1968

A numerical simulation of pressure distribution and radius of drainage in infinite radial aquifers - constant rate case

Alton John Nute

A NUMERICAL SIMULATION OF PRESSURE DISTRIBUTION AND RADIUS OF DRAINAGE IN INFINITE RADIAL AQUIFERS - CONSTANT RATE CASE

by

ALTON JOHN NUTE, 1939

A DISSERTATION 54

Presented to the Faculty of the Graduate School of the

UNIVERSITY OF MISSOURI-ROLLA

In Partial Fulfillment of the Requirements for the Degree

DOCTOR OF PHILOSOPHY

in

PETROLEUM ENGINEERING

1968

F. E. Kaveler
Advisor

M. D. Arnold

Ernest H. Stokes

D. R. Beveridge

J. P. Govier

B. C. Gillett

ABSTRACT

The diffusivity equation for the transient flow of slightly-compressible liquids has been solved for infinite radial aquifers, subject to constant terminal rates, by employing a Romberg integration of the Van Everdingen - Hurst explicit solution over the transformed integral limits for $.01<TD\leq 500$. For the dimensionless times of $.01\geq TD>500$, the classical solutions presented by Carslaw and Jaeger, Mortada, Theis, and others are incorporated in the digital analysis to yield dimensionless pressures for 40 selected dimensionless radius (RD) ratios between 1 and 64 for dimensionless time values of .0005 to 1000.0.

A new expression for dimensionless pressure-distribution, PD'(RD,TD), as a fraction of well bore pressure drop is presented with cross plots of the results obtained. These plots permit the solution of field problems involving PD', RD, and TD without the aid of the computer and without interpolation.

A radius of drainage relationship for an infinite radial aquifer is developed from the least squares polynominal curve fit of PD' = .01.

Additionally, an on-line mapping technique is presented which permits the aquifer pressure distribution to be displayed graphically on the I.B.M. 360/50 On-Line Printer.

ACKNOWLEDGEMENT

The author wishes to express his appreciation to Dr. R. E. Carlile, his advisor, and to Dr. M. D. Arnold and Professor J. P. Govier for their careful and thorough review of this dissertation.

The author also wishes to express his gratitude to Professor T. C. Wilson for his assistance in the transformation of integration limits which led to the eventual solution.

Finally, the author is deeply grateful to his parents, Mr. & Mrs. Cloren A. Nute, for their continued encouragement and support during these years in school.

TABLE OF CONTENTS

LIST OF FIGURES

LIST OF TABLES

LIST OF INSERTS

Chapter 1

INTRODUCTION

The unsteady-state flow of a slightly compressible liquid, such as water or oil, through porous media is the basis for a major part of the physical and mathematical research work carried on in hydrological and reservoir engineering. In many cases the solutions to various unsteady-state fluid flow problems have been developed as a result of the analogy between the theory of fluid flow and that of heat transfer.

Various solutions to the diffusivity equation for the unsteady-state flow of water or oil through an infinite radial reservoir, subject to a constant producing rate at the interior boundary, can be found in the literature. However, these solutions (for the most part derived analytically) have not been suitably evaluated numerically to be of value to the practicing hydrologist or petroleum engineer who needs a simple table, plot, or computer program to enable him to solve his field problems with the required degree of accuracy. This is a particular need with the existing solutions to the diffusivity equation giving the pressure distribution within and around a hydrocarbon reservoir. The work of Van Everdingen and Hurst(9) adequately treats the case where the pressure at the interior boundary (viz.r_D=1) is desired but their results are not well-suited to use with modern digital computer programs without tedious curve-fitting or numerical integration of their analytical expressions for dimensionless

pressure $P_D(t_D)$ at various dimensionless times (t_D).

The pressure distribution at points apart from the inner boundary of the reservoir is even less adequately covered in the literature. The point-source solution(13) is normally used for calculating the pressure distribution around a well interior to the bounds of a hydrocarbon reservoir, but this solution is unsatisfactory for calculating interference effects within the aquifers surrounding many petroleum reservoirs. Mortada(16) has presented the only results to date which can be used to accurately predict the pressure distribution within aquifers. These results, however, are in the form of plots which cannot be easily interpolated at non-integral r_D values or readily used in digital analyses.

The literature concerning the effective radius of drainage for radial reservoirs is in much the same state as that of pressure distribution. Many radius of drainage equations are available, but they have been derived for finite reservoirs and may or may not be suitable for infinite reservoirs. No simple method is available to predict the radius at which a given fractional pressure drop will occur within an infinite aquifer.

The object of this study was then to provide an easy means of:

1. Determining the pressure drop at any radial distance from the aquifer-hydrocarbon reservoir boundary at any time for an infinite radial system, constant rate case.

2. Determining the effective radius of drainage for the conditions set forth in 1) and to predict the radius at which any fractional pressure drop will occur at a given time after a constant producing rate has been initiated.

Chapter 2

LITERATURE REVIEW

An aquifer is considered to be of infinite areal extent when its exterior radius is so large relative to its interior boundary (represented by a wellbore or the outer boundary of a hydrocarbon reservoir) that the water movement in the vicinity of this exterior boundary is negligible during the time period under consideration (e.g., up to 20 years). If the pressure boundary (radius of drainage) reaches the exterior boundary of the aquifer during the above time period then the aquifer is considered to be of finite extent.

The pressure decline within an aquifer is, in most cases, an unsteady-state phenomenon due to the time-dependence of pressure within the porous stratum at a given point. As pressure changes on each element of the aquifer, the amount of water leaving each element is not the same as the amount entering that element due to the compressibility of the water.

2.1 Exponential Integral Solution

In 1935 Theis(1) showed that the unsteady-state flow of underground water into a radial sink area, such as a wellbore or hydrocarbon reservoir, is governed by the Diffusivity Equation (2-1).

$$\frac{\partial^2 \bar{s}}{\partial r^2} + \frac{1}{r}\frac{\partial \bar{s}}{\partial r} = \frac{S}{T}\frac{\partial \bar{s}}{\partial t} \qquad (2\text{-}1)$$

where:

S = the Coefficient of Storage (See Figure 2-1*).

$\bar{s}$ = the drawdown at any point r around a well.

T = Coefficient of Transmissibility (See Figure 2-2*).

r = the distance away from the discharge well.

t = the time of pumping.

The assumptions imposed on the derivation of Equation (2-1) are:

1. Darcy's Law applies.
2. The higher order term reflecting the rate-change of drawdown with distance $\left(\frac{\partial \bar{s}}{\partial r}\right)^2$ is negligible.
3. A single fluid is present that occupies the entire pore space.
4. The reservoir is horizontal, homogeneous, uniform in thickness, and of infinite radial extent.
5. The compressibility and viscosity of the fluid remain constant at all pressures.
6. The fluid density obeys the equation,

$$\rho = \rho_o e^{-c(p_o - p)} . \qquad (2\text{-}2)$$

Theis(1) has shown that the mathematical theory of heat conduction developed by Fourier and subsequent writers is applicable to hydraulic theory; hydraulic pressure being analogous to temperature, pressure-gradient to thermal-gradient, permeability to thermal conductivity, and specific yield to specific heat.

*Definitions of terms are given in the Appendix.

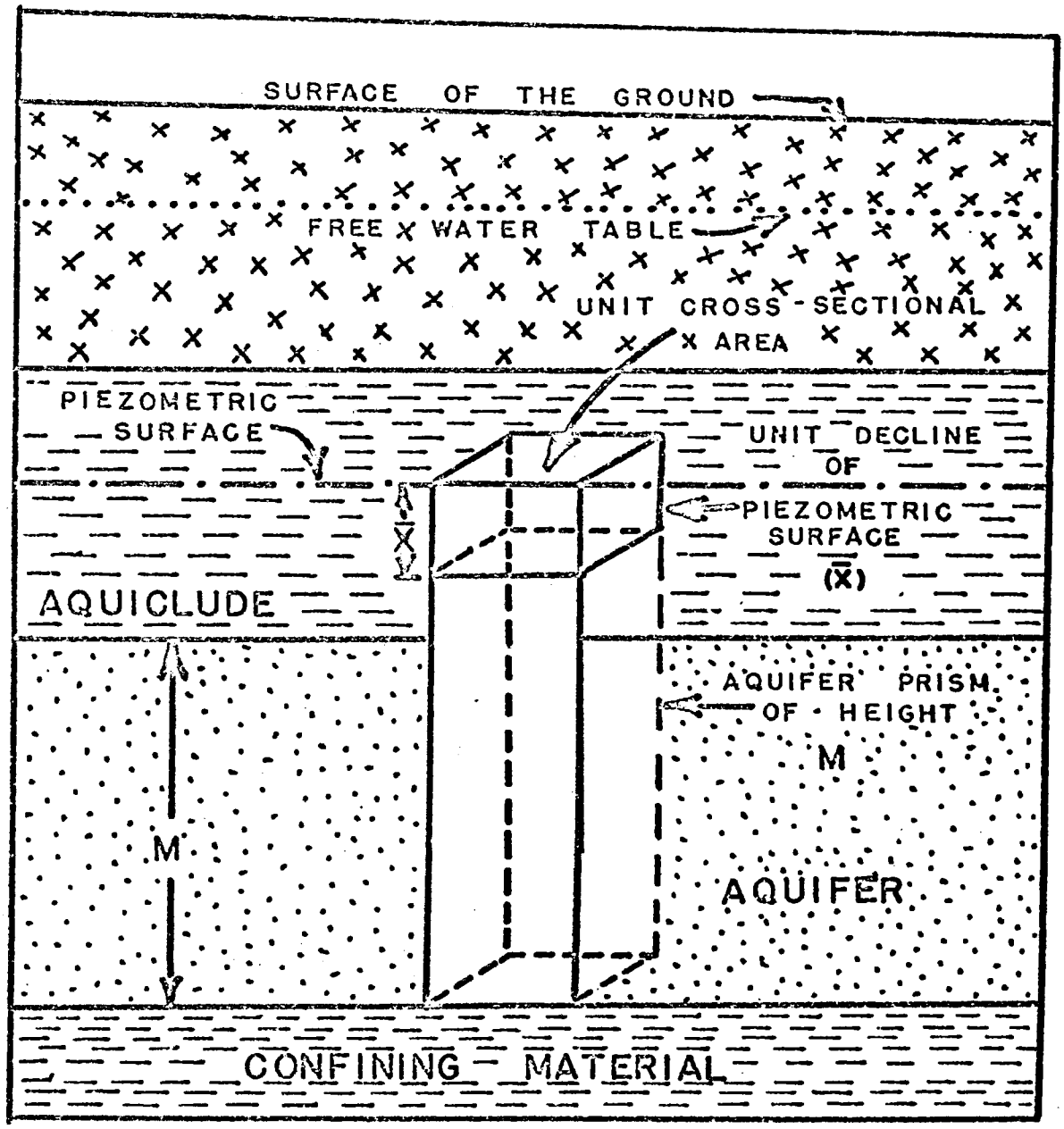

FIGURE 2-1

ARTESIAN AQUIFER

AND

STORAGE COEFFICIENT

(FROM REF. 4)

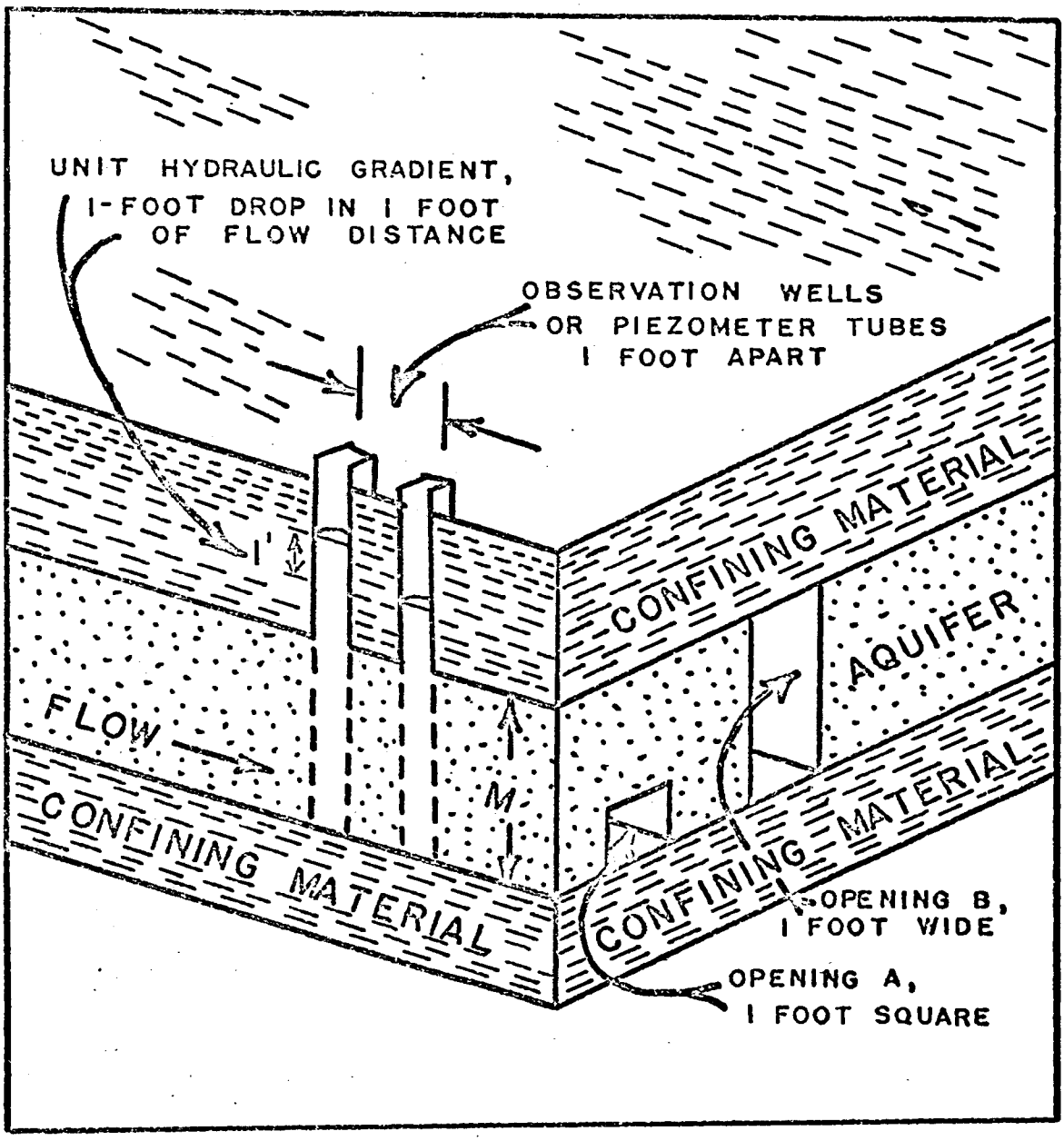

FIGURE 2-2

COEFFICIENTS OF TRANSMISSIBILITY AND PERMEABILITY

(FROM REF. 4)

Theis' solution to the differential equation for the radial flow of water in an elastic artesian aquifer for a constant discharge rate was derived from H. S. Carslaw's(2) two-dimensional heat flow equation:

$$v = (Q/4\pi\kappa t)e^{-(x^2+y^2)/4\kappa t} \qquad (2\text{-}3)$$

where:

v = temperature at the point x,y at time t.

Q = strength of the source (i.e., the amount of heat).

κ = Kelvin's coefficient of diffusivity, which is equal to the coefficient of conductivity divided by the specific heat per unit-volume.

t = time.

The effect of a continuous source of constant strength is derived from (2-3) (See Appendix B, page 231).

$$v_t = (\lambda/4\pi\kappa) \int_{\frac{x^2+y^2}{4\kappa t}}^{\infty} e^{-u}/u \; du \qquad (2\text{-}4)$$

Equation (2-4) when converted to radial form and expressed in hydrologic terms is:

$$\bar{s} = \frac{114.6Q}{\underline{T}} \int_{\frac{1.87r^2S}{\underline{T}t}}^{\infty} e^{-u}/u \; du \qquad (2\text{-}5)$$

where:

Q = discharge of the well, gallons per minute.

t = time since pumping started, days.

$u = 1.87\, r^2S/\underline{T}t$

$\underline{T}$ = Coefficient of Transmissibility, cubic feet of water per day per foot of aquifer width (See Figure 2-2).

S = Coefficient of Storage (See Figure 2-1).

$\bar{s}$ = water level at radius r from the pumped well, feet.

r = distance from the pumped well, feet.

The expression in Equation (2-5) cannot be integrated directly but can be approximated by the series(3):

$$\int_{\frac{1.87r^2S}{Tt}}^{\infty} e^{-u}/u \; du = W(u) = -.577216 - Ln(u) + u - \frac{u^2}{2(2!)} + \frac{u^3}{3(3!)} - \cdots \frac{u^n}{n(n!)} \quad . \qquad (2\text{-}6)$$

Values of W(u) have been tabulated by Wenzel(3) and Equation (2-5) can be solved for $\underline{T}$ by a type-curve matching process as indicated by Ferris(4) (See Figure 2-3).

This solution assumes the following:

1. The aquifer is homogeneous and isotropic.
2. The aquifer has infinite areal extent.
3. The discharge or recharge well fully penetrates the formation and receives water from the entire thickness of the aquifer.
4. The coefficient of transmissibility is constant at all times and at all places.
5. The well has an infinitesimal diameter.
6. Water removed from storage is discharged instantaneously with a decline in head.

Jacob(5) recognized that the terms beyond Ln(u) in Equation (2-6) were not significant when (u) becomes small (i.e., when t increases or r decreases) and that this series could be truncated without adding significant error to Theis' equation. Jacob's modified equation is:

$$\bar{s} = \frac{Q}{4\pi\underline{T}} \left[Ln \left(\frac{4\underline{T}t}{r^2S} \right) - .5772 \right] \qquad (2\text{-}7)$$

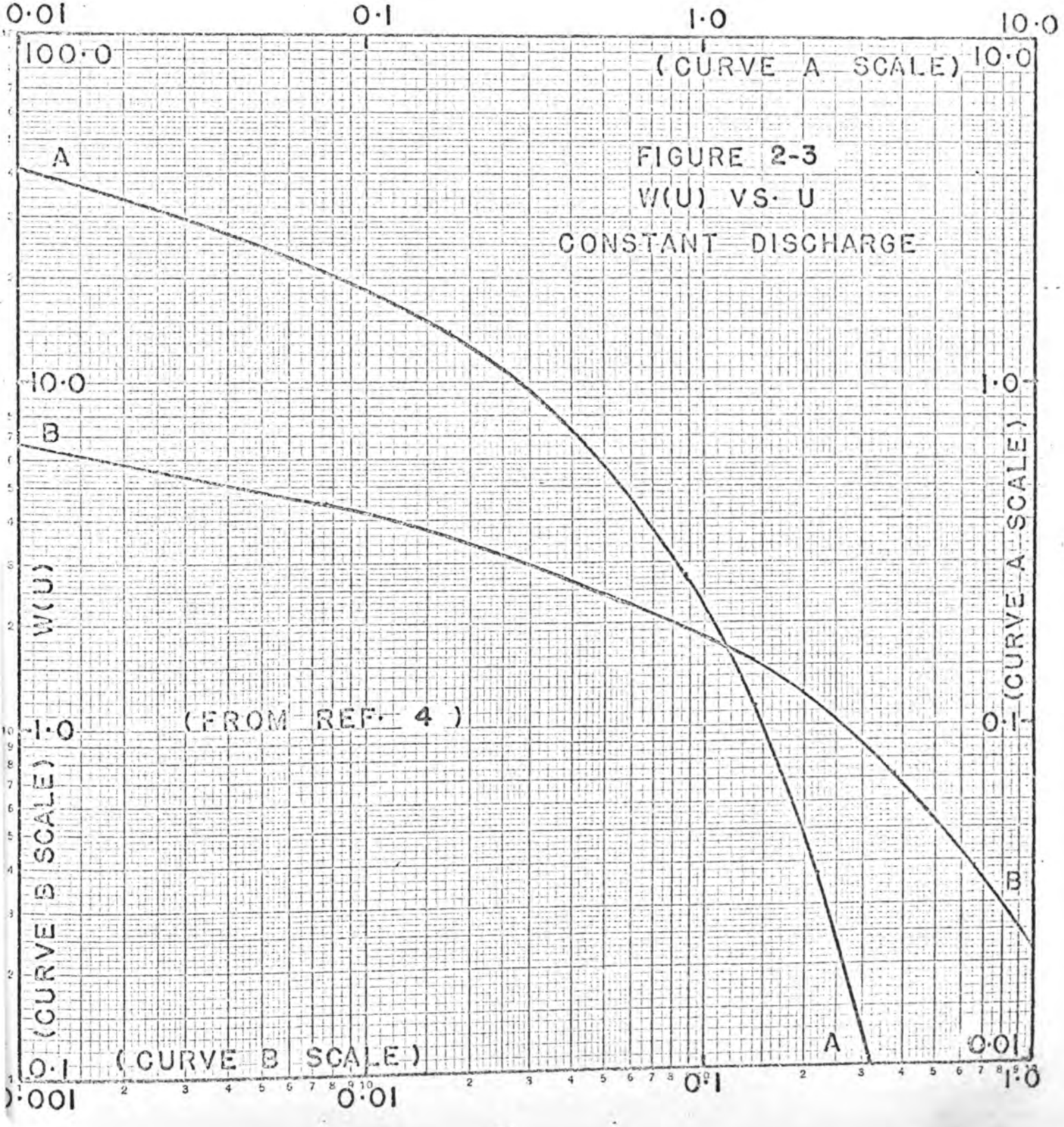
0·01
0·1
1·0
10·0
100·0
(CURVE A SCALE)
10·0
A
FIGURE 2-3
W(U) VS. U
CONSTANT DISCHARGE
10·0
1·0
B
W(U)
(CURVE B SCALE)
1·0
(FROM REF. 4)
0·1
(CURVE A SCALE)
B
A
0·1
(CURVE B SCALE)
0·01
0·001
0·01
0·1
1·0
U

or in standard hydrologic units:

$$\bar{s} = \frac{264Q}{\underline{T}} \left[\text{Log} \frac{0.3\underline{T}t}{r^2 S} \right] . \qquad (2\text{-}8)$$

In many cases the pumping rate, Q, as recorded in terms of daily or monthly discharge, is found to change continuously. With this variation in pumping rate, the methods previously described cannot be applied without tedious modifications. Stallman(6) introduced a method of approximating this varying discharge rate by a series of graphical steps. The analysis of each step is subsequently undertaken using the conventional equations. A type-curve for analyzing the observed drawdowns caused by this stepped pumping rate can be constructed by use of the Theis' non-equilibrium formula.

The water level drawdown, $\bar{s}$, used in the field of hydrology is analogous to the pressure drop used by petroleum engineers. Witherspoon and Neuman(7) have shown that this relation between $\bar{s}$ and a dimensionless pressure, P_D, is:

$$P_D = \frac{8.953 \times 10^{-5} Kh\bar{s}}{Q\mu} \qquad (2\text{-}9)$$

where:

K = permeability of reservoir, millidarcies.

h = thickness of reservoir, feet.

μ = viscosity of fluid, centipoise.

Q = pumping rate, gallons per minute.

$\bar{s}$ = drawdown of water level, feet.

2.2 The Finite Wellbore Solution:

The mathematical expression for pressure drop in an infinite homogeneous radial reservoir having a finite inner boundary (circular cylinder of radius r = a) was also developed in the theory of heat transfer. Carslaw and Jaeger(8) showed that the surface temperature v_s of an infinite region bounded internally by a circular cylinder of radius, a, with zero initial temperature and a constant heat flux of Q units per unit time per unit area at r = a is given by:

$$v_s = -\frac{2Q}{\pi K}\int_0^{\infty} \frac{\left(1-e^{-\kappa u^2 t}\right)\left[J_0(ur)Y_1(ua)-Y_0(ur)J_1(ua)\right]}{u^2\left[J_1^{\,2}(ua)+Y_1^{\,2}(ua)\right]}\,du \qquad (2\text{-}10)$$

where:

v_s = surface temperature at distance r from the wellbore, degrees.

Q = constant flux, heat units/unit time/unit area.

r = distance from the wellbore.

K = thermal conductivity.

a = radius of the inner circular cylinder.

κ = Kelvin's diffusivity coefficient.

t = time.

u = variable of integration.

J_0 = Bessel function of zero order, first kind.

Y_0 = Bessel function of zero order, second kind.

J_1 = Bessel function of first order, first kind.

Y_1 = Bessel function of first order, second kind.

Carslaw and Jaeger also present simplified expressions for both large and small values of $\kappa t/a^2$, dimensionless time (See Appendix B, pages 224 and 227).

Van Everdingen and Hurst(9) have presented a solution to the Diffusivity Equation (2-1) for the unsteady-state isothermal flow of a slightly compressible fluid encroaching into a homogeneous reservoir sink. This solution, developed by the application of Laplace transforms, gives an exact determination of the aquifer water encroachment across the aquifer-hydrocarbon reservoir boundary under the assumption that such encroachment is at constant terminal rate.

The pressure drop represented by $P_D = P_D(r_D,t_D)$ at the hydrocarbon reservoir boundary where $r_D = 1$ is

$$\left(\frac{\partial P_D}{\partial r_D}\right)_{r_D=1} = -1 \quad . \tag{2-11}$$

The minus sign is introduced to compensate for the pressure gradient direction relative to the radius of the reservoir. If the cumulative pressure drop is expressed as ΔP, then:

$$\Delta P = q(t_D)P_D(r_D,t_D) \tag{2-12}$$

where $q(t_D)$ is a constant relating the cumulative pressure drop with the pressure change for a unit rate of production. From Darcy's equation(10) for the rate of fluid flow into the well or reservoir per unit sand thickness

$$q_{(T)} = \frac{-2\pi K q(t_D)}{\mu} \left[\frac{\partial P_D(r_D,t_D)}{\partial r_D}\right]_{r_D=1} , \qquad (2\text{-}13)$$

the constant is found to be:

$$q(t_D) = \frac{q(T)\mu}{2\pi K} . \qquad (2\text{-}14)$$

The ΔP at unit reservoir radius (or well radius) for any constant rate of production is given by:

$$\Delta P = \frac{q_{(T)}\mu}{2\pi K} P_D(t_D) . \qquad (2\text{-}15)$$

Since the diffusivity equation is linear, the Duhamel Superposition Theorem(9) can be applied as a sequence of constant terminal rates in such a way that the pressure history at the aquifer-hydrocarbon reservoir boundary ($r_D = 1$) is reproduced. $P_D(t_D)$ is the cumulative pressure drop at the sand face per unit rate of production, Initially, that is at time zero, the cumulative pressure drop at any point in the formation is zero,

$$P_D(r_D, t_D = 0) = 0 . \qquad (2\text{-}16)$$

Hence, Van Everdingen and Hurst show that the cumulative pressure drop at any point in the reservoir since zero time is:

$$P_D(r_D,t_D) = \frac{2}{\pi} \int_0^\infty \frac{\left[1-e^{-u^2 t_D}\right]\left[J_1(u)Y_0(ur)-Y_1(u)J_0(ur)\right]}{u^2\left[J_1^2(u)+Y_1^2(u)\right]}\,du \quad . \tag{2-17}$$

Equation (2-17) is the explicit solution of the constant terminal rate case for an infinite radial reservoir. This solution can be shown to be analogous to the heat transfer equation of Carslaw and Jaeger, Equation (2-10) (See Appendix B, page 222).

To determine the cumulative pressure drop for a unit rate of production at the wellbore or field radius (where $r_D = 1$) Equation (2-17) changes to:

$$P_D(1,t_D) = \frac{2}{\pi} \int_0^\infty \frac{\left[1-e^{-u^2 t_D}\right]\left[J_1(u)Y_0(u)-Y_1(u)J_0(u)\right]}{u^2\left[J_1^2(u)+Y_1^2(u)\right]}\,du \quad . \tag{2-18}$$

Using the relationship:

$$J_1(u)Y_0(u)-J_0(u)Y_1(u) = \frac{2}{\pi u} \quad , \tag{2-19}$$

Equation (2-18) simplifies to:

$$P_D(t_D) = \frac{4}{\pi^2} \int_0^\infty \frac{\left[1-e^{-u^2 t_D}\right]}{u^3\left[J_1^2(u)+Y_1^2(u)\right]}\,du \quad . \tag{2-20}$$

Van Everdingen and Hurst solved Equation (2-20) for $P_D(t_D)$ at various values of t_D by numerical integration employing Simpson's Rule (See Figure 2-4 and Table 2-5).

Figure 2-4

Van Everdingen-Hurst P(t) Plot
Constant Rate Case

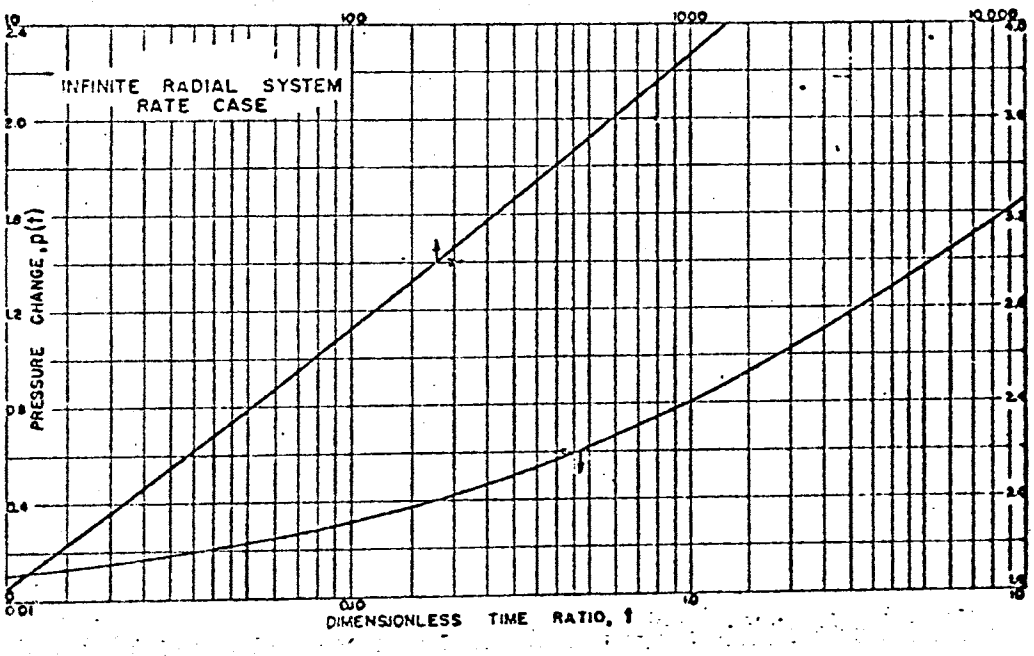

(From Reference 14)

Table 2-1

Van Everdingen and Hurst P(t) Results, Infinite Radial Aquifer-Constant Rate

t	$Q_{(t)}$	$P_{(t)}$	t	$Q_{(t)}$
$1.0(10)^{-2}$	0.112	0.112	$1.5(10)^{3}$	$4.136(10)^{3}$
5.0 "	0.278	0.229	2.0 "	5.315 "
$1.0(10)^{-1}$	0.404	0.315	2.5 "	6.406 "
1.5 "	0.520	0.376	3.0 "	7.590 "
2.0 "	0.608	0.424	4.0 "	9.757 "
2.5 "	0.689	0.469	5.0 "	11.88 "
3.0 "	0.758	0.503	6.0 "	13.95 "
4.0 "	0.898	0.564	7.0 "	15.99 "
5.0 "	1.020	0.616	8.0 "	18.00 "
6.0 "	1.140	0.659	9.0 "	19.99 "
7.0 "	1.251	0.702	$1.0(10)^{4}$	21.96 "
8.0 "	1.359	0.735	1.5 "	$3.146(10)^{3}$
9.0 "	1.469	0.772	2.0 "	4.079 "
1.0	1.570	0.802	2.5 "	4.994 "
1.5	2.032	0.927	3.0 "	5.891 "
2.0	2.442	1.020	4.0 "	7.634 "
2.5	2.838	1.101	5.0 "	9.342 "
3.0	3.209	1.169	6.0 "	11.03 "
4.0	3.897	1.275	7.0 "	12.69 "
5.0	4.541	1.362	8.0 "	14.33 "
6.0	5.148	1.436	9.0 "	15.95 "
7.0	5.749	1.500	$1.0(10)^{5}$	17.56 "
8.0	6.314	1.556	1.5 "	$2.538(10)^{4}$
9.0	6.861	1.604	2.0 "	3.308 "
$1.0(10)^{2}$	7.417	1.651	2.5 "	4.066 "
1.5 "	9.965	1.829	3.0 "	4.817 "
2.0 "	$1.229(10)^{3}$	1.960	4.0 "	6.267 "
2.5 "	1.455 "	2.067	5.0 "	7.699 "
3.0 "	1.681 "	2.147	6.0 "	9.113 "
4.0 "	2.088 "	2.282	7.0 "	10.51 "
5.0 "	2.482 "	2.388	8.0 "	11.89 "
6.0 "	2.860 "	2.476	9.0 "	13.26 "
7.0 "	3.228 "	2.550	$1.0(10)^{6}$	14.62 "
8.0 "	3.599 "	2.615	1.5 "	$2.126(10)^{5}$
9.0 "	3.942 "	2.672	2.0 "	2.781 "
$1.0(10)^{3}$	4.301 "	2.723	2.5 "	3.427 "
1.5 "	5.980 "	2.921	3.0 "	4.064 "
2.0 "	7.586 "	3.064	4.0 "	5.318 "
2.5 "	9.120 "	3.178	5.0 "	6.544 "
3.0 "	10.58 "	3.263	6.0 "	7.761 "
4.0 "	13.46 "	3.406	7.0 "	8.965 "
5.0 "	16.24 "	3.516	8.0 "	10.16 "
6.0 "	18.97 "	3.608	9.0 "	11.34 "
7.0 "	21.60 "	3.684	$1.0(10)^{7}$	12.52 "
8.0 "	24.23 "	3.750		
9.0 "	26.77 "	3.809		
$1.0(10)^{4}$	29.31 "	3.860		

(From Reference 9)

(This study gives values of $P_D(1,t_D)$, the dimensionless pressure at the sand face, for the constant terminal rate case for values of dimensionless time, t_D, ranging from .01 to 1000). They did not, however, attempt to solve Equation (2-17) numerically. As a result, their results are only applicable at the well or at the reservoir boundary and cannot be used at radius ratios other than $r_D = 1$.

In 1949, Muskat(11) presented another solution to the diffusivity equation for an infinite radial reservoir containing a slightly compressible fluid subject to constant terminal rate conditions:

$$\gamma=\gamma_i+\frac{q_0}{\pi^2 afr_f}\int_0^\infty \frac{\left[1-e^{-au^2t}\right]\left[J_0(ur)Y_1(ur_f)-Y_0(ur)J_1(ur_f)\right]}{u^2\left[J_1^2(ur_f)+Y_1^2(ur_f)\right]}\,du \qquad (2\text{-}21)$$

where:

κ = density of fluid.

f = porosity.

a = diffusivity constant, $k/f\kappa\mu$.

κ = compressibility of fluid.

μ = viscosity of fluid.

k = permeability of reservoir.

r_f = radius of the inner boundary.

q_0 = constant production rate.

At the field boundary, r_f, γ has the value:

$$\gamma_f = \gamma_i - \frac{2q_0}{\pi^3 a f r_f^2} \int_0^\infty \frac{\left(1-e^{-au^2t}\right) du}{u^3\left[J_1^2(ur_f)+Y_1^2(ur_f)\right]} \qquad (2\text{-}22)$$

On translating the decline in density $\gamma_i - \gamma_f$ to the corresponding pressure drop $\Delta p = p_i - p_f$ and introducing the dimensionless time variable, $\bar{t} = at/r_f^2$, Equation (2-22) becomes:

$$\Delta p = \frac{2Q\mu}{\pi^3 k} \int_0^\infty \frac{\left(1-e^{-z^2\bar{t}}\right) dz}{z^3\left[J_1^2(z)+Y_1^2(z)\right]} \qquad (2\text{-}23)$$

where:

Q = volumetric outflow per unit thickness at r_f measured at the surface, q_0/γ_0.

Muskat presented his results of Equation (2-23) in the form of a plot (See Figure 2-5) of dimensionless pressure versus dimensionless time at the inner boundary. He pointed out that Δp initially rises as $(\bar{t})^{\frac{1}{2}}$ and then asymptotically assumes a logarithmic variation with $\bar{t}$. Assuming the conditions of the constant rate solution, the curve in Figure 2-5 is a universal curve applicable to any infinite radial reservoir of constant efflux rate, regardless of the physical and geometrical parameters.

As is to be expected, Equation (2-23) shows that at any time after production is started, the pressure drop at the field boundary will be proportional to the water-influx rate.

Figure 2-5

Muskat's Constant Rate Q,
Δp versus t

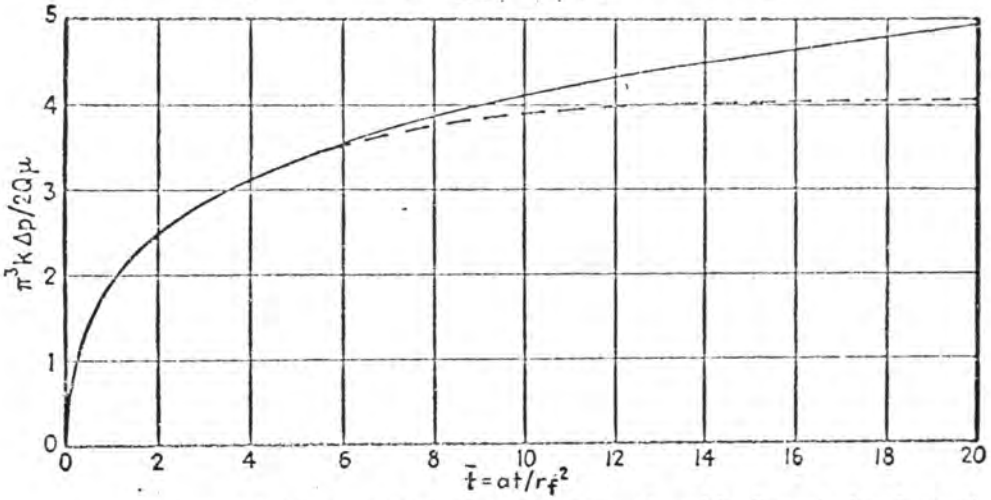

The calculated pressure drop Δp vs. the time t plotted in dimensionless form, at the internal boundary of water reservoirs, with constant water-withdrawal rate Q per unit thickness. Internal-boundary radius = r_f; permeability of water reservoir = k; μ = viscosity of water; κ = compressibility of water; f = porosity; $a = k/f\kappa\mu$. Solid curve refers to an infinite water reservoir. Dashed curve applies to a finite water reservoir with the pressure kept fixed at an external radius that is 6.3 times r_f.

Figure 2-6

Muskat's Δp versus
Cumulative Withdrawals

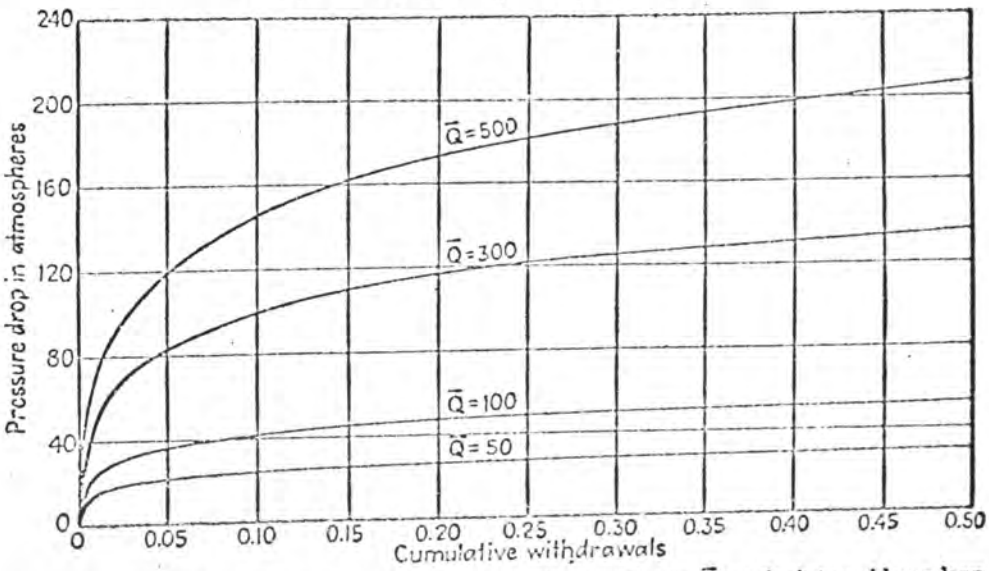

The calculated pressure drop for fixed withdrawal rates $\bar{Q}$, at the internal boundary of an infinite aquifer, vs. the cumulative withdrawals, expressed as a fraction of the pore volume of the oil reservoir, of radius r_f. $\bar{Q} = Q\mu/k$; Q = withdrawal rate from the aquifer per unit thickness; μ = water viscosity; k = permeability of aquifer. Water compressibility assumed = 4.5×10^{-5} per atmosphere.

(From Reference 11)

Muskat also presented a crossplot of Figure 2-5 which gives directly the variation of pressure decline for fixed cumulative water influx as a function of the rate of water withdrawal from the infinite aquifer (See Figure 2-6).

If the initial constant rate, Q_0, is changed at dimensionless time t_0 to Q_1, Equation (2-24) gives the pressure drop at the boundary, r_f, as:

$$\Delta p = \frac{2\mu}{\pi^3 k}\left[Q_0 I(\bar{t}) + (Q_1 - Q_0) I(\bar{t} - \bar{t}_0)\right] \qquad (2\text{-}24)$$

where $I(\bar{t})$ is the integral in Equation (2-23). The first term represents the projected pressure decline history if the rate had been maintained at Q_0. The second term gives the effect of the change employing the superposition principle of Duhamel, Stallman(12), and Van Everdingen and Hurst(9).

Muskat plotted Equation (2-24) in dimensionless form for fixed values of the ratio Q_1/Q_0, denoted by (r), assuming that the change in rate occured at $\bar{t} = 10 = \bar{t}_0$ (See Figure 2-7).

Horner(13) applied the so-called "point-source" solution to the diffusivity equation to the problem of pressure build-up in oil wells. Starting with Equation (2-1) in petroleum terms:

$$\frac{\partial^2 p}{\partial r^2} + \frac{1}{r}\frac{\partial p}{\partial r} = \frac{\phi\mu c}{K}\frac{\partial p}{\partial t} \qquad (2\text{-}25)$$

where:

r = distance from the center of the well, centimeters.

t = time, seconds.

p = reservoir pressure at radius r at time t, atmospheres.

ϕ = porosity of reservoir, fraction.

K = permeability of reservoir, darcies.

μ = viscosity of the fluid, centipoise.

c = compressibility of the fluid, vol/vol/atm.

Horner gave the reservoir pressure at radius r at any time t as:

$$p = p_0 + \frac{q\mu}{4\pi Kh} Ei\left(-\frac{r^2\phi\mu c}{4Kt}\right) \qquad (2\text{-}26)$$

where:

p_0 = initial reservoir pressure, atmospheres.

h = thickness of reservoir, centimeters.

q = constant production rate of well, cubic centimeters per second.

Equation (2-26), which is analogous to Theis' equation (2-5), where:

$$Ei(-X) = -\int_X^{\infty} e^{-u}/u \quad du \quad , \qquad (2\text{-}27)$$

is an exact solution of Equation (2-25) for the boundary conditions:

1. The external boundary is infinite and at constant pressure, p_0.
2. The internal boundary (i.e., well radius) is vanishing and has a constant flow rate q across it.

Figure 2-7

Muskat's Δp versus t
with Change in Q at Time t_1

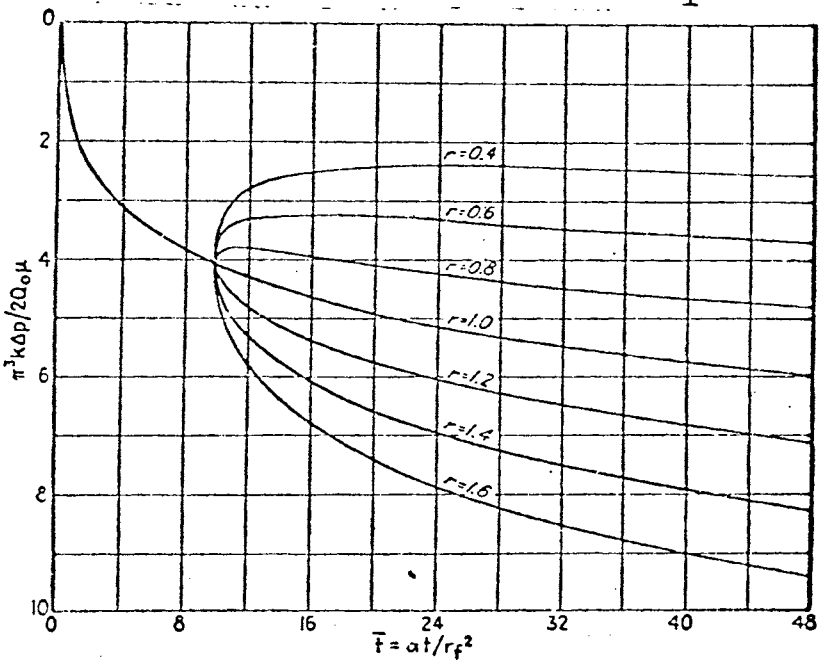

The calculated pressure drop Δp vs. the time t, plotted in dimensionless form, at the internal boundary of an infinite water reservoir with an initial withdrawal rate Q_o and a rate Q_1 after a time $\bar{t} = 10$; μ = water viscosity; κ = water compressibility; k = permeability of aquifer; f = porosity; r_f = internal radius of water reservoir; $r = Q_1/Q_o$; $a = k/f\kappa\mu$.

(From Reference 11)

Table 2-2

Chatas p(t) Results

Infinite radial system — Rate case.							
Dimensionless time t	Pressure change p(t)	Dimensionless time t	Pressure change p(t)	Dimensionless time t	Pressure change p(t)	Dimensionless time t	Pressure change p(t)
0	0	.06	.2500	3.0	1.1065	150.0	2.9212
.005	.0250	.07	.2680	4.0	1.2750	200.0	3.0638
.001	.0352	.08	.2845	5.0	1.3625	250.0	3.1726
.002	.0495	.09	.2999	6.0	1.4362	300.0	3.2630
.003	.0603	.1	.3144	7.0	1.4997	350.0	3.3394
.004	.0694	.15	.3750	8.0	1.5557	400.0	3.4057
.005	.0774	.2	.4241	9.0	1.6057	450.0	3.4641
.006	.0845	.3	.5024	10.0	1.6509	500.0	3.5164
.007	.0911	.4	.5645	15.0	1.8284	550.0	3.5643
.008	.0971	.5	.6167	20.0	1.9601	600.0	3.6078
.009	.1028	.6	.6622	30.0	2.1470	650.0	3.6476
.01	.1081	.7	.7024	40.0	2.2824	700.0	3.6842
.015	.1312	.8	.7387	50.0	2.3884	750.0	3.7184
.02	.1503	.9	.7716	60.0	2.4758	800.0	3.7505
.025	.1669	1.0	.8019	70.0	2.5501	850.0	3.7805
.03	.1818	1.2	.8572	80.0	2.6147	900.0	3.8058
.04	.2077	1.4	.9060	90.0	2.6718	950.0	3.8355
.05	.2301	2.0	1.0195	100.0	2.7233	1000.0	3.8586

(From Reference 14)

Horner assumed that the error introduced by treating the well radius as infinitely small could be considered to be negligible.

In 1953, Chatas(14) summarized the work of Van Everdingen and Hurst and further extended their results for higher and lower values of dimensionless time (t_D) (See Table 2-2).

Van Everdingen(15) investigated the pressure distribution around a producing well in relation to the effect of formation damage or skin effect on the productive capacity of the well. Using the following dimensionless quantities:

$$T = \frac{Kt}{\phi\mu c r_w^2}, \text{ and } p_{(T)} = \frac{2\pi Kh(p_r - p_w)}{q\mu}, \qquad (2\text{-}28)$$

Van Everdingen showed that Equation (2-17) can be approximated at large values of T (i.e., T>100) as:

$$p_{(T)} = \tfrac{1}{2}\left[\text{Ln}(T) + 0.809\right] \qquad (2\text{-}29)$$

and thus:

$$p_r - p_w = \frac{q\mu}{4\pi Kh}\left[\text{Ln}\left(\frac{Kt}{\phi\mu c r_w^2}\right) + 0.809\right]. \qquad (2\text{-}30)$$

For hydrocarbon well problems, Equation (2-30) holds since T usually exceeds 100 after a few seconds of production.

Mortada(16) discussed the problem of oilfield interference in water-drive reservoirs. He considered the problem of multiple oilfields located in a common aquifer and the effects of pressure drop in the various fields on the rate of water-influx into the reservoirs. In this paper, solutions were

presented to the diffusivity equation (Equation (2-25)) for values of dimensionless time (t_D) and dimensionless radius (r_D) for the constant rate case which are normally required for field analyses with the following boundary conditions:

1. $P_D(r_D,0) = 0$ (Uniform initial aquifer pressure).
2. $P_D(r_D,t_D) \rightarrow 0$ as $r_D \rightarrow \infty$ (Extensive aquifer). (2-31)
3. $\left(\frac{\partial P_D}{\partial r_D}\right)_{r_D = 1} = -1$ (Constant rate of water-influx).

Mortada's values for the dimensionless pressure $P_D(r_D, t_D)$ were obtained by several methods. For $t_D \leq .01$, the relationship

$$P_D(r_D,t_D) = \frac{2\sqrt{t_D}}{\sqrt{r_D}} \text{ ierfc} \left[\frac{r_D-1}{2\sqrt{t_D}}\right] \tag{2-32}$$

was solved, where(17);

$$\text{ierfc}(\bar{x}) = \frac{e^{-\bar{x}^2}}{\sqrt{\pi}} - \bar{x}\ \text{erfc}(\bar{x}) \quad . \tag{2-33}$$

For $t \geq 500$:

$$P_D(r_D,t_D) = \tfrac{1}{2}\left[-Ei\left(\frac{-r_D^2}{4t_D}\right)\right] \tag{2-34}$$

which is the point-source or exponential integral solution of Theis and Horner, where:

$$- Ei\left(\frac{-r_D^2}{4t_D}\right) = \int_{\frac{r_D^2}{4t_D}}^{\infty} e^{-\bar{x}}/\bar{x} \; d\bar{x} \quad . \qquad (2\text{-}35)$$

To bridge the gap between $t_D \leq .01$ and $t_D \geq 500$, Mortada used digital solutions to a set of finite-difference equations based upon the diffusivity equation. This technique provided values of $P_D(r_D,t_D)$ which showed no change in the third decimal place as the values of t_D were made progressively smaller.

Theis and Mortada are among the few authors who have investigated the pressure distribution away from the inner boundary (i.e., within the reservoir or aquifer). The Theis approach (Equation (2-7)) employs the exponential integral and is valid for pressure conditions that occur some distance away from the wellbore. The Mortada results, on the other hand, are valid at all points within the reservoir or aquifer. These results are presented in terms of dimensionless ratios of the radius where the pressure is desired to the radius where the flow rate is measured. Mortada's results are given in the form of graphs which are limited to a maximum radius ratio of 64 (See Figures 2-8 to 2-10). These graphical results are cumbersome to interpolate at non-integral radius ratios, and often it becomes necessary to solve the analytical expressions of Equations (2-32) and (2-35).

In order to obtain a dimensionless equation to facilitate one solution which can be used for application of

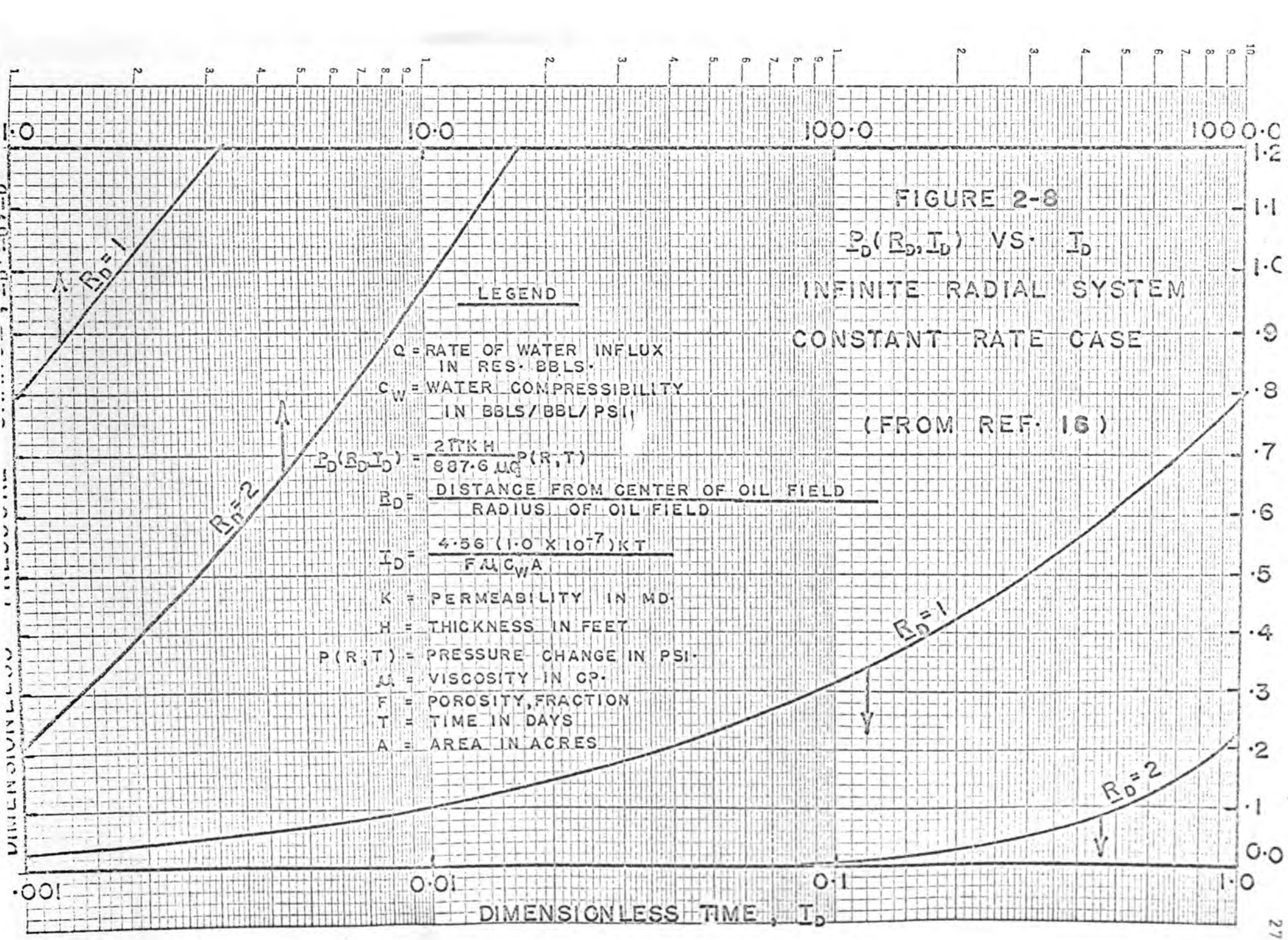
FIGURE 2-8
$P_D(R_D, T_D)$ VS. T_D
INFINITE RADIAL SYSTEM
CONSTANT RATE CASE
(FROM REF. 16)
LEGEND
Q = RATE OF WATER INFLUX IN RES. BBLS.
C_W = WATER COMPRESSIBILITY IN BBLS/BBL/PSI
$P_D(R_D,T_D) = \frac{2\pi KH}{887.6\,\mu Q} P(R,T)$
R_D = DISTANCE FROM CENTER OF OIL FIELD / RADIUS OF OIL FIELD
$T_D = \frac{4.56\,(1.0 \times 10^{-7})KT}{F\mu C_W A}$
K = PERMEABILITY IN MD.
H = THICKNESS IN FEET
P(R,T) = PRESSURE CHANGE IN PSI.
μ = VISCOSITY IN CP.
F = POROSITY, FRACTION
T = TIME IN DAYS
A = AREA IN ACRES
$R_D=1$
$R_D=2$
$R_D=1$
$R_D=2$
DIMENSIONLESS PRESSURE, P_D
DIMENSIONLESS TIME, T_D
.001
0.01
0.1
1.0
10.0
100.0
1000.0
0.0
.1
.2
.3
.4
.5
.6
.7
.8
.9
1.0
1.1
1.2

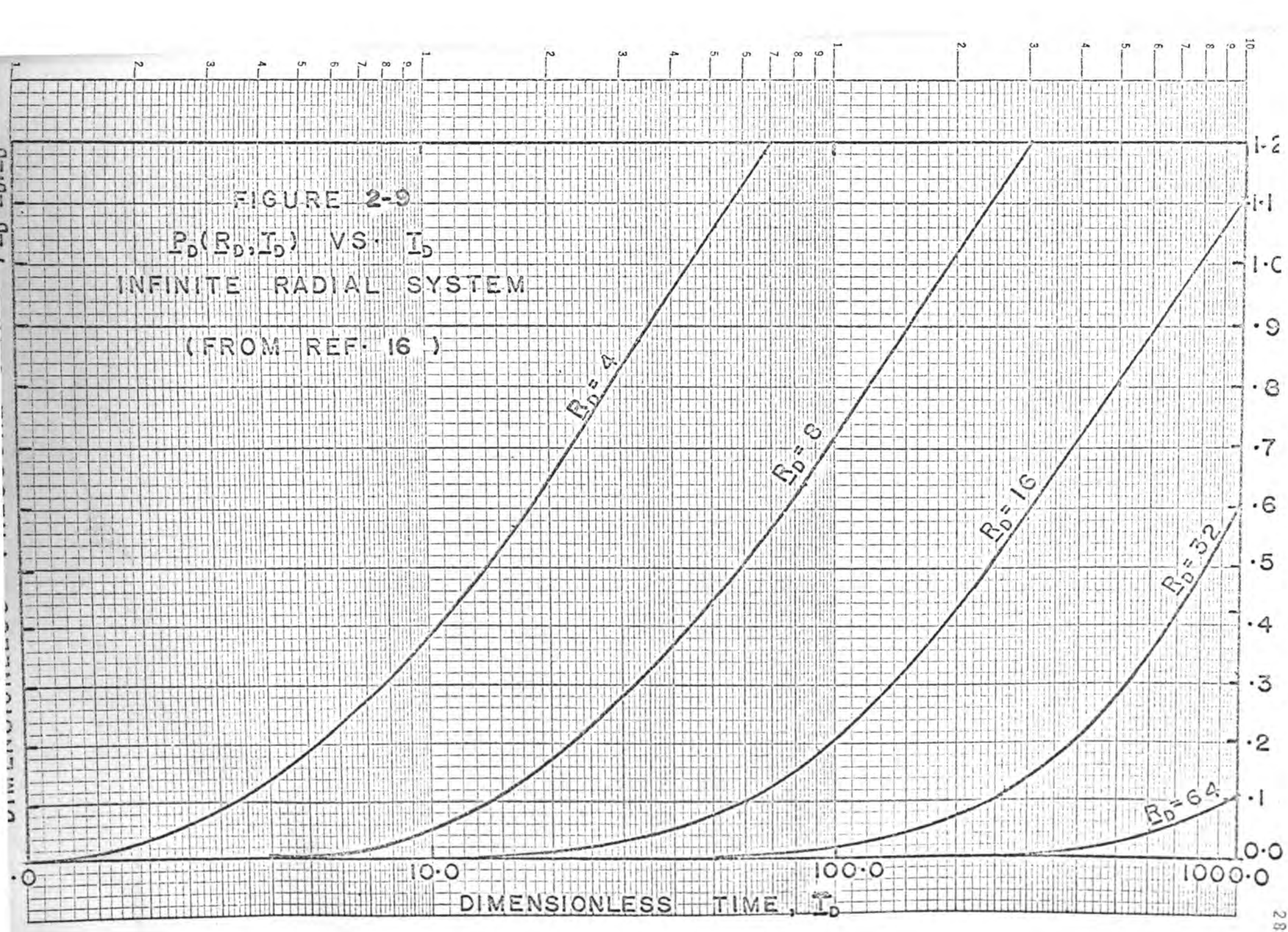
FIGURE 2-9
$P_D(R_D, T_D)$ VS. T_D
INFINITE RADIAL SYSTEM
(FROM REF. 16)
$R_D = 4$
$R_D = 8$
$R_D = 16$
$R_D = 32$
$R_D = 64$
1·2
1·1
1·0
·9
·8
·7
·6
·5
·4
·3
·2
·1
0·0
·0
10·0
100·0
1000·0
DIMENSIONLESS TIME, T_D

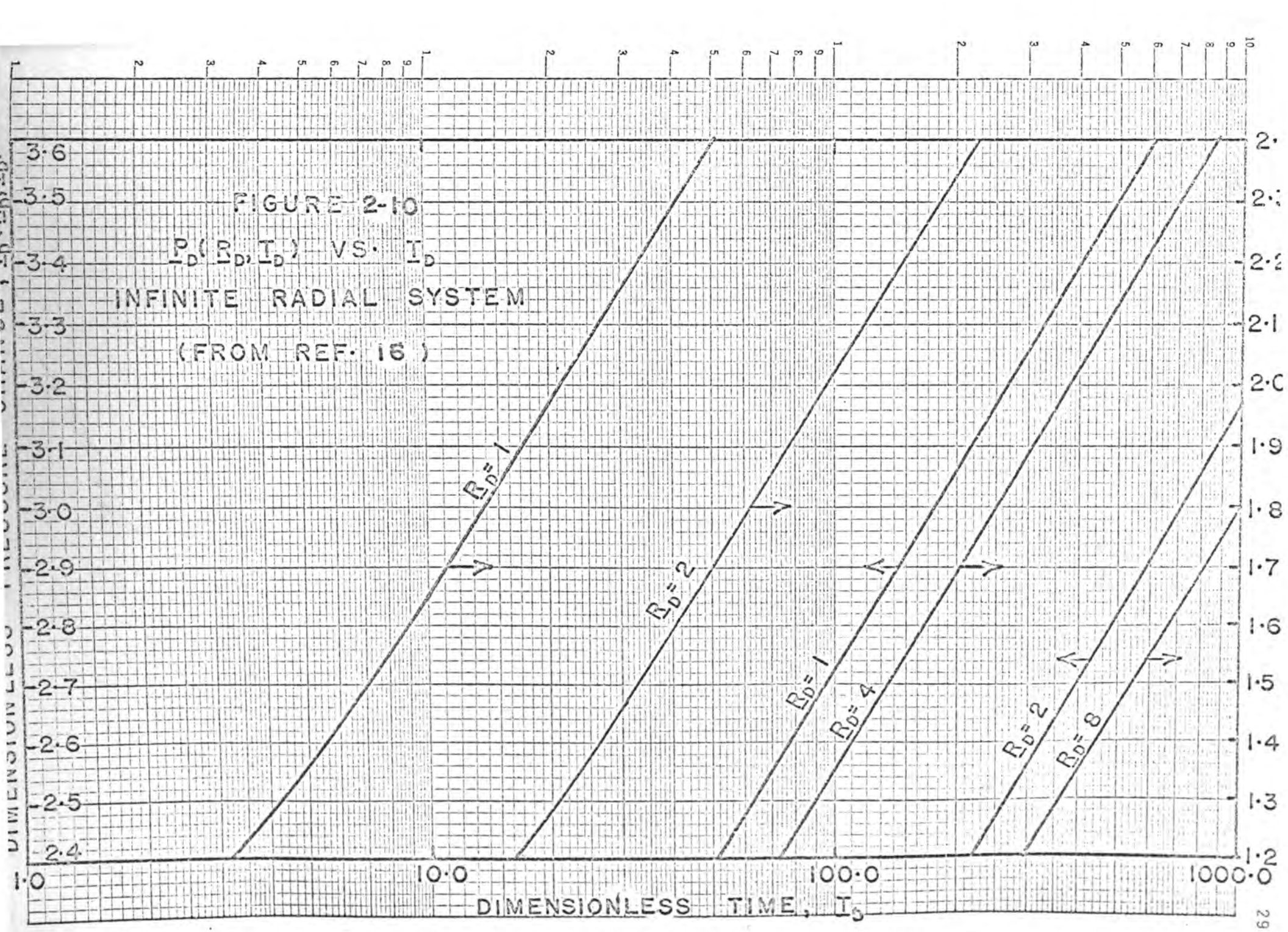
FIGURE 2-10
$P_D(R_D, t_D)$ VS. t_D
INFINITE RADIAL SYSTEM
(FROM REF. 16)
$R_D = 1$
$R_D = 2$
$R_D = 1$
$R_D = 4$
$R_D = 2$
$R_D = 8$
DIMENSIONLESS PRESSURE, P_D
DIMENSIONLESS TIME, t_D
3·6
3·5
3·4
3·3
3·2
3·1
3·0
2·9
2·8
2·7
2·6
2·5
2·4
2·
2·1
2·0
1·9
1·8
1·7
1·6
1·5
1·4
1·3
1·2
1·0
10·0
100·0
1000·0

different porosity, permeability, and fluid properties, Mortada, Van Everdingen-Hurst, and others have employed the following transformations:

Dimensionless Pressure:

$$P_D = \frac{2\pi KH\left(P_2-P_1\right)}{q\mu} \quad ; \tag{2-36}$$

Dimensionless Radius:

$$r_D = r/r_w, \text{ or } r_D = r/r_b \quad ; \tag{2-37}$$

Dimensionless Time:

$$t_D = \frac{Kt}{\phi\mu c r_w^2} \quad , \quad \text{or} \quad t_D = \frac{Kt}{\phi\mu c r_b^2} \quad . \tag{2-38}$$

Substituting these dimensionless parameters into Equation (2-25) yields:

$$\frac{\partial^2 P_D}{\partial r_D^2} + \frac{1}{r_D}\frac{\partial P_D}{\partial r_D} = \frac{\partial P_D}{\partial t_D} \quad . \tag{2-39}$$

Witherspoon, Mueller and Donovan(18) showed the relationship between the methods of analysis used by hydrologists and those commonly used by petroleum engineers. In oil-field terms, the Theis co-ordinates are:

$$P_D = \frac{wKH\Delta P}{q\mu} \quad \text{and} \quad \bar{t}_D = \frac{xKt}{\phi\mu c r^2} \tag{2-40}$$

Table 2-3

Definition of Terms in Theis Solution

Term	Definition	$w = 2\pi$ $x = 1.0$	$w = 7.082 \times 10^{-3}$ $x = 6.331 \times 10^{-3}$	$w = 8.953 \times 10^{-5}$ $x = 4.386 \times 10^{-6}$
K	Permeability	sq. cm.	md.	md.
H	Thickness	cm.	ft.	ft.
P	Pressure Drop	dynes/sq. cm.	psi.	ft. water
q	Flow Rate	cc./sec.	bbl./day	gal./min.
μ	Viscosity	poise	cp.	cp.
t	Time	sec.	days	min.
ϕ	Porosity	———	———	———
c	Compressibility	dynes/sq. cm.	psi.	psi.
r	Distance	cm.	ft.	ft.

(Ref. 18)

where (w) and (x) take on different values according to the dimensions selected (See Table 2-3).

These authors point out that Mortada's work shows that for reasonable values of real time, t, the Theis' point-source solution accurately represents the behavior of a slightly compressible system for all radial distances greater than about 30 times the radius of the pumping well, or in most cases about 15 feet or more away from the wellbore.

At early times and at short distances from the inner boundary, the point-source solutions are invalid. The error introduced by these solutions may be negligible in most reservoir problems, but in the calculation of interference effects in an aquifer the error introduced can be appreciable.

Buxton(19) provided a means for determining the pressure at various distances from the wellbore in an infinite reservoir subject to constant rate conditions. By using the point-source solution (Equation (2-34)) and digitally evaluating the explicit solution of the radial diffusivity equation obtained by Van Everdingen-Hurst (Equation (2-17)), Buxton prepared curves of $P(R,t_D)$ versus t_D for R ratios from 1 to 10. These results are of use mainly in an aquifer surrounding an oil reservoir. Buxton's results (See Figure 2-11 and Table 2-4) agree to within less than 1% with those of Van Everdingen-Hurst and Mortada.

Upon applying Simpson's rule for numerical integration to the explicit solution in Equation (2-17), Buxton succeeded in obtaining satisfactory results for a limited range of R

Figure 2-11

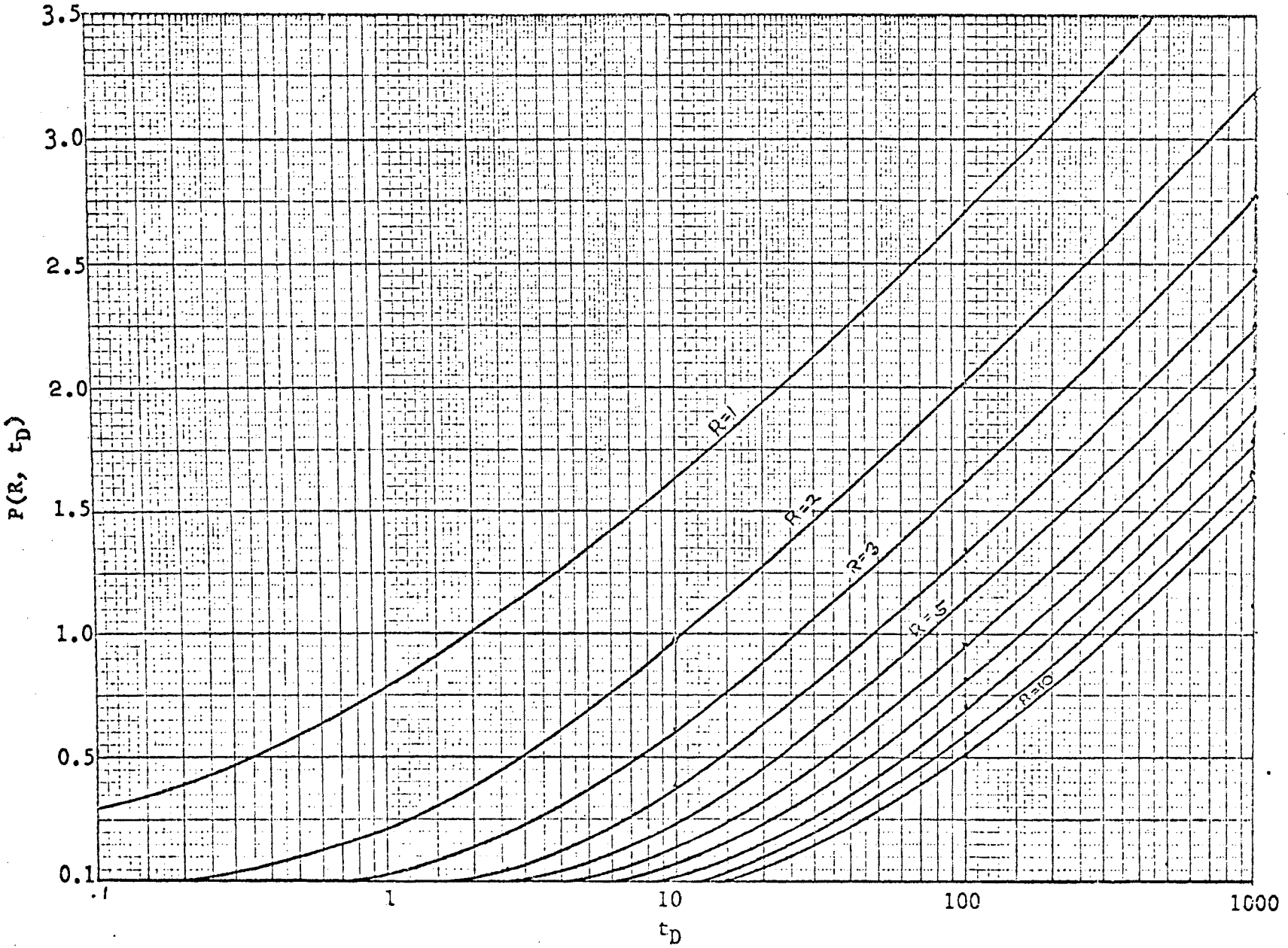

Pressure Distribution for Infinite Radial System-Constant Rate Case
(From Reference 19)

Figure 2-12

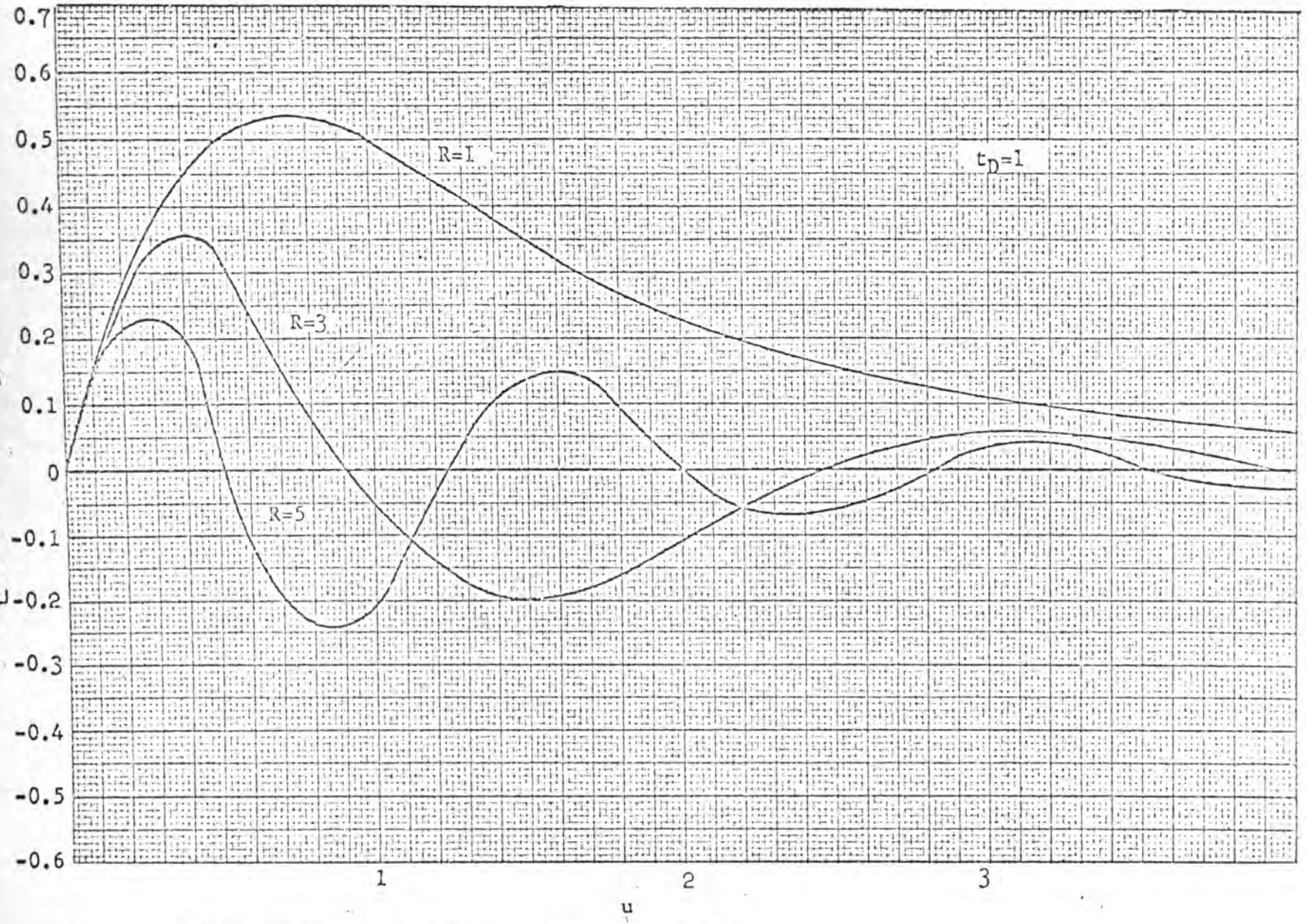

Effect of Radius on Function to be Integrated

(From Reference 19)

Table 2-4

MACHINE CALCULATED VALUES OF $P(R, t_D)$

t_D	R=1	R=2	R=3	R=4	R=5
0.01	0.107	0.004			
0.10	0.314	0.007	0.000		
1.0	0.802	0.225	0.055	0.009	0.004
5.0	1.361	0.705	0.381	0.196	0.100
10.0	1.651	0.980	0.621	0.391	0.248
30.0			1.081	0.812	0.623
50.0	2.396	1.712	1.320	1.041	0.841

t_D	R=6	R=7	R=8	R=9	R=10
1.0	0.000				
5.0	0.045	0.022	0.000		
10.0	0.151	0.093	0.044	0.032	0.018
20.0	0.335	0.242	0.162	0.122	0.085
30.0	0.475	0.367	0.270	0.215	0.163
50.0	0.680	0.557	0.445	0.373	0.305

(From Reference 19)

values. He found that a variable of integration value of 1000 gave an ordinate value of less than .00001 for the integral in Equation (2-17). Buxton also noted that the u^2 term in the denominator of Equation (2-17) caused the ordinate value (and hence the area under the curve) to become quite small for u values larger than 15. As a result of these observations, the following panel sizes were employed in Buxton's solution:

u Range	Panel Size
<15.8	.10
>15.8	3.0

Buxton was limited in his range of R values because of the oscillation occurring in the ordinate value of the integral (Equation (2-41)) at R values greater than 1:

$$\int_0^\infty \frac{\left[1-e^{-u^2 t_D}\right]\left[J_1(u)Y_0(uR)-Y_1(u)J_0(uR)\right]}{u^2\left[J_1^2(u)+Y_1^2(u)\right]}\,du \quad . \qquad (2\text{-}41)$$

This oscillation, shown in Figure 2-12, increased in frequency and decreased in magnitude as R was increased. For R values greater than 10, Buxton found that the numerical integration with Simpson's Rule of Equation (2-17) on the I.B.M. 650 computer no longer gave accurate results for $P(R,t_D)$.

Stevens and Thodos(20) considered the problem of interference between two wells producing from the same reservoir. Since they were principally interested in well interference, they used the Horner point-source solution to calculate the pressure distribution at various radii between two producing

Figure 2-13

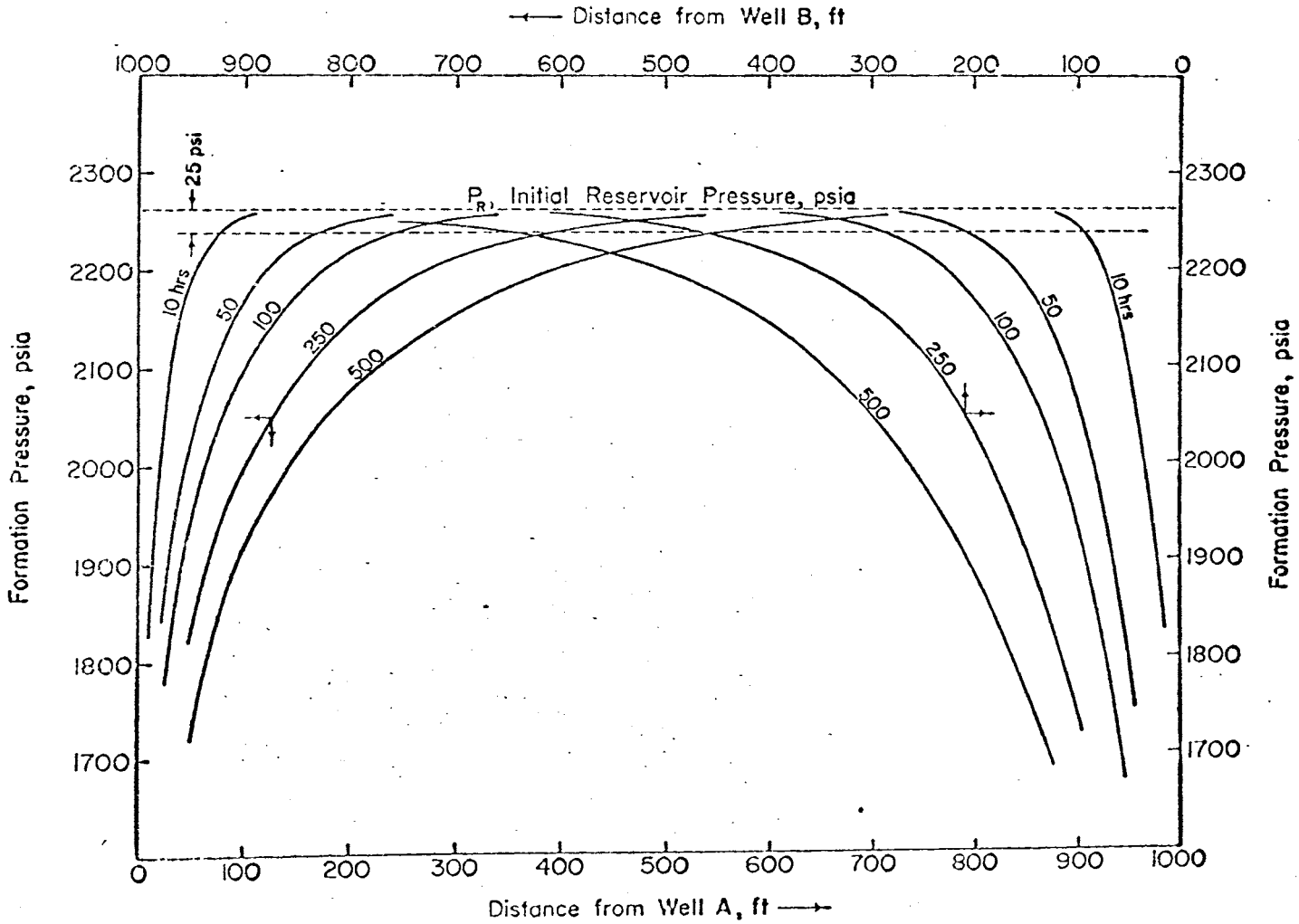

Pressure Profiles of Advancing Wave Fronts from Adjacent Wells and Interference Resulting from Their Interaction.

(From Reference 20)

wells. In determining the time of interference between the two wells, interference time was defined as that time when pressure waves from both wells exhibit a pressure decrease of 25 psi. at the same point in the formation (See Figure 2-13). Each well was assumed to act as a single well in an infinite reservoir until the pressure waves interfered at which time the production of each well falls below that which would be predicted by normal calculations. This approach is limited to a small number of wells due to the calculation of pressures at various radii at any time and the superposition of the individual pressure drops at each radius becoming extremely tedious as the number of wells is increased.

Edwardson(21) investigated formation temperature disturbances caused by mud circulation in the borehole. During this investigation he developed an approximate method of calculating the dimensionless temperature which he also called $P(r_D,t_D)$. This solution was for the unsteady-state temperature distribution in an infinite radial reservoir, constant terminal rate case. He also presented a summary of numerical results in tabular form (See Table 2-5) which was not previously available in Mortada's work and in addition, gave the following approximate expressions for $P_D(1,t_D)$, developed from polynominal approximations to his results:

$.01 \leq t_D < 500$ (Maximum error of .08%)

$$P_D(1,t_D) \simeq \frac{370.529\sqrt{t_D}+137.582(t_D)+5.69549(t_D)\sqrt{t_D}}{328.834+265.488\sqrt{t_D}+45.2157(t_D)+t_D\sqrt{t_D}} \qquad (2\text{-}42)$$

Table 2-5

$P(r_D, t_D)$ Values

t_D	$r_D = 2$	$r_D = 3$	$r_D = 5$	$r_D = 8$	$r_D = 10$	$r_D = 15$	$r_D = 20$	$r_D = 30$
4000	3.8591	3.4538	2.9434	2.4746	2.2526	1.8510	1.5687	1.1785
3000	3.7155	3.3102	2.8000	2.3315	2.1099	1.7095	1.4290	1.0438
2000	3.5131	3.1079	2.5980	2.1304	1.9095	1.5117	1.2347	0.8591
1500	3.3697	2.9645	2.4550	1.9881	1.7679	1.3726	1.0921	0.7330
1000	3.1677	2.7627	2.2537	1.7885	1.5697	1.1794	0.9126	0.5647
750	3.0245	2.6197	2.1114	1.6477	1.4303	1.0449	0.7848	0.4539
500	2.8231	2.4187	1.9115	1.4509	1.2364	0.8606	0.6132	0.3140
400	2.7125	2.3083	1.8021	1.3437	1.1314	0.7626	0.5242	0.2466
300	2.5702	2.1664	1.6617	1.2072	0.9982	0.6408	0.4168	0.1716
200	2.3703	1.9674	1.4658	1.0187	0.8164	0.4806	0.2826	0.09061
150	2.2293	1.8272	1.3285	0.8887	0.6929	0.3771	0.2021	0.05111
100	2.0317	1.6313	1.1385	0.7127	0.5291	0.2492	0.1124	0.01806
75	1.8927	1.4940	1.0068	0.5946	0.4224	0.1748	0.06692	0.00691
50	1.6991	1.3035	0.8274	0.4405	0.2888	0.09092	0.02602	0.00115
40	1.5939	1.2007	0.7326	0.3634	0.2252	0.06120	0.01356	0.00032
30	1.4600	1.0706	0.6154	0.2736	0.1552	0.03183	0.00486	0.00004
20	1.2755	0.8940	0.4624	0.1682	0.08081	0.00966	0.00071	
15	1.1482	0.7732	0.3643	0.1100	0.04515	0.00320	0.00012	
10	0.9751	0.6133	0.2441	0.05206	0.01579	0.00041		
7.5	0.8576	0.5080	0.1734	0.02660	0.00603	0.00006		
5.0	0.7011	0.3737	0.09613	0.00787	0.00101			
4.0	0.6200	0.3077	0.06490	0.00337	0.00029			
3.0	0.5217	0.2319	0.03568	0.00088	0.00004			
2.0	0.3960	0.1442	0.01223	0.00007				
1.5	0.3169	0.1003	0.00461	0.00001				
1.0	0.2204	0.04772	0.00077					
0.75	0.1634	0.02591	0.00014					
0.50	0.09938	0.00865	0.00001					
0.40	0.07212	0.00410						
0.30	0.04485	0.00127						
0.20	0.01973	0.00015						
0.15	0.00957	0.00002						
0.10	0.00263							

(From Reference 21)

Table 2-6

Comparison of Dependent and Independent Variables

Method	Dimensionless Independent Variable	Dimensionless Dependent Variable
Theis	$X = \frac{r^2 \phi \mu c}{4Kt}$	$E_i\ (-X)$
Mortada & V. E.-Hurst	$t_D = \frac{Kt}{\phi \mu c r_w^2}$	ΔP_D

(From Reference 22)

$t_D \geq 500$ (Maximum error of .01%)

$$P_D(1,t_D) \approx \left(\frac{1}{2}Lnt_D + .40454\right)\left(1+1/2t_D\right)+\frac{1}{4t_D} \quad . \qquad (2\text{-}43)$$

Mueller and Witherspoon(22) compared the variables used by Theis to those used by Mortada and Van Everdingen-Hurst (See Table 2-6). If the definition of dimensionless time in Equation (2-38) is based upon any radius in the infinite system, we then have

$$\bar{t}_D = \frac{Kt}{\phi\mu cr^2} \quad . \qquad (2\text{-}44)$$

The dimensionless time of Mortada (t_D) is related to that of Equation (2-44) by:

$$\bar{t}_D = \frac{t_D}{r_D^2} \quad . \qquad (2\text{-}45)$$

From Table 2-6 it can be seen that when (2-45) is compared to the Theis Equation (2-7) then:

$$\bar{t}_D = \frac{1}{4X} \quad , \qquad (2\text{-}46)$$

and:

$$\Delta P_D = \frac{E_i(-X)}{2} \quad . \qquad (2\text{-}47)$$

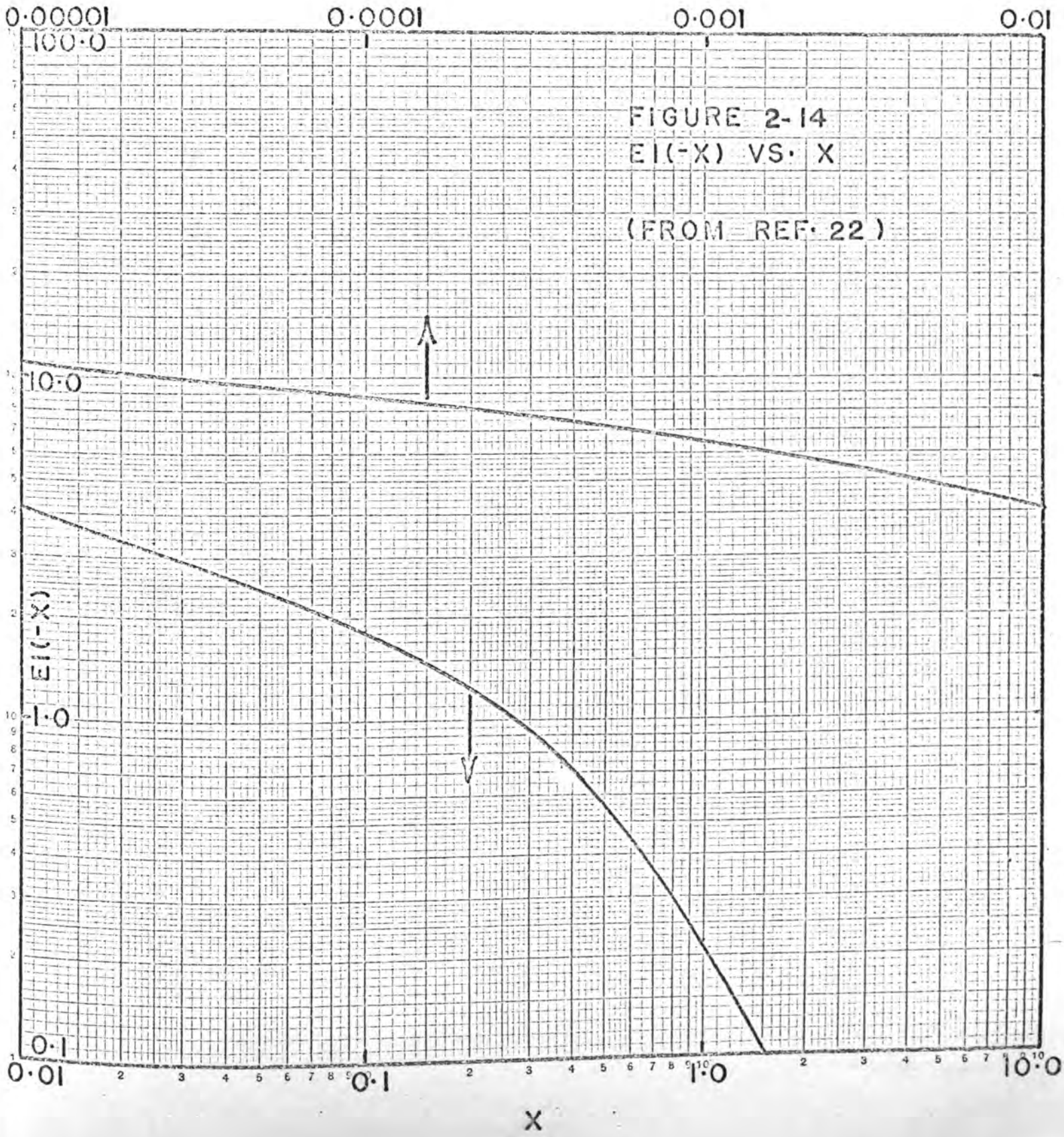

FIGURE 2-14
E1(-X) VS. X
(FROM REF. 22)

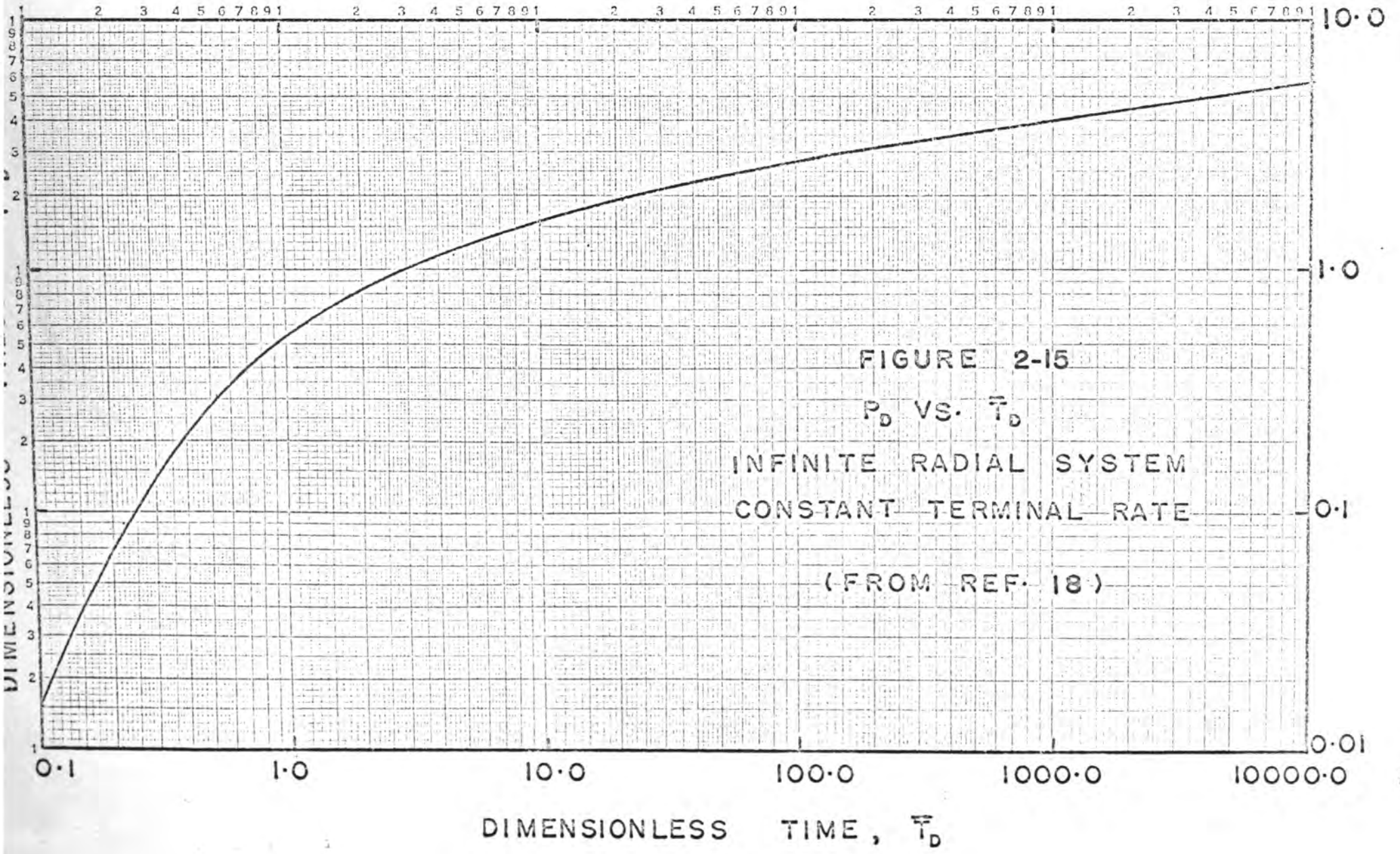

FIGURE 2-15

P_D VS. T_D

INFINITE RADIAL SYSTEM

CONSTANT TERMINAL RATE

(FROM REF. 18)

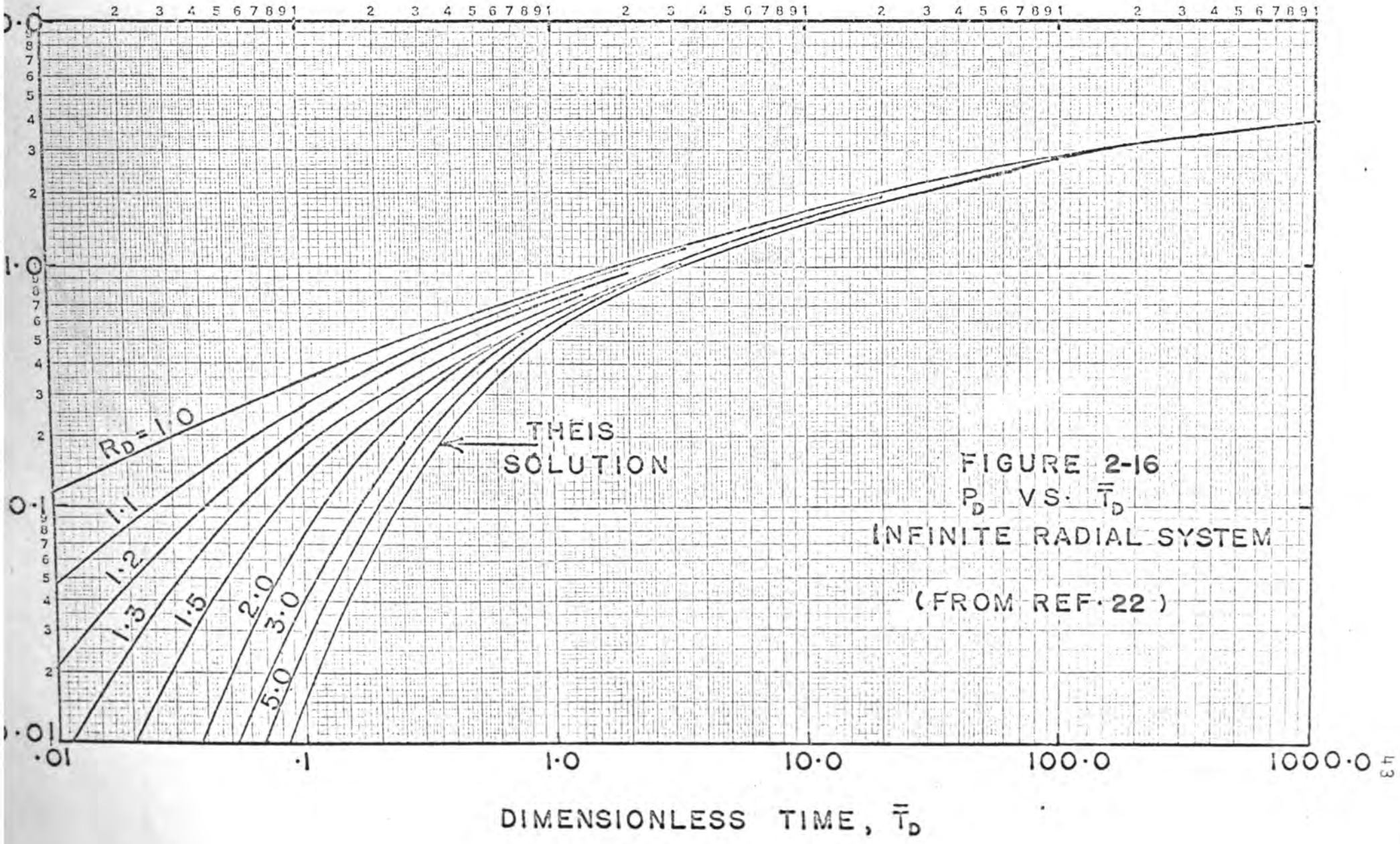

FIGURE 2-16
P_D VS. $\bar{T}_D$
INFINITE RADIAL SYSTEM
(FROM REF·22)

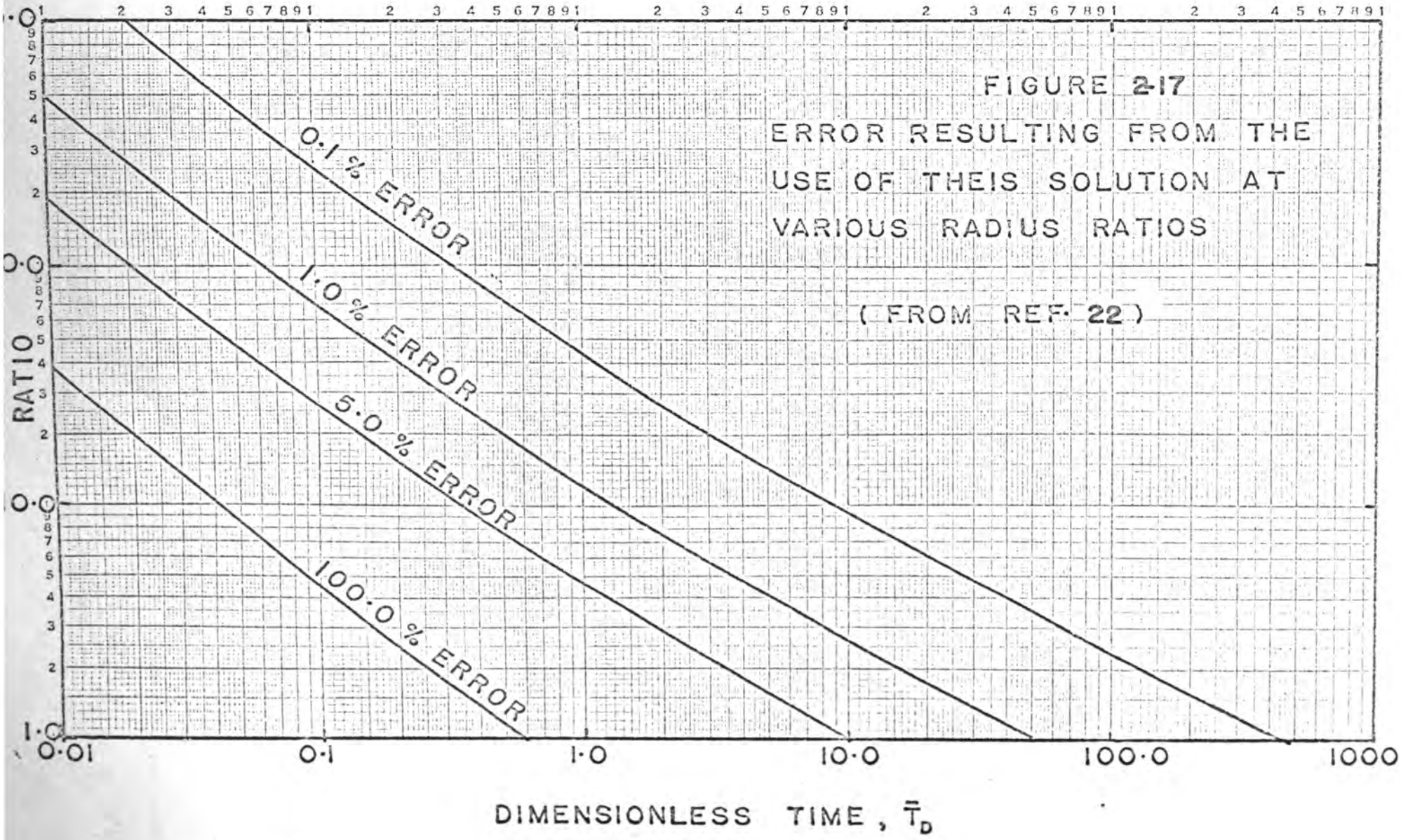

FIGURE 2-17
ERROR RESULTING FROM THE USE OF THEIS SOLUTION AT VARIOUS RADIUS RATIOS

(FROM REF. 22)

Mueller and Witherspoon adjusted the Theis results of Figure 2-14 and Figure 2-15 in accordance with the definitions of Equation (2-46) and Equation (2-47). They also modified Mortada's solutions of Figures 2-8, 2-9, and 2-10 by means of Equation (2-45). Their results were a family of curves shown in Figure 2-16 which converge on Theis' solution. Radius ratios not given in Mortada's work were taken from the results given by Mueller(23). Figure 2-16 shows that the Theis solution can be used for radius ratios greater than 20 for practical times ($t_D \geq .1$). Figure 2-17 shows the percent error that would result by using the Theis solution for various radius ratios instead of the Mortada solution.

2.3 Effective Radius of Drainage:

Aronofsky and Jenkins(24) presented the following expression for the effective drainage radius for a radial liquid system:

$$\text{Ln}\left(\frac{r_d}{r_w}\right) = \frac{2\pi Kh}{Q\mu}\left(P_0 - P_w\right) - 2T\left(\frac{r_w}{r_r}\right)^2 \qquad (2\text{-}48)$$

where:

$r_r >> r_w$

$T = Kt/\phi\mu\ \beta\ r_w^2$

r_d = effective radius of drainage, cm.

r_w = well radius, cm.

r_r = reservoir radius, cm.

β = liquid compressibility, atm^{-1}.

Q = production rate of the well, cc./sec.

K = permeability, darcies.

μ = viscosity, cps.

t = time, sec.

h = thickness of formation, cm.

P_0 = initial reservoir pressure, atm.

P_w = well pressure, atm.

ϕ = porosity, fraction.

Employing the common dimensionless pressure drop definition

$$P_{(T)} = \frac{2\pi Kh(P_0-P_w)}{Q\mu} \quad , \tag{2-49}$$

Equation (2-48) becomes

$$Ln(\frac{r_d}{r_w}) = P_{(T)} - 2T\ (\frac{r_w}{r_r})^2 \quad . \tag{2-50}$$

Since a value of the reservoir radius is required, Equation (2-50) is only applicable for finite radial reservoirs. When $(r_r/r_w)^2$ becomes much larger than unity, P(T) becomes:

$$P_{(T)} = \left[r_w/r_r\right]^2 + 2T\left[r_w/r_r\right]^2 - \frac{3}{4} + Ln\left[r_r/r_w\right] \tag{2-51}$$

and:

$$Ln\left[r_d/r_w\right] = Ln\left[r_r/r_w\right] - \frac{3}{4} \tag{2-52}$$

where $(r_w/r_r)^2$ is considered to be negligible. Then, since,

$$\text{Ln}(r_d/r_r) = -\frac{3}{4} \tag{2-53}$$

and;

$$(r_d/r_r) = e^{-\frac{3}{4}} = .472 \tag{2-54}$$

then;

$$r_d = 0.472\ r_r \quad . \tag{2-55}$$

This result gives the effective drainage radius for finite radial reservoirs under liquid flow conditions. The effective drainage radius thus stabilizes at about one-half (.472) the outer radius after only a small percentage of the liquid in place has been removed.

Figure 2-18 shows how the effective drainage radius, r_d, varies with time. This plot shows that, initially, r_d starts out near the wellbore and advances radially outward as flow continues. During this initial period r_d is independent of the outer boundary. During the later life of the reservoir r_d is independent of r_w but is dependent upon the outer radius, r_r, as can be seen in Figure 2-19, which also shows that the effective drainage radius builds up to .472 r_r.

Due to the apparent constancy of the pressure at various distances out in the reservoir, many authors have derived

Figure 2-18

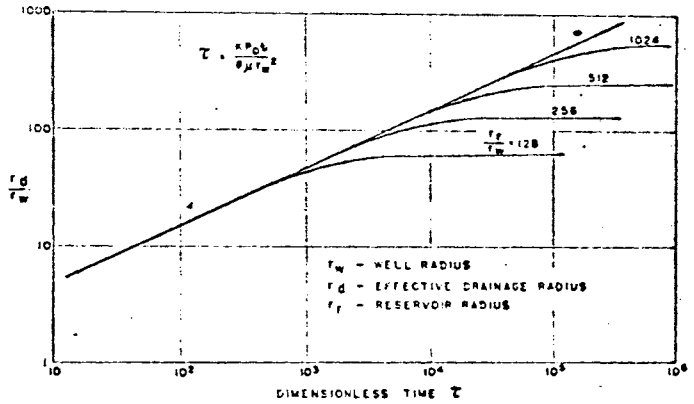

— Drainage Radius as a Function of Time.
(From Reference 24)

Figure 2-19

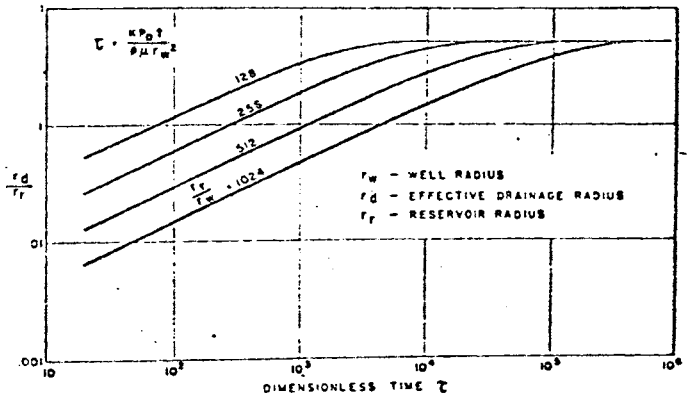

— Drainage Radius as a Function of Time.

(From Reference 24)

Table 2-7

Van Poolen's Summary of Various Radius-of-Drainage and Stabilization-time Equations

(Ref. 25)

Reference		(Ref. 26) P.E. Jones	(27) Tek, Grove, and Poettmann	(28) Muskat	(29) Browns-combe Kern M.D.H.	(14) Chatas radial	(30) Hutchinson Kern	(31) Hurst	(25) Present
Radius of drainage	c-g-s units	$4\sqrt{\frac{Kt}{\phi\mu c}}$	$4.29\sqrt{\frac{Kt}{\phi\mu c}}$	$2\sqrt{\frac{Kt}{\phi\mu c}}$	$1.784\sqrt{\frac{Kt}{\phi\mu c}}$	$2\sqrt{\frac{Kt}{\phi\mu c}}$	$1.5\sqrt{\frac{Kt}{\phi\mu c}}$	$2.6408\sqrt{\frac{Kt}{\phi\mu c}}$	$2\sqrt{\frac{Kt}{\phi\mu c}}$
	Field units	$\sqrt{\frac{Kt}{10\phi\mu c}}$	$\sqrt{\frac{Kt}{9\phi\mu c}}$	$\sqrt{\frac{Kt}{40\phi\mu c}}$	$\sqrt{\frac{Kt}{50\phi\mu c}}$	$\sqrt{\frac{Kt}{40\phi\mu c}}$	$\sqrt{\frac{Kt}{70\phi\mu c}}$	$\sqrt{\frac{Kt}{22.5\phi\mu c}}$	$\sqrt{\frac{Kt}{39.2\phi\mu c}}$
Stabilization time	c-g-s units	$\frac{\phi\mu cr^2}{16K}$	$\frac{\phi\mu cr^2}{18.45K}$	$\frac{\phi\mu cr^2}{4K}$	$\frac{\phi\mu cr^2}{3.18K}$	$\frac{\phi\mu cr^2}{4K}$	$\frac{\phi\mu cr^2}{2.25K}$	$\frac{\phi\mu cr^2}{6.97K}$	$\frac{\phi\mu cr^2}{4K}$
	Field units	$\frac{10\phi\mu cr^2}{K}$	$\frac{9\phi\mu cr^2}{K}$	$\frac{40\phi\mu cr^2}{K}$	$\frac{50\phi\mu cr^2}{K}$	$\frac{40\phi\mu cr^2}{K}$	$\frac{70\phi\mu cr^2}{K}$	$\frac{22.5\phi\mu cr^2}{K}$	$\frac{39.2\phi\mu cr^2}{K}$

expressions for the "radius of drainage". This drainage radius is usually defined as that distance beyond which the pressure change is only 1% of the change in pressure in effect at the wellbore. Some authors, however, have described this radius as that point across which only 1% of the flow occurs when 100% flow is being experienced at the wellbore.

Van Poolen(25) summarized the works of such authors as Jones(26), Tek(27), Muskat(28), Brownscombe and Kern(29), Chatas(14), Hutchinson and Kern(30), and Hurst, Haynie, and Walker(31). Van Poolen's summary table for the various radius of drainage equations developed by each of the above authors is given in Table 2-7. None of these equations, however, is derived for the effective drainage radius of an infinite radial reservoir subject to constant terminal rate conditions.

Nute(32) summarized the literature concerning pressure distribution in reservoirs and aquifers and pointed out the differences between the methods commonly used by hydrologists and those employed by petroleum engineers. It was also pointed out that the point-source or exponential integral solution of Theis and Horner was not sufficiently accurate for the ranges of dimensionless time normally used in aquifer studies, and that the Van Everdingen-Hurst approach must be used.

As a result of the above study, it was recommended that:

1. A method be developed which would permit the aquifer pressure to be calculated at various points in an infinite radial aquifer for different pumping rates and various pumping times. It was suggested that

this be accomplished by using a digital computer to solve the Van Everdingen-Hurst constant terminal rate solution to the diffusivity equation.

2. An equation be developed which would accurately predict the radius of drainage (the radius at which the pressure drop surrounding a well or reservoir could be considered to be negligible). This then would be an effective radius of drainage for the infinite radial system.

CHAPTER 3

GENERAL FORMULATION

3.1 Method of Formulation

When this investigation into the transient pressure distribution in aquifers surrounding oil fields was commenced it was decided that a numerical evaluation of the Van Everdingen and Hurst explicit constant terminal rate solution to the radial diffusivity equation (Equation 2-17) would be attempted rather than a finite difference solution as performed by Mortada(16). The main reasons for choosing to solve this problem by the more difficult numerical evaluation were:

1. By obtaining PD(1,TD) values by numerical evaluation of the Van Everdingen-Hurst equation, the table presented by Chatas could be checked.

2. The values of PD(RD,TD) obtained by numerical evaluation of Equation 2-17 could be checked against the finite-difference results presented by Mortada in Figures 2-8 through 2-10.

3. Computer time was not considered a factor in influencing the choice of type of solution to be attempted in this study.

4. The numerical evaluation of the explicit constant rate equation of Van Everdingen-Hurst was preferred since some doubt had been expressed in the past that useable PD(RD,TD) values could be obtained by this type of an approach due to oscillation.

3.2 Mathematical Considerations

No attempt was made in this study to derive any new equations for unsteady-state pressure distribution in infinite radial systems. Sufficient analytical solutions to the radial

diffusivity equation subject to a constant producing rate are already available in the literature (9) (11) (13). Although the necessary equations have been present in both the heat transfer and the petroleum literature for many years, very few numerical results for PD(RD,TD) have been presented for dimensionless radius ratios other than RD = 1.0. Mortada(16) presented some graphical results for PD(RD,TD) but the accuracy of these results is limited by the scale of his graphs (See Figures 2-8 to 2-10). Also, Mortada only published PD(RD,TD) curves for seven RD ratios and interpolation between these seven curves is difficult and inaccurate.

The availability of numerical values for PD(RD,TD) is limited partially because of the widespread use of the Theis or Exponential Integral solution to the radial diffusivity equation rather than the more accurate finite wellbore solution(9). The exponential integral solution has been used mainly because it is easy to solve and because numerical results are available(3), (4). For most well problems encountered by hydrologists and petroleum engineers, the exponential integral solution is sufficiently accurate; but for aquifer studies, Mueller and Witherspoon showed that the error introduced by using the exponential integral was considerable (See Figure 2-17).

It was further recognized that Buxton(19) attempted a numerical solution to the explicit Van Everdingen-Hurst equation (Equation 2-17) but was only partially successful in obtaining accurate PD(RD,TD) values. The oscillation of

the function being integrated (See Equation 2-17) limited the use of his Simpson's Rule technique to RD values less than 10 and dimensionless times below 50.

The Van Everdingen-Hurst equation for unsteady-state dimensionless pressure distribution is:

$$PD(RD,TD)=\frac{2}{\pi}\int_0^{\infty}\frac{\left[1-e^{-X^2TD}\right]\left[J_1(X)Y_0(X,RD)-Y_1(X)J_0(X,RD)\right]dX}{X^2\left[J_1^{\,2}(X)+Y_1^{\,2}(X)\right]} \quad . \qquad (3\text{-}1)$$

The main problem in obtaining numerical results for PD(RD,TD) is the oscillation of the complex function being integrated in Equation (3-1) and the lack of rapid convergence of this function for values of X close to zero. Also, the requirement of using a large upper limit of integration makes impractical the small panel size needed for accuracy.

The TD range over which Equation (3-1) must be integrated can be reduced by employing the simplifications for large and small dimensionless times presented by Carslaw and Jaeger(8). For $TD \leq .01$, Equation (3-1) reduces to:

$$PD(RD,TD)=\frac{2\sqrt{TD}}{\sqrt{RD}}\,\text{ierfc}\,\frac{RD-1}{2\sqrt{TD}}-\frac{(3RD+1)\sqrt{TD}}{4TD}\,i^2\text{erfc}\,\frac{RD-1}{2\sqrt{TD}} \quad . \qquad (3\text{-}2)$$

Equation (3-2) is similar to that used by Mortada except that an extra term has been added to improve the accuracy of the PD(RD,TD) values at small dimensionless times. For complete development of Equation (3-2) see Appendix B, page 224.

When TD exceeds 500, Carslaw and Jaeger showed that Equation (3-3) could be used to accurately predict PD(RD,TD). It's full development is also given in Appendix B, page 227.

$$PD(RD,TD) = \frac{1}{2}\left[\text{Ln}\ \frac{4Kt}{\phi\mu cr^2} - \gamma\right] . \qquad (3\text{-}3)$$

Equation (3-3) is identical to Mortada's expression for large TD, and is also an excellent approximation to the exponential integral solution of Lord Kelvin, Theis, and Horner (See Appendix B, page 229). Thus:

$$PD(RD,TD) = \frac{1}{2}\left[-E_i\ (-\frac{R_D^2}{4TD})\right] , \qquad (3\text{-}4)$$

where:

$$-E_i(\frac{RD^2}{4TD}) = \int_{\frac{RD^2}{4TD}}^{\infty} \frac{e^{-X}}{X}\, dX . \qquad (3\text{-}5)$$

The assumption of equivalance of Equations (3-3) and (3-4) at large TD values is discussed in detail in Appendix B, page 229. Equation (3-3) can be used provided

$$\frac{4TD}{RD^2} \geq 2000 . \qquad (3\text{-}6)$$

This provision is satisfied for RD = 1.0 when TD$\geq$500. Therefore for RD = 1, Equation (3-3) can be used to express the dimensionless pressure at any dimensionless time.

For this study, however, RD ratios other than 1.0 were required and therefore Equation (3-4) was preferred to Equation (3-3). If RD = 10, for example, applying Equation (3-5) leads to a TD value of at least 50,000. At RD = 10, Equation (3-3) would not be very accurate since TD = 500 was used as the lower limit of the exponential integral simplification in this study.

The following definitions of the dimensionless quantities TD, PD and RD were used in this investigation:

$$TD = Kt/\phi\mu c r_b^2 \quad , \tag{3-7}$$

$$PD = \frac{2\pi KH(p_i - p)}{q\mu} \quad , \tag{3-8}$$

and,

$$RD = r/r_b \quad . \tag{3-9}$$

For aquifer studies it is of interest to be able to define the dimensionless pressure at any RD and TD in terms of the dimensionless pressure PD(1,TD) at the inner boundary of the aquifer (RD = 1.0) at the same TD. For this reason, a new dimensionless quantity, PD', was developed in this study. PD' is defined as a fractional dimensionless pressure,

$$PD' = \frac{PD(RD,TD)}{PD(1,TD)} \quad . \tag{3-10}$$

And, from Equation (3-7):

$$PD' = \frac{2\pi KHP(r,t)/q\mu}{2\pi KHP(1,t)/q\mu} \quad , \tag{3-11}$$

so that

$$PD' = P(r,t)/P(1,t) \quad . \tag{3-12}$$

From Equation (3-12), it can be seen that PD' is also a fractional pressure change since it is a ratio of the pressure change existing at a radius r away from the inner boundary to the pressure existing at RD = 1.0 at the same instant of time.

When PD(RD,TD) is defined in terms of pressure-drop in the aquifer rather than pressure change, then:

$$PD(RD,TD) = \frac{2\pi KH(p_i-p)}{q\mu} \quad , \tag{3-13}$$

and:

$$PD(1,TD) = \frac{2\pi KH(p_i-p_b)}{q\mu} \quad , \tag{3-14}$$

thus:

$$PD' = (p_i-p)(p_i-p_b) \tag{3-15}$$

where:

p_i = the initial aquifer pressure

p_b = the pressure at the inner boundary.

Equation (3-15) shows that PD' is actually a fractional pressure-drop or the ratio of the pressure-drop (p_i-p) experienced at any radius r to the pressure-drop (p_i-p_b) occurring at the same TD at the inner boundary (RD = 1.0).

For the purpose of locating an effective radius of drainage for an infinite radial aquifer subject to a constant rate of production from its inner boundary, PD' can be assumed to be equal to .01. This assumption would indicate that at a radius r away from the inner boundary, the pressure change is 1% of the change occurring at the inner boundary.

3.3 The Problem of Oscillation

Buxton(19) found that Simpson's Rule could be used to integrate the function given in Equation (3-1) only for RD ratios from 1 to 10 and for TD values up to 50. For RD values greater than 10 oscillation of the function being integrated became severe and prohibited the continued application of Simpson's Rule. For TD values greater than 50, the function failed to converge rapidly at the origin.

Figures 3-1 to 3-5 show the variation of the function F(X) with the argument X for several TD and RD values. The function F(X) is given by:

$$F(X) = \frac{\left[1-e^{-X^2TD}\right]\left[J_1(X)Y_0(X,RD)-Y_1(X)J_0(X,RD)\right]}{X^2\left[J_1^2(X)+Y_1^2(X)\right]} \quad . \qquad (3\text{-}16)$$

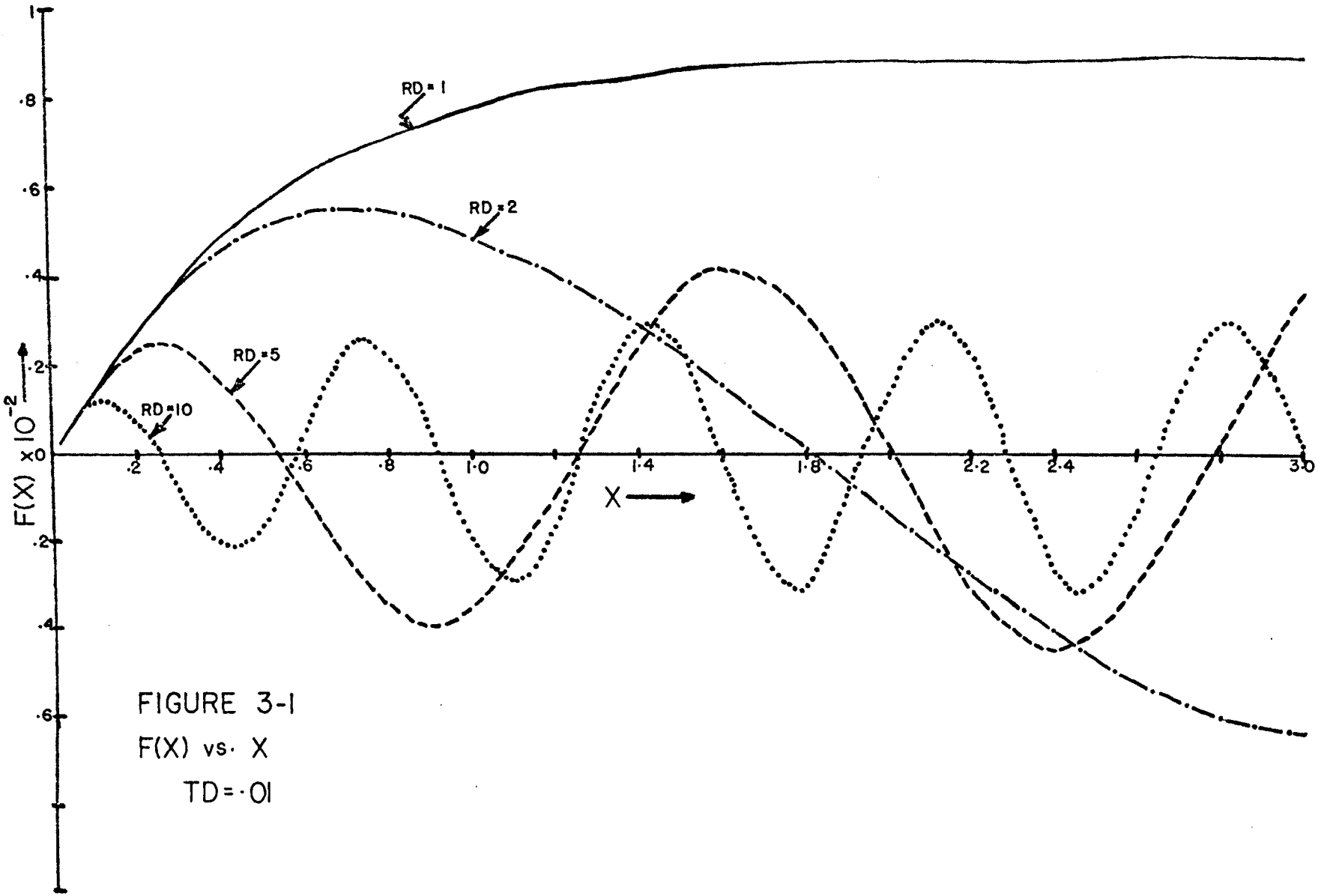

FIGURE 3-1
F(X) vs. X
TD = .01

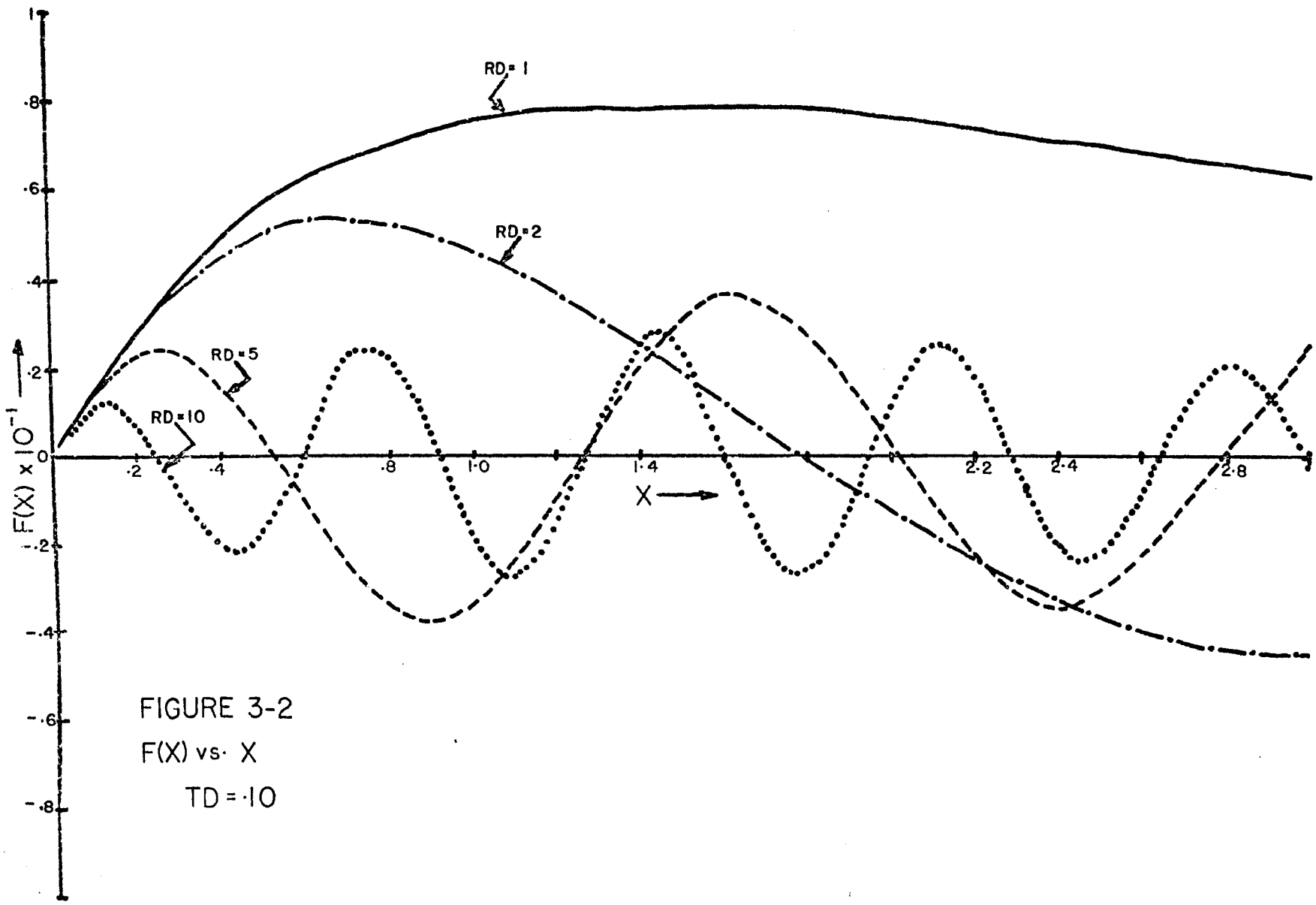

FIGURE 3-2

F(X) vs. X

TD = .10

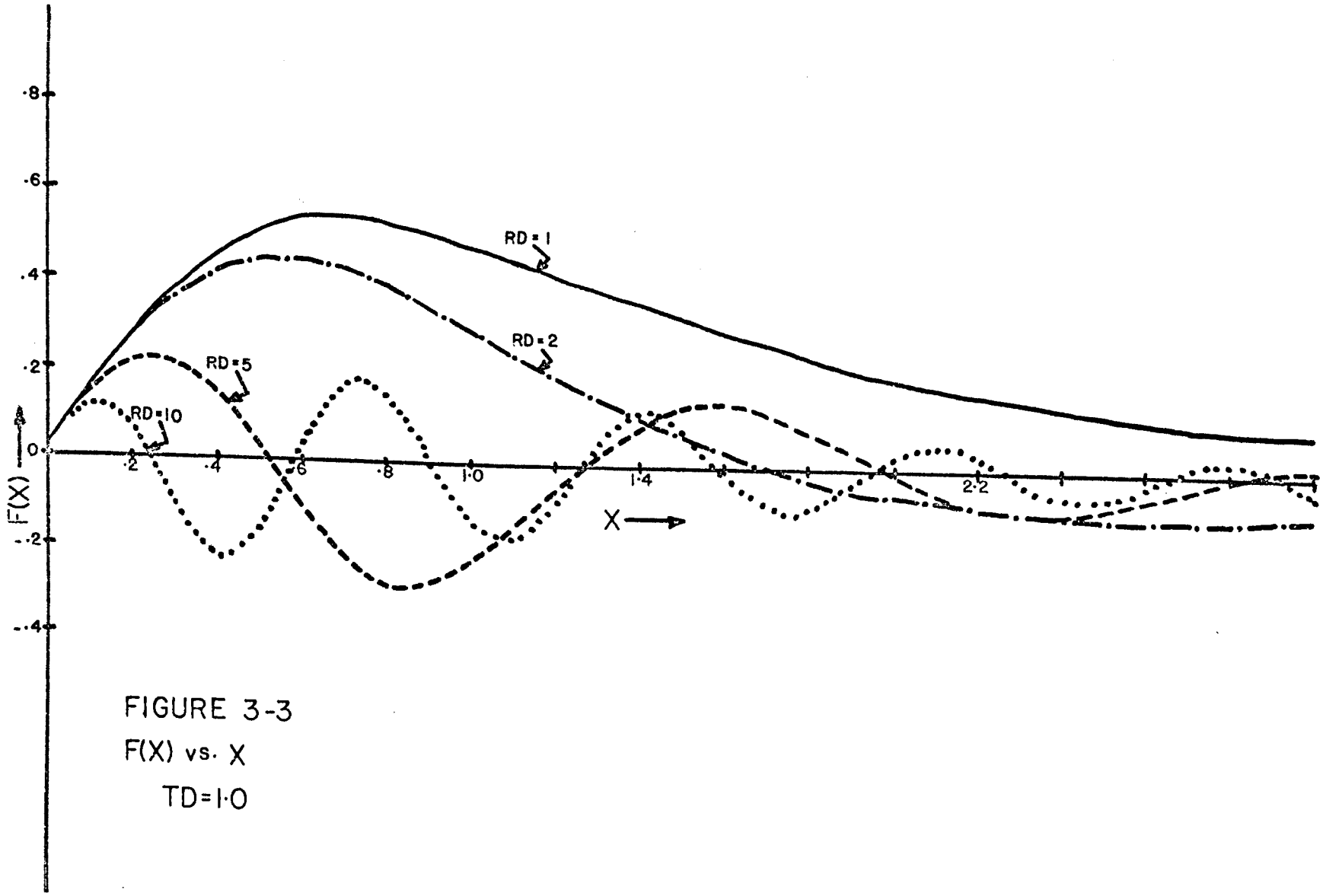

FIGURE 3-3
F(X) vs. X
TD=1·0

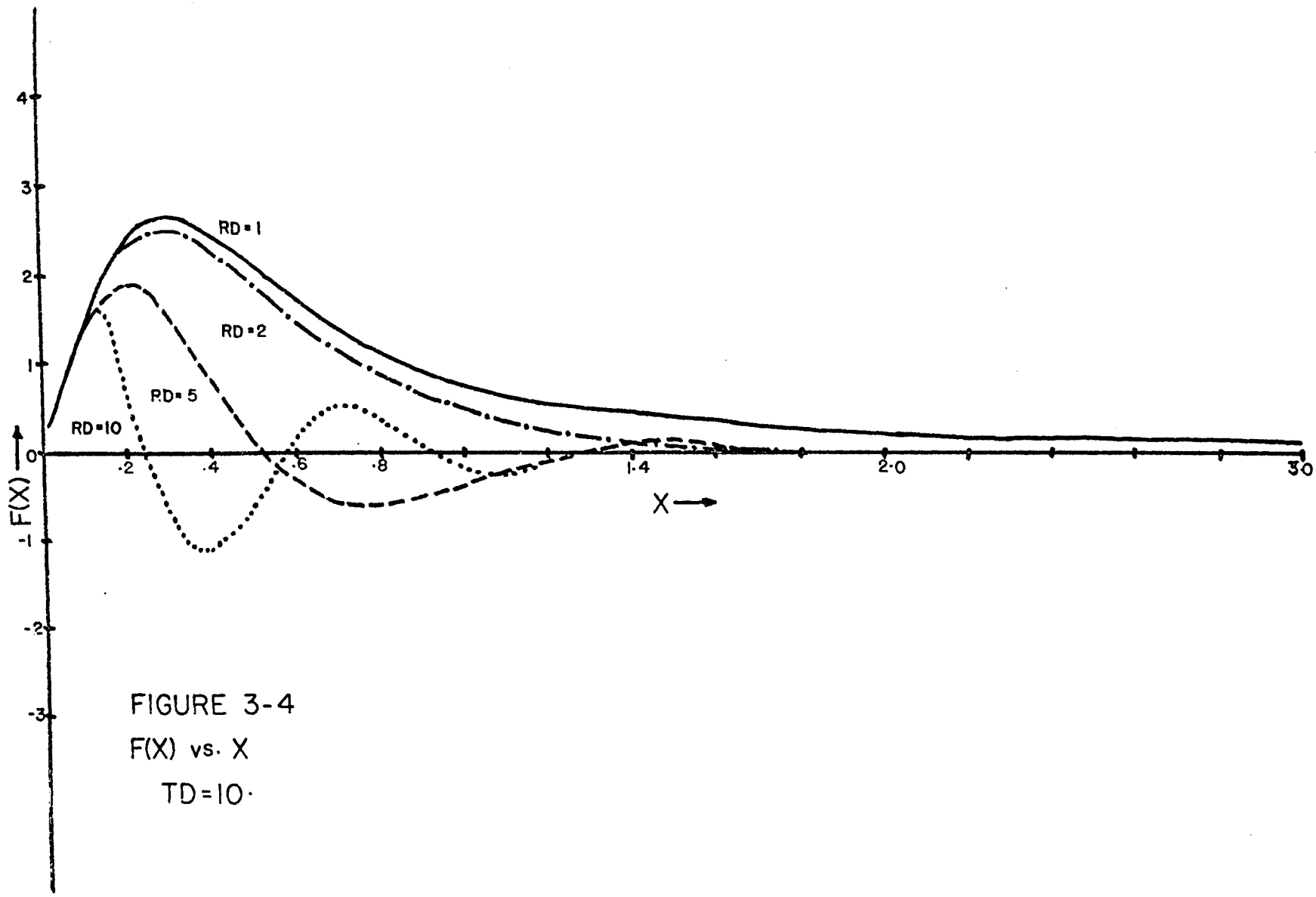

FIGURE 3-4
F(X) vs. X
TD=10.

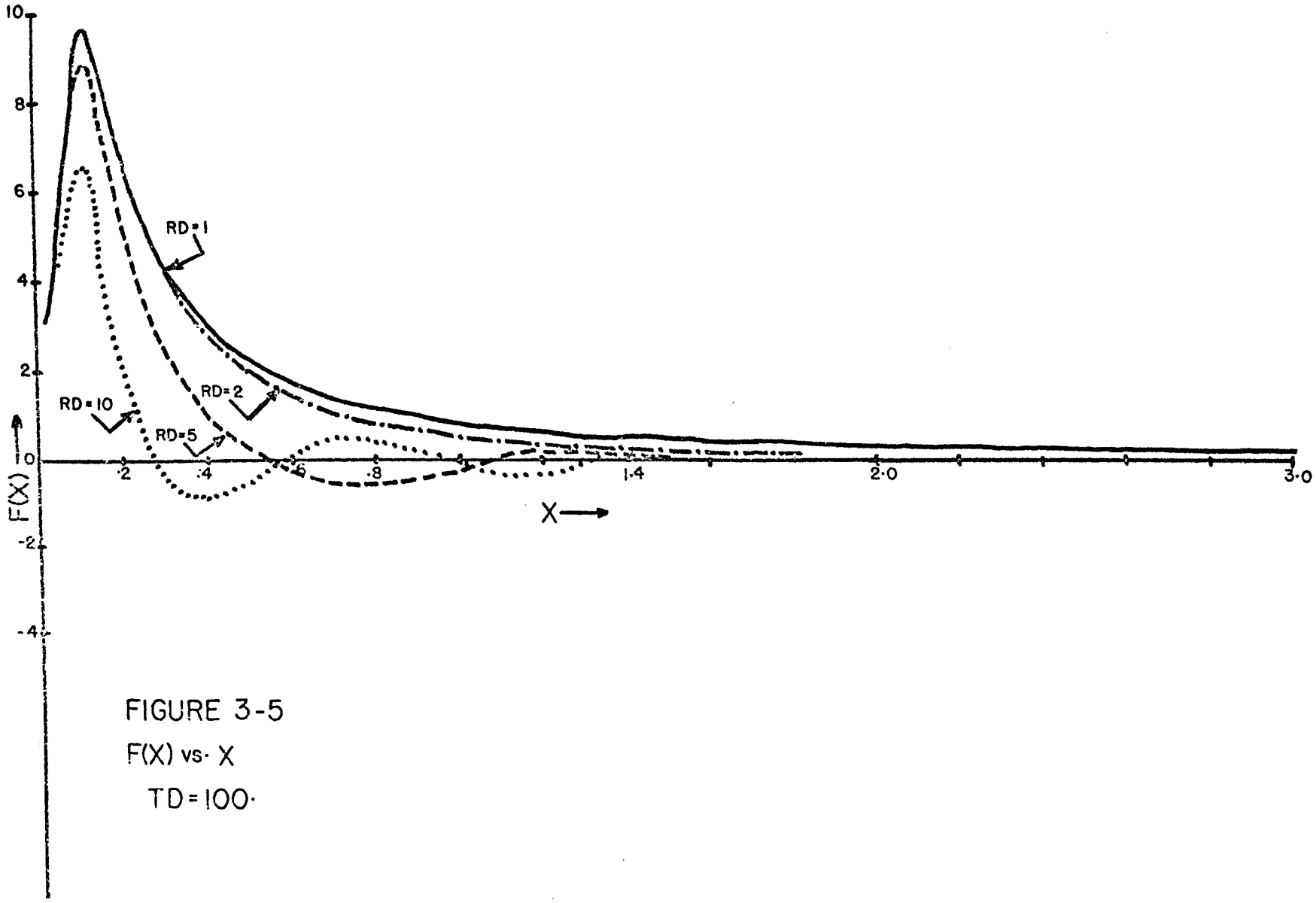

FIGURE 3-5

F(X) vs. X

TD = 100.

Figure 3-3, however, shows that for RD = 1.0, integration by numerical techniques should not be difficult as no oscillation of F(X) occurs regardless of the X value selected. As RD increases, however, oscillation becomes serious. At RD = 10, F(X) has changed sign nine times by the time X has reached 3.0. In addition to oscillating, F(X) also dampens out with increased X values. Because of this damping effect, the largest part of the area under the F(X) curve is obtained at small X values and any integration technique used must be accurate in this region. As X increases the value of F(X) rapidly decreases and by the time X>15.0, F(X) has become very small. Buxton pointed out that at X = 1000, F(X) was less than .00001.

Even though F(X) becomes small, any integration from zero to infinity must have an approximatingly large upper limit since even an F(X) value of .001 when extended over a long X distance will cause the value of the integral to change appreciably.

Figure 3-5 points out the problem of lack of rapid convergence of the function near the X origin. As can be seen for TD = 100 and RD = 10, F(X) is equal to 3.1 when X = .02. When F(X) is taken as zero at X = 0 and a straight line is assumed to connect F(0) to F(.02) then the area under the curve can be seriously miscalculated. Because of the rapid damping of the function, this error in area estimation can become a large part of the total area under the F(X) curve.

In general, the value of F(X) decreases with increasing X, with increasing RD ratios, and increases with increasing TD values. Oscillation increases with increasing RD ratios, with increasing X values, and with increasing TD values.

By the time TD = 100, as seen in Figure 3-5, the F(X) curve for small RD ratios has assumed a shape which can be approximated by the exponential integral function. This points out the reason for the simplification of Equation 3-1 at large TD values.

From Figures 3-1 to 3-5 it can be seen that even though at RD = 10 the oscillation is severe the oscillation is still equivalent. Equivalent oscillation refers to the fact that the area under a negative section of the F(X) curve is approximately equivalent to the area under the positive section immediately following. Because of this equivalence of areas the effect of oscillation is not actually as important as Buxton assumed. This is because the area added to the value of the integral is quite small once the severe oscillation starts since by this time the value of F(X) itself is also small. Therefore, any error caused by oscillation affecting the integration technique is significantly offset by the approximate cancellation of the areas above and below the X axis.

3.4 Variable Transformation

After the integration of the F(X) function (Equation 3-16) by a modified Trapezoidal Rule (discussed in Section

3.5) it was evident that the values of PD(1,TD) were beginning to deviate somewhat from those presented by Chatas at TD values above 25. Since the lack of rapid convergence near the origin seemed to be the cause of this deviation, a transformation of limits was developed which caused the values of $FT(\bar{X})$ (the transformed F(X) function) near the origin to become very small. $FT(\bar{X})$ is defined by Equation 3-20 where only the definition of X has been changed in the transformed case. In this way the error introduced by the step from X = 0 to the X location of the first evaluation of Equation (3-16) would be reduced in relative importance since the area added would be a very small fraction of the total area under the curve being integrated.

By the use of this transformation, it was possible to maintain a small panel size and at the same time obtain a very large upper limit for the integral of Equation (3-16).

The transformation was accomplished by setting:

$$u = \frac{\bar{X}}{1-\bar{X}} \quad . \tag{3-17}$$

u is equivalent to X in Equation (3-16) and the $\bar{X}$ of Equation (3-17) is a number such that: $0 \leq \bar{X} < 1$. This change of X definition is required to be consistent with the computer programs which use X as the variable of integration for both the untransformed and the transformed functions. Thus:

$$u^2 = \bar{X}^2/(1-\bar{X})^2 \tag{3-18}$$

and:

$$du = d\bar{X}/(1-\bar{X})^2 \quad . \tag{3-19}$$

Substituting these relationships into Equation (3-1) results in the following equation:

$$PD(RD,TD) = \frac{2}{\pi} \int_0^1 \frac{\left[1-e^{-u^2 TD}\right]\left[J_1(u)Y_0(u,RD)-Y_1(u)J_0(u,RD)\right]}{\bar{X}^2\left[J_1^2(u)+Y_1^2(u)\right]}\, d\bar{X} \tag{3-20}$$

The value of the function $FT(\bar{X})$ is shown in Figures 3-6 to 3-9. From these figures it can be seen that $FT(\bar{X})$ is very nearly zero at $\bar{X} = 0$ and the problem of rapid convergence near the origin is no longer a serious problem.

Although the oscillation seems more severe for large values of $\bar{X}$ in Figures 3-6 to 3-9 than in the untransformed F(X) plots (Figures 3-1 to 3-5), both functions do change sign in exactly the same manner and the transformation has simply squeezed the oscillations together and increased their amplitude.

Because of the decreased range of limits (from 0 to 1 rather than from 0 to ∞) it was possible to obtain a much smaller panel size and still maintain an upper limit of .999995 or approximately 200,000 in untransformed terms. This decreased panel size served to reduce the error caused by oscillation by causing more evaluations of $FT(\bar{X})$ to be

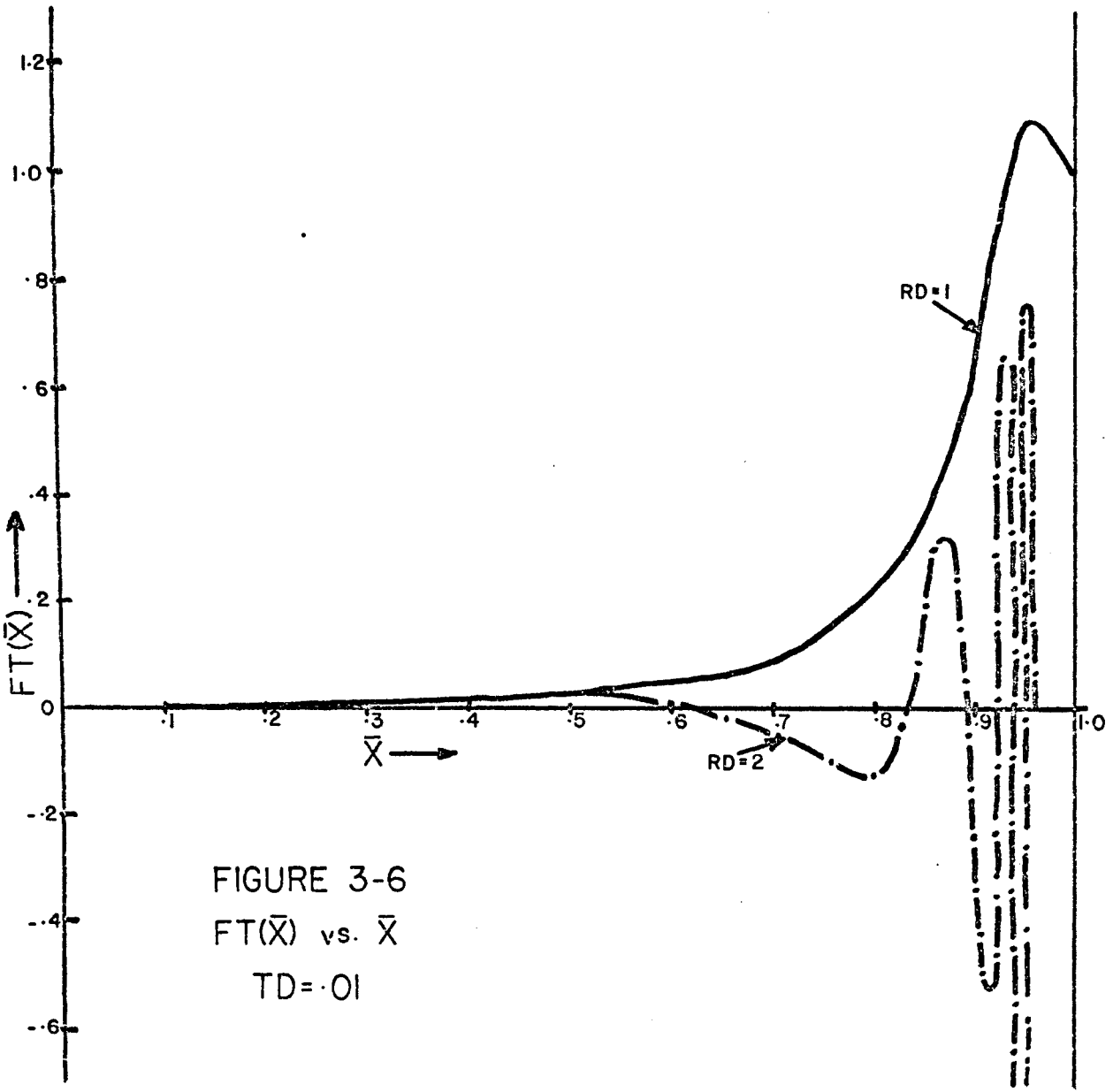

FIGURE 3-6
FT(X̄) vs. X̄
TD=·01

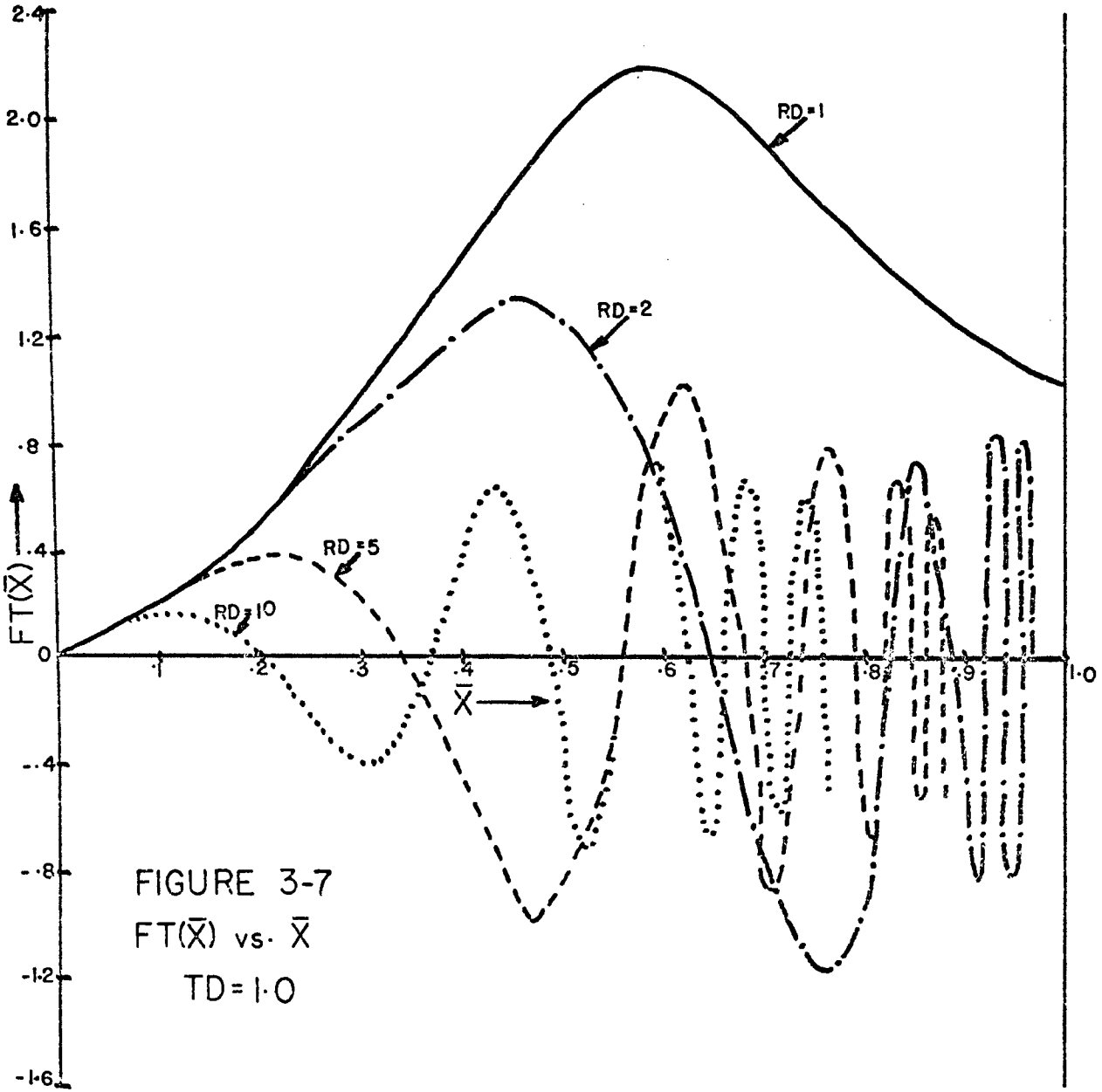

FIGURE 3-7
FT(X̄) vs. X̄
TD = 1·0

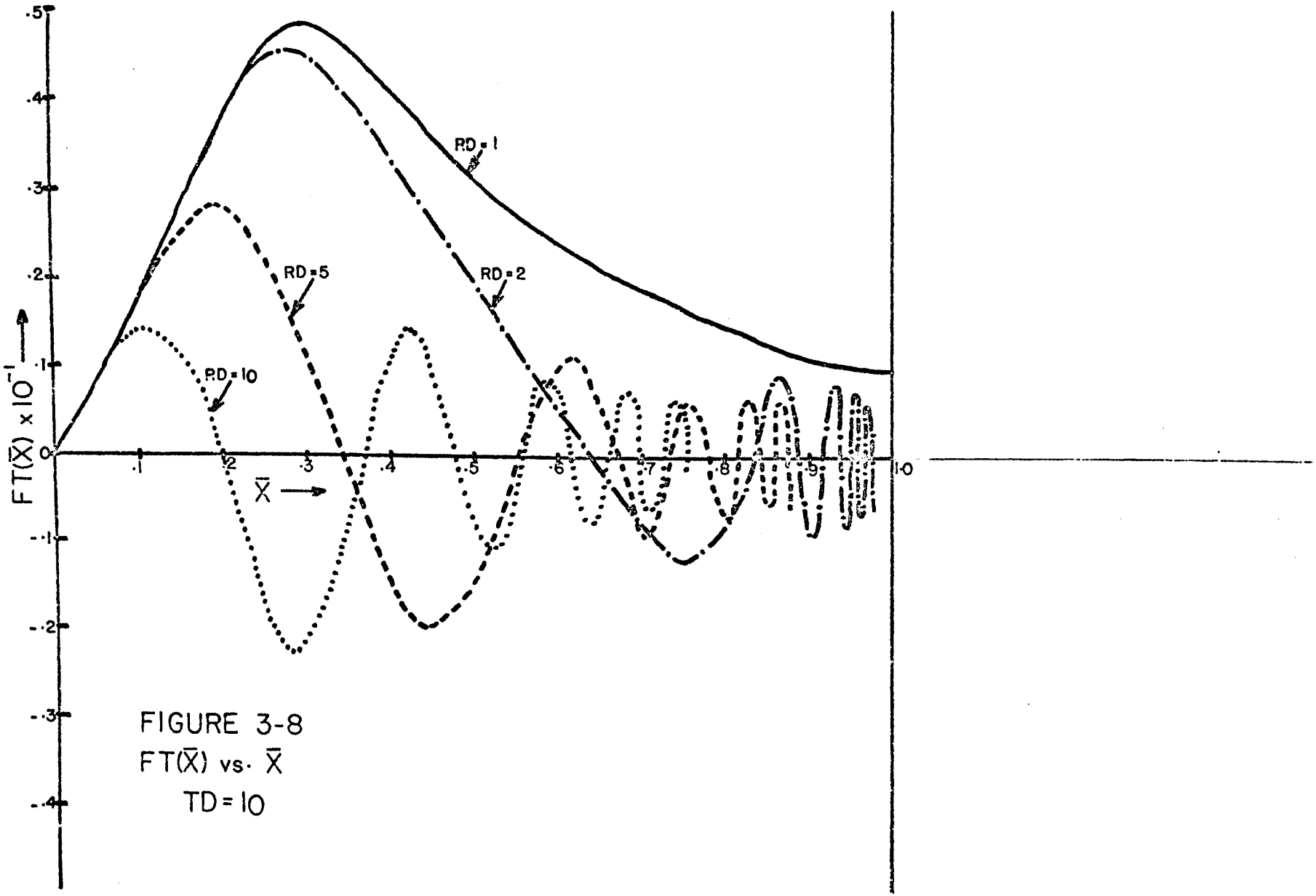

FIGURE 3-8
FT(X̄) vs. X̄
TD = 10

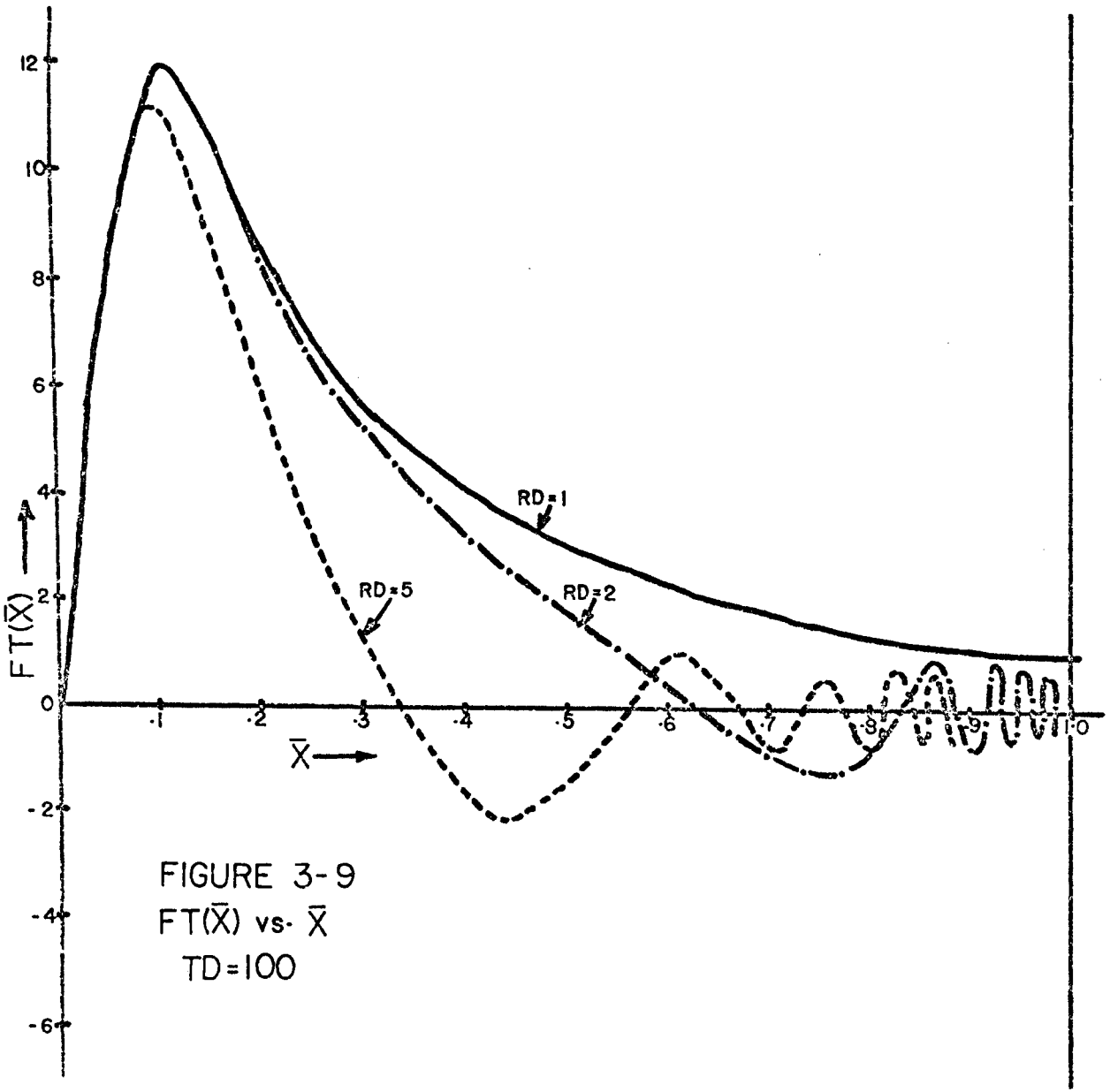

FIGURE 3-9
FT($\bar{X}$) vs. $\bar{X}$
TD=100

made before the sign changed than was possible before the transformation was made.

As can be seen from Figures 3-6 to 3-9, the area under any two successive oscillations is approximately the same once the severe oscillation begins and thus the value of the integral is not increased appreciably in this region. Integration error occurring in the region of high oscillation therefore does not seriously affect the accuracy of the PD(RD,TD) values obtained in this study except at TD values below 1.0.

Figure 3-6 indicates that for a TD value of .01 the area added in the region of high oscillation is a large part of the total area under the $FT(\bar{X})$ curve. This would indicate that any error in integration has a larger effect on the PD(RD,TD) values obtained than for large TD values (above 1.0). However, the error introduced for TD<1.0 does not seem to have a large effect on the value of PD(RD,TD) obtained. The untransformed function F(X) can be integrated quite accurately in the region below TD <1.0 since convergence for these low TD values is not a problem because of the low value of F(X) at small TD values. A comparison of RD ratios having a given fractional pressure PD' for the transformed and untransformed methods resulted in a difference in RD values of not more than 4.2%. This would seem to indicate that even for TD<1.0 the error introduced by the transformation is not unreasonably large.

3.5 Numerical Analysis Techniques

A. Program No. 2A - This program employs a modified Trapezoidal Rule to integrate the function F(X) of Equation (3-16). The integration of F(X) was accomplished without transformation of limits. The lower limit of integration was set at .02 and the upper limit was 2160. This technique is termed a modified Trapezoidal Rule because the area under the curve is obtained by forming a trapezoid with the panel size changing with increasing X. In order to be a true Trapezoidal Rule, the panel size would have to be the same throughout the range of integration. It was found necessary to impose a changing panel size to obtain a small panel size for small X values and still be able to have a larger panel size as X increased beyond 15.0. By using a changing panel size it was possible to have both a large upper limit and a small panel size in the region where it was required.

Figure 3-10 shows the principle employed in Program No. 2A.

Integration Technique Used in Program No. 2A

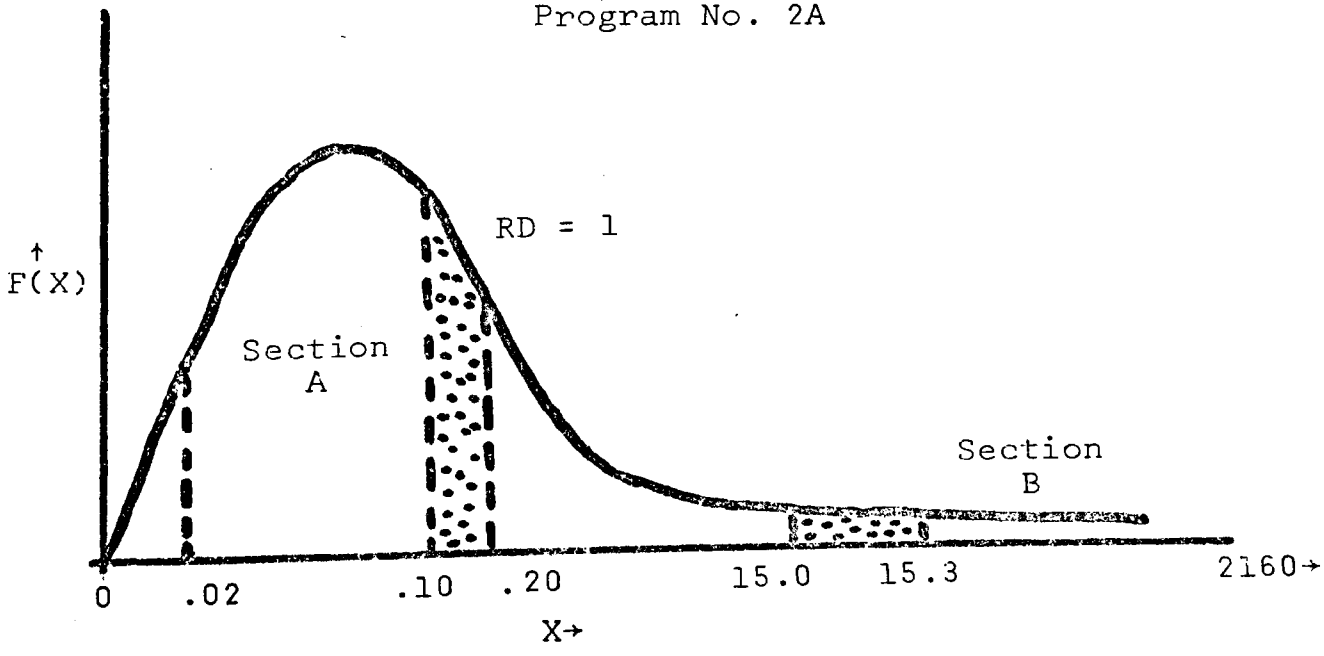

In Section A of Figure 3-10 a panel size of .10 was used. Starting at X = .02 and taking 150 of these panels resulted in Section B starting at 15.02. The panel size was then increased to .30 and 150 more panels were taken before changing to .50. The procedure of sectionally increasing panel size by .20 was repeated 12 times before an upper limit of approximately 2160 was reached.

As discussed in Section 3.4 and 3.5, the region X = 0 to X = .02 and the large panel size used (.10 or larger) caused the integration to become somewhat inaccurate at TD values above 25 and at large RD ratios. Program No. 2 was designed to improve upon this technique and to check the values of (RD - 1) obtained from Program No. 2A.

B. Program No. 2 - In this approach a Romberg integration was performed on the transformed function $FT(\bar{X})$ between the limits of 0 to 0.999995 with this upper limit being equivalent to an upper limit of 200,000 in Program No. 2A. The distance betwene 0 and .999995 was divided into $(2)^k$ equal panels. The value of k was allowed to increase from 1 to 10 and the function $FT(\bar{X})$ was integrated 10 times by the regular Trapezoidal Rule with the number of panels increasing from 2 to 1024.

The standard Trapezoidal Rule formula is given as:

$$T_N = H\left[\frac{FT_0}{2} + FT_1 + FT_2 + \ldots FT_{N-1} + \frac{FT_N}{2}\right] \qquad (3\text{-}21)$$

where:

$$h = \frac{b-a}{2^k} \quad (k=1,2,\ldots\ 10) \quad . \tag{3-22}$$

Double-precision evaluation of Equation (3-15) was impractical due to the excessively large computer time required for single-precision. The Romberg integration was preferred to either Simpson's Rule or the straight Trapezoidal Rule because it allowed the integration to be carried out with coarser intervals for which round-off error was less and maximum accuracy could be obtained. The effects of panel size and double-precision are discussed briefly in Section 3.6.

The Romberg integration operator used is

$$T_{2^k N}^{(m)} = \frac{4^k T_{2^k N}^{(m-1)} - T_{2^{k-1} N}^{(m-1)}}{4^k - 1} \tag{3-23}$$

where:

$$m = 0,1,2..\ 9$$

$$k = 1,2,\ldots\ 10$$

and,

$$N = \frac{b-a}{h} \quad . \tag{3-24}$$

Each successive entry in a column becomes more and more accurate since the error of Equation (3-23) is of the order:

$$\text{error} = 0(h^{2m+2}) \tag{3-25}$$

Table 3-1

SUCCESSIVE ROMBERG APPROXIMATIONS - $T_{2^k N}^{(m)}$

$2k$ \ m	0	1	2	3	4	5	6	7	8	9
2	$T_{2N}^{(0)}$									
4	$T_{4N}^{(0)}$	$T_{4N}^{(1)}$								
8	$T_{8N}^{(0)}$	$T_{8N}^{(1)}$	$T_{8N}^{(2)}$							
16	$T_{16N}^{(0)}$	$T_{16N}^{(1)}$	$T_{16N}^{(2)}$	$T_{16N}^{(3)}$						
32	$T_{32N}^{(0)}$	$T_{32N}^{(1)}$	$T_{32N}^{(2)}$	....	$T_{32N}^{(4)}$					
64	$T_{64N}^{(0)}$	$T_{64N}^{(1)}$	$T_{64N}^{(2)}$	....	....	$T_{64N}^{(5)}$				
128	$T_{128N}^{(0)}$	$T_{128N}^{(1)}$	$T_{128N}^{(2)}$	....	....	....	$T_{128N}^{(6)}$			
256	$T_{256N}^{(0)}$	$T_{256N}^{(1)}$	$T_{256N}^{(2)}$	....	....	....	.....	$T_{256N}^{(7)}$		
512	$T_{512N}^{(0)}$	$T_{512N}^{(1)}$	$T_{512N}^{(2)}$	....	....	....	.....	.....	$T_{512N}^{(8)}$	
1024	$T_{1024N}^{(0)}$	$T_{1024N}^{(1)}$	$T_{1024N}^{(2)}$	....	....	....	.....	.....	$T_{1024N}^{(8)}$	$T_{1024N}^{(9)}$

as (m = 0,1,2,...) and h→0.

Also, the agreement of successive entries in a row provides a good indication of the accuracy obtained.

For this study $T^{(9)}_{1024N}$ was taken as the value of the integral of $FT(\bar{X})$ from 0 to .999995 since this is the most accurate entry of all. The error introduced by this technique is discussed in Section 3.6.

3.6 Error Analysis

Each of the polynomial approximations employed in the analysis has error terms less than 10^{-7}; therefore, the error resulting from these approximations will be considered to be negligible as far as this analysis is concerned. These polynomial approximations were for the integrand functions of J_1, Y_o, Y_1, J_o, Erf(X), etc.

The error to be considered resulted from the numerical integration of $FT(\bar{X})$ by the Romberg technique.

There are two major parameters which must be optimized in order to accurately integrate Equation (3-17) by the Romberg technique. These are the upper limit of integration and the number of integration panels.

The selection of the upper limit of integration depends mainly upon the size of the argument (u,RD) which can be successfully evaluated by the computer routines such as SIN and COS. It was found that these routines would not operate when the argument (u,RD) was greater than 823,550. The use of the multiple angle expansions for the SIN(12X) and

the COS(12X) allowed arguments 12 times larger to be successfully evaluated and permitted an upper limit of .999995 to be used regardless of the TD-RD combination being integrated.

The use of transformed upper limits greater than .999995 resulted in changes in the PD(RD,TD) values in the sixth to seventh decimal place for all values compared. On the other hand, the use of .99995 as an upper limit caused the PD(RD,TD) values to differ in the fourth to fifth decimal place. As a result of these comparisons, .999995 was selected as the upper limit of integration best suited for all TD-RD combinations.

As previously mentioned, because of the increase in oscillation of $FT(\bar{X})$ as RD increases and the increase in magnitude of $FT(\bar{X})$ as TD increases, the optimum number of integration panels required to give a certain degree of accuracy also changes with TD and RD. In general, more panels are normally needed in order to achieve the same accuracy when the degree of oscillation increases. But, accuracy is also a function of the magnitude of $FT(\bar{X})$ for the TD being evaluated. If $FT(\bar{X})$ is large then a small error in the integration resulting from an insufficient number of panels can cause a fairly large change in the value of PD(RD,TD) calculated.

The amount of computer time required is also a factor in the selection of the number of integration panels to be used since the time increases with the number of panels. The following times were required to obtain the same PD(RD,TD) value with different numbers of panels:

No. of Panels	IBM 360/50 Computer Time
512	33 sec.
1024	42 sec.
2048	48 sec.

The main basis for choosing the number of integration panels was whether the value of the integral of $FT(\bar{X})$ failed to change significantly when the number of panels was doubled. It was found that in most cases the value of the regular trapezoidal integration of $FT(\bar{X})$ changed only in the third decimal place as the number of panels increased from 256 to 512 to 1024. This indicated that regardless of the oscillation of $FT(\bar{X})$, the trapezoidal integration with 1024 panels gave stabilized results. When the seventh, eighth, and ninth Romberg combinations of the ten trapezoidal answers were compared the results change beyond the sixth decimal place for all results.

It should be pointed out also that the use of 1024 integration panels between 0 and .999995 gave results for PD(1,TD) which are almost identical to those presented by Chatas. Because of this good reproduction of the accepted results and because of the relative stability of the answers obtained, 1024 panels were used for all TD-RD combinations being integrated.

In single-precision, 36 to 42 seconds of I.B.M. 360/50 computer time were required to obtain one PD(RD,TD) value when $.01<TD<500$. Double-precision computation required from 90 to 100 seconds of computer time to obtain the same PD(RD,TD) value. These times were based upon the ninth Romberg

combination being used as the value of the integral and 1024 panels being used for the integration between 0 and .999995 of Equation (3-17).

The slight variation in the time required when TD fell within the range requiring $FT(\bar{X})$ to be integrated by the Romberg technique resulted from the varying size of the argument (u,RD). Many different polynomial approximations were used to evaluate $FT(\bar{X})$ and the specific approximation selected depended upon the size of the argument (u,RD). Some of these approximations required a slightly longer period of time to be evaluated than did others.

Double-precision was performed to check the round-off error caused by the computer during the many repetitive calculations needed to obtain a PD(RD,TD) value. In all 12 spot-checks that were made for different combinations of TD and RD, the difference between the single-precision and the double-precision results was in at least the sixth decimal place or beyond. The results of these double-precision checks indicated that the PD(RD,TD) values presented in Tables 4-1 to 4-3 were accurate to at least the four decimal places shown in those tables.

Chapter 4

DISCUSSION OF RESULTS

4.1 Tabulated Values of PD(RD,TD)

Tables 4-1 to 4-3 give the numerical results obtained from this study for PD(RD,TD). These dimensionless pressure values were obtained from Program No. 1. PD(RD,TD) values have been presented for RD ratios from 1 to 64 and for TD values from .0005 to 1000. The results shown in Tables 4-1 to 4-3 have been given to four significant figures. If more accurate values of PD(RD,TD) are desired, the complete computer results are available in Appendix C, page 248. The RD ratios presented are sufficiently close together to allow accurate interpolation between columns. Interpolation is also possible between successive TD values in any column. Table 4-4 gives the results of 10 randomly selected interpolations between rows and 20 interpolations between columns. This table shows the error which would result from the use of interpolation from Tables 4-1 to 4-3 rather than the use of Program No. 1 to calculate PD(RD,TD). The average percent difference between the PD(RD,TD) values obtained by interpolation between RD columns in Table 4-1 and those produced by Program No. 1 was 6.40%. The maximum percent difference was 23.3%. Interpolation between TD values in the same RD column of Table 4-1 resulted in an average percent difference of 1.07% with a maximum of 2.97%. The interpolations mentioned above were made by selecting PD(RD,TD) values on either side of a particular PD(RD,TD) entry in Table 4-1. The difference

Table 4-1

FD(RD,TD) Values at Selected RD Ratios

for Various TD - Coast or Auto Cars

TD	RD = 1.0	RD = 1.1	RD = 1.2	RD = 1.3	RD = 1.4	RD = 1.5	RD = 1.6	RD = 1.7	RD = 1.8	RD = 1.9	RD = 2.0	RD = 2.5	RD = 3.0	RD = 3.5	RD = 4.0
.0005	.0050														
.0010	.0052	.0004													
.0020	.0402	.0029													
.0030	.0003	.0069	.0002												
.0040	.0394	.0111	.0007												
.0050	.0773	.0155	.0015	.0001											
.0060	.0844	.0200	.0025	.0002											
.0070	.0909	.0243	.0040	.0004											
.0080	.0969	.0286	.0055	.0007											
.0090	.1026	.0327	.0072	.0010	.0001										
.0100	.1078	.0368	.0089	.0015	.0002										
.0150	.1311	.0555	.0167	.0055	.0013										
.0200	.1503	.0719	.0271	.0105	.0031	.0002									
.0250	.1669	.0866	.0374	.0162	.0056	.0011	.0002								
.0300	.1817	.1000	.0474	.0224	.0088	.0025	.0007								
.0400	.2076	.1239	.0664	.0353	.0164	.0064	.0024								
.0500	.2300	.1456	.0839	.0483	.0250	.0114	.0051	.0005	.0001						
.0600	.2499	.1658	.1001	.0609	.0340	.0173	.0086	.0024	.0010	.0035					
.0700	.2680	.1811	.1153	.0732	.0432	.0237	.0127	.0048	.0024	.0042					
.0800	.2845	.1970	.1295	.0850	.0524	.0303	.0172	.0077	.0041	.0052					
.0900	.2999	.2118	.1429	.0964	.0615	.0371	.0220	.0109	.0061	.0064	.0029				
.1000	.3142	.2257	.1556	.1074	.0704	.0441	.0271	.0145	.0085	.0078	.0038				
.1500	.3751	.2852	.2109	.1566	.1125	.0785	.0541	.0249	.0233	.0182	.0107	.0016			
.2000	.4242	.3334	.2567	.1987	.1500	.1109	.0814	.0571	.0409	.0318	.0209	.0032	.0023		
.3000	.5024	.4106	.3310	.2686	.2142	.1688	.1324	.1011	.0782	.0627	.0461	.0099	.0034	.0011	
.4000	.5646	.4722	.3909	.3259	.2682	.2187	.1780	.1431	.1145	.0944	.0734	.0203	.0063	.0016	
.5000	.6168	.5240	.4416	.3749	.3149	.2627	.2189	.1797	.1486	.1251	.1006	.0331	.0108	.0029	
.6000	.6622	.5691	.4859	.4179	.3562	.3020	.2559	.2142	.1805	.1543	.1271	.0473	.0169	.0049	.0035
.7000	.7024	.6091	.5253	.4563	.3933	.3375	.2896	.2460	.2102	.1818	.1524	.0681	.0241	.0078	.0044
.8000	.7386	.6452	.5609	.4911	.4271	.3701	.3207	.2755	.2380	.2078	.1766	.0973	.0321	.0115	.0058
.9000	.7717	.6781	.5934	.5230	.4581	.4001	.3496	.3030	.2641	.2324	.1996	.0925	.0408	.0158	.0077
1.000	.8021	.7084	.6234	.5524	.4869	.4280	.3765	.3288	.2887	.2558	.2216	.1076	.0500	.0206	.0099
1.200	.8567	.7628	.6772	.6055	.5388	.4785	.4254	.3760	.3340	.2990	.2627	.1372	.0690	.0316	.0156
1.400	.9047	.8106	.7247	.6523	.5848	.5235	.4692	.4184	.3749	.3383	.3003	.1656	.0885	.0438	.0225
2.000	1.022	.9279	.8412	.7675	.6984	.6350	.5784	.5249	.4784	.4386	.3972	.2434	.1464	.0838	.0484
3.000	1.166	1.072	.9844	.9097	.8390	.7739	.7152	.6593	.6102	.5675	.5230	.3512	.2341	.1517	.0983
4.000	1.275	1.180	1.092	1.017	.9457	.8796	.8197	.7626	.7119	.6676	.6213	.4392	.3099	.2146	.1488
5.000	1.363	1.268	1.180	1.104	1.032	.9654	.9047	.8467	.7951	.7497	.7023	.5134	.3759	.2717	.1967
6.000	1.436	1.341	1.253	1.177	1.105	1.038	.9765	.9179	.8667	.8195	.7713	.5775	.4341	.3233	.2415
7.000	1.500	1.405	1.316	1.240	1.168	1.100	1.039	.9797	.9269	.8802	.8314	.6340	.4862	.3703	.2831
8.000	1.556	1.461	1.372	1.296	1.223	1.156	1.094	1.034	.9812	.9341	.8848	.6846	.5332	.4134	.3218
9.000	1.606	1.511	1.422	1.346	1.273	1.205	1.143	1.083	1.030	.9834	.9328	.7303	.5761	.4530	.3579
10.00	1.651	1.556	1.468	1.391	1.318	1.250	1.188	1.128	1.074	1.026	.9763	.7720	.6155	.4897	.3916
15.00	1.829	1.734	1.646	1.569	1.496	1.427	1.364	1.303	1.246	1.200	1.150	.9393	.7754	.6409	.5332
20.00	1.960	1.864	1.776	1.699	1.625	1.556	1.493	1.432	1.377	1.328	1.277	1.064	.8957	.7565	.6434
30.00	2.147	2.052	1.963	1.886	1.812	1.743	1.679	1.618	1.563	1.513	1.461	1.245	1.073	.9287	.8098
40.00	2.282	2.187	2.098	2.021	1.947	1.878	1.814	1.753	1.697	1.647	1.595	1.377	1.203	1.056	.9342
50.00	2.388	2.293	2.204	2.127	2.053	1.984	1.920	1.858	1.803	1.753	1.700	1.481	1.306	1.157	1.034
60.00	2.476	2.381	2.292	2.214	2.140	2.071	2.007	2.019	1.964	1.913	1.861	1.641	1.464	1.313	1.187
70.00	2.550	2.456	2.366	2.289	2.214	2.145	2.081	2.084	2.028	1.978	1.925	1.705	1.527	1.376	1.249
80.00	2.614	2.520	2.430	2.353	2.279	2.210	2.146	2.141	2.085	2.035	1.982	1.761	1.583	1.432	1.304
90.00	2.671	2.576	2.488	2.410	2.336	2.267	2.203	2.192	2.136	2.086	2.033	1.812	1.634	1.482	1.354
100.0	2.723	2.627	2.539	2.461	2.387	2.318	2.254	2.390	2.334	2.283	2.231	2.009	1.830	1.677	1.547
150.0	2.921	2.885	2.736	2.659	2.585	2.516	2.452	2.591	2.475	2.425	2.372	2.150	1.970	1.816	1.686
200.0	3.062	2.967	2.878	2.800	2.726	2.656	2.592	2.640	2.584	2.534	2.481	2.259	2.079	1.925	1.795
250.0	3.172	3.077	2.988	2.910	2.836	2.766	2.702	2.770	2.674	2.624	2.571	2.349	2.169	2.015	1.884
300.0	3.262	3.167	3.078	3.000	2.926	2.856	2.792	2.860	2.750	2.700	2.647	2.425	2.245	2.090	1.960
350.0	3.338	3.243	3.154	3.076	3.002	2.933	2.868	2.872	2.816	2.767	2.713	2.491	2.311	2.155	2.025
400.0	3.404	3.309	3.220	3.143	3.068	2.999	2.934	2.931	2.875	2.824	2.771	2.549	2.369	2.214	2.083
450.0	3.463	3.367	3.278	3.201	3.127	3.057	2.993	2.983	2.927	2.876	2.823	2.601	2.421	2.266	2.135
500.0	3.515	3.420	3.331	3.253	3.179	3.109	3.045	3.030	2.973	2.919	2.867	2.645	2.463	2.310	2.177
550.0	3.562	3.465	3.378	3.298	3.224	3.155	3.090	3.073	3.016	2.962	2.911	2.688	2.506	2.353	2.220
600.0	3.603	3.508	3.421	3.341	3.267	3.198	3.134	3.113	3.056	3.003	2.951	2.728	2.546	2.393	2.260
650.0	3.643	3.548	3.461	3.381	3.307	3.238	3.174	3.150	3.093	3.039	2.988	2.765	2.583	2.430	2.297
700.0	3.680	3.585	3.498	3.418	3.344	3.275	3.211	3.184	3.127	3.073	3.022	2.799	2.618	2.464	2.331
750.0	3.715	3.620	3.533	3.453	3.378	3.310	3.245	3.217	3.160	3.106	3.054	2.832	2.650	2.496	2.363
800.0	3.747	3.652	3.565	3.485	3.411	3.342	3.277	3.247	3.190	3.136	3.084	2.862	2.680	2.526	2.393
850.0	3.777	3.682	3.595	3.515	3.441	3.372	3.308	3.277	3.218	3.164	3.113	2.890	2.708	2.555	2.422
900.0	3.806	3.711	3.624	3.544	3.470	3.401	3.336	3.305	3.245	3.191	3.140	2.917	2.735	2.582	2.449
950.0	3.833	3.738	3.651	3.571	3.497	3.428	3.362	3.330	3.271	3.217	3.166	2.943	2.761	2.607	2.474
1000.	3.859	3.763	3.676	3.596	3.522	3.453	3.389	3.358	3.298	3.243	3.192	2.969	2.787	2.633	2.500

Table 4-2

PD(RD,TD) Values at Selected RD Ratios
for Various TD - Constant Rate Case

TD	RD = 4.5	RD = 5.0	RD = 5.5	RD = 6.0	RD = 6.5	RD = 7.0	RD = 7.5	RD = 8.0	RD = 8.5	RD = 9.0	RD = 9.5	RD = 10	RD = 15	RD = 16	TD
1.000	.0043	.0005	.0009												1.000
1.200	.0069	.0016	.0013												1.200
1.400	.0105	.0033	.0020	.0021	.0028										1.400
2.000	.0260	.0120	.0066	.0044	.0039										2.000
3.000	.0610	.0354	.0216	.0135	.0092	.0025	.0020								3.000
4.000	.1001	.0646	.0427	.0282	.0191	.0089	.0060	.0021	.0017	.0009	.0008	.0007			4.000
5.000	.1394	.0959	.0669	.0465	.0325	.0185	.0127	.0066	.0047	.0028	.0019	.0014			5.000
6.000	.1773	.1273	.0925	.0666	.0481	.0304	.0215	.0130	.0092	.0060	.0041	.0029			6.000
7.000	.2134	.1581	.1181	.0878	.0651	.0438	.0319	.0209	.0151	.0103	.0072	.0051			7.000
8.000	.2476	.1878	.1436	.1092	.0829	.0583	.0435	.0301	.0222	.0157	.0113	.0081			8.000
9.000	.2800	.2164	.1684	.1306	.1010	.0733	.0559	.0401	.0303	.0220	.0162	.0118	.0009		9.000
10.00	.3106	.2438	.1926	.1517	.1191	.0888	.0688	.0508	.0390	.0291	.0218	.0162	.0011	.0002	10.00
15.00	.4417	.3641	.3017	.2497	.2064	.1656	.1359	.1088	.0886	.0712	.0571	.0456	.0039	.0018	15.00
20.00	.5461	.4621	.3933	.3345	.2844	.2368	.2005	.1669	.1406	.1173	.0978	.0812	.0104	.0060	20.00
30.00	.7061	.6152	.5389	.4724	.4143	.3586	.3140	.2723	.2379	.2067	.1795	.1556	.0326	.0224	30.00
40.00	.8270	.7323	.6520	.5812	.5186	.4582	.4088	.3622	.3228	.2866	.2544	.2256	.0619	.0461	40.00
50.00	.9242	.8272	.7443	.6707	.6052	.5418	.4892	.4393	.3965	.3570	.3214	.2891	.0942	.0734	50.00
60.00	1.006	.9069	.8222	.7467	.6791	.6136	.5587	.5065	.4614	.4194	.3813	.3465	.1271	.1021	60.00
70.00	1.075	.9755	.8896	.8127	.7436	.6764	.6200	.5660	.5191	.4752	.4352	.3985	.1596	.1310	70.00
80.00	1.137	1.036	.9489	.8710	.8007	.7323	.6746	.6193	.5709	.5256	.4842	.4459	.1911	.1594	80.00
90.00	1.191	1.090	1.002	.9231	.8520	.7826	.7238	.6675	.6180	.5715	.5289	.4894	.2214	.1871	90.00
100.0	1.240	1.138	1.050	.9704	.8985	.8283	.7687	.7115	.6611	.6137	.5700	.5296	.2505	.2139	100.0
150.0	1.432	1.328	1.238	1.156	1.082	1.010	.9474	.8874	.8342	.7838	.7370	.6933	.3779	.3337	150.0
200.0	1.570	1.466	1.374	1.292	1.216	1.142	1.079	1.017	.9627	.9107	.8623	.8169	.4813	.4326	200.0
250.0	1.678	1.573	1.481	1.398	1.322	1.247	1.183	1.121	1.065	1.012	.9625	.9160	.5677	.5160	250.0
300.0	1.767	1.662	1.569	1.485	1.409	1.334	1.269	1.206	1.150	1.096	1.046	.9987	.6416	.5879	300.0
350.0	1.842	1.737	1.644	1.560	1.483	1.408	1.342	1.279	1.222	1.168	1.117	1.070	.7061	.6509	350.0
400.0	1.908	1.802	1.709	1.625	1.548	1.472	1.406	1.343	1.285	1.231	1.180	1.132	.7633	.7070	400.0
450.0	1.966	1.860	1.767	1.682	1.605	1.529	1.463	1.399	1.342	1.287	1.236	1.187	.8147	.7574	450.0
500.0	2.018	1.911	1.818	1.734	1.656	1.580	1.514	1.450	1.392	1.337	1.286	1.237	.8613	.8033	500.0
550.0	2.060	1.956	1.862	1.776	1.697	1.625	1.557	1.495	1.436	1.381	1.329	1.279	.9013	.8434	550.0
600.0	2.103	1.999	1.905	1.819	1.740	1.667	1.600	1.537	1.478	1.423	1.370	1.321	.9408	.8824	600.0
650.0	2.143	2.038	1.944	1.858	1.779	1.707	1.639	1.576	1.517	1.461	1.409	1.360	.9773	.9185	650.0
700.0	2.180	2.075	1.981	1.895	1.816	1.743	1.675	1.612	1.553	1.497	1.445	1.395	1.011	.9522	700.0
750.0	2.214	2.109	2.015	1.929	1.850	1.777	1.709	1.646	1.587	1.531	1.478	1.429	1.043	.9838	750.0
800.0	2.246	2.141	2.047	1.961	1.882	1.809	1.741	1.677	1.618	1.562	1.510	1.460	1.073	1.014	800.0
850.0	2.276	2.171	2.077	1.991	1.912	1.838	1.771	1.707	1.648	1.592	1.539	1.489	1.102	1.042	850.0
900.0	2.305	2.200	2.105	2.019	1.940	1.867	1.799	1.735	1.676	1.620	1.567	1.517	1.129	1.068	900.0
950.0	2.331	2.227	2.132	2.046	1.967	1.893	1.825	1.762	1.702	1.646	1.593	1.543	1.154	1.093	950.0
1000.	2.357	2.252	2.158	2.071	1.992	1.919	1.851	1.787	1.727	1.671	1.618	1.568	1.178	1.117	1000.

Table 4-3

PD(RD,TD) Values at Selected RD Ratios
for Various TD - Constant Rate Case

TD	RD = 20	RD = 25	RD = 30	RD = 32	RD = 35	RD = 40	RD = 45	RD = 50	RD = 55	RD = 60	RD = 64	TD
20.00	.0003											20.00
30.00	.0044	.0008										30.00
40.00	.0131	.0026	.0005									40.00
50.00	.0256	.0063	.0013	.0029								50.00
60.00	.0407	.0119	.0029	.0038								60.00
70.00	.0575	.0190	.0055	.0054	.0002							70.00
80.00	.0752	.0275	.0089	.0077	.0014							80.00
90.00	.0935	.0370	.0132	.0107	.0030	.0005						90.00
100.0	.1120	.0473	.0182	.0143	.0052	.0013						100.0
150.0	.2015	.1044	.0512	.0402	.0226	.0096	.0022	.0025	.0004	.0022		150.0
200.0	.2821	.1628	.0907	.0733	.0475	.0242	.0102	.0066	.0024	.0031		200.0
250.0	.3533	.2182	.1316	.1089	.0760	.0431	.0220	.0136	.0063	.0052	.0014	250.0
300.0	.4163	.2697	.1717	.1447	.1059	.0643	.0365	.0230	.0122	.0087	.0037	300.0
350.0	.4728	.3172	.2101	.1796	.1358	.0868	.0527	.0343	.0197	.0135	.0070	350.0
400.0	.5237	.3611	.2467	.2133	.1652	.1098	.0700	.0469	.0286	.0196	.0114	400.0
450.0	.5701	.4018	.2813	.2455	.1938	.1328	.0879	.0605	.0386	.0267	.0167	450.0
500.0	.6127	.4396	.3140	.2762	.2214	.1554	.1061	.0746	.0493	.0347	.0228	500.0
550.0	.6507	.4732	.3437	.3200	.2482	.1776	.1257	.0877	.0604	.0409	.0297	550.0
600.0	.6873	.5063	.3731	.3299	.2737	.1993	.1437	.1023	.0720	.0500	.0370	600.0
650.0	.7214	.5375	.4010	.3564	.2982	.2203	.1615	.1172	.0840	.0595	.0447	650.0
700.0	.7533	.5669	.4276	.3818	.3217	.2408	.1789	.1318	.0960	.0692	.0529	700.0
750.0	.7834	.5947	.4528	.4060	.3443	.2607	.1961	.1464	.1082	.0792	.0613	750.0
800.0	.8117	.6211	.4770	.4292	.3661	.2799	.2129	.1608	.1205	.0893	.0699	800.0
850.0	.8386	.6461	.5000	.4514	.3870	.2986	.2293	.1749	.1326	.0995	.0786	850.0
900.0	.8641	.6700	.5221	.4727	.4071	.3167	.2453	.1889	.1446	.1097	.0875	900.0
950.0	.8883	.6929	.5433	.4932	.4265	.3342	.2609	.2027	.1565	.1200	.0964	950.0
1000.	.9115	.7147	.5637	.5129	.4452	.3512	.2762	.2162	.1683	.1302	.1054	1000.

Table 4-4

PERCENT DIFFERENCE BETWEEN INTERPOLATED PD(RD,TD) VALUES AND THOSE PRODUCED BY PROGRAM NO. 1

Part A. Interpolation between RD columns in Figures 4-1 to 4-3

TD	RD	Interpolated PD(RD,TD)	Program PD(RD,TD)	Percent Difference
.02	1.1	.0887	.0719	23.3
400.0	1.1	3.312	3.309	.097
.60	2.0	.1364	.1271	7.3
1.2	2.0	.2740	.2627	4.3
8.0	5.0	.1956	.1878	4.2
40.0	10.0	.2371	.2256	5.1
90.0	10.0	.5009	.4894	2.4
300.0	25.0	.2940	.2697	9.0
550.0	40.0	.1370	.1776	22.9
800.0	55.0	.1251	.1205	3.8
.15	1.6	.0567	.0541	4.8
9.0	3.0	.5917	.5761	2.71
75.0	1.6	3.264	3.245	.59
9.0	7.0	.0785	.0733	7.1
950.0	6.0	2.050	2.046	.20
6.0	8.5	.0095	.0092	3.4
550.0	32.0	.3055	.3200	4.5
350.0	60.0	.0126	.0135	6.7
1000.0	40.0	.3607	.3512	2.7
.05	1.3	.0545	.0483	12.9
			Ave.	6.40
			Max.	23.3

Part B. Interpolation between TD rows in Figures 4-1 to 4-3

RD	TD	Interpolated PD(RD,TD)	Program PD(RD,TD)	Percent Difference
1.0	8.0	1.553	1.556	.19
1.0	750.0	3.714	3.715	.03
1.0	.004	.0617	.0621	.65
1.8	2.0	.4926	.4784	2.97
1.9	400.0	2.806	2.824	.64
50.0	400.0	.0474	.0469	1.07
32.0	90.0	.0110	.0107	2.80
7.5	15.0	.1347	.1359	.84
10.0	40.0	.2224	.2256	1.42
5.0	5.0	.0960	.0959	.11
			Ave.	1.07
			Max.	2.97

between the two PD(RD,TD) values chosen for interpolation was therefore about double what would be required when normally interpolating between columns or rows in Table 4-1. As a result of this large difference, the author believes that regular interpolation between RD columns in Table 4-1 should produce an average percent difference of less than 5.0% with a maximum of less than 10%. For regular interpolation between TD values in Table 4-1, the average percent difference should be less than 1.0% with a maximum less than 2.0%.

4.2 Comparison of PD(RD,TD) Results

The values obtained for PD(1,TD) can be checked against those of Chatas by comparing Table 4-1 to Table 2-2. The maximum percent difference between the results of this study and those of Chatas are listed below for the 3 different TD ranges. The 3 TD regions correspond to the region of Romberg integration and the two regions of simplification where integration was not required.

Table 4-5

TD Region	Maximum % Difference in PD(1,TD)
$.0005 \leq TD \leq .01$	0.28
$.01 < TD \leq 500$	0.06
$500 < TD < 1000$	0.13

In lieu of the excellent reproduction of Chatas' results in all three TD regions, it is believed that 3 of Chatas' PD(1,TD) values are in error. The PD(1,TD) values in question are given in Table 4-6 along with the values obtained in this study.

Table 4-6

TD	This Study	Chatas	Percent Difference
1.2	.8672	.8567	1.21
1.4	.9160	.9047	1.24
2.0	1.0195	1.0222	.27

Mortada's results for PD(RD,TD) shown in Figures 2-8 to 2-10 cannot be numerically compared since no tabulated results of Mortada's work are available. The results obtained in this study do, however, plot exactly on the curves presented in Figures 2-8 to 2-10.

In general, the results of this study compare favorably with those of Buxton presented in Table 2-4 and Figure 2-11. Points calculated in this study were plotted on Buxton's Figure 2-11 and any deviation was too small to be observed. No formal attempt was made to calculate all the percent differences between the results of this study and those presented by Buxton because the oscillation of the function F(X) and the lack of rapid convergence near the origin apparently affected Buxton's results for TD less than 50 and RD less than 10. As can be seen from Tables 2-4 and 2-2, Buxton's technique fails to reproduce Chatas' results even at TD equal to 50, whereas, the results of this study agree with those of Chatas for RD = 1 across the entire TD range to within 0.28%. Since Buxton did not reproduce Chatas' results at RD = 1.0 where oscillation is not a problem, the author did not deem a formal comparison of results necessary. A spot-check of 15 PD(RD,TD) values, however, indicated a maximum deviation of 10% between the results of this study and the PD(RD,TD) values presented by Buxton.

The PD(RD,TD) values presented by Edwardson in Table 2-5 agree with those of this study to within 2.0% except at the lowest five or six TD values in each of RD column.

Edwardson did not, however, point out whether his Table 2-5 was the result of a curve fit of Mortada's results (Figures 2-8 to 2-10) or whether Table 2-5 was the product of some other unmentioned technique developed by Edwardson himself. Since the origin of Table 2-5 was uncertain, no attempt to explain the deviation of results at low TD values can be reasonably made.

4.3 Tabulated (RD-1) Results

Table 4-7 gives the values of (RD-1) obtained from Program No. 2A for various fractional pressure values, PD'. This table contains the 30 values used to plot Figure 4-1 and these numerical results are tabulated for those interested in reproducing a work-plot similar to Figure 4-1 on a scale sufficient to allow field problems to be accurately solved without the use of the digital computer (See Insert 7).

Although the results of Table 4-7 are obtained from Program 2A, the author suggests that Program 2 be used in preference to Program 2A for further accuracy.

Table 4-8 gives the results of 30 spot-check comparisons of (RD-1) as produced by Program 2 and Program 2A. (RD-1) is the radius ratio at which the fractional pressure, PD', exists at a dimensionless time TD, minus 1.0.

The percent difference values of Table 4-8 were averaged and yielded a value of .62%. The maximum difference is 4.2%.

Table 4-7

RD -1 Values for Selected PD' Ratios at

Various TD - Constant Rate Case

TD	PD' = .01	PD' = .02	PD' = .05	PD' = .10	PD' = .20	PD' = .30	PD' = .40	PD' = .50	PD' = .60	PD' = .70	PD' = .80	PD' = .90	TD
.0010	.1009	.0899	.0739	.0604	.0454	.0356	.0280	.0219	.0165	.0118	.0075	.0036	.0010
.0020	.1424	.1268	.1042	.0851	.0639	.0501	.0395	.0308	.0233	.0167	.0107	.0051	.0020
.0030	.1740	.1550	.1273	.1041	.0779	.0611	.0483	.0375	.0284	.0203	.0130	.0063	.0030
.0040	.2008	.1787	.1468	.1198	.0899	.0704	.0555	.0433	.0328	.0234	.0150	.0071	.0040
.0060	.2452	.2183	.1793	.1463	.1097	.0859	.0677	.0528	.0399	.0285	.0183	.0087	.0060
.0100	.3156	.2809	.2304	.1881	.1408	.1102	.0869	.0677	.0511	.0366	.0233	.0112	.0100
.0200	.4630	.4074	.3241	.2609	.1951	.1529	.1208	.0943	.0714	.0510	.0327	.0159	.0200
.0400	.6063	.5502	.4574	.3705	.2736	.2132	.1675	.1306	.0987	.0705	.0451	.0218	.0400
.0600	.7694	.6647	.5497	.4506	.3339	.2587	.2031	.1577	.1191	.0850	.0543	.0262	.0600
.1000	.9689	.8741	.7018	.5702	.4262	.3307	.2579	.1998	.1502	.1071	.0683	.0329	.1000
.2000	1.366	1.215	.9801	.7963	.5861	.4564	.3561	.2741	.2053	.1455	.0925	.0444	.2000
.3000	1.680	1.457	1.194	.9608	.7074	.5475	.4281	.3292	.2455	.1733	.1099	.0527	.3000
.4250	1.948	1.740	1.403	1.151	.8331	.6398	.4987	.3839	.2855	.2010	.1270	.0606	.4250
.7000	2.512	2.201	1.780	1.425	1.042	.8019	.6193	.4755	.3536	.2477	.1557	.0743	.7000
1.000	2.974	2.611	2.108	1.686	1.226	.9371	.7225	.5514	.4096	.2860	.1784	.0845	1.000
1.500	3.577	3.153	2.547	2.030	1.467	1.116	.8588	.6510	.4813	.3348	.2081	.0981	1.500
2.200	4.317	3.804	3.042	2.418	1.741	1.317	1.005	.7606	.5577	.3873	.2394	.1121	2.200
3.000	5.025	4.387	3.513	2.783	1.992	1.500	1.142	.8602	.6263	.4337	.2672	.1243	3.000
5.000	6.399	5.593	4.455	3.512	2.492	1.858	1.401	1.044	.7575	.5189	.3178	.1463	5.000
10.00	8.905	7.766	6.142	4.801	3.355	2.471	1.836	1.352	.9664	.6527	.3956	.1794	10.00
15.00	10.76	9.405	7.414	5.762	3.985	2.910	2.144	1.564	1.108	.7428	.4459	.2005	15.00
25.00	13.70	11.95	9.384	7.241	4.944	3.561	2.593	1.868	1.309	.8671	.5133	.2286	25.00
40.00	17.02	14.87	11.63	8.919	6.011	4.280	3.077	2.191	1.515	.9904	.5800	.2560	40.00
100.0	26.73	23.00	17.73	13.36	8.754	6.065	4.247	2.944	1.984	1.265	.7230	.3121	100.0
150.0	32.54	27.97	21.40	16.01	10.36	7.082	4.895	3.350	2.229	1.404	.7931	.3388	150.0
200.0	37.37	32.07	24.45	18.19	11.66	7.897	5.407	3.665	2.416	1.508	.8449	.3580	200.0
300.0	45.42	38.88	29.48	21.77	13.76	9.194	6.208	4.150	2.699	1.663	.9203	.3856	300.0
425.0	53.68	45.86	34.61	25.40	15.86	10.46	6.979	4.609	2.962	1.804	.9879	.4098	425.0
750.0	70.49	60.00	44.93	32.62	19.95	12.90	8.425	5.451	3.433	2.052	1.103	.4501	750.0
1000.	80.90	68.75	51.29	37.02	22.40	14.33	9.259	5.925	3.693	2.186	1.164	.4711	1000.

Table 4-8

Comparison of (RD-1) Values

TD	PD'	Program No. 2	Program No. 2A	Percent Difference
.003	.01	.1740	.1738	.12
.003	.20	.0779	.0777	.26
.003	.80	.0130	.0129	.78
.006	.01	.2452	.2445	.29
.006	.20	.1097	.1091	.55
.006	.80	.0183	.0180	1.70
.425	.60	1.28552	1.28552	0.00
.425	.50	1.38391	1.38391	0.00
.70	.60	1.3546	1.3536	.074
.70	.50	1.4752	1.4755	.020
1.50	.60	1.4825	1.4813	.081
1.50	.50	1.6578	1.6510	.412
3.0	.01	5.1265	5.0249	2.0
3.0	.20	2.0042	1.9924	.54
3.0	.80	.2687	.2672	.58
6.0	.01	6.9536	6.9702	.27
6.0	.20	2.7000	2.6926	.26
6.0	.80	.3412	.3373	1.2
10.0	.60	1.9689	1.9664	.13
10.0	.50	2.3554	2.3522	.14
75.0	.01	23.2481	22.5527	3.1
75.0	.20	7.8149	7.7876	.35
75.0	.80	.6827	.6766	.90
100.0	.01	26.9689	25.8340	4.2
100.0	.20	8.8018	8.7564	.52
100.0	.80	.7245	.7239	.08
600.0	.01	63.3320	63.3320	0.0
600.0	.20	18.2315	18.2315	0.0
600.0	.80	1.0573	1.0573	0.0

4.4 Graphical (RD-1) Results

Figure 4-1 is a log-log plot of (RD-1) vs. TD over the TD range of .001 to 100.0. The fractional dimensionless pressure, PD', ranges from .01 to .99. Figure 4-1 can be used to obtain RD directly if TD and PD' are known. In the same way, if TD and RD are available, then PD' can easily be found from Figure 4-1. Finally, if PD' and RD are given, then TD can be obtained.

In order to improve the accuracy of the results when PD' values other than those given in Figure 4-1 are required, Figures 4-2 and 4-3 were prepared by cross-plotting Figure 4-1. By using all three plots, any problem involving TD, RD, and PD' can be rapidly solved without interpolation between curves (See Inserts at back).

Some qualitative aspects of Figure 4-1 should be mentioned. The reason for plotting the difference (RD-1) versus TD in Figure 4-1 rather than RD versus TD was that by subtracting 1.0 from each RD ratio the log-log plot became essentially a family of straight parallel lines.

As shown in Figure 4-1, the deviation from a true straight line begins at a PD' value of about .20 and gradually increases as PD' increases. Even at PD' = .99, however, the deviation from a straight line is small enough to allow a fit-factor to force the data to become a straight line if so desired. This technique would allow straight line equations to be obtained for the entire family of PD' curves.

The accuracy of the three separate routines used to calculate PD(RD,TD) can be seen from Figure 4-1 by noting

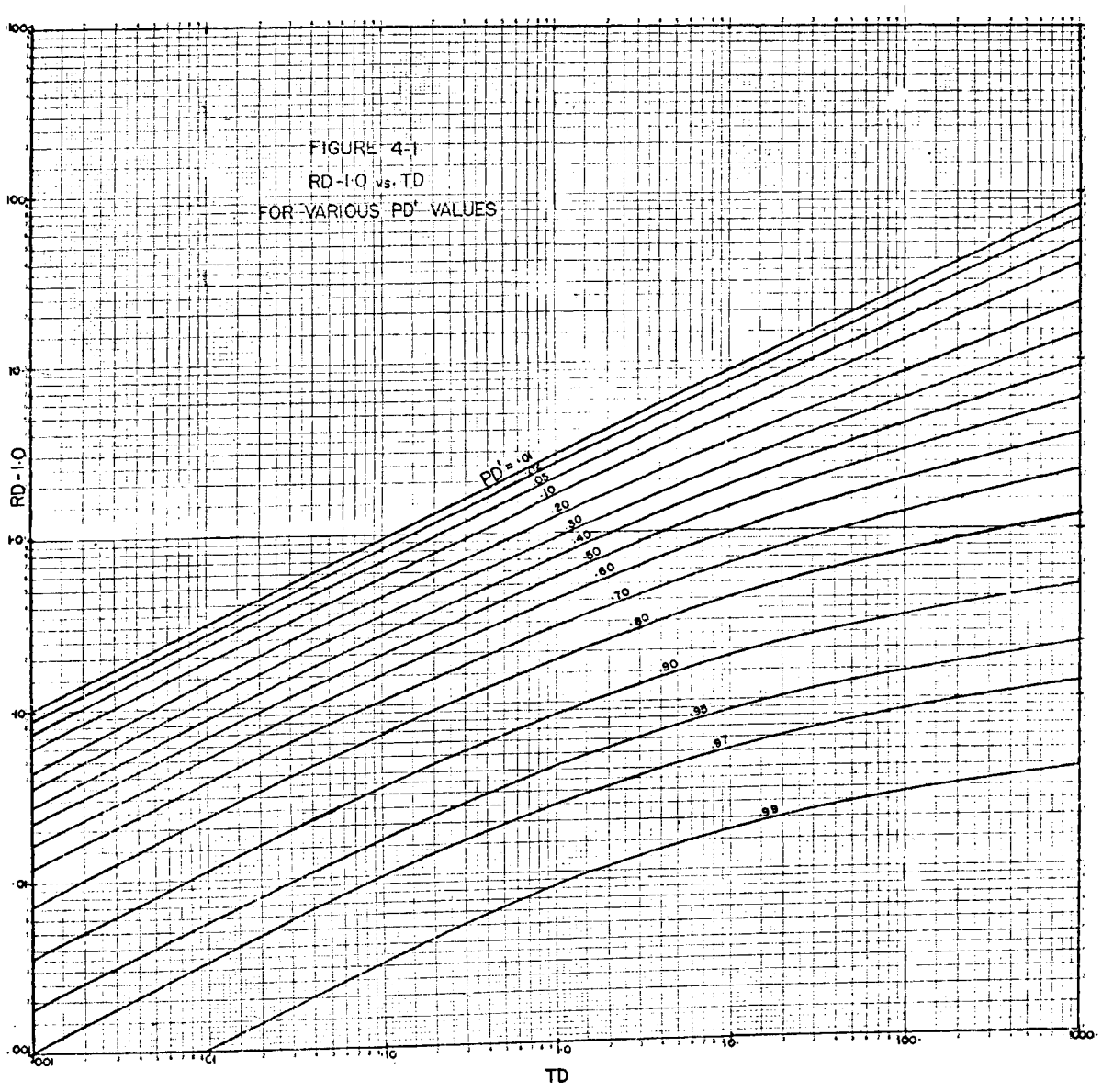
FIGURE 4-1
RD-1.0 vs. TD
FOR VARIOUS PD' VALUES
RD-1.0
TD
PD' = .01
.05
.10
.20
.30
.40
.50
.60
.70
.80
.90
.95
.97
.99
100
10
1.0
.1
.01
.001
.01
.1
1.0
10
100
1000

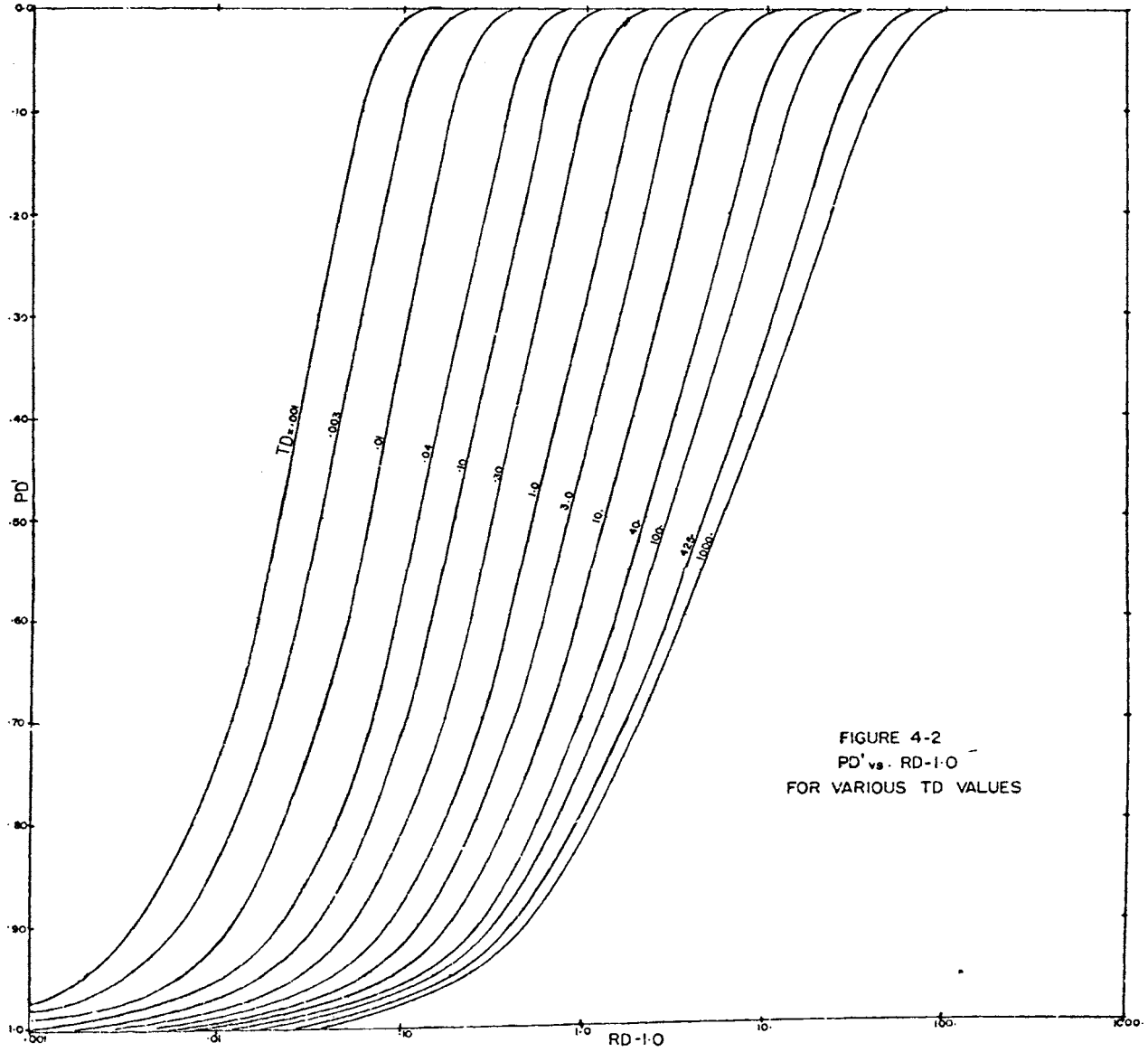

FIGURE 4-2
PD' vs. RD-1·0
FOR VARIOUS TD VALUES

FIGURE 4-3
PD' vs. TD
FOR VARIOUS RD-1.0 VALUES

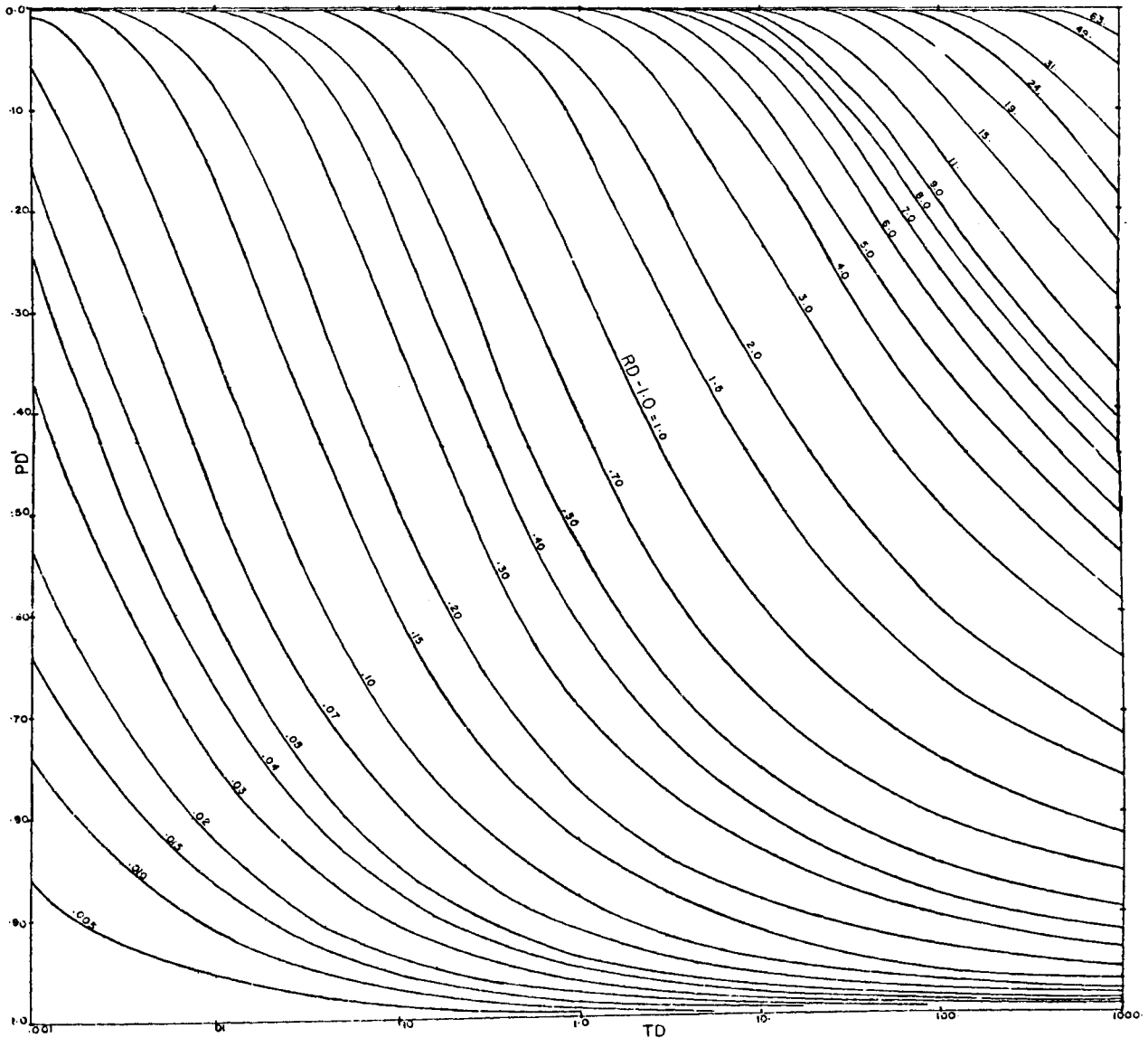

that there is no discontinuity of the PD' curves at TD = .01 and TD = 100. This also indicates that the gradual changing of the PD' lines to curves as PD' and TD increase is the result of physical phenomena rather than program inaccuracy.

Since the pressure distribution at some distance away from the oil-field boundary (RD = 1.0) would be approximately logarithmic (See Muskat, page 543), the small PD' values should give straight lines on a log-log plot. Small PD' values indicate that RD is far enough away from 1.0 so that only a small fraction of the pressure-drop at the inner boundary occurs at any given dimensionless time, TD. On the other hand, as PD' increases, RD decreases and the pressure distribution gradually becomes linear close to the inner boundary. This results in the gradual curvature of the PD' curves at TD values above 10. The logarithmic variation of pressure can also be noted from the spacing of the 15 PD' curves. The distance between any two successive PD' curves increases logarithmically as PD' increases.

The variation of fractional pressure-drop, PD', with the radius ratio RD can be seen from Figure 4-2. For any fixed dimensionless time the PD' curve consists of three regions. First there is a region of very high fractional pressure-drop immediately surrounding the inner boundary (RD = 1). The exact PD' experienced depends upon the value of TD or, since all the other factors in the definition of TD are constant, upon the producing time t. Regardless of the TD value chosen a very high fractional pressure-drop ($.95 \leq PD'$) is experienced within a short distance of the inner boundary.

This region of high pressure-drop surrounding an oil field is equivalent to the zone of high pressure-drop immediately surrounding an oil well.

In the second region the fractional pressure-drop undergoes the major part of its decline from PD$\geq$.95 to PD$\leq$.01 and RD increases by a factor of more than 10.

Since Figure 4-2 is for an infinite aquifer, a PD' of 0.0 will never be reached and RD increases rapidly in the third region as PD' becomes less than .01. It is due to this slow change in PD' in the third region that PD' = .01 is considered to be the effective radius of drainage for the infinite radial aquifer. Figure 4-2 allows the fractional pressure-drop PD' at any producing time t to be traced as RD increases.

Figure 4-3 shows that the fractional pressure-drop PD' at any radius RD in the aquifer increases very slowly as the oil field is first produced, then increases fairly rapidly as the time of production increases, and finally requires a very long producing time in order to increase above .95. By using Figure 4-3, the fractional pressure-drop at any radius ratio RD can be traced as the producing time increases.

4.5 Effective Radius of Drainage Equation

Figure 4-1 gives the variation of (RD-1) with TD for any fractional pressure-drop PD'. PD' was formed in this study so the fractional pressure change in the aquifer could

be evaluated. For the constant terminal rate case, PD(RD,TD) is not a fractional quantity and is defined as:

$$PD(RD,TD) = \frac{2\pi KH(p_i-p)}{q\mu} \quad , \tag{4-1}$$

while, for the constant terminal pressure case it is a true fractional pressure:

$$PD(RD,TD) = \frac{p_i-p}{p_i-p_b} \quad . \tag{4-2}$$

Equation 4-1 can be transformed into a fractional pressure-drop by dividing it by the dimensionless pressure PD(1,TD) at the inner boundary RD = 1 at the same TD.

$$PD' = \frac{2\pi KH(p_i-p)/q\mu}{2\pi KH(p_i-p_b)/q\mu} = \frac{p_i-p}{p_i-p_b} \quad / \tag{4-3}$$

The effective radius of drainage for an infinite radial aquifer was assumed to be the dimensionless radius RD where the fractional pressure-drop experienced was 1% of the pressure-drop at the inner boundary (RD = 1). Thus at the radius of drainage:

$$PD' = .01 \tag{4-4}$$

Figure 4-1 shows that for PD' = .01, the variation of (RD-1) with TD is a straight line on log-log paper. A straight line on log-log paper has an equation of the form:

$$Y = A(X)^N \quad . \tag{4-5}$$

By least-squares fitting of 30 data points taken from the PD' = .01 line in Figure 4-1, an equation for the effective drainage radius was obtained. This equation is:

$$RD = 2.915(TD)^{.48241} + 1.0 \quad . \tag{4-6}$$

Equation 4-6 has been developed especially for the infinite radial aquifer subject to a constant producing rate and therefore avoids selecting one of the several equations already present in the petroleum literature, none of which were specifically derived for an infinite radial system.

The RD values generated by the least-squares fit of the data for PD' = .01 had an average deviation of 1.4%. The use of Equation (4-6) to calculate RD ratios at 30 TD values not used in the least-squares fitting resulted in an average deviation of .547% between the RD ratios obtained from Equation (4-6) and those actually generated by Program No. 2. The complete results of this comparison are given in Table 4-9.

Table 4-9

COMPARISON OF RD RATIOS CALCULATED FROM EQUATION (4-6) AND THOSE GENERATED BY PROGRAM NO. 2

TD	ACTUAL RD	CALCULATED RD	% DEVIATION
0.0011	1.1039	1.1077	0.3437
0.0012	1.1089	1.1128	0.3477
0.0013	1.1138	1.1176	0.3416
0.0015	1.1229	1.1267	0.3426
0.0017	1.1313	1.1351	0.3404
0.0018	1.1352	1.1391	0.3482
0.0021	1.1465	1.1505	0.3438
0.0032	1.1793	1.1830	0.3133
0.0085	1.2904	1.2936	0.2479
106.3866	28.5723	28.7306	0.5543
127.6639	31.1074	31.2785	0.5500
170.2186	35.5840	35.7832	0.5600
212.7732	39.5039	39.7340	0.5824
319.1594	47.7852	48.0965	0.6516
531.9329	60.7852	61.2485	0.7623
638.3193	66.2461	66.7841	0.8122
851.0928	75.8867	76.5713	0.9021
957.4792	80.2422	80.9868	0.9280
15.0000	11.7627	11.7839	0.1801
2.2000	5.3169	5.2741	-0.8044
0.7000	3.5115	3.4608	-1.4429
0.4250	2.9480	2.9346	-0.4534
0.0600	1.7694	1.7528	-0.9384
25.0000	14.7021	14.7953	0.6339
0.0030	1.1738	1.1776	0.3261
0.0040	1.2003	1.2040	0.3133
0.0060	1.2445	1.2481	0.2858
150.0000	33.5410	33.7261	0.5518
200.0000	38.3730	38.5949	0.5783
300.0000	46.4180	46.7116	0.6326

AVERAGE DEVIATION OF RD = 0.5471%

4.6 Comparison of Various Radius of Drainage Equations

Table 4-10 gives the value of the radius of drainage obtained by the use of Equation 4-6 and the drainage radii resulting from the solution of each of the expressions previously available in the petroleum literature (See Table 2-7). As TD increases, the difference between the radius obtained by Equation (4-6) and the radii given by the other expressions becomes significant. The Hurst, Haynie, and Walker equation given as Equation (4-7) gives results closest to those obtained from Equation (4-6). This is as expected since the Hurst, Haynie, and Walker equation was developed by obtaining a relationship between the radii at which the PD(1,TD) curves for a series of finite systems start to deviate from the PD(1,TD) curve for an infinite system. This approach allowed a relationship to be obtained between TD and the radii of the individual finite systems. Equation (4-7) was developed by graphically determining the point of separation of the finite system curves from the infinite system PD(1,TD) curve. Because of this graphical evaluation, the Hurst, Haynie, Walker equation is not as accurate for an infinite system as Equation (4-6).

$$r \approx 2.6408\sqrt{Kt/\phi\mu c} \quad . \tag{4-7}$$

Hurst, Haynie, and Walker also gave the stabilization time as:

$$t_s = \frac{\phi\mu c r^2}{6.97K} \quad . \tag{4-8}$$

Table 4-10

COMPARISON OF THE VARIOUS RADIUS OF DRAINAGE EQUATIONS

TD=	0.00009378	TD=	0.93777782
TIME, DAYS=	0.01	TIME, DAYS=	100.00
PEJR=	1038.49	PEJR=	4849.00
TGPR=	1040.57	TGPR=	5057.20
MCVPR=	1019.44	MCVPR=	2944.04
HUTKR=	1014.55	HUTKR=	2454.79
HHWR=	1025.66	HHWR=	3566.00
BKMDHR=	1017.21	BKMDHR=	2721.33
AJNR=	1033.41	AJNR=	3833.40
TD=	0.00093778	TD=	9.37777805
TIME, DAYS=	0.10	TIME, DAYS=	1000.00
PEJR=	1121.72	PEJR=	13171.62
TGPR=	1128.30	TGPR=	13830.00
MCVPR=	1061.48	MCVPR=	7147.59
HUTKR=	1046.00	HUTKR=	5600.43
HHWR=	1081.14	HHWR=	9114.41
BKMDHR=	1054.43	BKMDHR=	6443.31
AJNR=	1101.38	AJNR=	9598.58
TD=	0.00937778	TD=	93.77778625
TIME, DAYS=	1.00	TIME, DAYS=	10000.00
PEJR=	1384.90	PEJR=	39490.04
TGPR=	1405.72	TGPR=	41572.04
MCVPR=	1194.40	MCVPR=	20440.40
HUTKR=	1145.48	HUTKR=	15547.86
HHWR=	1256.60	HHWR=	26660.01
BKMDHR=	1172.13	BKMDHR=	18213.26
AJNR=	1307.66	AJNR=	27094.31
TD=	0.09377778	TD=	937.7758789
TIME, DAYS=	10.00	TIME, DAYS=	100000.00
PEJR=	2217.16	PEJR=	122716.13
TGPR=	2283.00	TGPR=	129300.06
MCVPR=	1614.76	MCVPR=	62475.96
HUTKR=	1460.04	HUTKR=	47004.38
HHWR=	1811.44	HHWR=	82144.06
BKMDHR=	1544.33	BKMDHR=	55433.13
AJNR=	1933.66	AJNR=	80189.00

Equation (4-6) can be reduced to the form of Equation (4-7) by assuming that $r_b \rightarrow 0$ and that .48241 is approximately equal to .5000 (See Appendix B, page 245). If these modifications are made Equations (4-9) and (4-10) are obtained:

Radius of Drainage in C.G.S. Units

$$r = 2.76\sqrt{\frac{Kt}{\phi\mu c}} \qquad (4\text{-}9)$$

Stabilization Time in C.G.S. Units

$$t_s = \frac{\phi\mu c r^2}{7.62K} \; . \qquad (4\text{-}10)$$

As mentioned above, Equations (4-9) and (4-10) also show that the equation developed in this study (Equation (4-6)) is closer to the Hurst, Haynie, Walker equation than to any of the other equations presented by Van Poolen in Table 2-7.

Definition of terms in Table 4-10 are:

PEJR = P. E. Jones

TGPR = Tek, Grove, and Poettmann

MCVPR = Muskat, Chatas, and Van Poolen

HUTKR = Hutchinson and Kern

HHWR = Hurst, Haynie, and Walker

BKMDHR = Brownscombe and Kern

AJNR = Nute

4.7 On-Line Mapping Technique

The development of the mapping routine included in Program No. 3 allows the areal distribution of aquifer

pressure to be examined quickly and accurately. The use of this routine, in conjunction with the basic program to generate areal pressure distribution eliminates the tedious and often inaccurate hand-contouring of aquifer pressure data. The technique developed in this study allows a graphical representation of the areal pressure or pressure-drop distribution to be produced directly on the I.B.M. 360/50 on-line printer. The map produced is attached to the computer print-out and is designed to fill exactly two pages of print-out space. Furthermore, the routine is designed so that the map divides evenly between the two pages of output and this results in one-half of the grid appearing on each of the two output pages.

As can be seen of Figures 4-4 and 4-5, every other pressure contour is represented by a distinctive letter or character. Between each distinctive contour there is a blank contour. This alternating printed and blank contouring produces an easily interpreted map.

This mapping routine is designed to produce 53 contours above and 53 contours below the reference pressure with each letter or character having the value given in Table 4-11.

If the number of contours required either above or below the reference pressure exceeds the number of symbols available as shown in Table 4-11, then the routine picks up its own symbols. After printing the blank following either the Z (plus pressures) or the / (negative pressures) the program prints a * contour as as unreferenced contour and

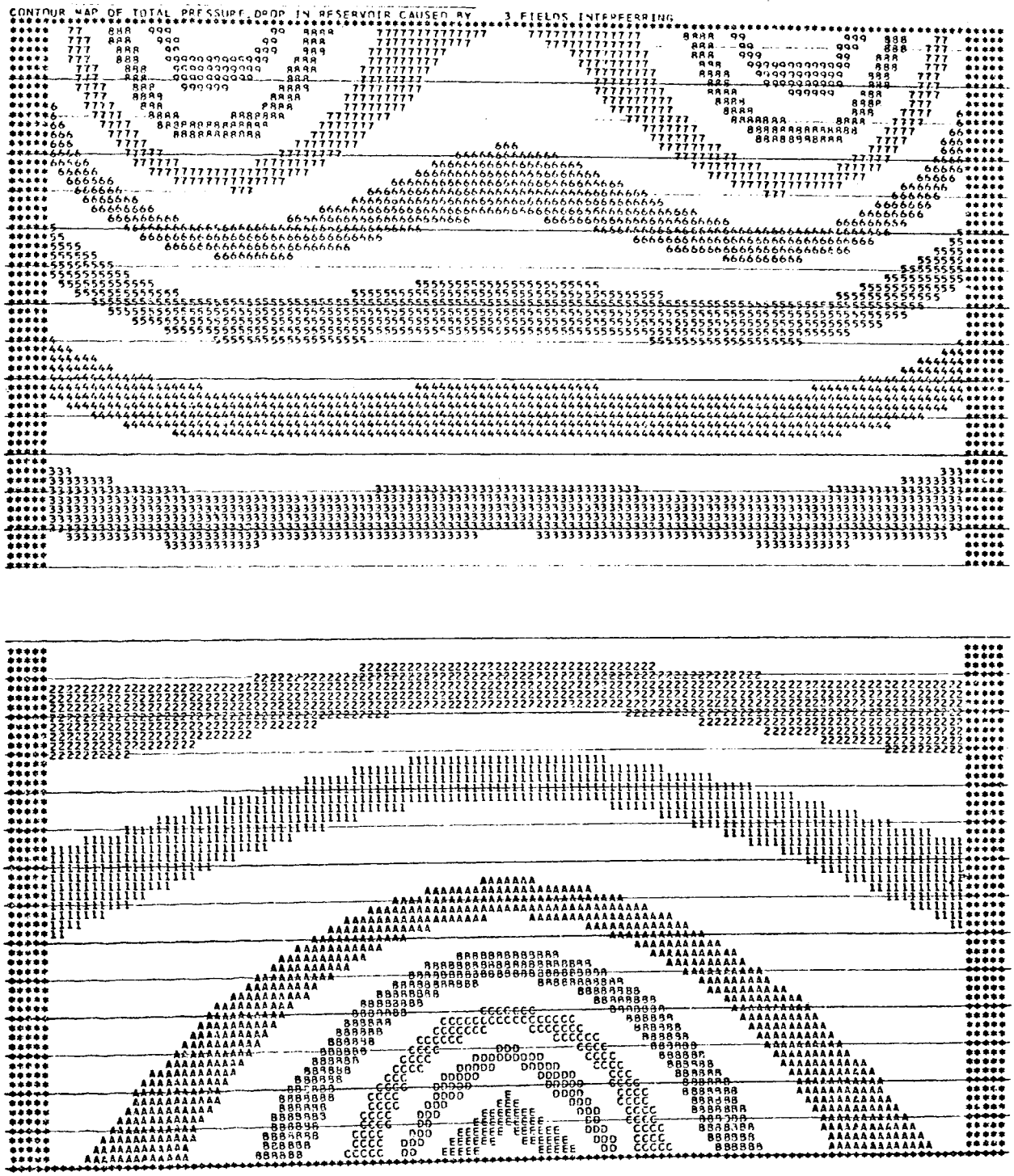

FIGURE 4-4

CONTOUR MAP OF THE TOTAL PRESSURE-DROP OCCURRING IN THE AQUIFER

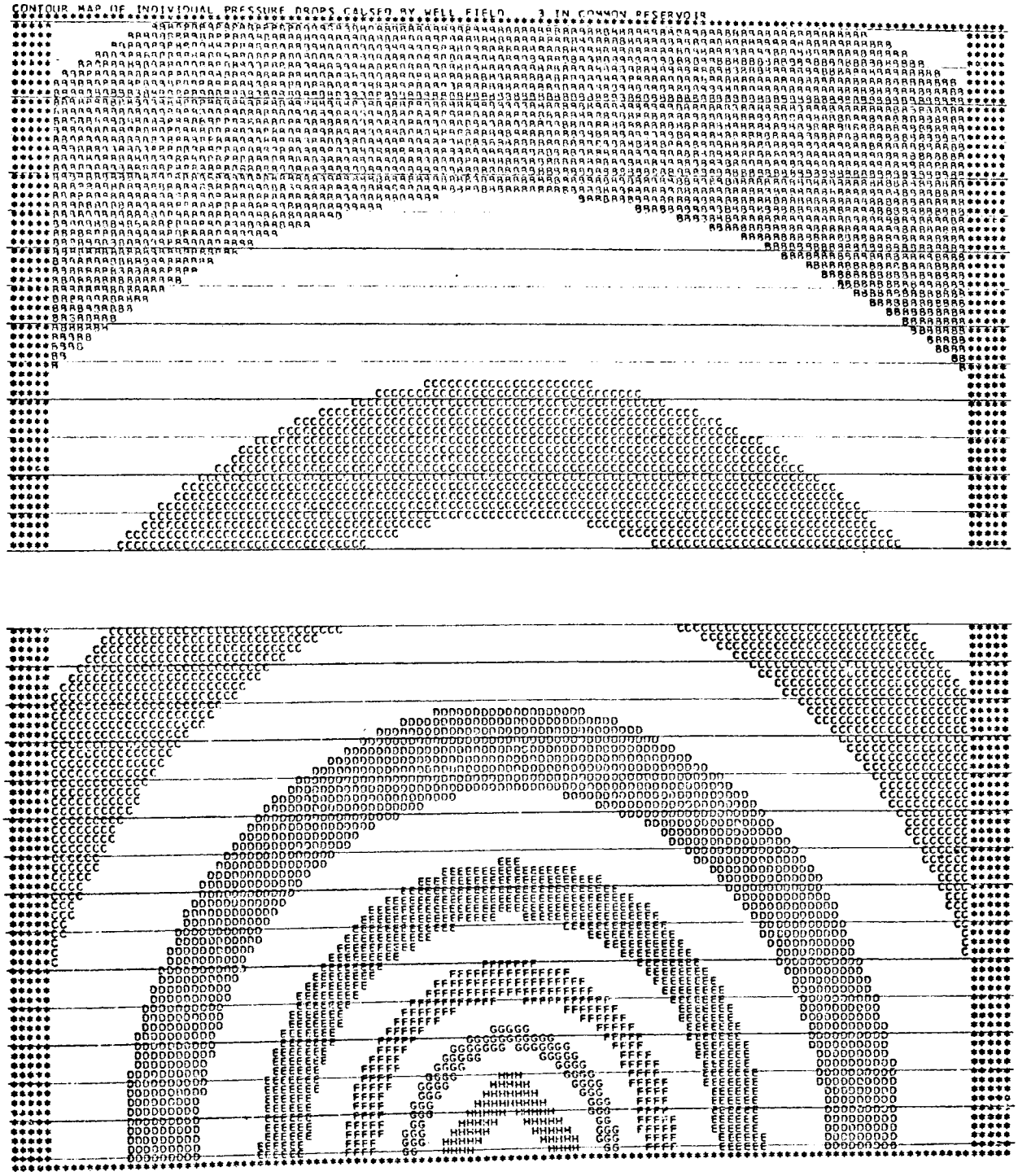

FIGURE 4-5

CONTOUR MAP OF THE PRESSURE-DROP CAUSED BY WELL-FIELD 3 .

Table 4-11

INTERPRETATION OF LETTERS AND SYMBOLS PRINTED AS CONTOURS ON THE MAPS PRODUCED

SYMBOLS	# of C.I. ABOVE REF.	SYMBOL	# of C.I. BELOW REF.
blank	53	blank	- 53
Z	52	/	- 52
blank	51	blank	- 51
Y	50	<	- 50
blank	49	blank	- 49
X	48	∂	- 48
blank	47	blank	- 47
W	46	%	- 46
blank	45	blank	- 45
V	44	"	- 44
blank	43	blank	- 43
U	42	❋	- 42
blank	41	blank	- 41
T	40	!	- 40
blank	39	blank	- 39
S	38	ε	- 38
blank	37	blank	- 37
R	36	¢	- 36
blank	35	blank	- 35
Q	34	=	- 34
blank	33	blank	- 33
P	32	+	- 32
blank	31	blank	- 31
O	30	,	- 30
blank	29	blank	- 29
N	28	.	- 28
blank	27	blank	- 27
M	26	-	- 26
blank	25	blank	- 25
L	24	*	- 24
blank	23	blank	- 23
K	22	$	- 22
blank	21	blank	- 21
J	20	0	- 20
blank	19	blank	- 19
I	18	9	- 18
blank	17	blank	- 17
H	16	8	- 16
blank	15	blank	- 15
G	14	7	- 14
blank	13	blank	- 13
F	12	6	- 12
blank	11	blank	- 11
E	10	5	- 10
blank	9	blank	- 9
D	8	4	- 8

Table 4-11 Continued

SYMBOLS	# of C.I. ABOVE REF.	SYMBOL	# of C.I. BELOW REF.
blank	7	blank	- 7
C	6	3	- 6
blank	5	blank	- 5
B	4	2	- 4
blank	3	blank	- 3
A	2	1	- 2
blank	1	blank	- 1
?	0	?	0

then starts with the blank preceeding either the 1 or the A. Due to this feature a map will be produced regardless of the contour interval selected but the symbols printed may not always have the meaning shown in Table 4-11.

As an example, permit a minimum pressure-drop to be 52 psi. and the maximum pressure-drop to be mapped to be 76 psi. Then, given a reference pressure-drop of 0 psi. and a contour interval of 1 psi., the routine would produce the following symbols on the map.

1. Print a Z contour (52 psi.)
2. Print a blank contour (53 psi.)

Having done 1 and 2, there are now no more positive symbols available so the routine would:

3. Print a # contour (54 psi.)
4. Print a * contour (55 psi.)

It then would skip to the negative symbols and:

5. Print a blank contour (56 psi.)
6. Print a 1 contour (57 psi.)
7. Continue printing the negative symbols until the blank following 0 (76 psi.) is printed.

The same type of a procedure would be followed if the pressures were -52 psi. to -76 psi.

1. Print a / contour (-52 psi.)
2. Print a blank contour (-53 psi.)

3. Print a # contour (-54 psi.)
4. Print a * contour (-55 psi.)
5. Print a blank contour (-56 psi.)
6. Print an A contour (-57 psi.)
7. Continue printing positive symbols until the blank following J (-76 psi.) is printed.

If the contour interval is properly chosen, however, there is no reason for the routine to print symbols in a fashion other than that given in Table 4-11. It must be remembered that 53 contours are available only if the first pressure-drop value printed is one interval above or below the reference pressure-drop. If the first pressure to be printed is 23 times the contour interval, then only 30 symbols remain before the symbols printed no longer have the meanings listed in Table 4-11.

An easy way to check the symbol meaning when both positive and negative symbols appear on a map is to use the plastic grid overlay and to check the various symbols against the numerical print-out pressure-drop values at the different grid points.

The key to the mapping routine is a special grid which allows the pressures to be calculated at 225 specific points in the aquifer. This grid is shown in Figure 4-6. Any point in the grid is referred to the point (0,0) in the upper left-hand corner of the grid. Rectangular coordinates of pressure locations can be readily converted into radial distances from well-field centers located either inside or

FIGURE 4-6

MAPPING GRID USED IN PROGRAM NO. 3

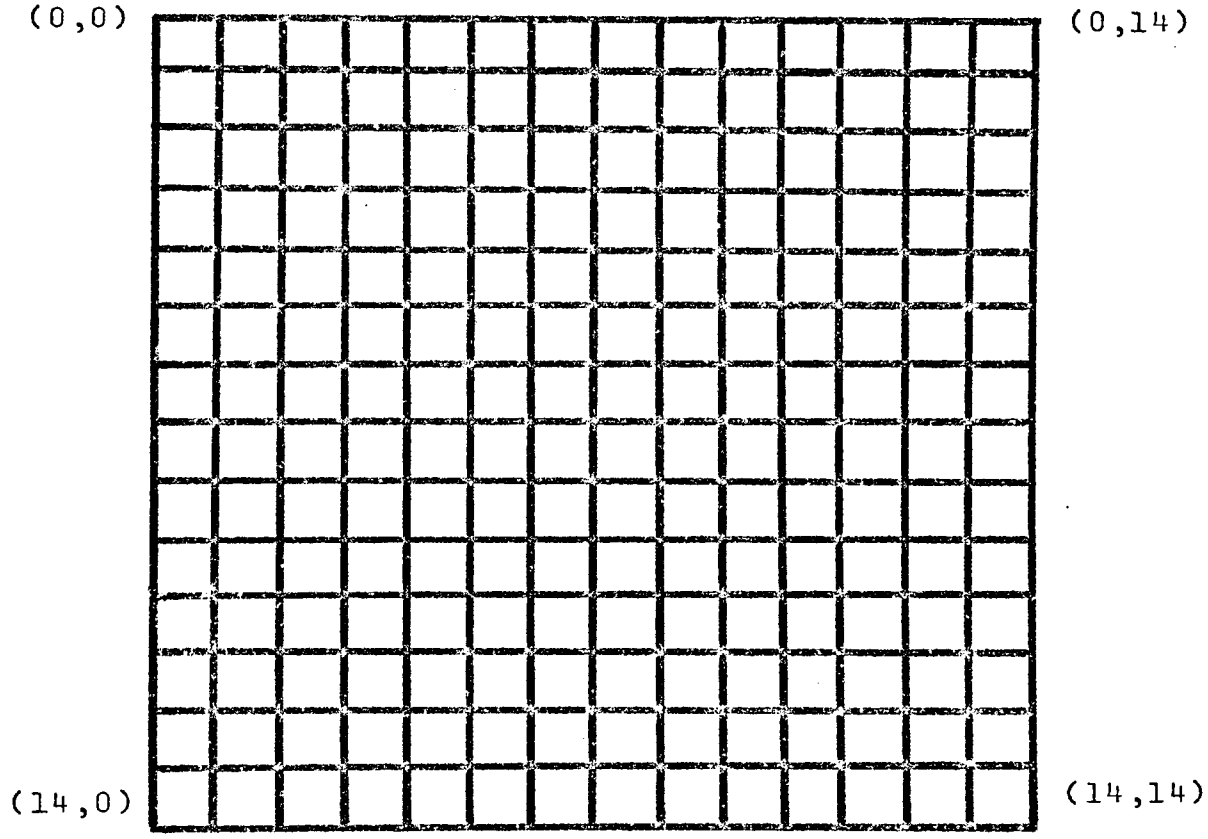

outside the grid itself.

Radial distances from the well-field centers can then be converted into dimensionless radii, RD. Once the required aquifer parameters, the producing time, and the constant producing rate have all been specified, the pressure or pressure-drop can easily be evaluated at each RD by means of a routine similar to Program No. 1. This routine calculates PD(RD,TD) at any RD and TD. PD(RD,TD) is then converted to real pressure or pressure-drop by means of the definition of PD(RD,TD) for the constant rate case (See Equation (1B-9), page 226).

The pressure values are calculated at all 225 grid locations for each well-field producing from the aquifer. These individual field pressures are then superimposed to give the total interference pressure resulting from all the well-fields producing together in the aquifer.

$$P_T(r,t_1) = P_1(r,t_1) + P_2(r,t_1) + \ldots P_n(r,t_n) \qquad (4\text{-}11)$$

Once the 225 grid pressures have been calculated, then the actual mapping routine uses these 225 values to linearly interpolate 12769 pressures for printing purposes. These 12769 pressures are printed in the locations in the aquifer section at which they actually occur.

For the numerical print-out of individual well-field pressure values, the grid points are numbered consectively from 1 to 225. Grid location (0,0) is labelled point 1 and

(0,14) becomes point 15. Numbering in this manner results in point (14,0) becoming 211, while (14,14) becomes point 225.

Because of the difference in the horizontal and vertical character spacing for the I.B.M. 360/50 software, the square grid section is distorted into a rectangular section. This causes circular contours to appear in the maps as ellipses.

This program is designed so that the contour interval and reference pressure can be varied for each map produced. Maps of the pressure distribution resulting from each individual well-field producing alone in the aquifer can be produced as well as a map of the pressure distribution resulting from all the well-fields interfering.

The mapping routine itself is quite versatile and can be separated if desired from the problem investigated and used alone for mapping any parameter. The 225 values to be mapped can be read in as data or generated internally by a computer routine.

For rapid analysis of the maps produced, a plastic grid-overlay (See Insert No. 1) can be used. This overlay contains the well-field locations and the various grid lines and allows rapid visualization of the pressures at various points in the aquifer section without additional detail being added which would make the maps themselves more difficult to interpret.

The application of the mapping routine is discussed in Section 5.5 for a typical field problem.

CHAPTER 5

APPLICATION OF RESULTS

5.1 Use of Tables to Check Their Accuracy

Problem: Given a dimensionless time of .10 and a fractional dimensionless pressure, PD' of .50, use Table 4-1 and Table 4-7 to check their accuracy.

1.) From Table 4-1, for RD = 1.0 and TD = .10:

$PD(1,TD) = .3142$

2.) From Table 4-7, for TD = .10 and PD' = .50:

$RD - 1.0 = .1998$

$RD = 1.1998$

$RD \doteq 1.20$

3.) From Table 4-1, for RD = 1.2 and TD = .10:

$PD(1.2,.10) = .1556$

4.) Thus:

$$PD' = \frac{PD(1.2,.10)}{PD(1.0,.10)} = \frac{.1556}{.3142} = .495$$

$PD' = .495$

5.) Comparing the calculated PD' of .495 to the given PD' of .500 results in an error of only .005 in the value of the fractional dimensionless pressure. This error would be insignificant when using Tables 4-1 and 4-7 to solve practical field problems.

5.2 Use of the Tables to Plot Curves Not Given in the Work Plots

Problem: Using Table 4-1 establish a (RD-1) curve of .10.

1.) From Table 4-1, letting RD = 1.1

RD - 1.0 = .10

then if TD = 1000: PD(1.1,1000) = 3.767
and TD = 1000: PD(1.0,1000) = 3.859

thus: PD' = 3.767/3.859 = .975

Point 1. PD' = .975

2.) By the same procedure:

TD = 100: PD(1.1,100) = 2.627
TD = 100: PD(1.0,100) = 2.723

then: PD' = .965

Point 2. PD' = .965

3.) Also:

TD = 1.0: PD(1.1,1.0) = .7084
TD = 1.0: PD(1.0,1.0) = .8021

so: PD' = .883

Point 3. PD' = .883

4.) Points 1, 2, and 3 are then plotted on Insert 9 (as shown). If more points were obtained by choosing other TD values when RD = 1.1, then the (RD-1) = .10 curve could be drawn as shown in Insert 9.

5.) In order to check the accuracy of the new curve plotted one more intermediate point on the curve is calculated.

TD = 10: PD(1.1,10) = 1.556
TD = 10: PD(1.0,10) = 1.651

thus: PD' = .943

Point 4. PD' = .943 and from Insert 9 at TD = 10 it can be seen that PD' = .943

5.3 Use of the Work Plots to Calculate PD',(RD-1), and TD If Any Two of These Parameters are Given and the Third Is Desired

Problem: Find the dimensionless radius ratio, RD, at which there is a fractional dimensionless pressure-drop, PD', of .53 when the dimensionless time, TD, is .153.

The value of (RD-1) can be estimated from any of the three work plots, but it is desired to show here a method which will allow the answer to be obtained without guessing.

1.) Go to Insert 8 (Figure 4-2) and find (RD-1) values for at least 1 TD value on either side of TD = .153 for PD' = .53.

Point A: (RD-1) = .185 @ TD = .10
Point B: (RD-1) = .295 @ TD = .30
Point C: (RD-1) = .490 @ TD = 1.0

The above points are shown on Insert 8.

2.) Using the three sets of (RD-1) and TD values from step 1, plot a PD' = .53 curve on Insert 7 (Figure 4-1).

3.) Find the value of (RD-1) when TD = .153 by using the new PD' = .53 curve plotted in Step 2.

(RD-1) = .223 (PD' = .53 & TD = .153) Point X

4.) Add 1.0 to the (RD-1) value obtained to get RD.

RD = 1.223

Problem 5.32: Find the dimensionless time, TD, at which the fractional dimensionless pressure-drop, PD' = .232 at a RD value of 1.57.

1.) Go to Insert 9 and find TD values for at least 1 (RD-1) value on either side of (RD-1) = .57 for PD' = .232.

Point K - TD = .103 @ (RD-1) = .40
Point L - TD = .183 @ (RD-1) = .50
Point M - TD = .355 @ (RD-1) = .70
Point N - TD = .790 @ (RD-1) = 1.0

The above points are shown on Insert 9.

2.) Using the four sets of TD and (RD-1) values from Step 1, plot a PD' = .232 curve on Insert 7.

3.) Find the value of TD when (RD-1) = .57 by using the new PD' = .232 curve plotted in Step 2.

TD = .230 (PD' = .232 & (RD-1) = .57)

Problem 5.33: Find the fractional dimensionless pressure, PD' at a radius ratio, RD = 27 when TD = 350.

1.) Go to Insert 7 and find PD' values for at least 1 TD value on either side of TD = 350 for (RD-1) = 26.

Point D - PD' = .01 @ TD = 93
Point E - PD' = .02 @ TD = 130
Point F - PD' = .05 @ TD = 230
Point G - PD' = .10 @ TD = 440

The above points are shown on Insert 7.

2.) Using the four sets of TD and PD' values from Step 1, plot a (RD-1) = 26 curve on Insert 9.

3.) Find the value of PD' when TD = 350 by using the new (RD-1) = 26 curve plotted in Step 2.

PD' = .08

Thus by using the techniques shown in Problems 5.31, 5.32, and 5.33 it is possible to solve any field problem involving the fractional dimensionless pressure-drop, PD', the dimensionless time, TD, and the dimensionless radius ratio, RD. Furthermore, it has been shown that the solutions to these problems can be obtained without inaccurate estimation or interpolation.

5.4 Calculation of an Effective Drainage Radius

Problem: An observation well is located in an infinite radial aquifer 3.57 miles from a new municipal well-field which is starting production. If the new field pumps 5000 bbls/day, when will the observation well be included in the well-field's drainage radius? Also, find the radius of drainage after two months of constant production.

Aquifer Data:

Porosity - 15%

Permeability - 200 md.

Compressibility of the water - 5×10^{-6} vol/vol/psi.

Viscosity of water - 1 cp.

Well-field Data:

Field radius - 528 ft.

Starting with the radius of drainage equation developed in this study, the dimensionless time TD is calculated.

$$RD = 2.915\ (TD)^{.48241} + 1.0$$

$$\frac{RD - 1.0}{2.915} = (TD)^{.48241}$$

Then from the statement of the problem and the well-field data:

$$RD = \frac{3.57}{.10} = 35.7$$

thus:

$$34.7/2.915 = (TD)^{.48241}$$

TD = 170 (Also from Figure 4-1, TD is 170) at (RD-1) of 34.7

The surface area of the well-field is:

$$\text{Area} = 640\ (r_w)^2(3.14)$$

$$A = 640(.10)^2(3.14)$$

$$A = 20.1 \text{ acres}$$

$$TD = 170 = \frac{Kt(4.56 \times 10^{-7})}{\phi \mu c_w A}$$

thus:

$$t = \frac{170(.15)(1.0)(20.1)(5 \times 10^{-6})}{200(4.56 \times 10^{-7})}$$

$$t = 28.1 \text{ days}$$

Thus the observation well will be inside the effective drainage area of the well-field at the ends of 28.1 days, regardless of the pumping rate.

At the end of two months production:

$$TD = \frac{200(61)(4.56 \times 10^{-7})}{(.15)(1.0)(20.1)(5 \times 10^{-6})}$$

$$TD = 369$$

then going to the drainage equation:

$$RD = 2.915\ (369)^{.48241} + 1.0$$

$$RD = 2.915(17.3) + 1.0$$

$$RD = 51.4$$

then since RD = r/r_w:

$$r = RD(r_w) = 51.4(.10) = 5.14 \text{ miles}$$

The radius of drainage at the end of two months will be 5.14 miles away from the center of the well-field.

5.5 On-line Mapping of Interference Pressure-Drop in a Radial Aquifer

Problem: Map the areal pressure-drop distribution in an extensive aquifer containing 2 municipal well-fields and one waste-disposal well-field. The following information is available for the system.

Aquifer Data:

Shape - Radial
Radius - 200 miles
Permeability - 200 md.
Porosity - 10%
Thickness - 90 ft.
Viscosity of water - 1 cp.
Compressibility of water - 5×10^{-6} vol/vol/psi
Depth of aquifer - 800 ft.

Well-field Information:

Field No. 1 - Waste Disposal
Location - 6.5 mi. south of Point A
3.5 mi. east of Point A
Field Radius - .75 mi.
Injection Rate - 2500 bbls/day
Injection Period - 1000 days

Field No. 2 - Municipal Supply
Location - 7.0 mi south of Point A
- 7.0 mi east of Point A
Field Radius - 1 mi.
Producing Rate - 5000 bbls/day
Producing Period - 2000 days

Field No. 3 - Municipal Supply
Location - 11.0 mi. south of Point A
- 1.5 mi. east of Point A
Field Radius - 1.5 mi.
Producing Rate - 7500 bbls/day
Producing Period - 4000 days

Point A is taken as grid location (0,0) and the data is read into Program No. 3 as described in Section 6.63, page 188. Inserts 2 through 6 are the maps of the aquifer pressure-drop distribution produced for this problem. The values of the individual contours can be determined either from Table 4-11 or from the overlay in conjunction with the print-out of the pressure-drops occurring at the various grid points (See Tables 5-1 to 5-4).

As can be seen from Inserts 2 and 3, the proper choice of contour interval can greatly improve the ease of map interpretation. Insert 2 was produced with a contour interval of 5 psi. and the areal pressure-drop distribution can be readily visualized. Insert 3, which is also a map of the total pressure-drop, used a 1 psi. contour interval. This insert, while serving to point out the detailed pressure-drop distribution, has become somewhat harder to rapidly examine for over-all distribution.

This example, while not an actual field problem, is presented in order to demonstrate the type of results obtained for the solution of a typical aquifer mapping problem. The problem presented here is concerned with water supply reservoirs rather than producing oil fields but the mapping

occurs in the same manner for both types of problems.

In order to verify the correctness of the maps produced the total pressure-drop at one grid point is calculated by slide rule in the following manner.

At grid-point (4,6) (point 80 is the individual well-field print-outs) the total pressure-drop is the sum of the pressure-drops resulting from the three well-fields producing alone in the aquifer. These individual pressure-drops are:

A. Pressure-drop resulting from Field 1 injecting alone in the aquifer.

well-field area = $3.14(.75)^2(640) = 1130$ acres

$$TD = Kt/\phi\mu cA = \frac{4.56 \times 10^{-7}(1000)(200)}{.10(.30)(5 \times 10^{-6})(1130)}$$

$$TD_1 = 537.$$

$$P_1(r,t) = \frac{887.6(.30)(-2500)}{6.28(200)(90)} \; PD(RD,TD)$$

The radial distance from point (4,6) to the location of the center of well-field 1 at (3.5, 6.5) is:

$$r_1 = SQRT\ ((4.0 - 3.5)^2 + (6.0 - 6.5)^2)$$

$$r_1 = .707 \text{ mi.}$$

The radius of well-field 1 is .75 mi., therefore:

$$RD = .707/.75 = .944$$

Since RD<1.0, point 80 must lie inside the boundary of well-field 1 and therefore it is assumed to have the same pressure-drop as exists at RD = 1.0.

By means of Table 4-1 the value of dimensionless pressure, PD(1,537) is found by interpolation:

$$PD(1,537) = 3.548$$

thus:

$$P_1(r,t) = \frac{(887.6)(.30)(-2500)(3.548)}{6.28(200)(90)}$$

$$P_1(r,t) = -20.9 \text{ psi.} \quad \text{(Computer result = -18.5 psi.)}$$

B. Pressure-drop resulting from well-field 2 producing alone from the aquifer.

well-field area = $3.14(1)^2(640) = 2010$ acres

$$TD/\phi\mu cA = \frac{4.56 \times 10^{-7}(200)(2000)}{.10(.30)(5 \times 10^{-6})(2010)} = 605$$

$$TD_2 = 605$$

The radial distance between point (4,6) and the location of the center of well-field 2 at (7.0, 7.0) is:

$$r_2 = \text{SQRT}\ ((7.0 - 4.0)^2 + (7.0 - 6.0)^2)$$

$$r_2 = 3.16 \text{ mi.}$$

The radius of well-field 2 is 1.0 mile, therefore:

$$RD = 3.16$$

From Table 4-1, PD(3.16, 605) is found by double interpolation between TD rows and between RD columns as:

$$PD(3.16, 605) = 2.461$$

thus:

$$P_2(r,t) = \frac{887.6(.30)(5000)(2.461)}{6.28(200)(90)}$$

$P_2(r,t)$ = 29.0 psi. (Computer result = 27.4 psi.)

C. Pressure-drop resulting from well-field 3 producing alone in the aquifer.

well-field area = $3.14(1.5)^2(640)$ = 4525 acres

$$TD_3 = kt/\phi\mu cA = \frac{4.56 \times 10^{-7}(200)(4000)}{(.10)(.30)(5 \times 10^{-6})(4525)}$$

TD_3 = 537

The radial distance between point (4,6) and the location of well-field's 3 center at (11.0, 1.5) is:

$$r_3 = \text{SQRT}((4. - 11.)^2 + (6. - 1.5)^2)$$

r_3 = 8.32 mi.

The radius of well-field 3 is 1.5 mi., therefore:

RD_3 = 5.55

From Table 4-2, PD(5.55, 537) is found by double interpolation to be:

PD(5.55, 537) = 1.851

thus:

$$P_3(r,t) = \frac{887.6(.30)(7500)(1.851)}{6.28(200)(90)}$$

$P_3(r,t)$ = 32.8 psi. (Computer result = 36.8 psi.)

Therefore, the total pressure-drop experienced when all 3 well-fields interfere is:

$$P_T(r,t) = P_1(r,t) + P_2(r,t) + P_3(r,t)$$

$$P_T(r,t) = -20.9 + 29.0 + 32.8$$

$$P_T(r,t) = 50.9 \text{ psi.} \quad \text{(Computer result = 45.5 psi.)}$$

Using the plastic overlay on the map of total pressure-drop contoured at 1 psi. intervals (Insert 3) it is found that the pressure-drop at point (4,6) is represented on the map as a (W). A (W) indicates (by referring to Table 4-11) that the pressure-drop at point (4,6) is 46 contour intervals above the reference pressure-drop which in this case is 0 psi. The symbol (W) produced on the map is therefore the proper symbol to represent the actual pressure-drop of 45.5 psi.

The values of the pressure-drop calculated in this example differ slightly from those calculated by the computer due to the interpolation performed and because of slide-rule error.

TABLE 5-1

CHANGE AT VARIOUS GRID-POINTS RESULTING FROM 3 FIELDS

X-COOD.	Y-COOD.	PRESSURE CHANGE
0.0	0.0	33.7113
1.0000	0.0	34.3227
2.0000	0.0	34.8636
3.0000	0.0	35.3316
4.0000	0.0	35.7107
5.0000	0.0	35.9662
6.0000	0.0	36.0501
7.0000	0.0	35.9167
8.0000	0.0	35.5411
9.0000	0.0	34.9288
10.0000	0.0	34.1122
11.0000	0.0	33.1387
12.0000	0.0	32.0579
13.0000	0.0	30.9137
14.0000	0.0	29.7404
0.0	1.0000	35.4118
1.0000	1.0000	36.0878
2.0000	1.0000	36.7005
3.0000	1.0000	37.2632
4.0000	1.0000	37.7657
5.0000	1.0000	38.1573
6.0000	1.0000	38.3523
7.0000	1.0000	38.2645
8.0000	1.0000	37.8471
9.0000	1.0000	37.1115
10.0000	1.0000	36.1163
11.0000	1.0000	34.9398
12.0000	1.0000	33.6554
13.0000	1.0000	32.3213
14.0000	1.0000	30.9781
0.0	2.0000	37.2044
1.0000	2.0000	37.9281
2.0000	2.0000	38.5953
3.0000	2.0000	39.2591
4.0000	2.0000	39.9370
5.0000	2.0000	40.5564

6.0000	2.0000	40.9564
7.0000	2.0000	40.9647
8.0000	2.0000	40.4915
9.0000	2.0000	39.5687
10.0000	2.0000	38.3127
11.0000	2.0000	36.8575
12.0000	2.0000	35.3115
13.0000	2.0000	33.7473
14.0000	2.0000	32.2084
0.0	3.0000	39.1101
1.0000	3.0000	39.8399
2.0000	3.0000	40.5002
3.0000	3.0000	41.2358
4.0000	3.0000	42.1616
5.0000	3.0000	43.1846
6.0000	3.0000	43.9796
7.0000	3.0000	44.1813
8.0000	3.0000	43.6123
9.0000	3.0000	42.3728
10.0000	3.0000	40.7149
11.0000	3.0000	38.8717
12.0000	3.0000	36.9927
13.0000	3.0000	35.1567
14.0000	3.0000	33.3996
0.0	4.0000	41.1840
1.0000	4.0000	41.8477
2.0000	4.0000	42.3409
3.0000	4.0000	42.9941
4.0000	4.0000	44.2545
5.0000	4.0000	46.0455
6.0000	4.0000	47.6433
7.0000	4.0000	48.2348
8.0000	4.0000	47.4419
9.0000	4.0000	45.6001
10.0000	4.0000	43.2982
11.0000	4.0000	40.9215
12.0000	4.0000	38.6360
13.0000	4.0000	36.4957
14.0000	4.0000	34.5088
0.0	5.0000	43.5499
1.0000	5.0000	44.0810
2.0000	5.0000	44.0805
3.0000	5.0000	44.0477
4.0000	5.0000	45.6955
5.0000	5.0000	49.1070
6.0000	5.0000	52.3931
7.0000	5.0000	53.8421
8.0000	5.0000	52.3664
9.0000	5.0000	49.2494
10.0000	5.0000	45.9310
11.0000	5.0000	42.8748
12.0000	5.0000	40.1396
13.0000	5.0000	37.6909
14.0000	5.0000	35.4838
0.0	6.0000	46.4252
1.0000	6.0000	46.9183
2.0000	6.0000	46.1612
3.0000	6.0000	43.5833
4.0000	6.0000	45.4876
5.0000	6.0000	52.4032

6.0000	6.0000	58.8933
7.0000	6.0000	63.1433
8.0000	6.0000	58.7985
9.0000	6.0000	52.9253
10.0000	6.0000	48.2613
11.0000	6.0000	44.5092
12.0000	6.0000	41.3680
13.0000	6.0000	38.6579
14.0000	6.0000	36.2696
0.0	7.0000	50.0648
1.0000	7.0000	50.9520
2.0000	7.0000	50.2645
3.0000	7.0000	47.4608
4.0000	7.0000	49.0880
5.0000	7.0000	56.1396
6.0000	7.0000	64.9124
7.0000	7.0000	64.6969
8.0000	7.0000	64.1281
9.0000	7.0000	55.2565
10.0000	7.0000	49.7202
11.0000	7.0000	45.5653
12.0000	7.0000	42.1882
13.0000	7.0000	39.3209
14.0000	7.0000	36.8197
0.0	8.0000	54.6414
1.0000	8.0000	56.5424
2.0000	8.0000	56.7257
3.0000	8.0000	55.7527
4.0000	8.0000	56.1805
5.0000	8.0000	59.0573
6.0000	8.0000	63.5037
7.0000	8.0000	66.5675
8.0000	8.0000	61.4399
9.0000	8.0000	55.0170
10.0000	8.0000	49.9524
11.0000	8.0000	45.9000
12.0000	8.0000	42.5284
13.0000	8.0000	39.6384
14.0000	8.0000	37.1073
0.0	9.0000	60.1983
1.0000	9.0000	64.0782
2.0000	9.0000	64.8144
3.0000	9.0000	62.7912
4.0000	9.0000	60.9494
5.0000	9.0000	60.5244
6.0000	9.0000	60.8938
7.0000	9.0000	60.3211
8.0000	9.0000	57.4278
9.0000	9.0000	53.2894
10.0000	9.0000	49.2156
11.0000	9.0000	45.5878
12.0000	9.0000	42.4113
13.0000	9.0000	39.6158
14.0000	9.0000	37.1319
0.0	10.0000	66.2672
1.0000	10.0000	70.1551
2.0000	10.0000	71.0663
3.0000	10.0000	69.1752
4.0000	10.0000	64.0151
5.0000	10.0000	61.0399

6.0000	10.0000	59.1331
7.0000	10.0000	57.1834
8.0000	10.0000	54.5401
9.0000	10.0000	51.3300
10.0000	10.0000	47.9972
11.0000	10.0000	44.8293
12.0000	10.0000	41.9262
13.0000	10.0000	39.2962
14.0000	10.0000	36.9155
0.0	11.0000	69.6801
1.0000	11.0000	70.3689
2.0000	11.0000	71.2646
3.0000	11.0000	72.4301
4.0000	11.0000	64.8533
5.0000	11.0000	60.4956
6.0000	11.0000	57.4985
7.0000	11.0000	54.9210
8.0000	11.0000	52.2765
9.0000	11.0000	49.4631
10.0000	11.0000	46.5936
11.0000	11.0000	43.8041
12.0000	11.0000	41.1757
13.0000	11.0000	38.7384
14.0000	11.0000	36.4928
0.0	12.0000	66.4710
1.0000	12.0000	70.3811
2.0000	12.0000	71.1884
3.0000	12.0000	68.9054
4.0000	12.0000	62.9138
5.0000	12.0000	58.7095
6.0000	12.0000	55.5258
7.0000	12.0000	52.8081
8.0000	12.0000	50.2301
9.0000	12.0000	47.6638
10.0000	12.0000	45.1108
11.0000	12.0000	42.6212
12.0000	12.0000	40.2416
13.0000	12.0000	37.9988
14.0000	12.0000	35.9021
0.0	13.0000	60.6310
1.0000	13.0000	64.6422
2.0000	13.0000	65.3432
3.0000	13.0000	62.7268
4.0000	13.0000	59.2005
5.0000	13.0000	55.9570
6.0000	13.0000	53.1372
7.0000	13.0000	50.6019
8.0000	13.0000	48.2063
9.0000	13.0000	45.8701
10.0000	13.0000	43.5749
11.0000	13.0000	41.3366
12.0000	13.0000	39.1796
13.0000	13.0000	37.1233
14.0000	13.0000	35.1782
0.0	14.0000	55.2999
1.0000	14.0000	57.5686
2.0000	14.0000	58.1681
3.0000	14.0000	57.0852
4.0000	14.0000	55.0605
5.0000	14.0000	52.7607

6.0000	14.0000	50.4798
7.0000	14.0000	48.2807
8.0000	14.0000	46.1461
9.0000	14.0000	44.0530
10.0000	14.0000	41.9952
11.0000	14.0000	39.9815
12.0000	14.0000	38.0274
13.0000	14.0000	36.1473
14.0000	14.0000	34.3513

TABLE 5-2

PRESSURE CHANGES AT VARIOUS GRID-POINTS CAUSED BY FIELD 1

P(1 1)=	-9.5300
P(2 1)=	-9.8660
P(3 1)=	-10.1145
P(4 1)=	-10.2475
P(5 1)=	-10.2475
P(6 1)=	-10.1145
P(7 1)=	-9.8660
P(8 1)=	-9.5300
P(9 1)=	-9.1365
P(10 1)=	-8.7117
P(11 1)=	-8.2753
P(12 1)=	-7.8408
P(13 1)=	-7.4169
P(14 1)=	-7.0085
P(15 1)=	-6.6184
P(16 1)=	-10.2475
P(17 1)=	-10.6881
P(18 1)=	-11.0249
P(19 1)=	-11.2094
P(20 1)=	-11.2094
P(21 1)=	-11.0249
P(22 1)=	-10.6881
P(23 1)=	-10.2475
P(24 1)=	-9.7495
P(25 1)=	-9.2298
P(26 1)=	-8.7117
P(27 1)=	-8.2089
P(28 1)=	-7.7285
P(29 1)=	-7.2737
P(30 1)=	-6.8455
P(31 1)=	-11.0249
P(32 1)=	-11.6183
P(33 1)=	-12.0950
P(34 1)=	-12.3666
P(35 1)=	-12.3666
P(36 1)=	-12.0950
P(37 1)=	-11.6183
P(38 1)=	-11.0249
P(39 1)=	-10.3869
P(40 1)=	-9.7495
P(41 1)=	-9.1365
P(42 1)=	-8.5585
P(43 1)=	-8.0186

```
P(  44  1)=     -7.5168
P(  45  1)=     -7.0509
P(  46  1)=    -11.8468
P(  47  1)=    -12.6663
P(  48  1)=    -13.3784
P(  49  1)=    -13.8128
P(  50  1)=    -13.8128
P(  51  1)=    -13.3784
P(  52  1)=    -12.6663
P(  53  1)=    -11.8468
P(  54  1)=    -11.0249
P(  55  1)=    -10.2475
P(  56  1)=     -9.5300
P(  57  1)=     -8.8739
P(  58  1)=     -8.2753
P(  59  1)=     -7.7285
P(  60  1)=     -7.2276
P(  61  1)=    -12.6663
P(  62  1)=    -13.8128
P(  63  1)=    -14.9430
P(  64  1)=    -15.7300
P(  65  1)=    -15.7300
P(  66  1)=    -14.9430
P(  67  1)=    -13.8128
P(  68  1)=    -12.6663
P(  69  1)=    -11.6183
P(  70  1)=    -10.6881
P(  71  1)=     -9.8660
P(  72  1)=     -9.1365
P(  73  1)=     -8.4849
P(  74  1)=     -7.8988
P(  75  1)=     -7.3683
P(  76  1)=    -13.3784
P(  77  1)=    -14.9430
P(  78  1)=    -16.8098
P(  79  1)=    -18.5373
P(  80  1)=    -18.5373
P(  81  1)=    -16.8098
P(  82  1)=    -14.9430
P(  83  1)=    -13.3784
P(  84  1)=    -12.0950
P(  85  1)=    -11.0249
P(  86  1)=    -10.1145
P(  87  1)=     -9.3264
P(  88  1)=     -8.6340
P(  89  1)=     -8.0186
P(  90  1)=     -7.4664
P(  91  1)=    -13.8128
P(  92  1)=    -15.7300
P(  93  1)=    -18.5373
P(  94  1)=    -22.9249
P(  95  1)=    -22.9249
P(  96  1)=    -18.5373
P(  97  1)=    -15.7300
P(  98  1)=    -13.8128
P(  99  1)=    -12.3666
P( 100  1)=    -11.2094
P( 101  1)=    -10.2475
P( 102  1)=     -9.4263
P( 103  1)=     -8.7117
```

```
P(  104   1)=      -8.0806
P(  105   1)=      -7.5168
P(  106   1)=     -13.8128
P(  107   1)=     -15.7300
P(  108   1)=     -18.5373
P(  109   1)=     -22.9249
P(  110   1)=     -22.9249
P(  111   1)=     -18.5373
P(  112   1)=     -15.7300
P(  113   1)=     -13.8128
P(  114   1)=     -12.3666
P(  115   1)=     -11.2094
P(  116   1)=     -10.2475
P(  117   1)=      -9.4263
P(  118   1)=      -8.7117
P(  119   1)=      -8.0806
P(  120   1)=      -7.5168
P(  121   1)=     -13.3784
P(  122   1)=     -14.9430
P(  123   1)=     -16.8098
P(  124   1)=     -18.5373
P(  125   1)=     -18.5373
P(  126   1)=     -16.8098
P(  127   1)=     -14.9430
P(  128   1)=     -13.3784
P(  129   1)=     -12.0950
P(  130   1)=     -11.0249
P(  131   1)=     -10.1145
P(  132   1)=      -9.3264
P(  133   1)=      -8.6340
P(  134   1)=      -8.0186
P(  135   1)=      -7.4664
P(  136   1)=     -12.6663
P(  137   1)=     -13.8128
P(  138   1)=     -14.9430
P(  139   1)=     -15.7300
P(  140   1)=     -15.7300
P(  141   1)=     -14.9430
P(  142   1)=     -13.8128
P(  143   1)=     -12.6663
P(  144   1)=     -11.6183
P(  145   1)=     -10.6881
P(  146   1)=      -9.8660
P(  147   1)=      -9.1365
P(  148   1)=      -8.4849
P(  149   1)=      -7.8988
P(  150   1)=      -7.3683
P(  151   1)=     -11.8468
P(  152   1)=     -12.6663
P(  153   1)=     -13.3784
P(  154   1)=     -13.8128
P(  155   1)=     -13.8128
P(  156   1)=     -13.3784
P(  157   1)=     -12.6663
P(  158   1)=     -11.8468
P(  159   1)=     -11.0249
P(  160   1)=     -10.2475
P(  161   1)=      -9.5300
P(  162   1)=      -8.8739
P(  163   1)=      -8.2753
```

```
P(  164   1)=      -7.7285
P(  165   1)=      -7.2276
P(  166   1)=     -11.0249
P(  167   1)=     -11.6183
P(  168   1)=     -12.0950
P(  169   1)=     -12.3666
P(  170   1)=     -12.3666
P(  171   1)=     -12.0950
P(  172   1)=     -11.6183
P(  173   1)=     -11.0249
P(  174   1)=     -10.3869
P(  175   1)=      -9.7495
P(  176   1)=      -9.1365
P(  177   1)=      -8.5585
P(  178   1)=      -8.0186
P(  179   1)=      -7.5168
P(  180   1)=      -7.0509
P(  181   1)=     -10.2475
P(  182   1)=     -10.6881
P(  183   1)=     -11.0249
P(  184   1)=     -11.2094
P(  185   1)=     -11.2094
P(  186   1)=     -11.0249
P(  187   1)=     -10.6881
P(  188   1)=     -10.2475
P(  189   1)=      -9.7495
P(  190   1)=      -9.2298
P(  191   1)=      -8.7117
P(  192   1)=      -8.2089
P(  193   1)=      -7.7285
P(  194   1)=      -7.2737
P(  195   1)=      -6.8455
P(  196   1)=      -9.5300
P(  197   1)=      -9.8660
P(  198   1)=     -10.1145
P(  199   1)=     -10.2475
P(  200   1)=     -10.2475
P(  201   1)=     -10.1145
P(  202   1)=      -9.8660
P(  203   1)=      -9.5300
P(  204   1)=      -9.1365
P(  205   1)=      -8.7117
P(  206   1)=      -8.2753
P(  207   1)=      -7.8408
P(  208   1)=      -7.4169
P(  209   1)=      -7.0085
P(  210   1)=      -6.6184
P(  211   1)=      -8.8739
P(  212   1)=      -9.1365
P(  213   1)=      -9.3264
P(  214   1)=      -9.4263
P(  215   1)=      -9.4263
P(  216   1)=      -9.3264
P(  217   1)=      -9.1365
P(  218   1)=      -8.8739
P(  219   1)=      -8.5585
P(  220   1)=      -8.2089
P(  221   1)=      -7.8408
P(  222   1)=      -7.4664
P(  223   1)=      -7.0940
P(  224   1)=      -6.7295
P(  225   1)=      -6.3764
```

TABLE 5-3

PRESSURE CHANGES AT VARIOUS GRID-POINTS CAUSED BY FIELD 2

P(1 2)=	15.7104
P(2 2)=	16.5171
P(3 2)=	17.3065
P(4 2)=	18.0482
P(5 2)=	18.7020
P(6 2)=	19.2206
P(7 2)=	19.5564
P(8 2)=	19.6729
P(9 2)=	19.5564
P(10 2)=	19.2206
P(11 2)=	18.7020
P(12 2)=	18.0482
P(13 2)=	17.3065
P(14 2)=	16.5171
P(15 2)=	15.7104
P(16 2)=	16.5171
P(17 2)=	17.4629
P(18 2)=	18.4124
P(19 2)=	19.3304
P(20 2)=	20.1645
P(21 2)=	20.8457
P(22 2)=	21.2974
P(23 2)=	21.4562
P(24 2)=	21.2974
P(25 2)=	20.8457
P(26 2)=	20.1645
P(27 2)=	19.3304
P(28 2)=	18.4124
P(29 2)=	17.4629
P(30 2)=	16.5171
P(31 2)=	17.3065
P(32 2)=	18.4124
P(33 2)=	19.5564
P(34 2)=	20.7028
P(35 2)=	21.7878
P(36 2)=	22.7120
P(37 2)=	23.3475
P(38 2)=	23.5759
P(39 2)=	23.3475
P(40 2)=	22.7120
P(41 2)=	21.7878
P(42 2)=	20.7028
P(43 2)=	19.5564
P(44 2)=	18.4124
P(45 2)=	17.3065
P(46 2)=	18.0482
P(47 2)=	19.3304
P(48 2)=	20.7028
P(49 2)=	22.1398
P(50 2)=	23.5760

```
P(  51  2)=      24.8773
P(  52  2)=      25.8266
P(  53  2)=      26.1810
P(  54  2)=      25.8266
P(  55  2)=      24.8773
P(  56  2)=      23.5760
P(  57  2)=      22.1398
P(  58  2)=      20.7028
P(  59  2)=      19.3304
P(  60  2)=      18.0482
P(  61  2)=      18.7020
P(  62  2)=      20.1645
P(  63  2)=      21.7878
P(  64  2)=      23.5760
P(  65  2)=      25.4926
P(  66  2)=      27.3959
P(  67  2)=      28.9329
P(  68  2)=      29.5507
P(  69  2)=      28.9329
P(  70  2)=      27.3959
P(  71  2)=      25.4926
P(  72  2)=      23.5760
P(  73  2)=      21.7878
P(  74  2)=      20.1645
P(  75  2)=      18.7020
P(  76  2)=      19.2206
P(  77  2)=      20.8457
P(  78  2)=      22.7120
P(  79  2)=      24.8773
P(  80  2)=      27.3959
P(  81  2)=      30.2415
P(  82  2)=      33.0007
P(  83  2)=      34.3117
P(  84  2)=      33.0007
P(  85  2)=      30.2415
P(  86  2)=      27.3959
P(  87  2)=      24.8773
P(  88  2)=      22.7120
P(  89  2)=      20.8457
P(  90  2)=      19.2206
P(  91  2)=      19.5564
P(  92  2)=      21.2974
P(  93  2)=      23.3475
P(  94  2)=      25.8266
P(  95  2)=      28.9329
P(  96  2)=      33.0007
P(  97  2)=      38.3867
P(  98  2)=      42.4642
P(  99  2)=      38.3867
P( 100  2)=      33.0007
P( 101  2)=      28.9329
P( 102  2)=      25.8266
P( 103  2)=      23.3475
P( 104  2)=      21.2974
P( 105  2)=      19.5564
P( 106  2)=      19.6729
P( 107  2)=      21.4562
P( 108  2)=      23.5759
P( 109  2)=      26.1810
P( 110  2)=      29.5507
```

```
P(  111   2)=      34.3117
P(  112   2)=      42.4642
P(  113   2)=      42.4642
P(  114   2)=      42.4642
P(  115   2)=      34.3117
P(  116   2)=      29.5507
P(  117   2)=      26.1810
P(  118   2)=      23.5759
P(  119   2)=      21.4562
P(  120   2)=      19.6729
P(  121   2)=      19.5564
P(  122   2)=      21.2974
P(  123   2)=      23.3475
P(  124   2)=      25.8266
P(  125   2)=      28.9329
P(  126   2)=      33.0007
P(  127   2)=      38.3867
P(  128   2)=      42.4642
P(  129   2)=      38.3867
P(  130   2)=      33.0007
P(  131   2)=      28.9329
P(  132   2)=      25.8266
P(  133   2)=      23.3475
P(  134   2)=      21.2974
P(  135   2)=      19.5564
P(  136   2)=      19.2206
P(  137   2)=      20.8457
P(  138   2)=      22.7120
P(  139   2)=      24.8773
P(  140   2)=      27.3959
P(  141   2)=      30.2415
P(  142   2)=      33.0007
P(  143   2)=      34.3117
P(  144   2)=      33.0007
P(  145   2)=      30.2415
P(  146   2)=      27.3959
P(  147   2)=      24.8773
P(  148   2)=      22.7120
P(  149   2)=      20.8457
P(  150   2)=      19.2206
P(  151   2)=      18.7020
P(  152   2)=      20.1645
P(  153   2)=      21.7878
P(  154   2)=      23.5760
P(  155   2)=      25.4926
P(  156   2)=      27.3959
P(  157   2)=      28.9329
P(  158   2)=      29.5507
P(  159   2)=      28.9329
P(  160   2)=      27.3959
P(  161   2)=      25.4926
P(  162   2)=      23.5760
P(  163   2)=      21.7878
P(  164   2)=      20.1645
P(  165   2)=      18.7020
P(  166   2)=      18.0482
P(  167   2)=      19.3304
P(  168   2)=      20.7028
P(  169   2)=      22.1398
P(  170   2)=      23.5760
```

```
P(  171   2)=       24.8773
P(  172   2)=       25.8266
P(  173   2)=       26.1810
P(  174   2)=       25.8266
P(  175   2)=       24.8773
P(  176   2)=       23.5760
P(  177   2)=       22.1398
P(  178   2)=       20.7028
P(  179   2)=       19.3304
P(  180   2)=       18.0482
P(  181   2)=       17.3065
P(  182   2)=       18.4124
P(  183   2)=       19.5564
P(  184   2)=       20.7028
P(  185   2)=       21.7878
P(  186   2)=       22.7120
P(  187   2)=       23.3475
P(  188   2)=       23.5759
P(  189   2)=       23.3475
P(  190   2)=       22.7120
P(  191   2)=       21.7878
P(  192   2)=       20.7028
P(  193   2)=       19.5564
P(  194   2)=       18.4124
P(  195   2)=       17.3065
P(  196   2)=       16.5171
P(  197   2)=       17.4629
P(  198   2)=       18.4124
P(  199   2)=       19.3304
P(  200   2)=       20.1645
P(  201   2)=       20.8457
P(  202   2)=       21.2974
P(  203   2)=       21.4562
P(  204   2)=       21.2974
P(  205   2)=       20.8457
P(  206   2)=       20.1645
P(  207   2)=       19.3304
P(  208   2)=       18.4124
P(  209   2)=       17.4629
P(  210   2)=       16.5171
P(  211   2)=       15.7104
P(  212   2)=       16.5171
P(  213   2)=       17.3065
P(  214   2)=       18.0482
P(  215   2)=       18.7020
P(  216   2)=       19.2206
P(  217   2)=       19.5564
P(  218   2)=       19.6729
P(  219   2)=       19.5564
P(  220   2)=       19.2206
P(  221   2)=       18.7020
P(  222   2)=       18.0482
P(  223   2)=       17.3065
P(  224   2)=       16.5171
P(  225   2)=       15.7104
```

TABLE 5-4

PRESSURE CHANGES AT VARIOUS GRID-POINTS CAUSED BY FIELD 3

P(	1	3) =	27.5309
P(	2	3) =	27.6717
P(	3	3) =	27.6717
P(	4	3) =	27.5309
P(	5	3) =	27.2561
P(	6	3) =	26.8601
P(	7	3) =	26.3597
P(	8	3) =	25.7738
P(	9	3) =	25.1212
P(	10	3) =	24.4199
P(	11	3) =	23.6855
P(	12	3) =	22.9314
P(	13	3) =	22.1684
P(	14	3) =	21.4052
P(	15	3) =	20.6484
P(	16	3) =	29.1422
P(	17	3) =	29.3130
P(	18	3) =	29.3130
P(	19	3) =	29.1422
P(	20	3) =	28.8106
P(	21	3) =	28.3365
P(	22	3) =	27.7430
P(	23	3) =	27.0558
P(	24	3) =	26.2993
P(	25	3) =	25.4956
P(	26	3) =	24.6636
P(	27	3) =	23.8183
P(	28	3) =	22.9715
P(	29	3) =	22.1321
P(	30	3) =	21.3065
P(	31	3) =	30.9229
P(	32	3) =	31.1340
P(	33	3) =	31.1340
P(	34	3) =	30.9229
P(	35	3) =	30.5158
P(	36	3) =	29.9395
P(	37	3) =	29.2272
P(	38	3) =	28.4137
P(	39	3) =	27.5309
P(	40	3) =	26.6062
P(	41	3) =	25.6614
P(	42	3) =	24.7132
P(	43	3) =	23.7738
P(	44	3) =	22.8517
P(	45	3) =	21.9529
P(	46	3) =	32.9088
P(	47	3) =	33.1758
P(	48	3) =	33.1758
P(	49	3) =	32.9088
P(	50	3) =	32.3984
P(	51	3) =	31.6857
P(	52	3) =	30.8193
P(	53	3) =	29.8471
P(	54	3) =	28.8106
P(	55	3) =	27.7430
P(	56	3) =	26.6689
P(	57	3) =	25.6058

```
P(  58  3) =      24.5652
P(  59  3) =      23.5548
P(  60  3) =      22.5791
P(  61  3) =      35.1482
P(  62  3) =      35.4960
P(  63  3) =      35.4960
P(  64  3) =      35.1482
P(  65  3) =      34.4919
P(  66  3) =      33.5926
P(  67  3) =      32.5232
P(  68  3) =      31.3504
P(  69  3) =      30.1273
P(  70  3) =      28.8923
P(  71  3) =      27.6717
P(  72  3) =      26.4820
P(  73  3) =      25.3331
P(  74  3) =      24.2300
P(  75  3) =      23.1750
P(  76  3) =      37.7077
P(  77  3) =      38.1783
P(  78  3) =      38.1783
P(  79  3) =      37.7077
P(  80  3) =      36.8369
P(  81  3) =      35.6753
P(  82  3) =      34.3354
P(  83  3) =      32.9088
P(  84  3) =      31.4607
P(  85  3) =      30.0328
P(  86  3) =      28.6496
P(  87  3) =      27.3239
P(  88  3) =      26.0616
P(  89  3) =      24.8638
P(  90  3) =      23.7295
P(  91  3) =      40.6816
P(  92  3) =      41.3510
P(  93  3) =      41.3510
P(  94  3) =      40.6816
P(  95  3) =      39.4796
P(  96  3) =      37.9398
P(  97  3) =      36.2366
P(  98  3) =      34.4919
P(  99  3) =      32.7783
P( 100  3) =      31.1340
P( 101  3) =      29.5759
P( 102  3) =      28.1090
P( 103  3) =      26.7322
P( 104  3) =      25.4411
P( 105  3) =      24.2300
P( 106  3) =      44.2047
P( 107  3) =      45.2258
P( 108  3) =      45.2258
P( 109  3) =      44.2047
P( 110  3) =      42.4622
P( 111  3) =      40.3652
P( 112  3) =      38.1783
P( 113  3) =      36.0455
P( 114  3) =      34.0305
P( 115  3) =      32.1542
P( 116  3) =      30.4170
P( 117  3) =      28.8106
```

```
P(  118   3)=       27.3239
P(  119   3)=       25.9453
P(  120   3)=       24.6636
P(  121   3)=       48.4634
P(  122   3)=       50.1880
P(  123   3)=       50.1880
P(  124   3)=       48.4634
P(  125   3)=       45.7848
P(  126   3)=       42.8664
P(  127   3)=       40.0599
P(  128   3)=       37.4817
P(  129   3)=       35.1482
P(  130   3)=       33.0413
P(  131   3)=       31.1340
P(  132   3)=       29.3997
P(  133   3)=       27.8150
P(  134   3)=       26.3597
P(  135   3)=       25.0173
P(  136   3)=       53.6439
P(  137   3)=       57.0453
P(  138   3)=       57.0453
P(  139   3)=       53.6439
P(  140   3)=       49.2835
P(  141   3)=       45.2258
P(  142   3)=       41.7059
P(  143   3)=       38.6757
P(  144   3)=       36.0455
P(  145   3)=       33.7361
P(  146   3)=       31.6857
P(  147   3)=       29.8471
P(  148   3)=       28.1841
P(  149   3)=       26.6689
P(  150   3)=       25.2796
P(  151   3)=       59.4120
P(  152   3)=       62.6569
P(  153   3)=       62.6569
P(  154   3)=       59.4120
P(  155   3)=       52.3353
P(  156   3)=       47.0224
P(  157   3)=       42.8664
P(  158   3)=       39.4796
P(  159   3)=       36.6321
P(  160   3)=       34.1816
P(  161   3)=       32.0347
P(  162   3)=       30.1273
P(  163   3)=       28.4136
P(  164   3)=       26.8601
P(  165   3)=       25.4411
P(  166   3)=       62.6569
P(  167   3)=       62.6569
P(  168   3)=       62.6569
P(  169   3)=       62.6569
P(  170   3)=       53.6439
P(  171   3)=       47.7134
P(  172   3)=       43.2902
P(  173   3)=       39.7649
P(  174   3)=       36.8369
P(  175   3)=       34.3354
P(  176   3)=       32.1542
P(  177   3)=       30.2227
```

```
P(  178   3)=       28.4916
P(  179   3)=       26.9248
P(  180   3)=       25.4956
P(  181   3)=       59.4120
P(  182   3)=       62.6569
P(  183   3)=       62.6569
P(  184   3)=       59.4120
P(  185   3)=       52.3353
P(  186   3)=       47.0224
P(  187   3)=       42.8664
P(  188   3)=       39.4796
P(  189   3)=       36.6321
P(  190   3)=       34.1816
P(  191   3)=       32.0347
P(  192   3)=       30.1273
P(  193   3)=       28.4136
P(  194   3)=       26.8601
P(  195   3)=       25.4411
P(  196   3)=       53.6439
P(  197   3)=       57.0453
P(  198   3)=       57.0453
P(  199   3)=       53.6439
P(  200   3)=       49.2835
P(  201   3)=       45.2258
P(  202   3)=       41.7059
P(  203   3)=       38.6757
P(  204   3)=       36.0455
P(  205   3)=       33.7361
P(  206   3)=       31.6857
P(  207   3)=       29.8471
P(  208   3)=       28.1841
P(  209   3)=       26.6689
P(  210   3)=       25.2796
P(  211   3)=       48.4634
P(  212   3)=       50.1880
P(  213   3)=       50.1880
P(  214   3)=       48.4634
P(  215   3)=       45.7848
P(  216   3)=       42.8664
P(  217   3)=       40.0599
P(  218   3)=       37.4817
P(  219   3)=       35.1482
P(  220   3)=       33.0413
P(  221   3)=       31.1340
P(  222   3)=       29.3997
P(  223   3)=       27.8150
P(  224   3)=       26.3597
P(  225   3)=       25.0173
```

CHAPTER 6

COMPUTER PROGRAMS FOR PRESSURE DISTRIBUTION AND RADIUS OF DRAINAGE

The computer programs evaluating Equation (2-17) constitute a major part of this study. This section contains the detailed descriptions of these computer programs including user instructions, flow diagrams, and summaries of program identifiers. Complete listings of all programs and subroutines are inserted at the rear of this report.

6.1 Introduction to the Programs

All the programs in this study are written in Fortran IV and developed on the IBM 360/50 system. The programs are presented in two segments; first, the mainline programs which consist of data input, various numerical operations employed, and output operations; and second, the subroutine packages which consist of the routines for performing the required repetitive calculations necessary in order to calculate PD(RD,TD).

6.2 Discussion of Subroutines Used in Programs No. 1, 2, 2A, and 3

The following section describes the subroutines contained in each of the four computer programs used in this study. These subroutines have been appropriately named SUBTB, SUBTA, ERFC, BESJO, BESYO, BESJ1, and BESY1.

1. SUBTA - Solutions to the Exponential Integral, Ei(X), for the argument $X = (RD)^2/4TD$. Two different

polynomial approximations are used, depending on the value of X relative to 1.0. These polynomial approximations are given in Section F, page 238.

2. SUBTB - The value of PD(RD,TD) is calculated for any given RD and TD values. The evaluation is accomplished by three different routines depending on the size of TD. For TD$\leq$.01 and for TD>500, simplified expressions are used to obtain PD(RD,TD). (See Section B page 224.) For .01<TD$\leq$500, the integral of Equation (3-16) is evaluated by the Romberg technique. Program No. 2A has a SUBTB subroutine different than the other three programs. For Program 2A, the expression for TD$\leq$.01 is the same as Mortada's Equation 4. For .01<TD$\leq$100, Program 2A uses the modified Trapezoidal method rather than the Romberg method.

3. ERFC - The Error Function, the Complementary Error Function, and the integral of the Complementary Error Function are evaluated for the argument X, where X = (RD - 1.0)/(2. * SQRT(TD)). (See Section E, page 236.) Program No. 2A does not evaluate the Complementary Error function of X since it is not required in the expression for TD$\leq$.01.

4. BESY0 - The value of the Bessel function, zero order, second kind, (Y_0) is calculated for the value of ARG brought into the subroutine. Depending on whether ARG is greater or less than 3.0, two different polynomial approximations are used to evaluate the function (See Equations (2B-1) and (2B-2), page 234). The SIN expansion (See Appendix B, page 242) has been added to permit extra large arguments to be used.

5. BESJ0 - The value of the Bessel function, zero order, first kind, (J_0) is calculated for the argument ARG. The polynomial approximations used are given in Equations (2A-1) and (2A-2), page 233. The COS expansion (See Equation (3A-7), page 241) is also used.

6. BESY1 - The Bessel function of first order, second kind, (Y_1) is evaluated for the argument ARG. The approximations are given by Equations (2D-1) and (2D-2), page 235.

7. BESJ1 - The Bessel function of first order, first kind, (J_1) is evaluated for the argument ARG. The approximations are given by Equations (2C-1) and (2C-2), page 234.

6.3 Program No. 1 - PD(RD,TD) Values

6.31 Program Description:

6.31.1 Objective:

Program No. 1 is designed to calculate the dimensionless pressure PD(RD,TD) for each value of dimensionless radius, RD, and each value of dimensionless time, TD, supplied by the input data cards.

6.31.2 Advantages of This Program:

1. Any number of PD values can be calculated as long as a TD value and a RD value are available from the input data.

2. The values of PD(1,TD) previously obtained from Van Everdingen-Hurst's or Chatas' tables can be checked against those calculated by this program.

3. The values of PD(RD,TD) previously obtained only from Mortada's plots or table can easily be calculated by Program No. 1. Radius ratios and dimensionless times not given by Mortada are now available through the use of this program.

4. All practical radius ratios and dimensionless times can be used in this program. Since this study is concerned principally with aquifer pressure distribution, only TD values between .0005 and 1000 have been investigated. RD values from 1.0 to 64 have been used in this study, but ratios greater than 64 can be handled by the program.

5. This program is based upon an evaluation of the explicit equations for PD(RD,TD) rather than the usual finite difference solutions to the radial diffusivity equation. This allows a more accurate value of PD(RD,TD) to be obtained.

6. Since this program is based upon the concept of the interior boundary of the radial system having a finite area, the dimensionless pressures obtained are much more accurate than those previously obtained from "point-source" solutions to the diffusivity equation. This increase in accuracy is especially important at radius ratios close to 1.0 and at small dimensionless times.

6.31.3 Limitations of This Program:

1. In its present form, PD(RD,TD) values are calculated for only one RD value at a time for multiple TD values. In order to run more than one RD value at a time, a DO-LOOP must be added prior to statement 4.

2. The time required to calculate the PD(RD,TD) values can range from less than three minutes to more than an hour, depending upon the magnitude of the TD values selected and the number of PD(RD,TD) values being sought.

3. At the present time, radius ratios greater than 64 and dimensionless times outside the range of .0005 to 1000 have not been used in this program. Values outside these ranges, however, should not affect the operation or accuracy of this program.

6.31.4 Data Required By This Program:

1. The number of TD values being read in as data.

2. The desired RD value at which PD values are required for the TD values read in as data.

3. The TD values at which PD is to be calculated for the RD value already read in Step 2.

6.31.5 Operation of This Program:

Once the required dimensionless parameters (TD and RD) have been supplied, the program calculates PD(RD,TD) by solving one of three explicit equations available for the dimensionless pressure.

A. If TD≤.01, Equation (3-2) is solved with the aid of Subroutine ERFC.

B. If TD>500, Equation (3-3) is solved with the help of Subroutine SUBTA.

C. If .01<TD≤500, Equation (3-16) is solved by the Mainline Program starting with statement 30.

In case C, Equation (3-16) is solved by the Romberg integration technique. A maximum of $(2)^{10}$ panels is employed and the combination of 10 Trapezoidal approximations was found to produce PD(1,TD) values which compare favorably to the accepted values of Chatas.

The Bessel functions J0, J1, Y0, and Y1 required to solve Equation (3-16) are furnished by the proper polynomial approximations contained in the 4 Bessel function subroutines BESJ0, BESJ1, BESY0, and BESY1.

6.32 List of Symbols

NOTE: All symbols used in Program No. 1 are the same as those given for Program No. 2 (See page 157).

6.33 User Instructions for Program No. 1 - PD(RD,TD) Values

6.33.1 Program Input:

It is imperative for the input data to be supplied in the correct manner. Although the data input is relatively simple for Program No. 1, the order of data cards and the necessary formats are listed below to prevent any difficulties which might otherwise occur.

CARD NO.	FORMAT	VARIABLE NAME	DESCRIPTION
1	I5	I	Contains the number of values of TD to be read as data.
2	E18.8	RD	Contains the RD value at which the PD(RD,TD) will be calculated.
3 to I+2	E18.8	TD	The next I cards contain the values of TD at which PD(RD,TD) is desired.

6.33.2 Program Output:

Program No. 1 prints the value of PD(RD,TD) for each of the I values of TD read in for the RD location specified. It also prints RD and the TD values at which PD(RD,TD) is calculated.

6.34 PROGRAM NO. 1

BLOCK DIAGRAM

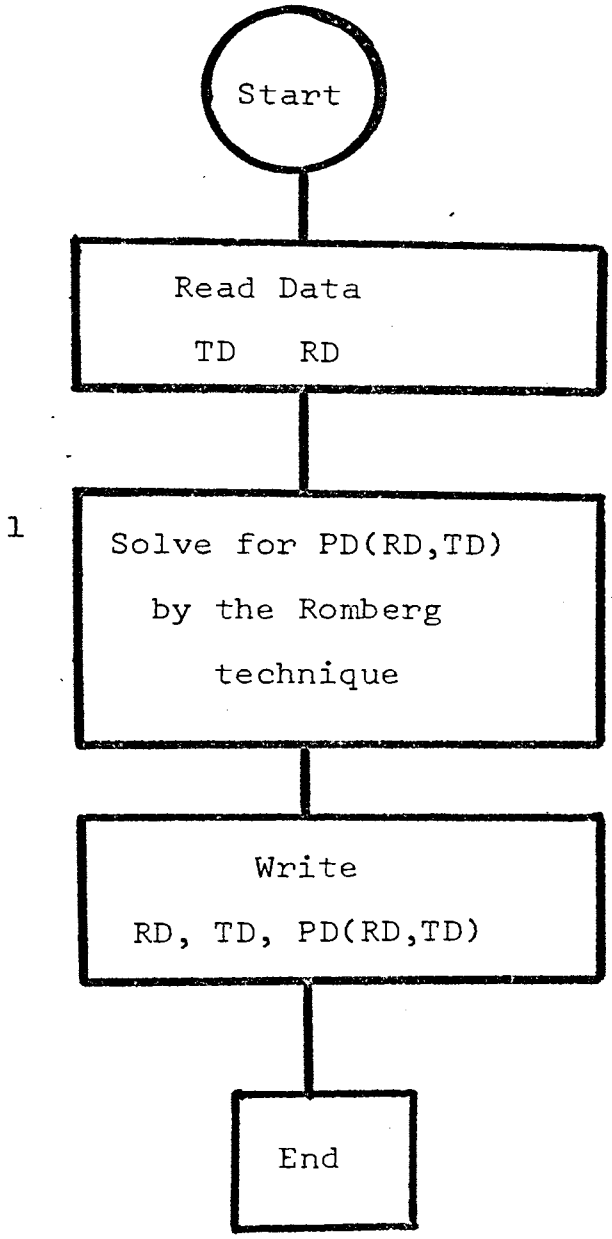

6.35 Flow Diagram
Program No. 1 - Calculation of PD(RD,TD)

A.) Main Line Program

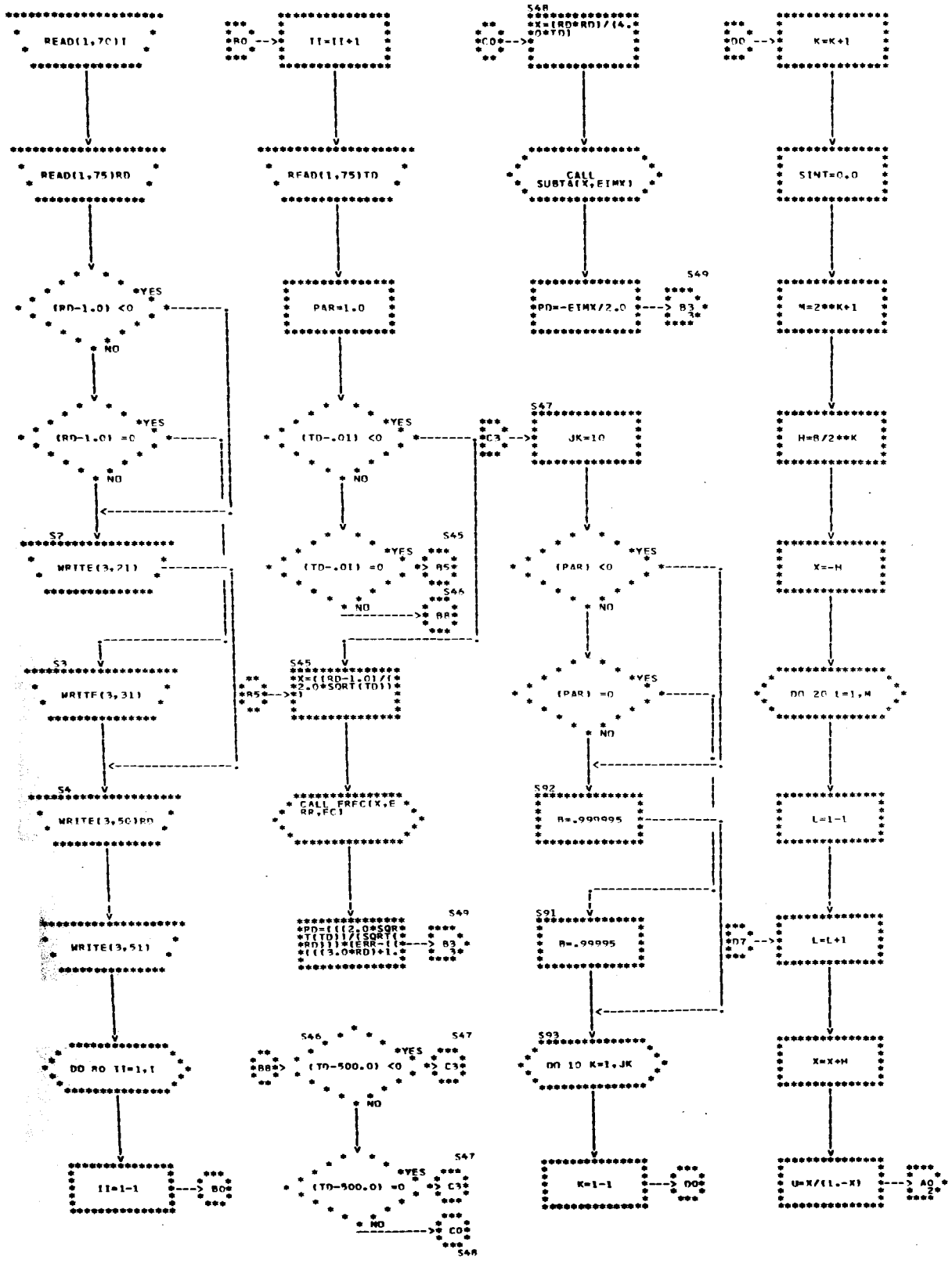

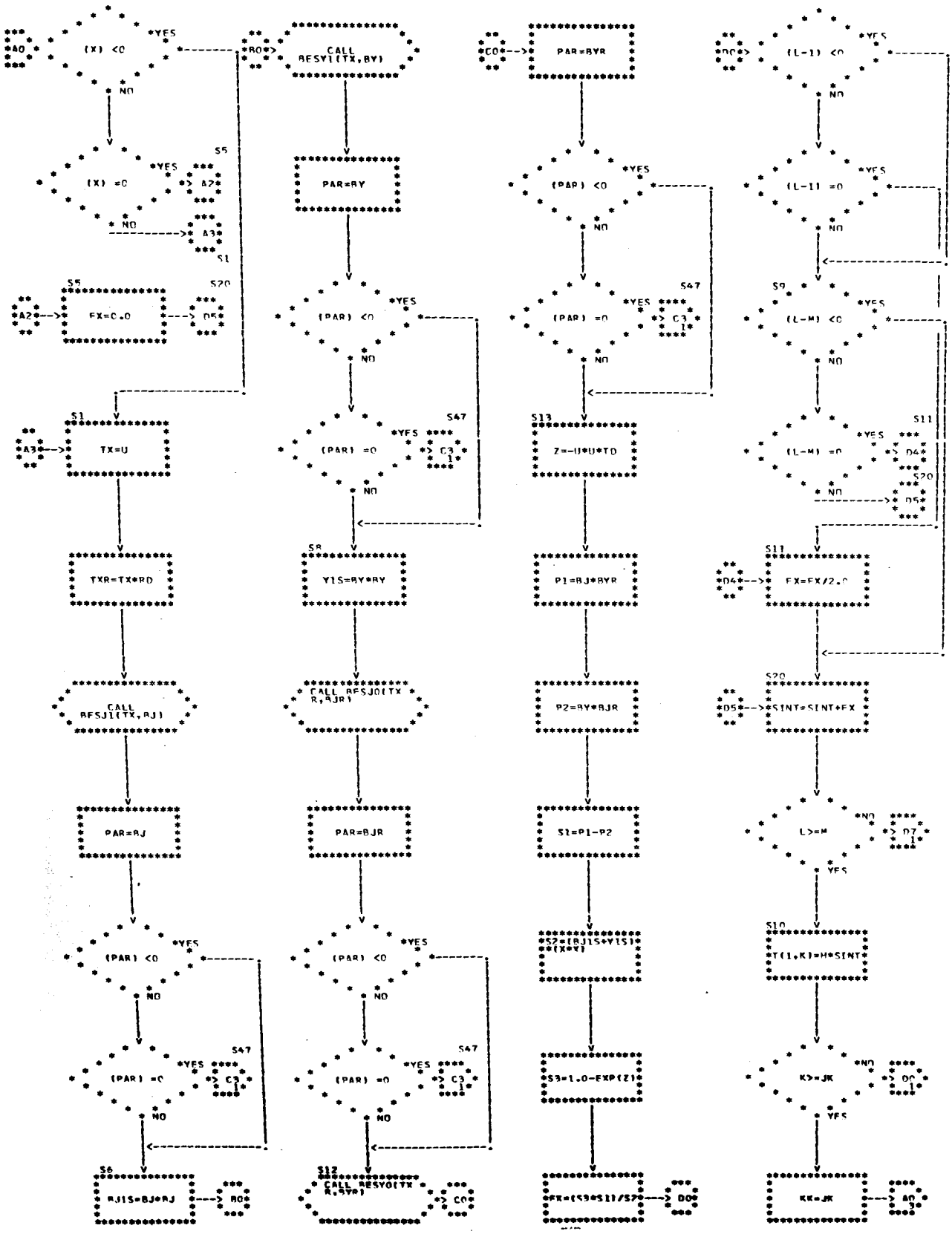
A0
(X) <0
YES
NO
A2
(X) =0
A3
S5
S1
S20
FX=0.0
D5
TX=U
TXR=TX*RD
CALL RESJ1(TX,RJ)
PAR=RJ
(PAR) <0
(PAR) =0
C3
RJ1S=RJ*RJ
R0
CALL RESY1(TX,RY)
PAR=RY
S8
Y1S=RY*RY
CALL RESJ0(TXR,RJR)
PAR=RJR
S12
CALL RESY0(TXR,RYR)
C0
PAR=RYR
S13
Z=-U*U*TD
P1=RJ*RYR
P2=RY*RJR
S1=P1-P2
S2=(RJ1S+Y1S)*(X*Y)
S3=1.0-EXP(Z)
FX=(S3*S1)/S2
D0
D0
S9
(L-1) <0
(L-1) =0
(L-M) <0
(L-M) =0
S11
D4
FX=FX/2.0
SINT=SINT+FX
L>=M
D7
S10
T(1,K)=H*SINT
K>=JK
KK=JK

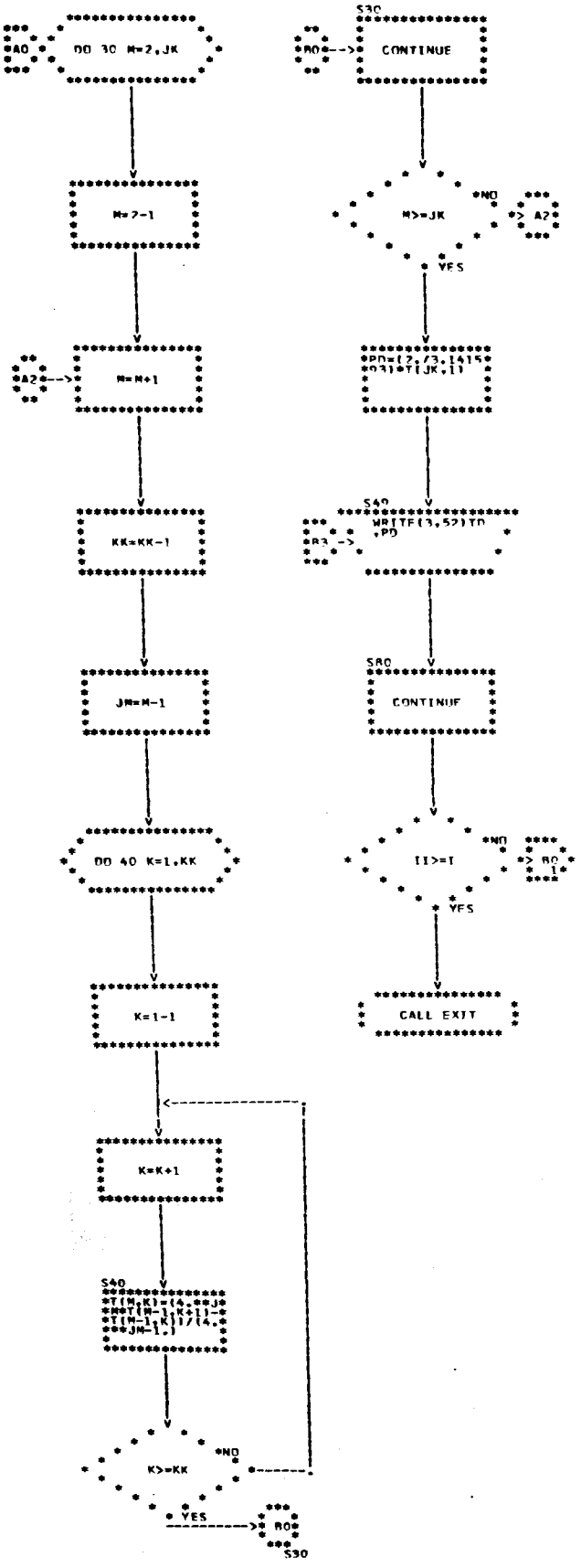
A0
DO 30 M=2,JK
M=2-1
A2
M=M+1
KK=KK-1
JM=M-1
DO 40 K=1,KK
K=1-1
K=K+1
S40
*T(M,K)=(4.**J*
**T(M-1,K+1)-*
T(M-1,K))/(4.
**JM-1.)
K>=KK
*NO
* YES
B0
S30
S30
B0
CONTINUE
M>=JK
*NO
*> A2
* YES
PI=(2./3.1415*
*J)*T(JK,1)
S40
WRITE(3,52)TD
,PD
B3
SR0
CONTINUE
II>=I
*NO
*> B0
1
* YES
CALL EXIT

6.4 Program No. 2 - Fractional Pressure Location

6.41 Program Description:

6.41.1 Objective:

Program No. 2 is designed to calculate the dimensionless radius, RD, at which a given fracitonal dimensionless pressure, PD', occurs at a specified dimensionless time, TD.

6.41.2 Advantages of This Program:

1. The radius at which the aquifer pressure-drop is a given fraction of the well-field pressure-drop can easily be determined at any dimensionless time.

2. The radius calculated will be within .01% of the radius at which the desired fractional dimensionless pressure PD' occurs, regardless of the dimensionless time or the PD' value selected.

3. If the fractional dimensionless pressure, PD', is specified as .01, then an accurate value of the effective radius of drainage can be obtained for an infinite radial reservoir subject to a constant producing rate under unsteady-state fluid flow conditions.

6.41.3 Limitations of This Program:

1. For $.01 < TD \leq 500$, this program may require up to 15 minutes to obtain the required radius, RD, at which the specified PD' occurs at the given TD. The time required can

be significantly reduced if the percent error is increased to .1%.

2. At present, only TD values from .0005 to 1000 have been calculated, but values outside this range should not present difficulties in the operation of this program.

6.41.4 Data Required By This Program:

1. The values of the fractional dimensionless pressure, PD', for which RD is desired at the TD values which are to follow in Step 2.

2. The values of dimensionless time, TD, and the starting values of RD (always equal to 1.0).

6.41.5 Operation of This Program:

Once the required values of PD' and TD have been read in along with the starting RD = 1.0 values, the program calculates the corresponding PD(1,TD) value. Next it increases RD to 2.0 and calculates PD(RD,TD) for the same TD value. The fractional dimensionless pressure is obtained by PD(RD,TD)/PD(1,TD). This value of PD' is then checked against the required PD' value for which RD is being sought. If these two PD' values are not the same, then the RD value is changed. If the last PD' calculated is larger than the desired PD', then RD is doubled and a new PD(RD,TD) calculated. A new PD' is then formed and checked against the desired PD'. This procedure is continued until a RD value is obtained at which the calculated PD' value is less than the desired PD' value.

When an RD has been found where PD' is less than that requested, then an iterative procedure is followed. The last two RD values are subtracted and one-half their difference is added to the smaller value (RD_1). Using this new RD value (RD_2), PD(RD,TD) and PD' are again calculated. If PD' is still smaller than the desired PD' then the difference between the smaller RD_1 and the new RD_2 value is formed and one-half of this is again added to RD_1 to give RD_3 and PD' is calculated once more.

If PD' becomes larger than the desired PD' value, then the difference between the current RD value and the last RD value giving a smaller PD' is taken and one-half of this difference is added to the current RD value. PD(RD,TD) and PD' are then recalculated.

This type of procedure is continued until an RD value is obtained which is less than .01% different than the previous RD value selected. The PD' value calculated at this RD ratio should be extremely close to the desired PD' value since the two RD values compared have PD' values on either side of the desired PD' value and still differ by only .01%.

The TD, RD, and PD' values are printed as the search continues. The last RD value printed is the radius ratio at which the desired PD' occurs.

The PD(RD,TD) values are obtained by solving the explicit equations given in Section 3.2 for the three different TD ranges (See pages 54 to 56). Equation (3-16) is solved by the Romberg technique using $(2)^{10}$ panels and taking the combination of 10 Trapezoidal approximations.

The ERFC subroutine contains the term added to Mortada's equation for TD$\leq$.01 (See Equation (1B-13), page 227).

The Bessel function subroutines have the SIN and COS expansions which allow extremely large arguments to be evaluated.

6.42 List of Symbols Used In Program No. 2

PROGRAM SYMBOL	PROBLEM SYMBOL	DEFINITION
MAINLINE PROGRAM		
PDF	PD'	Fractional dimensionless pressure PD' = PD(RD,TD)/PD(1,TD).
TD	TD	Dimensionless time, $Kt/\phi\mu cr_b^2$.
RD	RD	Dimensionless radius, r/r_b.
DELR	----	Percent difference between the radius RDL where PDF is less than the desired PDF value and the radius RDS where PDF is larger than the desired PDF value.
SUBROUTINE SUBTB		
PAR	----	Control value for size of the upper limit of the integral in Equation(3-20).
JK	----	Number of Trapezoidal approximations made for the Romberg combination.
B	.999995	The upper limit of the integral in Equation (3-20).
M	----	Number of panels used (maximum of 2^{10}).
H	----	Size of the individual panels.
U	----	Variable of integration, $\bar{X}/(1.-\bar{X})$.
$\bar{X}$	----	Variable of integration.

PROGRAM SYMBOL	PROBLEM SYMBOL	DEFINITION
SUBROUTINE SUBTB		
FX	----	Value of the function 3-20 at any $\bar{X}$ value before integration occurs.
TX	----	U.
TXR	----	U * RD.
BJ1S	----	BJ * BJ.
Y1S	----	BY * BY.
BJ, BY	----	Values of the Bessel functions of zero order, first and second kinds.
BJR, BYR	----	Values of the Bessel functions of first order, first and second kinds.
SINT	----	Sum of the FX values.
T(1,K)	----	Value of the integral in Equation (3-20) from the Trapezoidal technique.
T(M,K)	----	Value of the integral in Equation (3-20) obtained from the Romberg combination of several Trapezoidal approximations.
SUBROUTINE SUBTA		
X	----	Argument, $RD^2/(4 * TD)$.
EIMX	Ei(-X)	Value of the Exponential Integral with the argument -X.
SUBROUTINE ERFC		
X	----	Argument, (RD-1)/(2 *SQRT(TD)).
T	----	1./(1. + .3275911(X)).
A	----	e^{-X^2}
ERFX	ERF(X)	Error Function of X (given by Equation (2E-7)).
ERR	IERFC(X)	Integral of the Complementary Error Function of X (given by Equation (2E-3)).

PROGRAM SYMBOL	PROBLEM SYMBOL	DEFINITION
SUBROUTINE ERFC		
EC	ERFC(X)	Complementary Error Function of X (given by Equation (2E-4)).
SUBROUTINES BESJO, BESYO, BESY1, and BESJ1		
ARG	----	Argument brought into the subroutine.
ASIN, ACOS	SIN, COS	SIN and COS of a number.
PIE	π	3.141593.
S12,C12	SIN 12X COS 12X	Expressions for the SIN and COS of extremely large arguments (See Equations (3B-6) and (3A-7)).

6.43 User Instructions for Program No. 2 - Fractional Pressure Location

6.43.1 Program Input:

The following data should be read in exactly as listed below in order for this program to operate properly.

CARD NO.	FORMAT	VARIABLE NAME	DESCRIPTION
1 - 3	10X,E18.8	PDF(JJ)	Each card contains one value of the fractional dimensionless pressure PD'.
4 - 5	10X,2E18.8	TD, RD	Each of the next 2 cards contains one value of TD and one value of RD (RD must be 1.0).

6.43.2 Program Output:

Program No. 2 prints the value of PD' and each corresponding RD ratio selected by the program until two successive RD ratios have been obtained which have PD' values both above and below the desired PD' value. The two RD ratios also are within .01% of each other. This program also prints the requested PD' value read in as data and the value of TD at which the PD' occurs at the calculated RD ratio.

6.44 PROGRAM NO. 2

BLOCK DIAGRAM

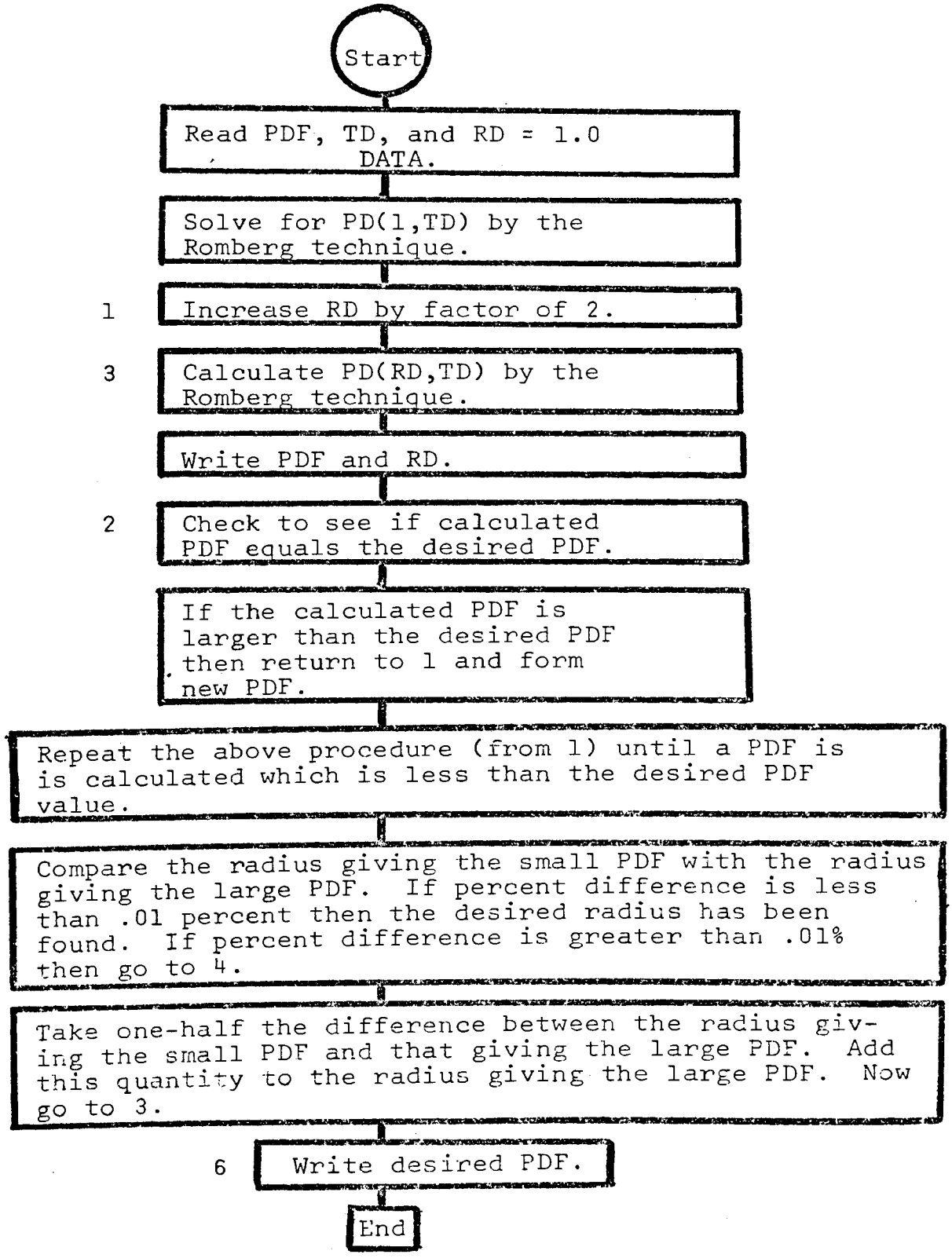

6.45 Flow Diagram
Program No. 2 - Calculation of Fractional
Pressure Drop - Romberg

A.) Main Line Program

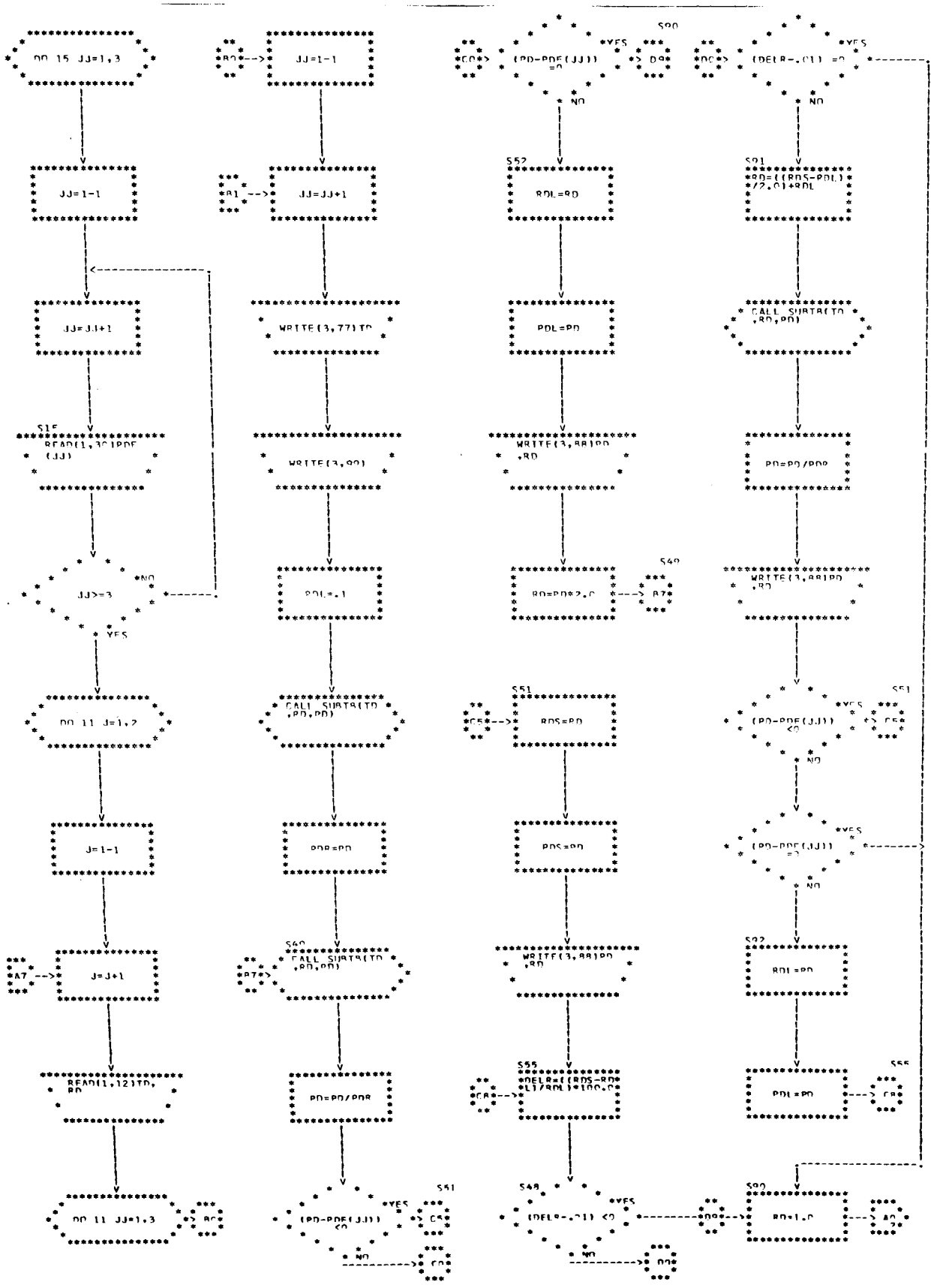

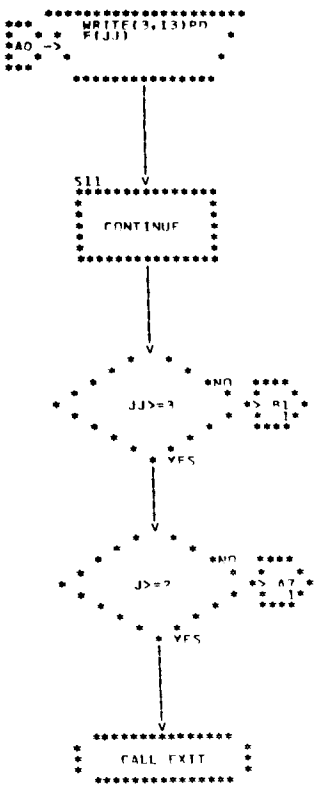
WRITE(3,13)PD
F(JJ)
AO ->
511
CONTINUE
JJ>=3
NO
YES
J>=2
NO
YES
CALL EXIT

B.) SUBROUTINE SUBTA(TD,RD,PD)

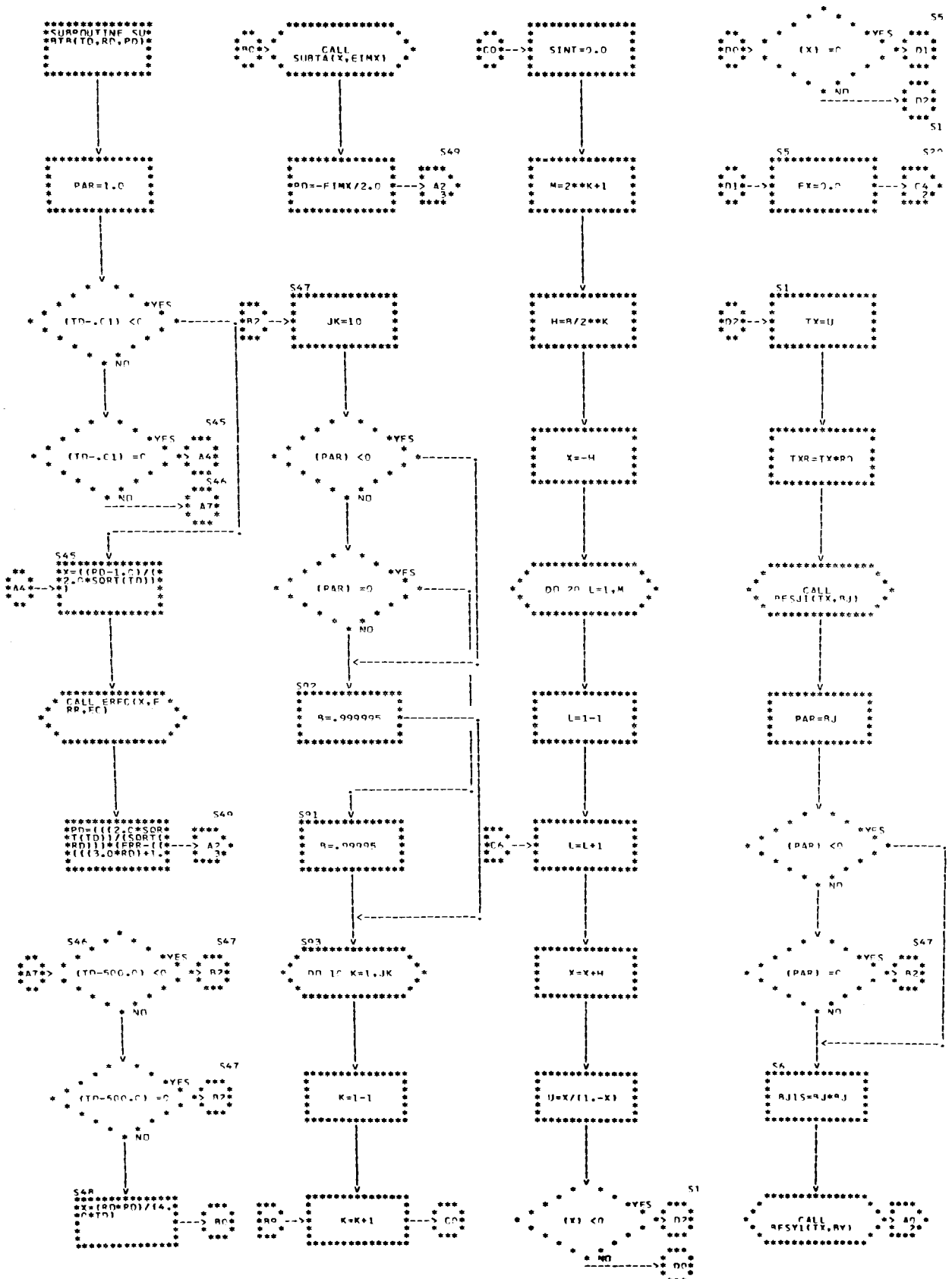

FLOWCHARTER II

SUBROUTINE SUBTR(TD,RD,PD)

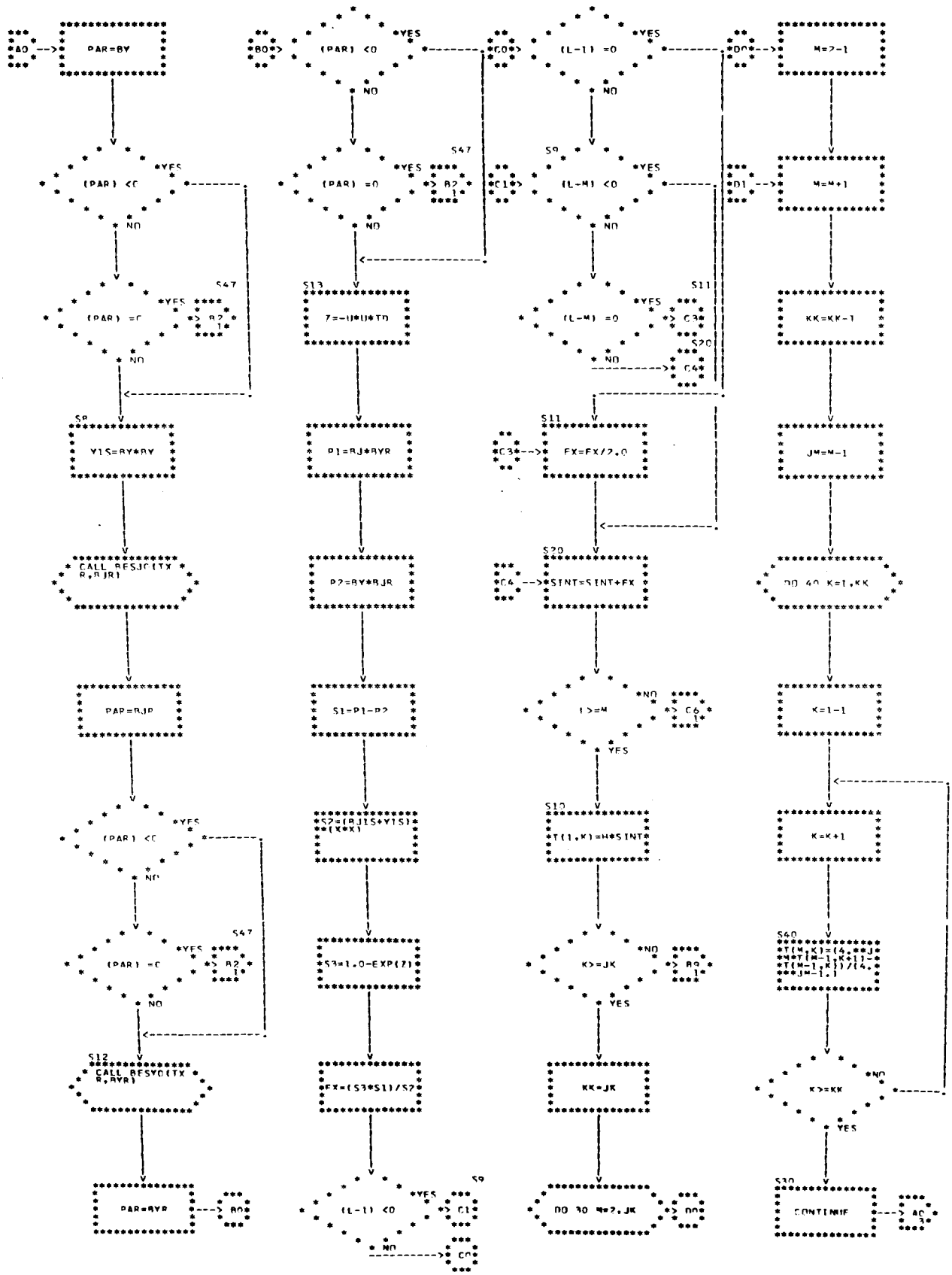

FLOWCHARTER II

SUBROUTINE SUBTA(TO,PD,PO)

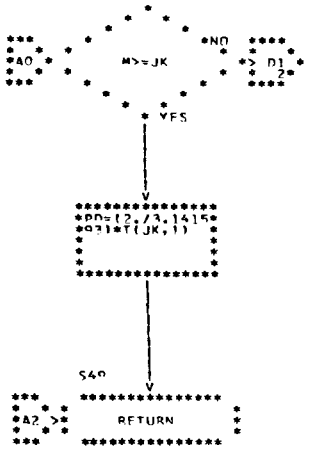

FLOWCHARTER II

C.) SUBROUTINE SUBTA(X,FIMX)

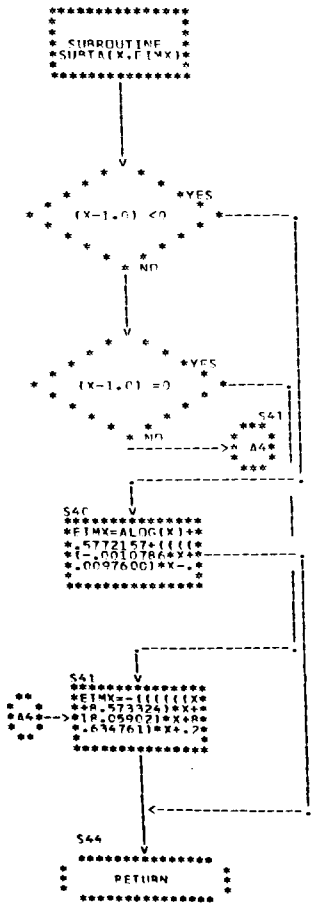

FLOWCHARTER II

D.) SUBROUTINE EREC(Y,ERR,EC)

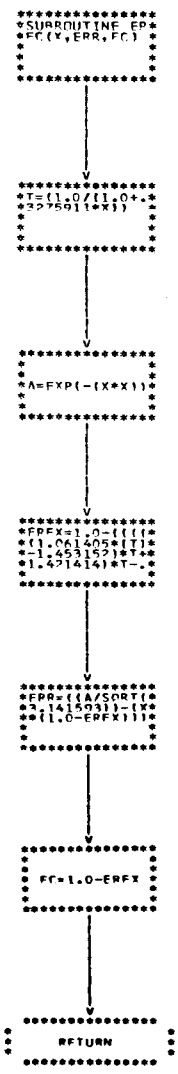

E.) SUBROUTINE BESJ0(ARG,BJ)

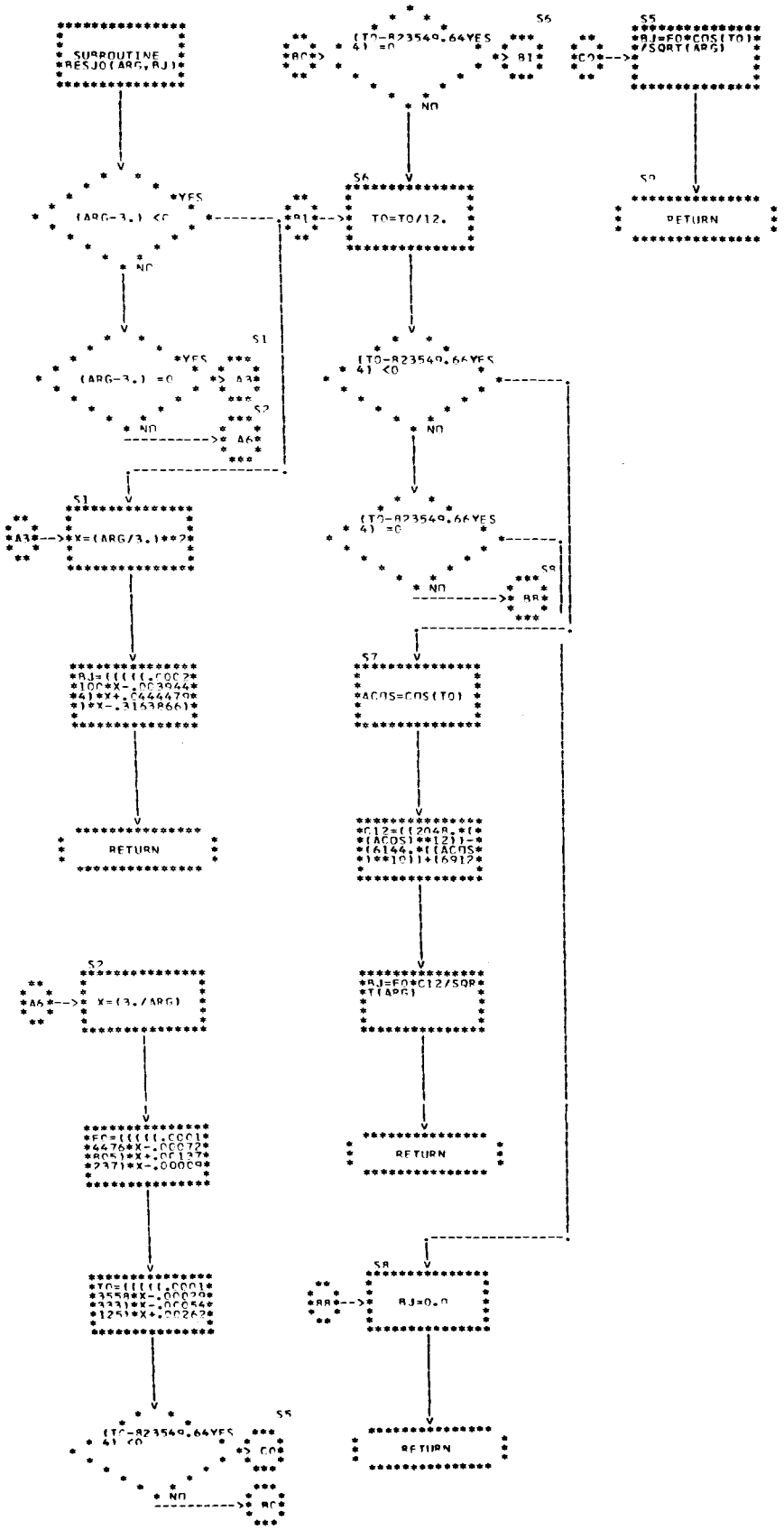

FLOWCHARTER II

F.) SUBROUTINE BESYO(ARG,BY)

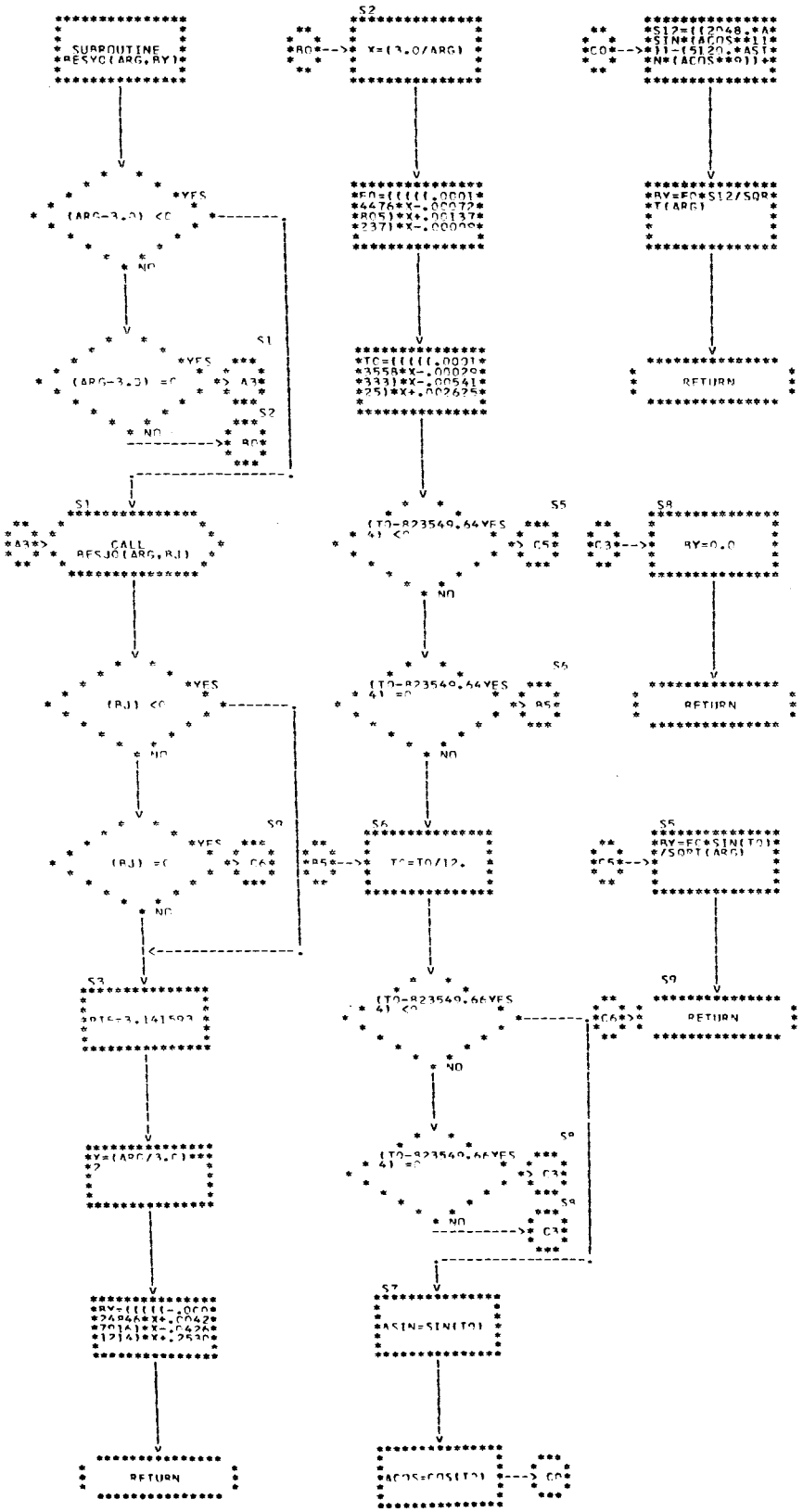

FLOWCHARTER II

G.) SUBROUTINE RESJI(ARG,RJ)

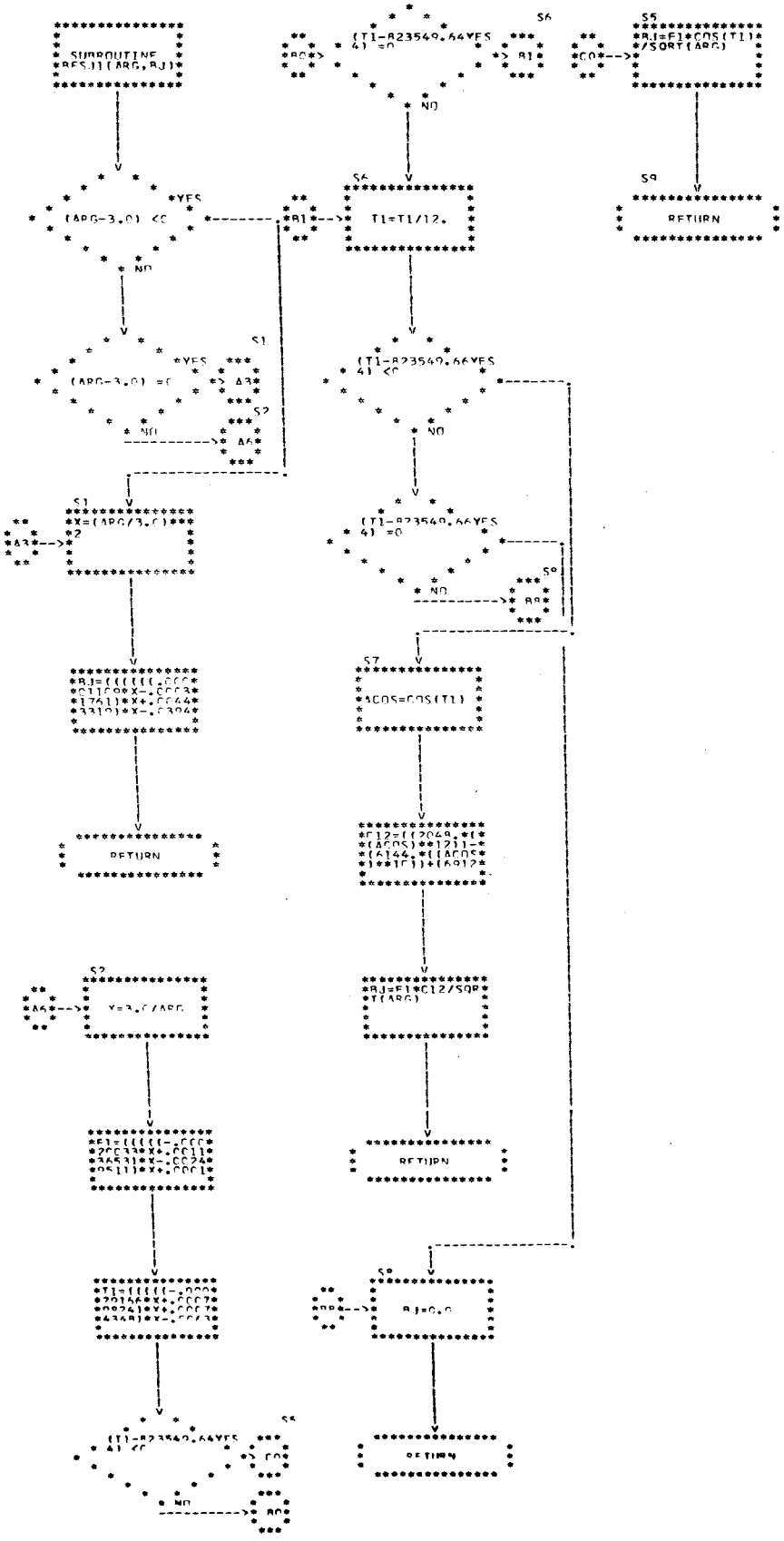

FLOWCHARTER II

B.) SUBROUTINE BESY1(ARG,BY)

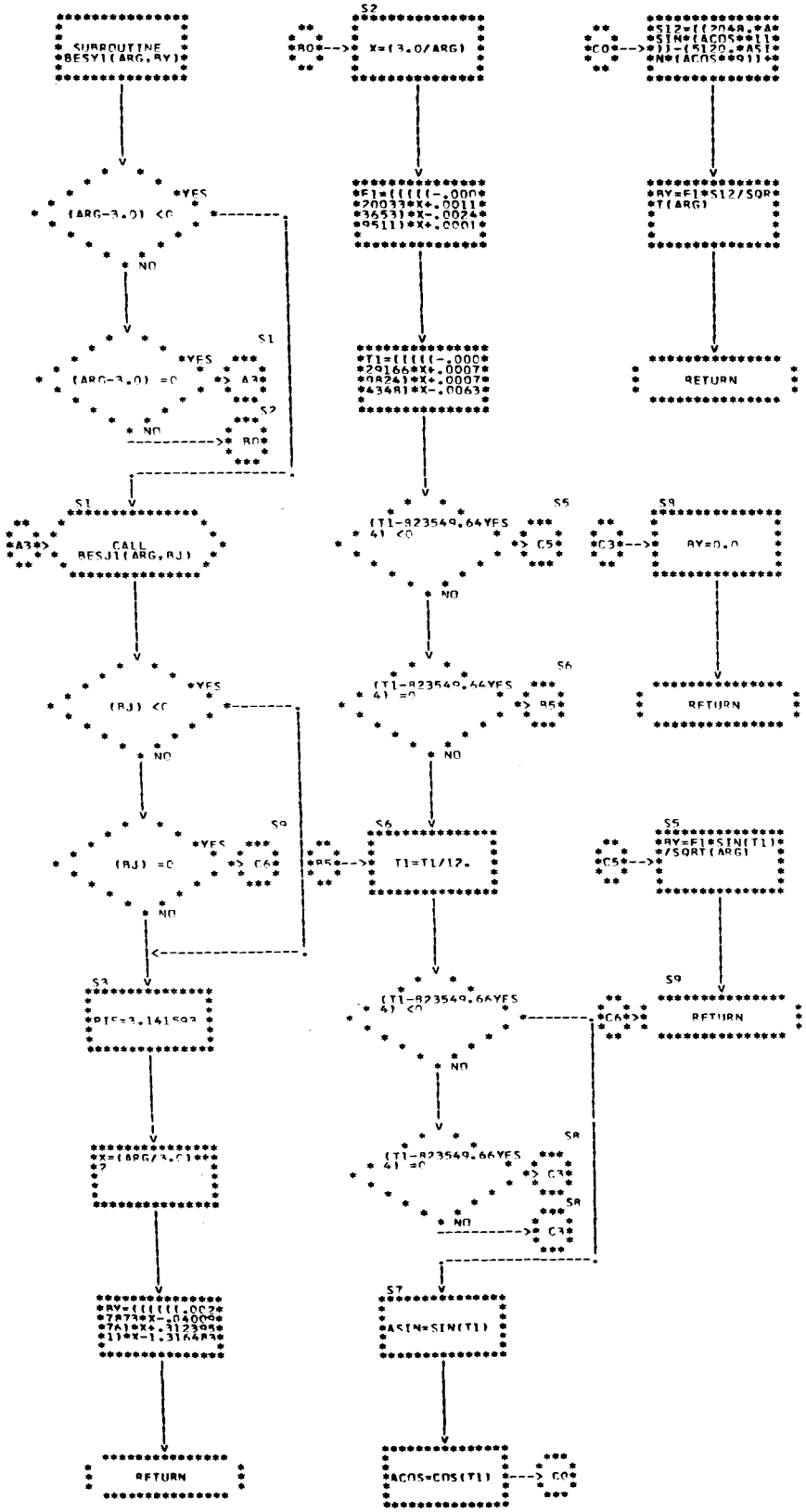

6.5 Program No. 2A - Fractional Pressure Location

6.51 Program Description:

6.51.1 Objective:

Program No. 2A, like Program No. 2, is designed to calculate the dimensionless radius, RD, at which a given fractional dimensionless pressure, PD', occurs at a specified dimensionless time, TD. This program operates exactly the same way as Program No. 2, except that the integration of Equation (2-17) for $.01<TD\leq100$ is accomplished by a modified Trapezoidal procedure rather than by the Romberg technique.

6.51.2 Advantages of This Program:

The advantages of this particular program are the same as those listed for Program No. 2 (See page 154). Program No. 2A, however, was used to obtain the values of RD-1 presented in Table 4-7, page 90.

6.51.3 Limitations of This Program:

1. In general, the restrictions mentioned for Program No. 2 also apply to this program.

2. The accuracy of the individual PD values slowly decreases as TD becomes greater than 10 but less than 100. For this reason, Program No. 2 is preferred over this program since it requires a few minutes less running time. This inaccuracy in PD values does not, however, significantly affect the RD values obtained from this program.

3. The time required to obtain a RD value is approximately 1 minute more for this program than for Program No. 2.

6.51.4 Data Required By This Program:

The data required by this program is identical to that listed for Program No. 2 (See Part 6.41.4, page 155).

6.51.5 Operation of This Program:

This program operates exactly the same way as Program No. 2, except that the integration of Equation (2-17) for $.01<TD\leq 100.$ is accomplished by a modified Trapezoidal procedure rather than by the Romberg technique.

The ERFC subroutine in this program does not contain the extra term, but is exactly the same as the expression used by Mortada (See Equation (1B-10), page 226).

The Bessel function subroutines do not have the provision for extra large arguments of the SIN and COS functions. This provision was not required in this program because the upper limit used for the integral was about 2100. Since the largest RD value used was less than 100, then the arguments of the Bessel functions always remained less than about 210,000. Arguments of this size did not require expansions of the SIN and COS functions in order to operate successfully.

6.52 List of Symbols Used In Program No. 2A

PROGRAM SYMBOL	PROBLEM SYMBOL	DEFINITION

NOTE: All symbols except those listed below from Subroutine SUBTB are similar to those already described for Program 2, page 157.

SUBROUTINE SUBTB

AREA	----	The area under the curve integrated from X = .02 up to the current value of X.
YA	----	The value of the function inside the integral at any given X value.
DX	----	The size of the individual panels used for the integration.
X	----	Variable of integration.
XR	----	X * RD.
YB	----	Equal to YA.
DELA	----	The increment of area added by the latest panel.

PROGRAM SYMBOL	PROBLEM SYMBOL	DEFINITION
SUBROUTINE SUBTB		
TA	----	The sum of the previous area plus the area added by the latest panel considered.

6.53 User Instructions for Program No. 2A - Fractional Pressure Location

6.53.1 Program Input:

NOTE: The input for Program No. 2A is identical to that described for Program No. 2 (See page 160) and therefore will not be repeated here.

6.53.2 Program Output:

NOTE: The output for Program No. 2A is also identical to that already described for Program No. 2 (See page 160) and therefore will not be mentioned here.

6.54 PROGRAM NO. 2A

BLOCK DIAGRAM

NOTE: The Block Diagram for Program No. 2A is identical to that for Program No. 2 already given on page 161 and therefore will not be repeated here. However, a Trapezoidal technique is used in step number 3 rather than the Romberg method given for Step 3 of Program No. 2.

6.55 Flow Diagram
Program No. 2A - Calculation of Fractional Pressure Drop - Trapezoidal

A.) Main Line Program

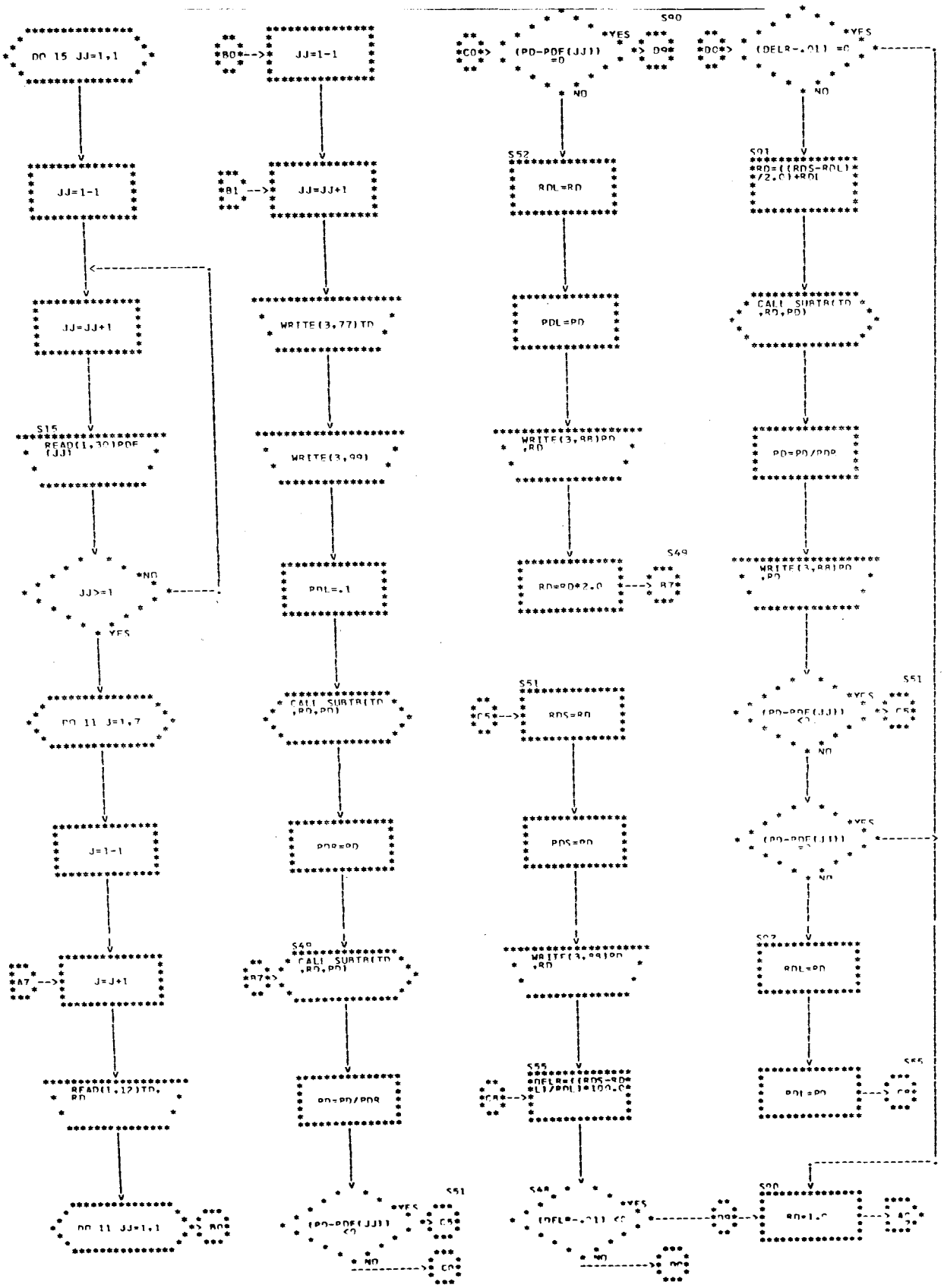

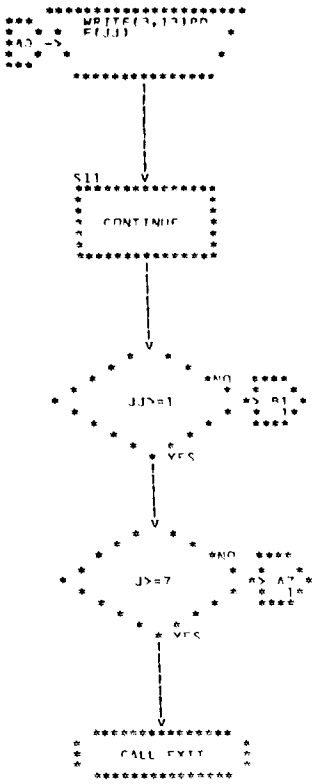
WRITE(3,12)DD
F(JJ)
A0 ->
S11
CONTINUE
JJ>=1
*NO
*> B1
*YES
J>=7
*NO
*> A7
*YES
CALL EXIT

FLOWCHARTER II

B.) SUBROUTINE SUBTR(TD,RD,PD)

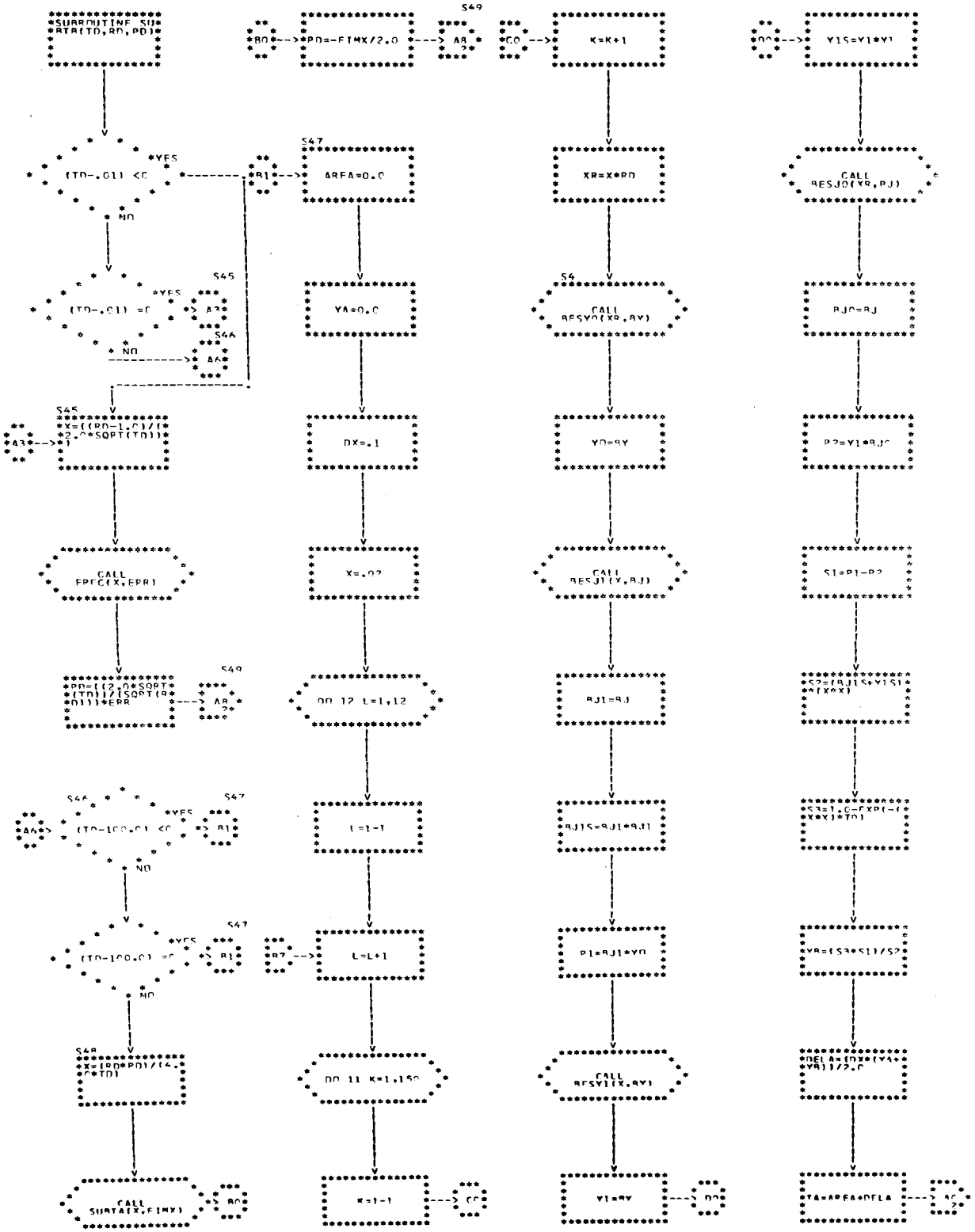

FLOWCHARTER II
SUBROUTINE SUBTA(TD,RD,PD)

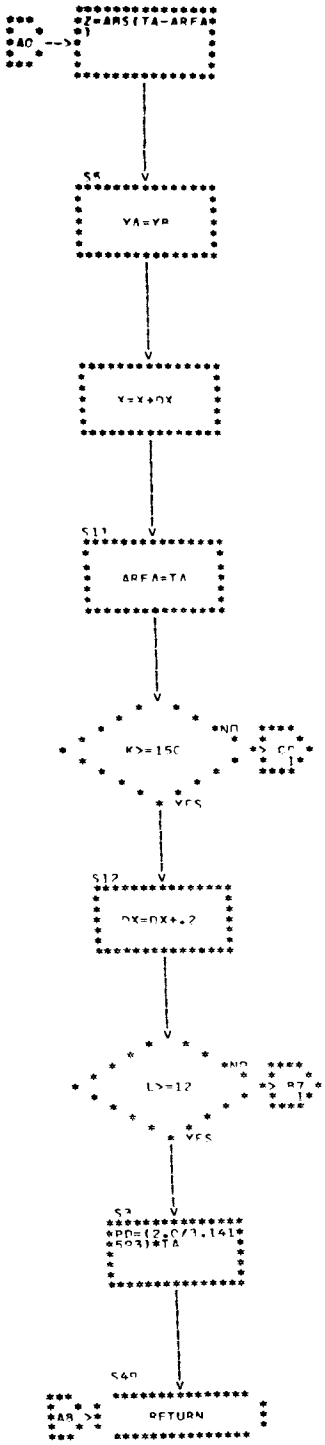

C.) SUBROUTINE EREC(X,ERR)

FLOWCHARTER II

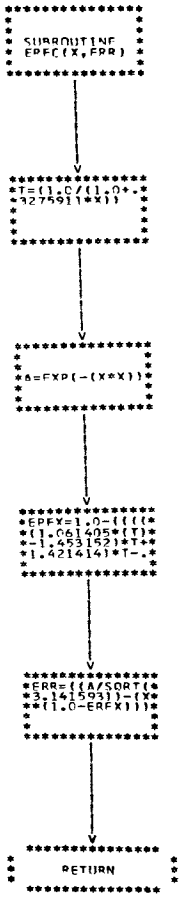

D.) SUBROUTINE SUBTA(X,FIMX)

FLOWCHARTER II

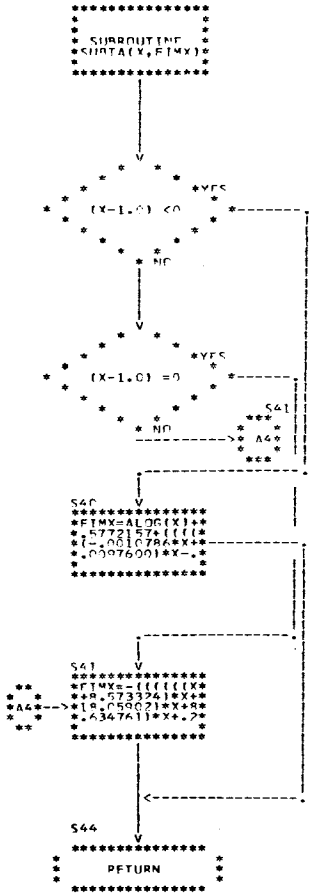

FLOWCHARTER II

E.) SUBROUTINE BESYO(ARG,BY)

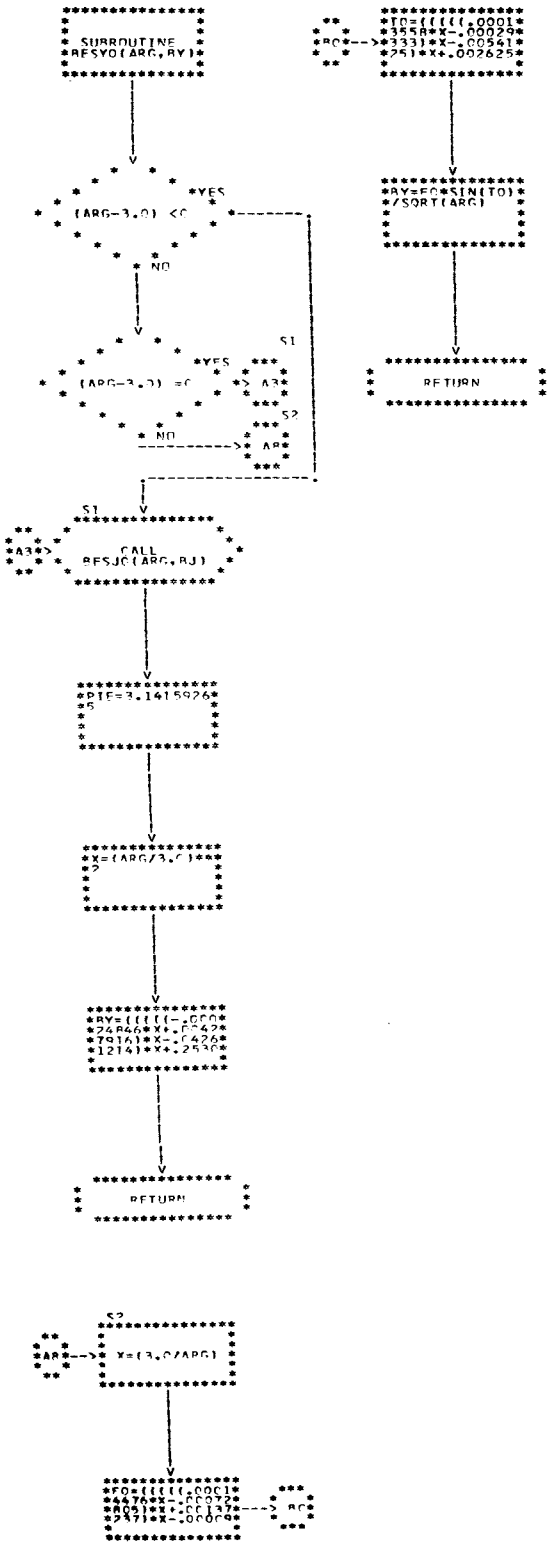

FLOWCHARTER II

F.) SUBROUTINE BESJO(ARG,BJ)

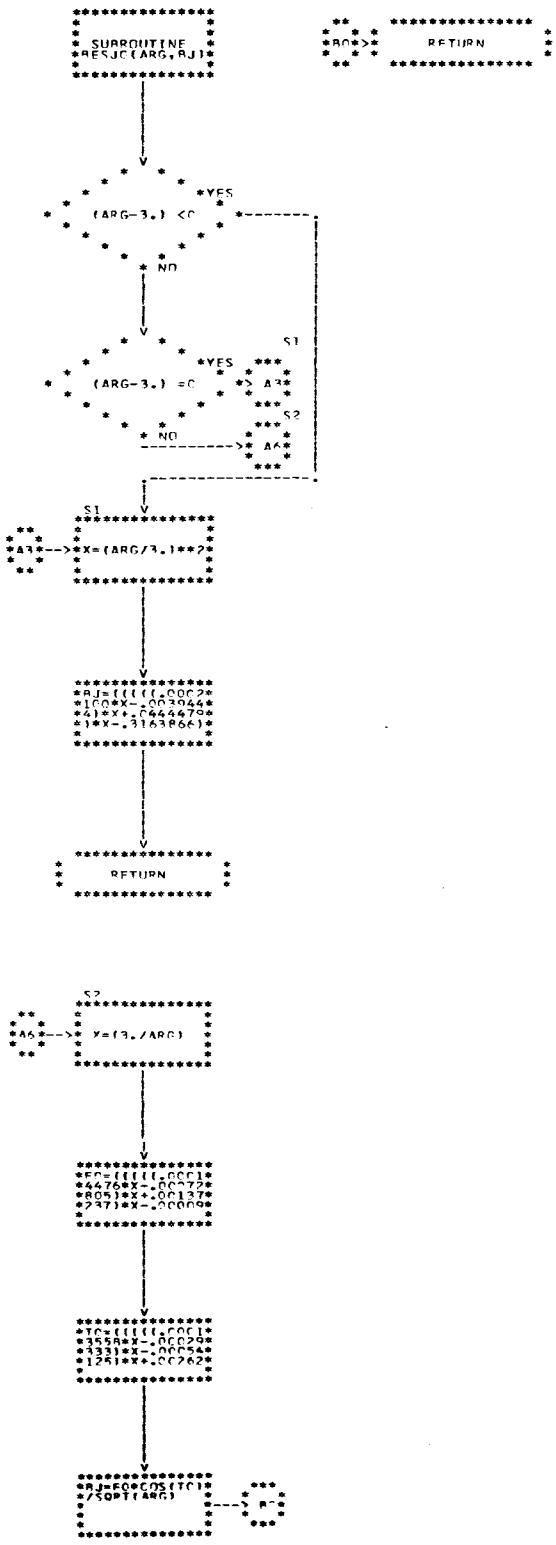

FLOWCHARTER II

G.) SUBROUTINE BESY1(ARG,BY)

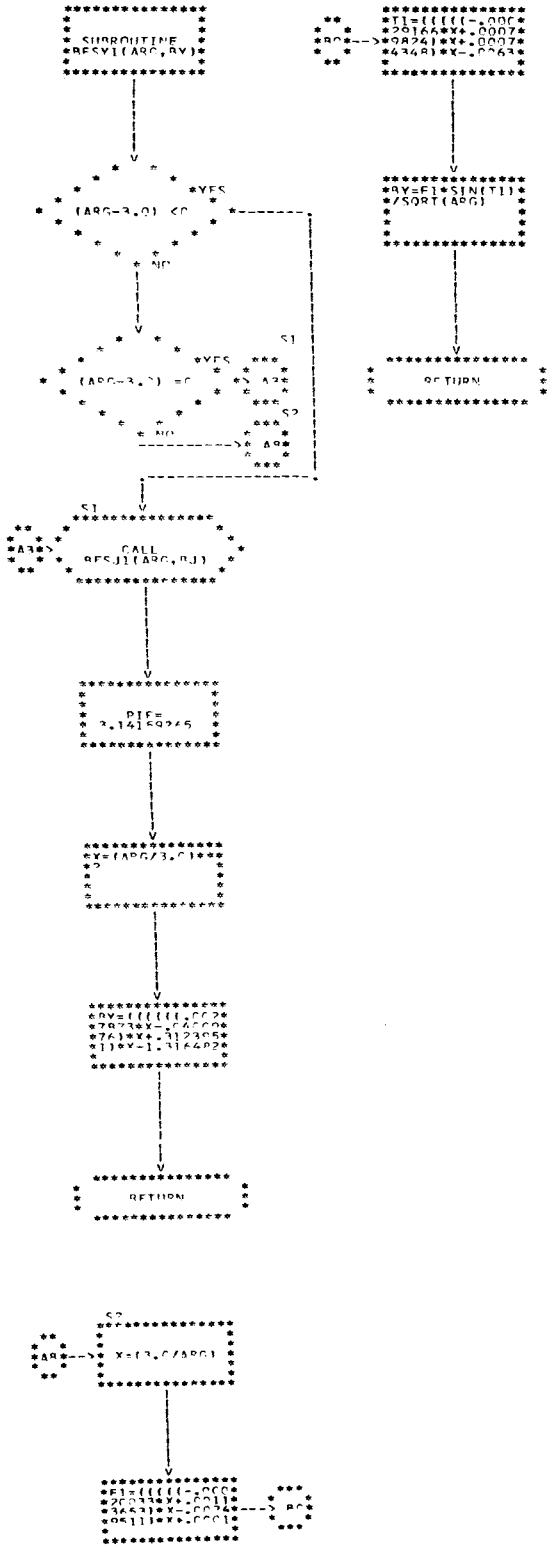

FLOWCHARTER II

H.) SUBROUTINE BESJ1(ARG,BJ)

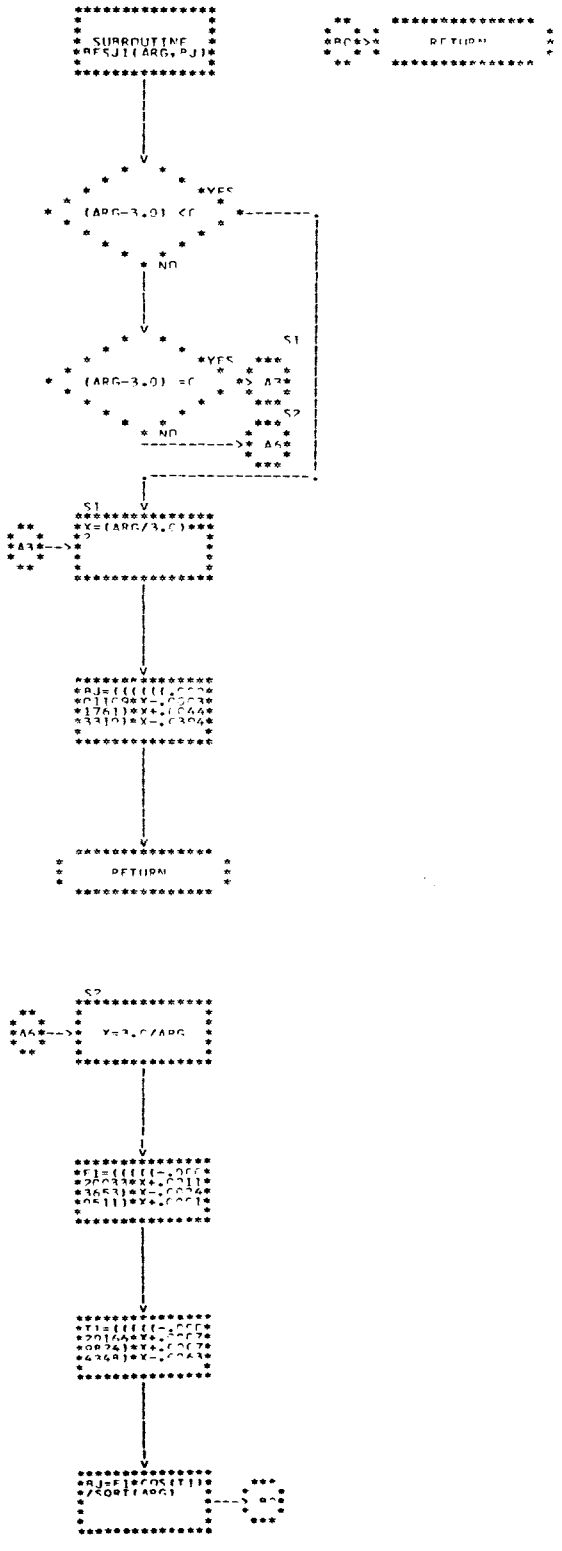

6.6 Program No. 3 - On-Line Mapping Technique

6.61 Program Description:

6.61.1 Objective:

Program No. 3 is designed to map directly from the on-line printer the pressure-drop distribution in a square section of an infinite radial aquifer surrounding a number of radial oil-fields each producing at a constant rate.

6.61.2 Advantages of This Program:

1. Any number of well-fields can be mapped. These fields can be located anywhere inside or outside the grid-section chosen for pressure mapping.

2. Data can be furnished in any units provided that the proper conversion constants are supplied in statements 35, 36, and 38 of the program.

3. Varying production rates can be used for the fields provided a superposition routine for the pressure-drop resulting from each production rate, over the corresponding time-step, is added prior to statement number 43.

4. Fifty-three contours above the reference contour and 53 below are possible without any duplication of symbols. This will normally allow for contouring at 5 or 10 psi. drop per contour.

5. A map of the pressure-drop resulting from all the fields in the aquifer interference region is produced as

well as maps of the pressure-drop caused by each field producing alone in the aquifer.

6. A listing of the pressure-drop occurring at each of the 225 grid-points is produced for each of the fields acting by itself and for the combined effect of the fields interferring.

7. A map containing more than 12,700 pressure-drop values is produced by interpolation from only 225 calculated pressure-drops. This significantly reduces the time required to map with the detail desired.

8. The actual aquifer pressure rather than the pressure-drop can be mapped provided the pressure-drop values are subtracted from the initial aquifer pressure (PINT) prior to statement number 43.

9. The tedious and often inaccurate job of hand-contouring pressure values to investigate areal pressure distribution is eliminated.

10. The maps produced are of a useful size and the alternating black (printed) and white (blank) contours serve to highlight the pressure distribution.

6.61.3 Limitations of This Program:

1. In the form shown by the flow charts and listed in Insert 13, this program will handle only 3 well-fields producing from the aquifer. More fields can be examined by changing the dimension statements and do-loop indexes.

2. In its present form, the data must be supplied in the units described in the definition section. The constants in statements 35, 36, and 38 can be modified if other units are desired for the input-data.

3. Since the 15 x 15 map-grid requires 225 pressure-drop values in order to perform the interpolation and to map the pressure-drop distribution, the program must generate the 225 pressure-drops at the selected grid-points. These points are fixed and the number and location of these points can not be changed. This program will not map pressure-drop values supplied by data cards but only those pressure values generated internally.

4. Pressure-drops which occur inside well-field boundaries will be slightly different than the true pressure-drops at these points. This is due to the assumption that the pressure-drop anywhere in the well-field is the pressure-drop existing at the well-field boundary (RD = 1.0). Interference pressure-drops at points inside a well-field boundary caused by another field's production are calculated properly. Only the assumption of uniform pressure-drop within a field producing alone in the aquifer limits the exactness of the maps produced.

5. Each of the well-fields must have produced at a constant rate for the period of time (t) employed to calculate the dimensionless time, TD.

6. The time required to complete mapping can range from less than 3 minutes to well over an hour depending on the values of TD calculated and the number of well-fields in the aquifer.

7. The contour interval must be selected so that not more than 53 contours will fall on either side of the reference contour selected. The mapping will occur even if more than 53 contours are required, but there will be duplication of symbols.

8. Circular pressure-drop contours appear on the maps as ellipses. This distortion is caused by the difference between the character spacing horizontally and vertically. When mapping with the on-line printer, the even spacing of the grid-points can not be reproduced without system changes internally.

6.61.4 Data Required by This Program:

The following data are required in order for the mapping to occur in the proper manner:

1. One value each of aquifer permeability, aquifer thickness, viscosity of the water, aquifer porosity, initial aquifer pressure, compressibility of the water, and the proper unit conversion constant are required.

2. The number of grid-points (fixed at 225) and the number of well-fields in the aquifer are required.

3. Two hundred and twenty-five values of the X-coordinates and 225 values of the Y-coordinates of the map-grid used in the program are required. These values are in reference to the (X = 0, Y = 0) location in the upper-most left-hand corner of the grid.

4. One value of well-field radius, length of time at constant producing rate, and the constant producing rate for each well-field located in the aquifer are required.

5. Values for the X and Y-coordinates of the well-field centers for each well-field in the aquifer are required.

6. Values of the control variable, reference pressure, and contour pressure interval for each map desired is required.

6.61.5 Operation of This Program:

Once the required aquifer data has been read, the program calculates the pressure-drop at each of the 225 grid locations due to each well-field producing alone with its center at the specified point in the aquifer. These pressure-drops are then stored. Once the pressure-drop at each grid-point has been calculated and stored for each producing field, then the several values of pressure-drop at each grid-point are superimposed to give the total pressure-drop caused by all the fields in the aquifer at that particular grid-point.

For each of the more than 12,700 pressure-drop values required for each map produced, the program determines a map symbol (a letter or a character) which depends upon the value of the pressure-drop relative to the reference pressure-drop supplied in the data input. These symbols are then printed on the IBM 360/50 on-line printer in the exact locations that they occur in the grid-system. Each map appears as a two page rectangular section of the aquifer.

However, this section is actually a square section which has undergone distortion due to the limitations of the IBM 360/50 software.

6.62 List of Symbols Used In Program No. 3

PROGRAM SYMBOL	PROBLEM SYMBOL	DEFINITION
MAINLINE PROGRAM		
AK	K	Reservoir permeability (millidarcies).
H	H	Reservoir thickness (feet).
AMU	μ	Viscosity of water (centipoises).
POR	ϕ	Porosity of the reservoir (fraction).
PINT	p_i	Initial reservoir pressure (pounds per square inch absolute).
CW	c_w	Compressibility of water (volume per volume per pounds per square inch).
CON	4.56×10^{-7}	Unit conversion constant.
NS	----	Number of grid-points on the map.
N	----	Number of well-fields in the aquifer.
XY	X,Y	Coordinates of the grid-points on the map (miles).
RB	r_b	Well-field radius (miles).
T	t	Length of time at the constant producing rate (days).
Q	q	Constant producing rate from the well-fields (barrels per day).
C	----	Location of the well-field centers (miles).

PROGRAM SYMBOL	PROBLEM SYMBOL	DEFINITION
MAINLINE PROGRAM		
DELX DELY	---- ----	X and Y distances between the well-field centers and any grid-point (miles).
R	r	Radius from a well-field center to a grid-point (miles).
RD	RD	Dimensionless radius, r/r_b.
AREA	A	Area of a well-field (acres).
TD	TD	Dimensionless time, $Kt/\phi\mu cA$.
P	p	Individual pressure-drop at a point in the aquifer (pounds per square inch absolute).
PT	p_T	Total pressure-drop at a point in the aquifer (pounds per square inch absolute).
APLOT	----	The value of this variable controls whether the total or individual pressure-drop will be mapped. APLOT = 0 for total, APLOT = 1, 2, 3... for individual.
RCON	----	Reference pressure-drop contour (pounds per square inch absolute).
CONI	----	Pressure-drop contour interval for mapping (pounds per square inch absolute).
AP	----	Either P or PT (pounds per square inch absolute).
IRMIN	----	Family of pressure-drop values that are less than RCON.
IRPLS	----	Family of pressure-drop values that are greater than RCON.
IR	----	Pressure-drop values that are equal to RCON.

NOTE: All subroutine symbols used in Program No. 3 are the same as those described for the subroutines in Program No. 2 (See page 157).

6.63 User Instructions for Program No. 3 - On-Line Mapping

6.63.1 Program Input:

This program is quite complex in operation and therefore the data must be entered in exactly the manner specified below.

CARD NO.	FORMAT	VARIABLE NAME	DESCRIPTION
1	7F12.4	AK,H,AMU, POR,PINT	Contains the aquifer permeability, thickness, the viscosity of water, aquifer porosity, and initial aquifer pressure.
2	2E18.8	CW,CON	Contains the compressibility of water, and the unit conversion constant.
3	2I5	NS,N	Contains the number of grid-points (225) and the number of well-fields in the aquifer.
4-18	15F4.1	XY(I,1)	Contains the 225 X-coordinates of the grid-points, 15 per card going horizontally across the grid starting with the top row, left-hand corner.
19-33	15F4.1	XY(I,2)	Same as 4-18 only the Y-coordinates. At the upper left-hand corner (X = 0, Y = 0). In the lower right-hand corner (X = 15, Y = 15).
34-(N+33)	3F12.4	RB,T,Q	Next N cards contain the well-field data, radius of the field, producing time, and producing rate.

CARD NO.	FORMAT	VARIABLE NAME	DESCRIPTION
34+N	15F4.1	C(II,1) C(II,2)	Contains the N X-coordinates and the N Y-coordinates of the well-field centers. All X values come first, then all Y values on a single card unless more than 7 well-fields are located in the aquifer.
(N+35) - (2N+36) - 34+2 (N+1)	10X,3F7.2	APLOT RCON CONI	Next N+1 cards contain data, for mapping each card must have one value each for APLOT, RCON, and CONI.

Description of the mapping-routine parameters:

APLOT = 0 — The total pressure-drop resulting from the superposition of N well-fields will be mapped.

APLOT = 1,2,3 ... — The individual pressure-drops resulting from fields 1,2,3 ... will be mapped.

RCON — Reference contour value, normally RCON = 0 when mapping pressure-drop. If pressure itself is being mapped, then RCON equals the initial aquifer pressure in psi.

CONI — Contour interval selected. Must be chosen so that not more than 53 contours will fall above and below the value of RCON.

6.63.2 Program Output:

Program No. 3 prints the value of the total pressure-drop, resulting from N fields interfering, at each of the 225 grid-points. It also prints the 225 values of the pressure-drop resulting from each of the N fields producing alone in the aquifer. The pressure-drop values are labeled P(---,---) or PT(---), where the first blank contains the grid-point number and the second blank is for the field number.

After printing all the pressure-drops calculated at the 225 grid-points, the program begins its mapping routine. First a map of the total pressure-drop resulting from the N well-fields interfering is produced on the IBM 360/50 on-line printer. This map is followed by maps of the areal pressure-drop distribution for each of the N well-fields acting alone in the aquifer.

6.64 PROGRAM NO. 3

BLOCK DIAGRAM

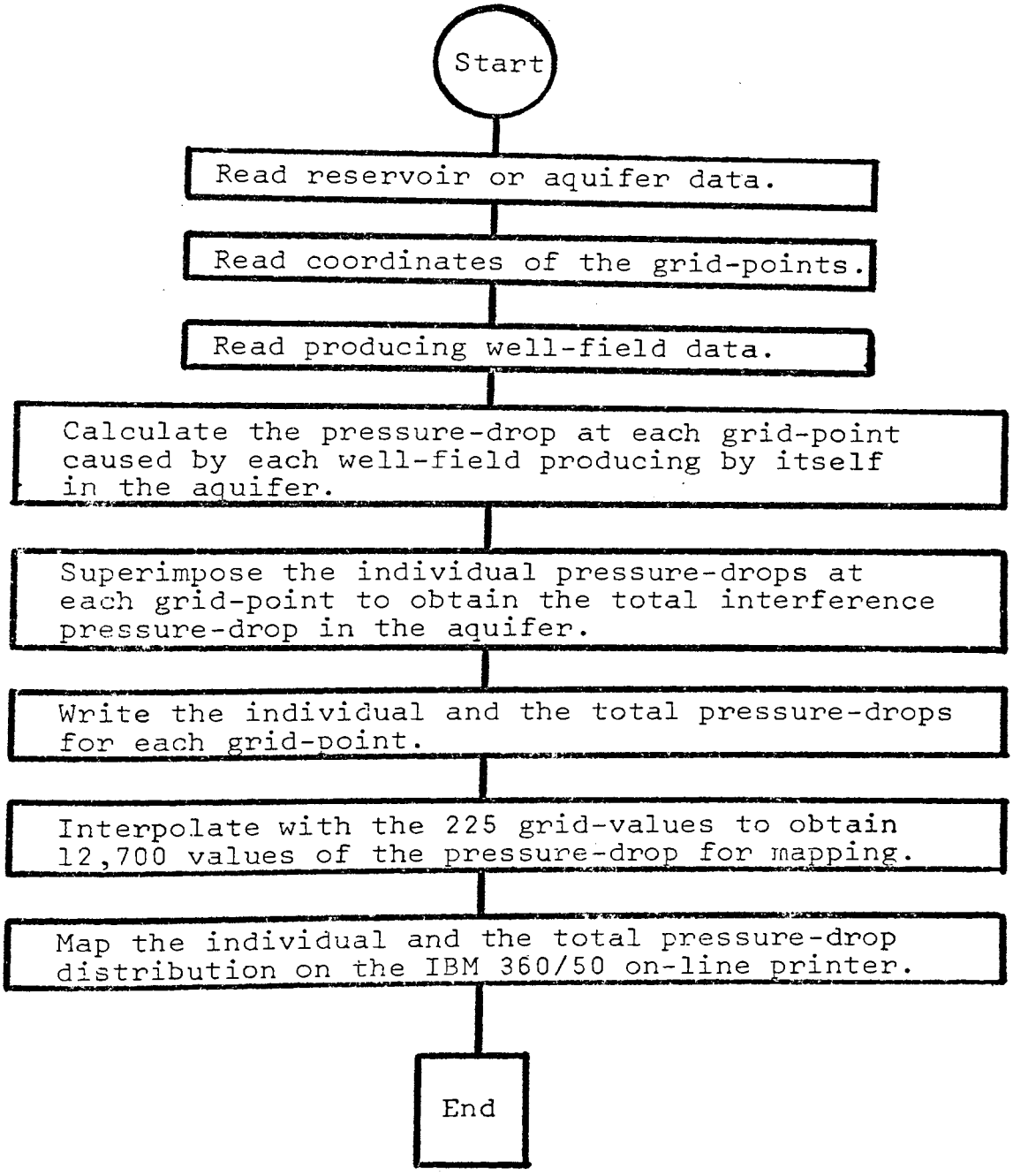

6.65 Flow Diagram
Program No. 3 - Mapping By On-Line Printer

A.) Main Line Program

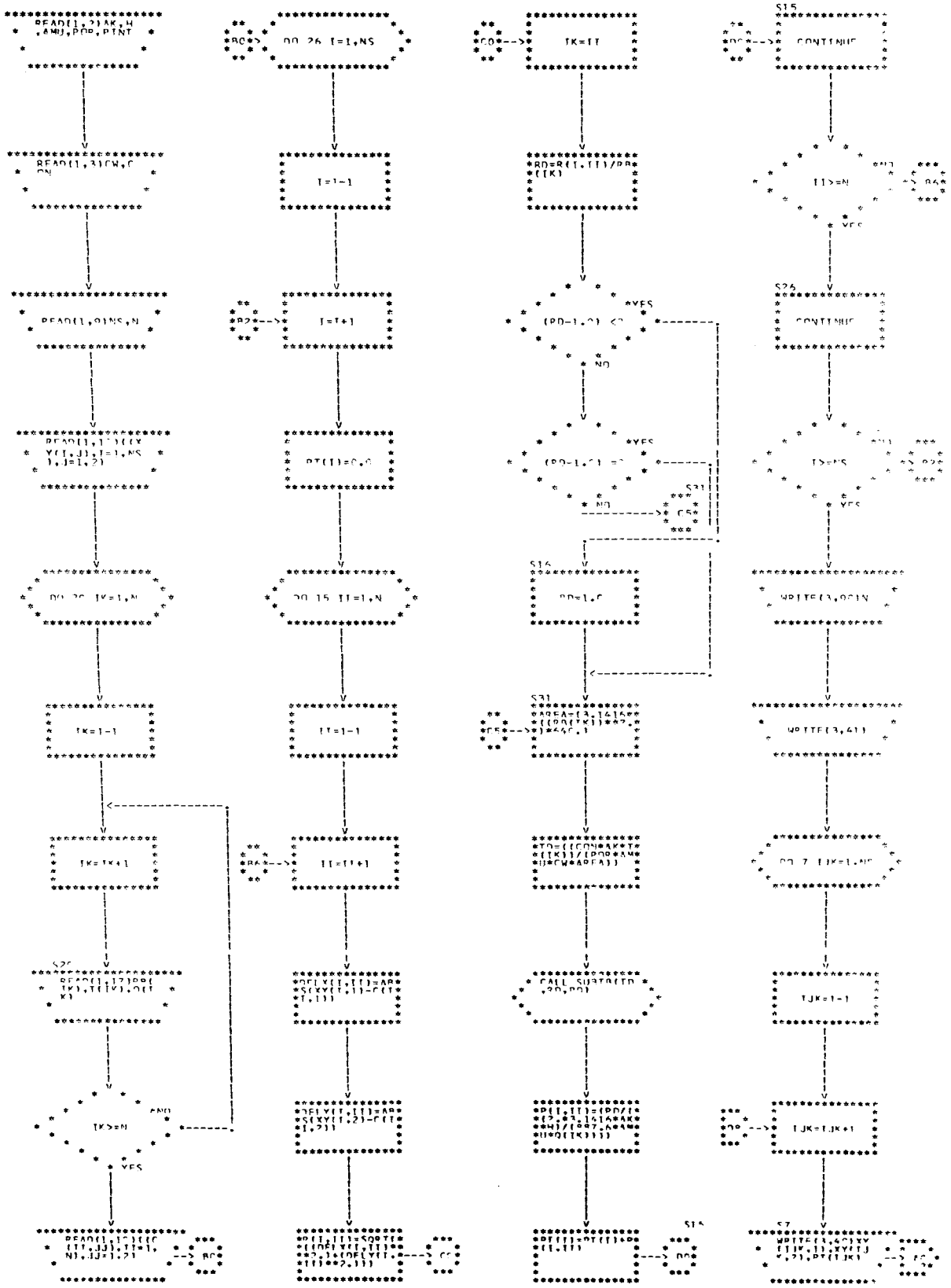

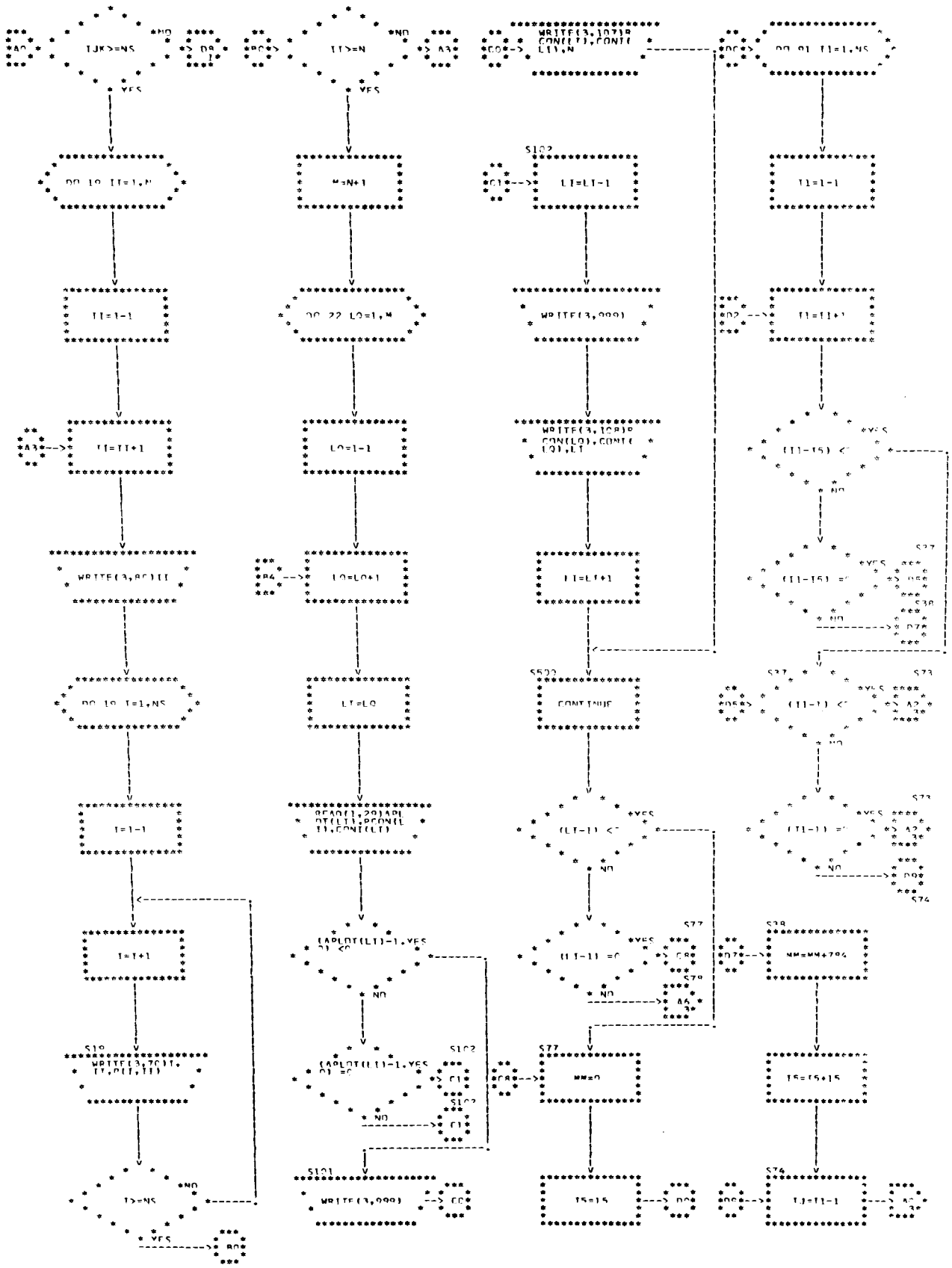
IJK>=NS
NO
YES
DO 10 II=1,N
II=1-1
II=II+1
WRITE(3,80)II
DO 10 I=1,NS
I=1-1
I=I+1
I>=NS
YES
II>=N
M=N+1
DO 22 LO=1,M
LO=1-1
LO=LO+1
LT=LO
READ(1,20)APL
LT=LT-1
WRITE(3,999)
WRITE(3,100)
CONTINUE
(LT-1) <
(II-1) =0
MM=MM+PW
MM=0
IS=IS+15
IS=15
DO 91 II=1,NS
II=1-1
II=II+1
(II-15) <
(II-1) <
IJ=II-1
WRITE(3,70)II,
II,P(I,II)
WRITE(3,999)

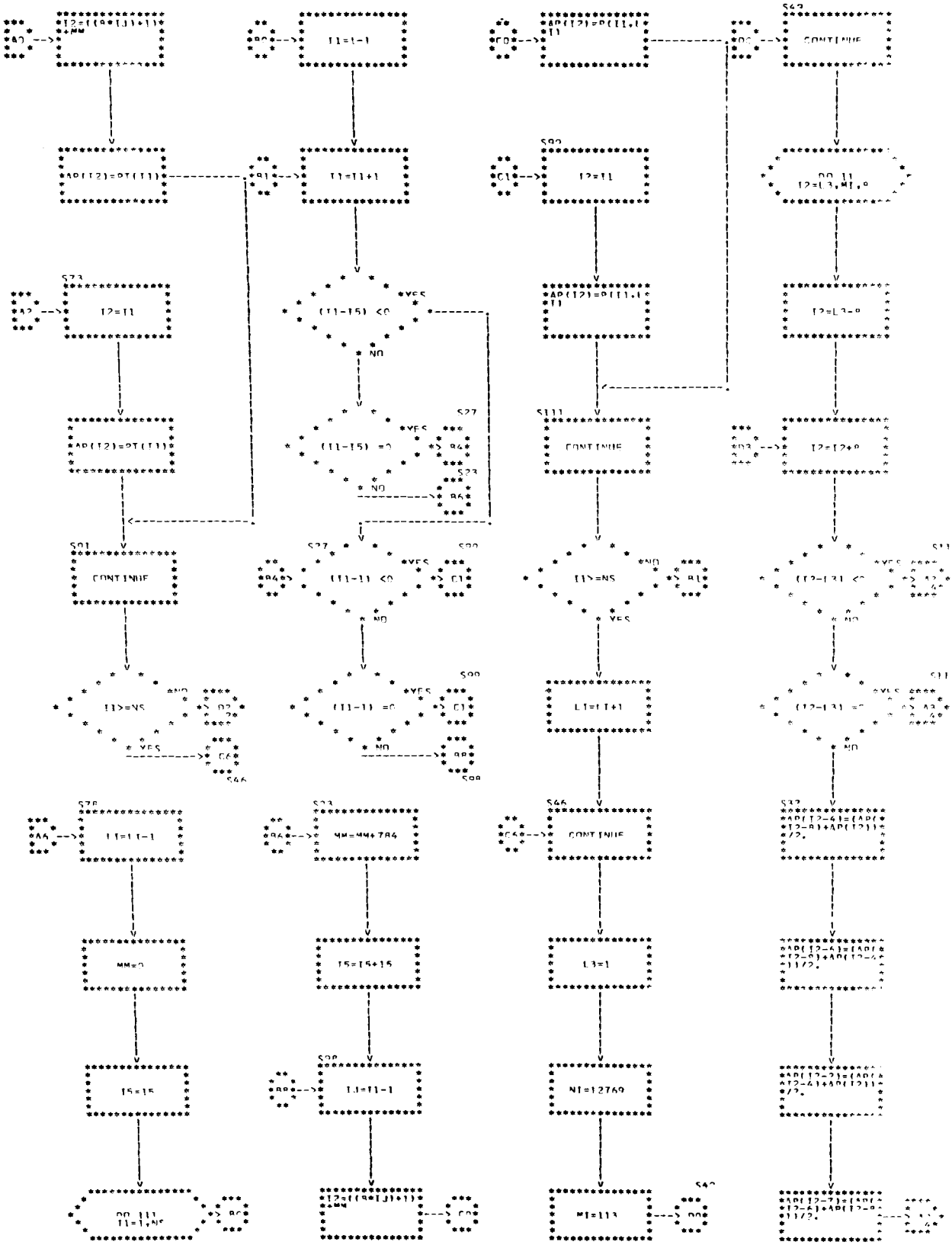

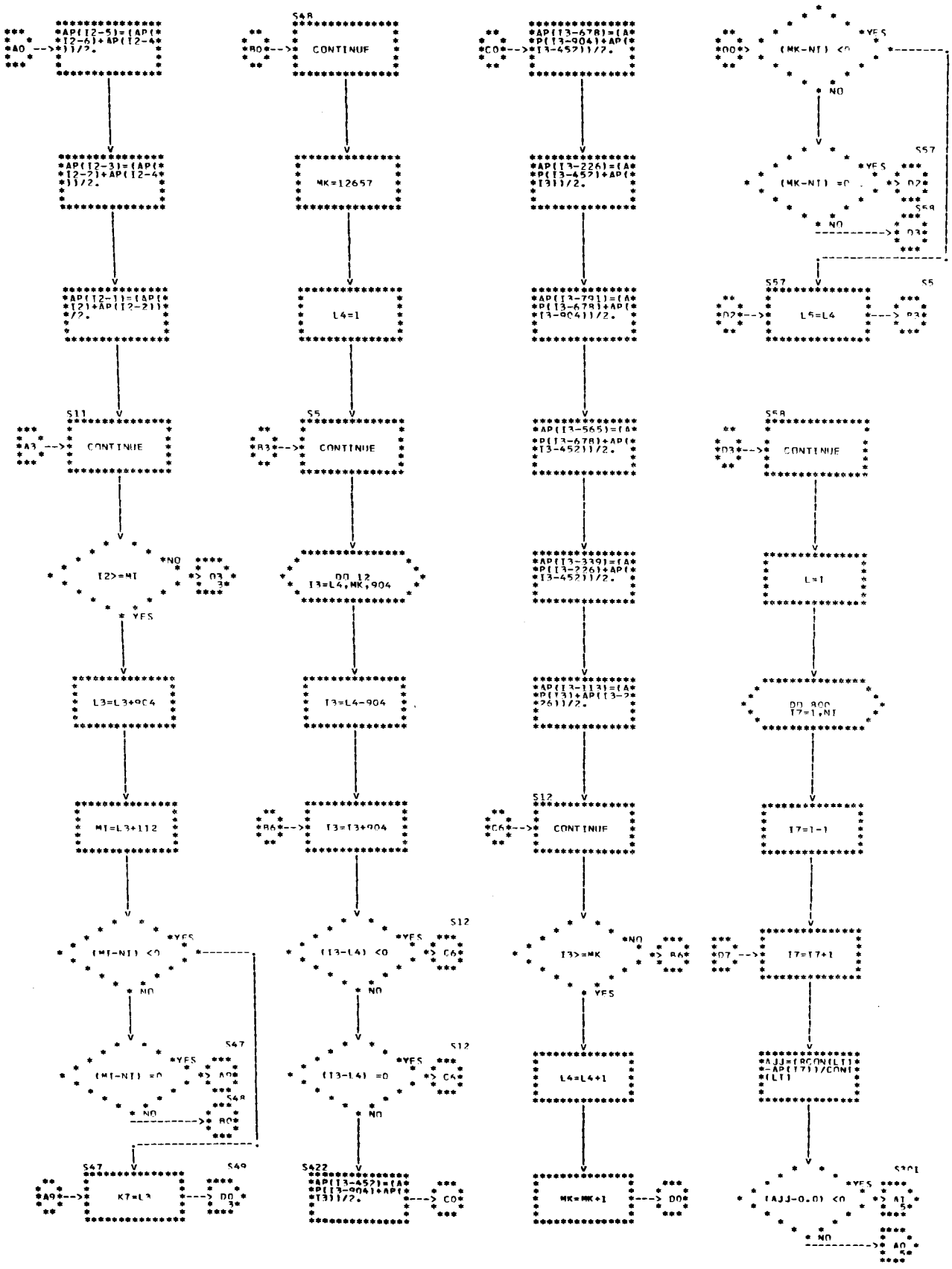
A0
AP(I2-5)=(AP(*I2-6)+AP(I2-4*))/2.
AP(I2-3)=(AP(*I2-2)+AP(I2-4*))/2.
AP(I2-1)=(AP(*I2)+AP(I2-2))*/2.
A3
CONTINUE
I2>=MI
NO
YES
L3=L3+904
MI=L3+112
(MI-NI) <0
NO
(MI-NI) =0
YES
NO
A9
K7=L3
DO 3
B0
CONTINUE
MK=12657
L4=1
B3
CONTINUE
DO 12 I3=L4,MK,904
I3=L4-904
B6
I3=I3+904
S12
(I3-L4) <0
YES
C6
NO
S12
(I3-L4) =0
YES
C4
NO
S422
AP(I3-4521)=(AP(I3-9041)+AP(I3))/2.
C0
AP(I3-678)=(AP(I3-9041)+AP(I3-4521))/2.
AP(I3-226)=(AP(I3-4521)+AP(I3))/2.
AP(I3-791)=(AP(I3-678)+AP(I3-9041))/2.
AP(I3-565)=(AP(I3-678)+AP(I3-4521))/2.
AP(I3-339)=(AP(I3-226)+AP(I3-4521))/2.
AP(I3-113)=(AP(I3)+AP(I3-226))/2.
C6
CONTINUE
I3>=MK
NO
B6
YES
L4=L4+1
MK=MK+1
DO 0
D0
(MK-NI) <0
YES
NO
S57
(MK-NI) =0
YES
D2
NO
D3
S57
L5=L4
S6
B3
D2
S58
CONTINUE
D3
L=1
DO 900 I7=1,NI
I7=1-1
D7
I7=I7+1
S201
(AJJ-0.0) <0
YES
A1
NO
A0
AJJ=(RCON(LT)-AP(I7))/CONI*(LT)

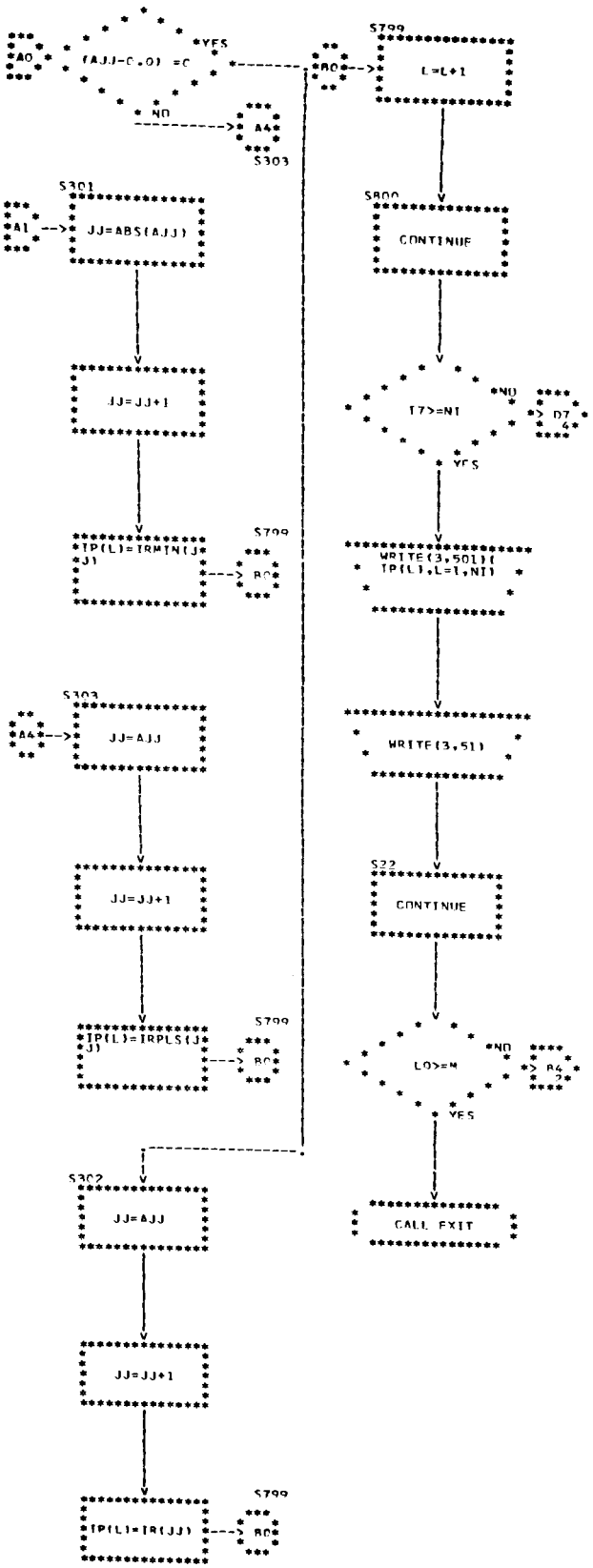
A0
(AJJ-C.0) =C
*YES
*NO
A4
S303
S301
A1
JJ=ABS(AJJ)
JJ=JJ+1
IP(L)=IRMIN(J
J)
S799
B0
S303
A4
JJ=AJJ
JJ=JJ+1
IP(L)=IRPLS(J
J)
S799
B0
S302
JJ=AJJ
JJ=JJ+1
IP(L)=IR(JJ)
S799
B0
S799
B0
L=L+1
S800
CONTINUE
I7>=NI
*NO
D7
4
*YES
WRITE(3,501)(
IP(L),L=1,NI)
WRITE(3,51)
S22
CONTINUE
LO>=M
*NO
B4
3
*YES
CALL EXIT

CHAPTER 7

CONCLUSIONS AND FUTURE INVESTIGATIONS

7.1 Conclusions

A method of calculating the dimensionless pressure PD(RD,TD) at any RD and TD value has been developed. The method developed employs a numerical evaluation of the explicit Van Everdingen-Hurst equation for the dimensionless pressure distribution in an infinite radial aquifer subject to a constant producing rate from the inner boundary. This approach allows accurate values of PD(RD,TD) to be obtained over a RD range from 1 to 64 for TD values from .0005 to 1000.

A new quantity termed the fractional dimensionless pressure, PD', has been created. PD' is used to investigate the distance away from the inner boundary at which a given fraction of the pressure-drop at the inner boundary is experienced. RD values have been obtained for 12 fractional dimensionless pressures ranging from .01 to .99.

A new and more accurate radius of drainage equation for infinite radial systems subject to constant producing rates has also been obtained by a least-squares curve fit of 30 RD-1 values. These RD-1 values correspond to various TD values at which PD' is .01. The use of this new equation avoids the question of selecting the proper radius of drainage equation from among the several expressions already available in the literature, none of which were specifically designed for an infinite radial system.

Finally, a technique for mapping pressure distribution in an infinite radial aquifer has been developed. This technique allows a square section of the aquifer to be mapped directly on the IBM 360/50 on-line printer. By the use of the program presented, a graphical representation of the areal pressure distribution resulting from several oil fields producing from a common aquifer can be obtained without the time-consuming process of contouring computer print-out pressure values. A built-in interpolation procedure also allows the map produced to have a much finer detail than what would normally result from contouring the print-out pressure values. This added detail is obtained with only a slight increase in computer time.

A study of this nature would be highly impractical without the aid of the digital computer. However, with the computer, the necessary equations can be numerically evaluated in a reasonable length of time. This study serves to point out the need to re-evaluate many of the techniques available in the petroleum literature which have heretofore been bypassed because of their highly complex nature or because of the large number of repetitive computations necessary to obtain suitable solutions.

7.2 Topics for Future Investigation

A.) Modification of Program No. 3 - A routine for the superposition of the pressure changes resulting from a series of different constant producing rates should be added to Program No. 3. This routine would then allow oil fields with declining production rates over the period of time being investigated to be mapped on the on-line printer. The routine could make step-wise calculations of PD(RD,TD) for each of a series of constant producing rates extending over the time steps t_1, t_2, t_3, ...t_N. The resulting pressure-drop would then be added to obtain the areal pressure distribution in the aquifer at time t_N.

B.) Constant Terminal Pressure Solution - The constant terminal pressure case for an infinite radial aquifer should be investigated along the same lines as undertaken in this study. The Romberg technique should be applied to Van Everdingen-Hurst's Equation (VI-26) after a transformation of limits has been performed similar to that discussed in Section 3.4. The PD(RD,TD) results obtained could then be compared to those presented by Jaeger(33).

The initial work on this problem was undertaken by the author and the results of the computer

program developed suggested that with future work suitable PD(RD,TD) values could be obtained. This initial work pointed out the need of plotting the function being integrated so that the correct type of transformation can be selected. As a result of the techniques used to evaluate the integral in the explicit constant pressure solution, the author believes that the tables of PD(RD,TD) given by Jaeger are not as accurate as is commonly desired.

C.) Radius of Drainage Equation - If PD(RD,TD) values can be obtained in the manner suggested in Part B, then an equation for the effective radius of drainage in an infinite radial aquifer can be developed for the constant pressure case. Since PD is a fractional dimensionless pressure for the constant pressure case, it would not be necessary to calculate a PD' as was required in this study. The drainage equation obtained when PD = .01 for the constant pressure case could then be compared to the equation developed in this study for the constant rate case.

D.) Curve Fit of RD-1 Values - The values of RD-1 given in Table 4-7 could easily be fitted by a least squares technique. If a fit-factor is used, the equations obtained should be a family of

straight lines in the form of the radius of drainage equation developed in Section 4.5. If PD' values other than those given in Table 4-7 were obtained from the cross-plots (Figures 4-2 and 4-3), then sufficient equations for RD-1 could be found to allow a simple computer program to be developed which would interpolate between these equations and would thus reduce the computer time required to locate RD for any TD and PD'.

E.) Mapping Routine - The mapping routine of Program No. 3 could be used to map the areal distribution of variables other than pressure-drop. The author has already used this routine to map the temperature distribution in the converter wall surrounding a copper tuyere. Some of the problems well-suited for the on-line mapping routine would be:

1. The mapping of aquifer pressure for underground gas storage problems.
2. The mapping of temperature profiles in underground thermal combustion and steam injection projects.
3. The graphical display of any reservoir parameter for which 225 values can be located on the 15 by 15 grid of Program No. 3.

F.) Aquifer Studies - Programs No. 2 and 3 and Figures 4-1, 4-2, and 4-3 now permit the drawdown occuring around producing municipal supply reservoirs to be examined provided the aquifer is large relative to the well-field itself. It is suggested that

various hydrologic problems be investigated using the capabilities developed by this study. The areal drawdown maps produced could be compared to those already on file at the Water Resources Division of the United States Geological Survey which have been prepared by contouring measured drawdowns in selected observation wells.

G.) Other Computer Models - By using the programs presented in this study for calculating PD(1,TD) and PD(RD,TD) it should now be possible to expand the basic model used in this study to include such variations as a dipping formation, aquifer shapes other than circular, various boundary effects, areal permeability variations, and varying formation thickness.

The techniques required to incorporate these modifications into the basic programs now developed are available in the petroleum literature in many cases. The programs developed in this study offer the foundation on which one can build more complex computer models to similuate the unsteady-state pressure distribution in aquifers.

BIBLIOGRAPHY

1. Theis, Charles V.: "The Relationship Between the Lowering of the Piezometric Surface and the Rate and Duration of Discharge of a Well Using Ground-Water Storage", Trans., Am. Geophys. Union, 16 (1935) 519.

2. Carslaw, H. S.: Introduction to the Mathematical Theory of the Conduction of Heat in Solids, 2nd Ed., Oxford Univ. Press, New York, (1921) 152.

3. Wenzel, L. K.: "Methods for Determining Permeability of Waterbearing Material with Special Reference to Discharging Well Methods", U. S. Geol. Survey Water-Supply Paper No. 887, (1942) 192.

4. Ferris, J. C., Knowles, D. B., Brown, R. H. and Stallman, R. W.: "Theory of Aquifer Tests", U. S. Geol. Survey Water-Supply Paper No. 1536-E, Washington, D. C. (1962).

5. Jacob, C. E.: "Flow of Ground Water", Chap. 5 in Rouse and Hunter, Engineering Hydraulics, New York, John Wiley and Sons, (1950).

6. Stallman, R. W.: "Continuously Varying Discharge Without Vertical Leakage", U. S. Geol. Survey Water-Supply Paper No. 1536-E, (1962) 174.

7. Witherspoon, P. A. and Neuman, S. P.: "Evaluating a Slightly Permeable Caprock in Aquifer Gas Storage: I. Caprock of Infinite Thickness", Jour. Pet. Tech., (July, 1967) 949.

8. Carslaw, H. S. and Jaeger, J. C.: "The Laplace Transformation: Problems on the Cylinder and Sphere", Chap. 13 in Carslaw and Jaeger, Conduction of Heat in Solids, Oxford Univ. Press, New York, (1947) 327.

9. Van Everdingen, A. F. and Hurst, W. E.: "The Application of Laplace Transformations to Flow Problems in Reservoirs", Trans., AIME, (1949) 186, 305.

10. Darcy, Henry: Les Fontaines Publiques de la Ville de Dijon (The Water Supply of Dijon), Paris, Victor Dalmont, (1856) 647.

11. Muskat, Morris: Physical Principals of Oil Production, McGraw-Hill, New York, (1949) 197.

12. Stallman, R. W.: "Non-Equilibrium-Type Curve Modified for Two-Well Systems", U. S. Geol. Survey Ground Water Note No. 3, (1952).

13. Horner, D. H.: "Pressure Build-up in Wells", Third World Petroleum Congress, E. J. Brill, Ed., Leiden, (1951) Sec. II, 503.

14. Chatas, Angelo T.: "A Practical Treatment of Non-Steady State Flow Problems in Reservoir Systems", Pet. Engr., (May, June, and August, 1953), B-38, B-42, and B-44.

15. Van Everdingen, A. K.: "The Skin Effect and Its Influence on the Productive Capacity of a Well", Trans., AIME, (1953) 198, 171.

16. Mortada, M.: "A Practical Method of Treating Interference in Water-Drive Reservoirs", Trans., AIME, (1955) 204, 217.

17. "Tables of the Error Function and Its Derivative", National Bureau of Standards, Ams-41, Washington, D. C., (1954).

18. Witherspoon, P. A., Mueller, T. D. and Donovan, R. W.: "Evaluation of Underground Gas-Storage Conditions in Aquifers Through Investigations of Ground-Water Hydrology", Jour. Pet. Tech., (May, 1962) 555.

19. Buxton, Thomas S.: "Pressure Distribution in Radial, Infinite, Single Phase Reservoirs Produced at a Constant Flow Rate", M.S. Thesis, Okla. State Univ., (1959) 45.

20. Stevens, W. F. and Thodos, George: "Prediction of Approximate Time of Interference Between Adjacent Wells", Jour. Pet. Tech., (October, 1959) 79.

21. Edwardson, M. S., Girner, H. M., Parkisons, H. R., Williams, C. D. and Matthews, C. S.: "Calculation of Formation Temperature Disturbances Caused by Mud Circulation", Jour. Pet. Tech., (April, 1962) 416.

22. Mueller, T. E. and Witherspoon, P. A.: "Pressure Interference Effects within Reservoirs and Aquifers", Jour. Pet. Tech., (April, 1965) 471.

23. Mueller, T. D.: "Transient Response of Non-Homogeneous Aquifers", Soc. Pet. Engr. Jour., (March, 1962) 33.

24. Aronofsky, J. S. and Jenkins, R.: "A Digital Computer Application to the Investigation of Aquifer Properties", Jour. Pet. Tech., (July, 1966) 827.

25. Van Poolen, H. K.: "Radius of Drainage and Stabilization Time Equations", Oil and Gas Jour., (Sept. 14, 1964) 138.

26. Jones, P. E.: "Reservoir Limit Test on Gas Wells", Jour. Pet. Tech., (June, 1962) 613.

27. Tek, M. H., Grove, M. L. and Poettmann, F. H.: "Method for Predicting the Back-Pressure Behavior of Low-Permeability Natural-Gas Wells", Trans., AIME, (1957) 210.

28. Muskat, Morris: Flow of Homogeneous Fluids through Porous Media, McGraw-Hill, New York, (1946) 657.

29. Brownscombe, E. R. and Kern, L. R.: "Graphical Solution of Single-Phase Flow Problems", Pet. Engr., (1951) B-70.

30. Hutchinson, T. O. and Kern, L. R.: (Personal Communication to Van Poolen, H. K.), Given by Van Poolen in Reference 29.

31. Hurst, W. E., Haynie, C. K. and Walker, R. N.: "Some Problems in Pressure Build-up", SPE-145, Dallas, Soc. Pet. Engr., (October, 1961).

32. Nute, Alton J.: "Some Aspects of Transient Flow Behavior in Artesian Aquifers and in Hydrocarbon Reservoirs Surrounded by Artesian Aquifers", M.S. Thesis, Univ. of Missouri-Rolla, (1967) 67.

33. Jaeger, J. C.: "Numerical Values for the Temperature in Radial Heat Flow", Jour. Math. Phys., (1956) 34, 316.

34. "Handbook of Mathematical Functions", U. S. Dept. of Commerce, Nat. Bureau Standards, Applied Math. Series 55, (1966) 1046.

35. "C.R.C. Standard Mathematical Tables, 11th Ed.", Chemical Rubber Publ. Co., Cleveland, Ohio, (1957) 480.

36. Carlile, R. E. and Gillett, B. E.: "Fortran Programming for Engineers", Tech. Manual Reprinted from Oil and Gas Jour., (1968) 94.

37. Pirson, Sylvain J.: Oil Reservoir Engineering, New York, McGraw-Hill, (1958) 735.

38. Merriam, D. F. and Harbaugh, J. W.: "Computer Helps Map Oil Structures", Oil and Gas Jour., (1963) 61, 47, 158.

39. Harbaugh, J. W.: "Balgol Program for Trend-Surface Mapping Using an IBM 7090 Computer", Kansas Geol. Survey Spec. Dist. Pub. 3, (1963) 1.

40. "International Symposium - Applications of Statistics, Operations Research, and Computers in the Mineral Industry - Part A", Quarterly Colo. Sch. Mines, (October, 1964) vol. 59, 4.

41. "Computer in the Mineral Industries, Part 2", Stanford Univ. Publ., Geol. Sciences, (1964) vol. 9, 2.

42. Perry, R. L. and Berggren, W. P.: "Transient Heat Conduction in Hollow Cylinders after Sudden Change of Inner Surface Temperature", Univ. Calif. Publ. In Engr., Univ. Calif. Press, (1944) 5, 59.

43. Germant, Andrew: "Transient Temperature around Heating Pipes Maintained at Constant Temperature", Jour. Appl. Phys., (1946) 17, 1076.

44. Guerro, E. T.: "How to Find Radius of Drainage", Art. 78 of Reservoir Engr. Series, Oil and Gas Jour., (May 10, 1965) 172.

45. Mortada, M.: "Oilfield Interference in Aquifers of Non-Uniform Properties", Trans., AIME, (1960) 219, 412.

46. Theim, Gunther: Hydrologische Methoden (Hydrologic Methods), Leipzig, J. B. Bebhardt, (1906) 56.

47. Slichter, C. S.: "Theoretical Investigation of the Motion of Ground Waters", U. S. Geol. Survey 19th Ann. Rpt., (1899); U. S. Geol. Survey Ground Water Note No. 22, (1954).

48. Turneaure, F. E. and Russell, H. L.: Public Water Supplies, New York, John Wiley and Sons, (1901).

49. Wyckoff, R. D., Botset, H. G. and Muskat, Morris: "Flow of Liquids through Porous Media under the Action of Gravity", Physics, vol. 3, (1932) 2, 90.

50. Tolman, C. F.: Ground Water, New York, McGraw-Hill, (1937) 387.

51. Leggette, R. M.: "The Mutual Interference of Artesian Wells on Long Island, N. Y.", Trans. Am. Geophys. Union, (1937) 493.

52. Muskat, Morris: "The Flow of Compressible Fluids through Porous Media and Some Problems in Heat Conduction", Physics, 5, (March, 1934) 71.

53. Jacob, C. E.: "Correction of Drawdowns Caused by a Pumped Well Tapping less than the Full Thickness of an Aquifer", U. S. Geol. Survey Water Supply Paper 1536-I, (1963) 341.

54. Hantush, M. S. and Jacob, C. E.: "Non-Steady Radial Flow in an Infinite Leaky Aquifer", Trans., Am. Geophys. Union, (1955) 36, 95.

55. Jacob, C. E. and Lohman, S. W.: "Non-Steady Flow to a Well of Constant Drawdown in an Extensive Aquifer", Trans., Am. Geophys. Union, (1952) 33, 559.

56. Hurst, W. E.: "Water Influx Into a Reservoir and Its Application to the Equation of Volumetric Balance", Trans., AIME, (1943) 151, 57.

57. Wilson, T. C.: "Water Encroachment-An Approximation", M.S. Thesis, Univ. of Missouri-Rolla, (1965) 29.

58. Carter, R. D. and Tracy, G. W.: "An Improved Method for Calculating Water Influx", Trans., AIME, (1960) 219, 415.

59. Van Everdingen, A. F., Timmermen, E. H. and McMahan, J. J.: "Application of the Material Balance Equation to a Partial Water-Drive Reservoir", Trans., AIME, (1953) 198, 51.

60. Katz, D. L., Tek, M., Coats, K. H., Katz, M. L., Jones, S. C. and Miller, M. C.: Movement of Underground Water In Contact With Natural Gas, Am. Gas Ass., New York, (February, 1963).

61. Schilthuis, R. J.: "Active Oil and Reservoir Energy", Trans., AIME, (1963) 118, 37.

62. Hurst, W. E.: "The Simplification of the Material Balance Formula by the Laplace Transformation", Trans., AIME, (1958) 213, 292.

63. Katz, D. L., Vary, J. A. and Elenbaas, J. R.: "Design of Gas Storage Fields", Trans., AIME, (1959) 216, 44.

64. Coats, K. H., Tek, M. R. and Katz, D. L.: "Method for Predicting the Behavior of Mutually Interferring Gas Reservoirs Adjacent to a Common Aquifer", Trans., AIME, (1959) 216, 460.

65. Katz, M. L., Tek, M. R. and Coats, K. H.: "Effect of Unsteady Aquifer Motion on the Size of an Adjacent Gas Storage Reservoir", Trans., AIME, (1959) 216, 18.

66. Yoo, H. D., Katz, D. L., White, R. R. and Tek, M. R.: "Methods for Predicting the Volume of Gas and Oil Reservoirs Associated with Active Water Drive", Pet. Engr., (September, 1959) 10, B-27.

67. Katz, D. L., Cornell, D., Kobayashi, R., Poettmann, F. H., Vary, J. A., Elenbaas, J. R. and Weinaug, C. F.: Handbook of Natural Gas Engineering, New York, McGraw-Hill, (1959).

68. Theis, C. V.: "The Significance and Nature of the Cone of Depression in Ground-Water Bodies", Econ. Geol., (1938) 33, 889.

69. Kellogg, F. H.: "Rate of Depletion of Water Bearing Sands", Miss. State Geol. Survey, (1950) 5.

70. De Wiest, R. J. M.: Geohydrology, John Wiley and Sons, New York, (1965).

71. Rowan, G. and Clegg, M. W.: "An Approximate Method for Transient Radial Flow", Soc. Pet. Engr. Jour., (September, 1962) 225.

72. Hall, H. N.: "Compressibility of Reservoir Rocks", Trans., AIME, (1953) 198, 309.

73. Geertsma, J.: "The Effect of Fluid Pressure Decline on Volumetric Changes in Porous Rocks", Trans., AIME, (1957) 210, 331.

74. Hurst, W. E.: "Interference between Oilfields", Trans., AIME, (1960) 219, 175.

75. Jacob, C. E.: "On the Flow of Water in an Elastic Artesian Aquifer", Trans., Am. Geophys. Union, (1940) 21, 574.

76. Hurst, W. E.: "Unsteady Flow of Fluids in Oil Reservoirs", Physics, (January, 1934) 5.

77. Agarwal, R. G., Al-Hussainy, R. and Ramey, H. J.: "The Importance of Water Influx in Gas Reservoirs", Jour. Pet. Tech., (November, 1965) 1336.

78. Brauer, E. B.: "Simplification of the Superposition Principle for Pressure Analysis at Variable Rates", Soc. Pet. Engr., Dallas, (1965) 1184.

79. Coats, K. H., Rapoport, L. A., McCord, J. R. and Drews, W. P.: "Determination of Aquifer Influence Functions from Field Data", Jour. Pet. Tech., (December, 1964) 1417.

80. Jargon, J. R. and Van Poolen, H. K.: "Unit Response Function from Varying-Rate Data", Jour. Pet. Tech., (August, 1965) 8, 965.

81. Odeh, A. S. and Jones, L. G.: "Pressure Drawdown Analysis, Variable-Rate Case", Jour. Pet. Tech., (August, 1965) 8, 961.

82. Howard, D. S. and Rachford, H. H.: "Comparison of Pressure Distributions during Depletion of Tilted and Horizontal Aquifers", Trans., AIME, (1956) 207, 92.

83. Hubbert, King M.: "Darcy's Law and the Field Equations of the Flow of Underground Fluids", Trans., AIME, (1956) 207, 222.

84. Brown, R. H., Ferris, J. G., Jacob, C. E., Knowles, D. B., Meyer, R. R., Skibitzke, H. E., Theis, C. V.: "Methods of Determining Permeability, Transmissibility, and Drawdown", U. S. Geol. Survey Water-Supply Paper 1536-I, (1963).

VITA

The author, Alton John Nute, was born on November 15, 1939 in Bangor, Maine. He received his primary and secondary education in the Lincoln, Maine Public School System graduating from Mattanawcook Academy in June, 1958.

He began his college studies at the University of Michigan in September, 1958. After completing one year of college he worked for over a year at the Eastern Fine Paper and Pulp Division of Standard Packaging Corporation, Lincoln, Maine.

In September, 1960 he transferred to the University of Maine and graduated from that institution in January, 1964 with a B.S. in Chemical Engineering.

After graduation from the University of Maine, he entered the University of Missouri-Rolla and received a second B.S. degree in Petroleum Engineering in May, 1965.

During the summers of 1964 and 1965 he was employed by Texaco, Inc. as a roughneck and an engineering assistant in the Houma District, Louisiana.

He received an M.S. in Petroleum Engineering in May, 1967 and continued working towards the Doctor of Philosophy Degree in Petroleum Engineering. He has held the position of Graduate Teaching Assistant in Petroleum Engineering since September, 1966. Since February, 1968, he has also held a National Aeronautics and Space Administration Pre-Doctoral Traineeship.

He has accepted permanent employment with Texaco, Inc. at their Research Laboratories in Bellaire, Texas.

APPENDIX A

PART 1. NOMENCLATURE

A	= Surface area of the well-field.
a	= Lower limit of integration.
a	= Muskat's diffusivity constant, $k/f\phi\mu$.
a	= Constant, see Equation (2E-7), page 237.
a	= Radius of the inner boundary.
B_0	= Oil formation volume factor.
b	= Upper limit of integration.
c	= Compressibility of the fluid.
C_w	= Compressibility of the water.
e	= Constant, 2.71828.
Ei(-X)	= Exponential integral of (-X).
erfc	= Complementary Error Function, defined by Equation (2E-3), page 236.
f	= Porosity of the aquifer.
f_0	= Variable, defined by Equation (2A-2), page 233.
f_1	= Variable, defined by Equation (2C-2), page 235.
F(X)	= Function integrated by the Trapezoidal Rule, defined by Equation (3-16), page 58.
$FT(\bar{X})$	= Function integrated by the Romberg method, defined by Equation (3-20), Page 67.
H	= Net sand or aquifer thickness.
h	= Panel size used for integration in the Romberg method, $(b-a)/2^k$.
h	= Unit thickness, Carslaw and Jaeger.
h	= Thickness of the reservoir.

$I(\bar{t})$ = Integral in Equation (2-23).

ierfc = Integral of the Complementary Error Function, defined by Equation (2E-3), page 236.

i^2erfc = Second integral of the Complementary Error Function, defined by Equation (2E-1), page 236.

J_0 = Bessel function, zero order, first kind.

J_1 = Bessel function, first order, first kind.

K Variable ranging from 1 to 10.

K Permeability of the aquifer.

K = Carslaw and Jaeger's thermal conductivity.

k = Permeability of the reservoir.

Log = Common logarithim, base 10.

Ln = Naperian logarithim, base e.

M = Aquifer prism height.

m = Variable ranging from 1 to 9.

N = Number of equal integration panels, (b-a)/h.

$\bar{P}$ = Meinzer's permeability coefficient, see definitions, page 221.

ΔP = Mortada's pressure-drop.

ΔP = Cumulative pressure-drop, $q(t_D)\ P_D(r_D,t_D)$

PD = Nute's dimensionless pressure, $\frac{2\pi KH\ (p_i - p)}{q\mu}$

P_D = Mortada's dimensionless pressure, $\frac{2\pi KH\ (P_2 - P_1)}{q\mu}$

PD' = Nute's fractional dimensionless pressure, defined by Equation (3-10), page 56.

P_D = Dimensionless pressure-drop, $\frac{8.953 \times 10^{-5}\ Kh\bar{s}}{Q\mu}$

ΔP_D = Mortada's and Van Everdingen-Hurst's dimensionless dependent variable, see Equation (2-47), page 40..

P_0 = Initial reservoir pressure.

P_R = Initial reservoir pressure.

P_r = Aquifer pressure at a radius r.

P_w = Pressure at the well-bore.

PD(1,TD) = Nute's dimensionless pressure at the inner boundary at a dimensionless time TD.

PD(RD,TD) = Nute's dimensionless pressure at any radius ratio RD at a dimensionless time TD.

$PD(1,t_D)$ = Dimensionless pressure at the well-bore or inner boundary at a dimensionless time t_D.

$P(R,t_D)$ = Buxton's dimensionless pressure at a radius ratio R at a dimensionless time t_D.

P(r,t) = Pressure-drop at a radius r at a time t.

$\underline{P}(\underline{r},\underline{t})$ = Mortada's dimensionless pressure at $\underline{r}$ and $\underline{t}$.

$P(r_D,t_D)$ = Edwardson's dimensionless temperature at any r_D and any t_D.

$P_{(T)}$ = Van Everdingen's dimensionless pressure, shown in Table 2-1 and Figure 2-4 and equivalent to $P_D(t_D)$.

$P_{(T)}$ = Aronofsky and Jenkin's dimensionless pressure.

$P_D(r_D,t_D)$ = Van Everdingen-Hurst's and Mortada's dimensionless pressure at r_D and t_D.

$P_D(t_D)$ = Van Everdingen-Hurst's dimensionless pressure at the inner boundary at a dimensionless time t_D.

$P_T(r,t)$ = Total pressure-drop at a radius r at time t.

Δp = $p_i - p_f$, pressure-drop.

p = Pressure at radius r at time t.

P_b = Pressure at the inner boundary of the aquifer.

P_f = Final aquifer pressure.

P_i = Initial aquifer pressure.

P_0 = Initial fluid pressure.

$p(t)$ = Chatas' dimensionless pressure-drop of Table 2-2.

Q = Constant flux, heat units/unit time/unit area.

Q = Rate of discharge of a well.

Q = Strength of the source (i.e., the amount of heat).

$\bar{Q}$ = $Q\mu/k$, withdrawal rate (Muskat).

Q_0 = Initial constant production rate (Muskat).

Q = Volumetric outflow per unit thickness at r_f, but measured at the surface, q_0/γ_0 (Muskat).

Q_1 = Constant production rate at time 1.

q = Constant discharge or production rate.

q = Carslaw and Jaeger's rate of flux, Q/T.

q_0 = Muskat's constant production rate.

$q_{(T)}$ = Van Everdingen-Hurst's rate of fluid flow into an inner cylinder per unit sand thickness H.

$q(t_D)$ = $q_{(T)}\mu/2\pi K$

RD = Nute's dimensionless radius, r/r_b.

r = Distance away from the discharge well.

r = Muskat's production ratio, Q_1/Q_0.

$\underline{r}$ = Mortada's dimensionless radius, r/r_b or r/r_w.

r_b = Radius of the inner boundary of the well-field.

r_{ab} = Distance between producing well A and observation well B.

r_D = Mortada's dimensionless radius, r/r_w or r/r_b.

r_d = Aronofsky and Jenkin's effective radius of drainage.

r_e = Constant radius of drainage.

r_f = Carslaw and Jaeger's radius of the inner boundary.

r_f = Muskat's radius of the inner boundary.

r_r = Reservoir radius, Aronofsky and Jenkin.

r_w = Radius of the well-bore.

S = Coefficient of storage, see Definitions, page 220.

$\bar{s}$ = Theis' drawdown at any point r around a well or well-field.

T_D = Same as $\bar{t}_D$, dimensionless time based on any radius r.

T = Van Everdingen dimensionless time, $Kt/\phi\mu cr_w^2$.

$\underline{T}$ = Coefficient of transmissibility, see Definitions, page 220.

TD = Nute's dimensionless time, $Kt/\phi\mu cr_b^2$.

T = Carslaw and Jaeger's unit time.

T_N = Trapezoidal Rule approximation to the integral of FT(X), defined by Equation (3-21), page 74.

$T_2{}^{(m)}_{k_N}$ = Romberg combination of k Trapezoidal approximations to the integral of Equation (3-20), see Table 3-1.

t = Theis pumping time or just time itself.

$\bar{t}$ = Muskat's dimensionless time, at/r_f^2.

$\underline{t}$ = Mortada's dimensionless time, $\frac{4.56 \times 10^{-7} kt}{f\mu C_w A}$

t_D = Mortada's dimensionless time, see Equation (2-38), page 30.

$\bar{t}_D$ = Dimensionless time based on any radius r,

$$\frac{xKt}{\phi \mu c r^2}$$

t_s = Time of stabilization, defined by Equation (4-8), page 101.

u = Variable, $\bar{X}/1 - \bar{X}$.

u = $1.87\ r^2 S/\underline{T}t$.

u = Variable of integration.

v = Temperature at radius r at time t.

v = Carslaw and Jaeger's change in temperature at point x,y at time t.

v_s = Surface temperature at a distance r from the well-bore.

v_t = Change in temperature at x,y at time t for a continuous source of constant strength.

$v_{(t)}$ = Surface temperature at time t, defined by Equation (1D-3), page 231.

$W(u)$ = Well function of (u), given by Equation (2-6) and shown in Figure 2-3.

w = Constant, depends on the units used, see Table 2-3, page 31.

X = Argument, definition varies.

X = Variable of integration, Trapezoidal Rule, given by Equation (3-16), page 58.

X = Theis' dimensionless independent variable, see Table 2-7.

$\bar{X}$ = A number between 0 and 1.0.

x = A constant, depends on the units used, see Table 2-3.

x = x coordinate (horizontal) of location in grid.

$\bar{x}$ = Level of decline of piezometric surface.

$\bar{x}$ = Variable of integration.

Y_0 = Bessel function, zero order, second kind.

Y_1 = Bessel function, first order, second kind.

y = y coordinate (vertical) of location in grid.

z = Variable of integration.

Z = Argument, see Section E, page 236.

β = Aronofsky and Jenkin's liquid compressibility.

γ = Euler's constant, .5772.

γ = Muskat's liquid density.

γ_f = Final liquid density at r_f.

γ_i = Muskat's initial liquid density.

γ_0 = Density of outflow liquid at the surface (Muskat).

ϕ = Aquifer porosity.

ρ = Density of fluid at pressure p.

ρ = Constant, .3275911.

ρ_0 = Initial density of fluid at pressure p_0.

κ = Kelvin's coefficient of diffusivity, $K/\phi\mu c$.

κ = Muskat's compressibility of the fluid.

T = Aronofsky and Jenkin's dimensionless time.

$\Psi_{(t')}$ = Function equal to λ.

μ = Viscosity of the fluid.

λ = Constant.

π = 3.14159.

θ_0 = Variable, defined by Equation (2B-2), Page 234.

θ_1 = Variable, defined by Equation (2C-2), Page 235.

$|E|$ = Absolute value of the error resulting from the use of any polynomial approximation.

∂ = Partial of a quantity.

∞ = Infinity.

Δ = Change in quantity.

$\int$ = Integral of.

PART 2. DEFINITIONS

Coefficient of Storage: The volume of water released or taken into storage per unit surface area of an aquifer per unit change of the component of head normal to that surface. Figure 2-1 shows a prism of height, m, which can be used to define this coefficient. This prism extends vertically from top to bottom of the aquifer and laterally so that its cross-sectional area is coextensive with the aquifer-surface area over which the head change occurs. The volume of water released from storage in this prism, m, for any head change $\bar{X}$, divided by the product of the prism's cross-sectional area and the change in head, $\bar{X}$, results in a dimensionless number, S, which is the coefficient of storage.

Coefficient of Transmissibility: Theis introduced this coefficient, T, which is expressed as the rate of flow of water, at the prevailing water temperature, in gallons per day, through a vertical strip of aquifer one foot wide extending the full saturated height of an aquifer under a hydraulic gradient of 100 percent. A hydraulic gradient of 100 percent means a one-foot drop in the head in one-foot of flow distance in the aquifer. The coefficient is shown in Figure 2-2. T is equal to the product of the coefficient of permeability, $\bar{P}$, and the thickness of the saturated aquifer, m.

Coefficient of Permeability: This coefficient, $\bar{P}$, is a measure of a material's capacity to transmit water. As expressed by Meinzer, it is the rate of flow of water in gallons per day through a cross-sectional area of one square foot under a hydraulic gradient of one foot per foot at a temperature of 60° F. This coefficient is shown in Figure 2-2.

APPENDIX B

DERIVATION OF EQUATIONS

PART 1 - Conversion of the heat transfer equations of Carslaw and Jaeger(8) to the equivalent pressure distribution equations for an infinite radial reservoir having a finite inner boundary r_f and subject to a constant producing rate, Q.

Section A: For the constant rate case where $\kappa t/a^2$ is of medium size ($.01 \leq TD \leq 500$), Carslaw and Jaeger give the following expression for the temperature at any radius r at time t (See Equation 17, page 339):

(1A-1)

$$v = \frac{-2Q}{\pi K} \int_0^\infty \frac{(1-e^{-\kappa u^2 t})\left[J_0(ur)Y_1(ua)-Y_0(ur)J_1(ua)\right]}{u^2\left[J_1^2(ua)+Y_1^2(ua)\right]}\,du$$

and since,

(1A-2)

$$\kappa = \frac{K}{\phi\mu c} \text{ and; } a = r_f$$

then:

(1A-3)

$$\frac{vK}{Q} = \frac{2}{\pi} \int_0^\infty \frac{(1-e^{-\frac{Ktu^2}{\phi\mu c}})\left[J_1(ur_f)Y_0(ur)-Y_1(ur_f)J_0(ur)\right]}{u^2\left[J_1^2(ur_f)+Y_1^2(ur_f)\right]}\,du$$

where:

(1A-5)

$$u = \frac{X}{r_f} \qquad \text{and:} \quad \frac{r}{r_f} = RD$$

$$dX = r_f du \qquad TD = \frac{Kt}{\phi \mu c r_f^2}$$

thus:

(1A-6)

$$\frac{vK}{r_f Q} = \frac{2}{\pi} \int_0^{\infty} \frac{(1-e^{-X^2 TD}) \left[J_1(X) Y_0(X,RD) - Y_1(X) J_0(X,RD) \right] dX}{X^2 \left[J_1^2(X) + Y_1^2(X) \right]}$$

then for a unit thickness, h, and a unit time, T, with a unit area, $2\pi r_f$:

(1A-7)

$$v = P(r,t) \quad \text{and} \quad q = Q/T$$

(1A-8)

$$\frac{vK}{r_f Q} \left(\frac{hT 2\pi r_f}{887\mu} \right) = \frac{2\pi Kh}{887 \mu q} P(r,t) = PD(RD,TD)$$

thus (1A-1) is equivalent to the Van Everdingen-Hurst Equation (V1-21) on page 313, where:

(1A-9)

$$PD(RD,TD) = \frac{2}{\pi} \int_0^{\infty} \frac{(1-e^{-X^2 TD}) \left[J_1(X) Y_0(X,RD) - Y_1(X) J_0(X,RD) \right] dX}{X^2 \left[J_1^2(X) + Y_1^2(X) \right]} .$$

Section B: For the constant rate case where $\kappa t/a^2 < .01$ ($TD < .01$) Carslaw and Jaeger give the following approximate expression for Equation (1A-1) (See Equation (18), page 339).

(1B-1)

$$v = \frac{2Q\sqrt{\kappa a t}}{K r}\left[\text{ierfc}\left(\frac{r-a}{2\sqrt{\kappa t}}\right) - \frac{(3r+a)\sqrt{\kappa t}}{4ar}\, i^2\text{erfc}\left(\frac{r-a}{2\sqrt{\kappa t}}\right) + \ldots\right]$$

and:

(1B-2)

$$\left[\text{ierfc}\left(\frac{r-r_f}{2\sqrt{\frac{\kappa t}{\phi\mu c}}}\right) - \frac{(3r+r_f)\sqrt{\frac{Kt}{\phi\mu c}}}{4r_f r}\, i^2\text{erfc}\left(\frac{r-r_f}{2\sqrt{\frac{\kappa t}{\phi\mu c}}}\right) + \ldots\right]$$

(1B-3)

$$\frac{v}{Q} = \frac{\frac{2}{r_f}\sqrt{\frac{Ktr_f}{\phi\mu cr}}}{K/r_f}\left[\text{ierfc}\,\frac{\frac{r}{r_f}-\frac{r_f}{r_f}}{\frac{2}{r_f}\sqrt{\frac{Kt}{\phi\mu c}}} - \frac{\left(\frac{3r}{r_f}+\frac{r_f}{r_f}\right)\sqrt{\frac{Kt}{\phi\mu c}}}{\frac{4r_f r}{r_f}}\, i^2\text{erfc}\,\frac{\frac{r}{r_f}-\frac{r_f}{r_f}}{\frac{2}{r_f}\sqrt{\frac{Kt}{\phi\mu c}}}\right]$$

(1B-4)

$$\frac{v}{Q} = \frac{2\sqrt{Kt/\phi\mu cr_f^2}}{\sqrt{RD}(K/r_f)}\left[\text{ierfc}\,\frac{RD-1}{2\sqrt{\frac{Kt}{\phi\mu cr_f^2}}} - \frac{(3RD+1)\sqrt{\frac{Kt}{\phi\mu c}}}{4r}\, i^2\text{erfc}\,\frac{RD-1}{2\sqrt{\frac{Kt}{\phi\mu cr_f^2}}}\right]$$

where:

(1B-5)

$$RD = \frac{r}{r_f} \quad \text{and} \quad TD = \frac{Kt}{\phi \mu c r_f^2}$$

so:

(1B-6)

$$\frac{v}{Q} = \frac{2\sqrt{TD}}{\frac{K}{r_f}\sqrt{RD}} \left(\text{ierfc} \frac{RD-1}{2\sqrt{TD}} - \frac{(3RD+1)\sqrt{\frac{Kt}{\phi \mu c}}}{4r} i^2\text{erfc} \frac{RD-1}{2\sqrt{TD}} \right)$$

(1B-7)

$$\frac{Kv}{Qr_f} = \frac{2\sqrt{TD}}{\sqrt{RD}} \left(\text{ierfc} \frac{RD-1}{2\sqrt{TD}} - \left(\frac{(3RD+1)\sqrt{TD}}{4RD} i^2\text{erfc} \frac{RD-1}{2\sqrt{TD}} \right) \right) .$$

Thus since $v = P(r,t)$ by the analogy of temperature in heat transfer theory to pressure in fluid flow theory, and since (1B-7) was derived for a unit thickness, h, with a fluid of viscosity, μ, and with Q as a constant unit flow rate per unit time per unit area at $r = r_f$, then:

(1B-8)

T = 1 unit time

h = 1 unit thickness

$2\pi r_f$ = 1 unit area

and furthermore since the surface area at $r=r_f$ is equal to $2\pi r_f h=A$, then by Mortada's definition:

(1B-9)

$$PD(RD,TD) = \frac{2\pi Kh}{887q\mu} P(r,t).$$

Mortada also gives:

(1B-10)

$$PD(RD,TD) = \frac{2\sqrt{TD}}{\sqrt{RD}} \text{ ierfc } \frac{RD-1}{2\sqrt{TD}}$$

and since the right hand side of (1B-10) equals the first term of the right hand side of (1B-7), then:

(1B-11)

$$\frac{Kv}{Qr_f} = \frac{2\pi Kh}{887q\mu} P(r,t) = PD(RD,TD)$$

and thus:

(1B-12)

$$\left(\frac{Kv}{Qr_f}\right) \frac{hT2\pi r_f}{\mu 887} = \frac{2\pi Kh}{887q\mu} P(r,t) = PD(RD,TD)$$

where: $q = Q/T$ and 887 is the conversion factor to Mortada's definition of PD(RD,TD).

So (1B-13) is obtained, which is Mortada's expression for TD<.01, plus an extra term.

(1B-13)

$$PD(RD,TD) = \frac{2\sqrt{TD}}{\sqrt{RD}}\ \text{ierfc}\ \frac{RD-1}{2\sqrt{TD}} - \frac{(3RD+1)\sqrt{TD}}{4RD}\ i^2\text{erfc}\ \frac{RD-1}{2\sqrt{TD}} \cdot$$

Section C: For large values of $\kappa t/a^2$ (TD> 500) Carslaw and Jaeger give the following approximation to (1A-1):

(1C-1)

$$v = \frac{Qa}{2K}\ \text{Ln}\ \left(\frac{4\kappa t}{Cr^2}\right)$$

(1C-2)

$$\frac{vK}{Q} = \frac{r_f}{2}\left(\text{Ln}\ \frac{4Kt}{Cr^2\phi\mu c}\right)$$

thus:

(1C-3)

$$\frac{vK}{Q} = \frac{r_f}{2}\left(\text{Ln}\ \frac{4Kt}{C\phi\mu cr^2}\right) = \frac{r_f}{2}\left(\text{Ln}\ \frac{4Kt}{\phi\mu cr^2} - \text{Ln}C\right)$$

and since Ln C = γ = .57722 (Euler's constant), then:

(1C-4)

$$\frac{vK}{Q} = \frac{1}{2}\left(\text{Ln}\ \frac{4Kt}{\phi\mu cr^2} - \gamma\right) \cdot$$

(1C-1) is the expression for a line source emitting $2\pi aQ$ units of heat per unit time per unit area at r = a per unit thickness, h.

Mortada(16), Page 224 gives:

(1C-5)

$$PD(RD,TD) = \frac{1}{2}\left[\text{Ln}\ \frac{4Kt}{\phi\mu cr^2} - \gamma\right]$$

and from (1B-11):

$$\frac{Kv}{Qr_f} = \frac{2\pi Kh}{887q\mu}\ P(r,t) = PD(RD,TD)$$

so:

$$\frac{Kv}{Qr_f}\left(\frac{2\pi hr_f}{887\mu}\right) = \frac{2\pi Khv}{887Q\mu}$$

and: $v = P(r,t)$

$q = Q/T$

thus:

(1C-6)

$$PD(RD,TD) = \frac{2\pi Kh}{887q\mu}\ P(r,t)$$

and from (1C-3) and (1C-6):

(1C-7)

$$PD(RD,TD) = \frac{1}{2}\left(Ln\frac{4Kt}{\phi\mu cr^2} - \gamma\right) \quad .$$

(1C-7) can be seen to be equivalent to Mortada's equation for TD>500, Equation (1C-5).

Equation (1C-5) is also the Lord Kelvin point source solution or the Theis exponential integral for large values of TD.

(1C-8)

$$PD(RD,TD) = \frac{1}{2}\left(-Ei\ (-\frac{RD^2}{4TD})\right)$$

where:

(1C-9)

$$-E_i\ (\frac{RD^2}{4TD}) = \int_{\frac{RD^2}{4TD}}^{\infty} \frac{e^{-x}}{x}\ dx$$

The equivalence of Equation (1C-5) and Equation (1C-8) at large TD can be shown in the following manner. By approximation, E_i can be given as:

(1C-10)

$$E_i(-X) = Ln\ X + .57722 + \cdots$$

$$-E_i(-X) = -Ln\ X - .57722$$

since:

$$X = \frac{RD^2}{4TD}$$

then:

$$-E_i(-\frac{RD^2}{4TD}) = -Ln\ (\frac{RD^2}{4TD}) - .57722$$

$$-E_i(-\frac{RD^2}{4TD}) = -\left[Ln(RD^2) - Ln(4TD)\right] - .57722$$

$$-E_i(-RD^2/4TD) = -Ln(RD^2) + Ln(4TD) - .57722$$

and since:

$$\begin{array}{rr} Ln\ 4 = & 1.38629 \\ - & .57722 \\ \hline & .80907 \end{array}$$

then:

(1C-11)

$$-E_i(-RD^2/4TD) = \left[Ln(\frac{TD}{RD^2}) + .80907\right]$$

thus from Equation (1C-8), ½ times the left hand side of Equation (1C-11) is defined as PD(RD,TD), so:

(1C-12)

$$PD(RD,TD) = \frac{1}{2}\left[Ln\frac{TD}{RD^2} + .80907\right]$$

(1C-12) is the equation of Van Everdingen and Hurst(19) (See Equation (V1-15), Page 312, for large values of TD.) Equation (1C-12) is then equal to the point source solution of Mortada, Equation (1C-5).

Mortada states that Equation (1C-5) holds if:

(1C-13)

$$\frac{4TD}{RD^2} \geq 2000 \text{ or if for } RD = 1.0, \text{ then } TD \geq 500$$

Mueller and Witherspoon(24) also showed that less than .1% error resulted from using Equation (1C-5) for all RD values when $TD \geq 500$.

Section D: Continuous Source Derivation.

The effect of a continuous source or sink of constant strength is derived from Equation (2-3) as follows:

(1D-1)

Let: $Q = \Psi(t')dt'$

then:

(1D-2)

$$v(x,y,t) = \int_0^t \left[\Psi(t')/4\pi\kappa(t-t')\right] e^{-(x^2+y^2)/4\kappa(t-t')} \, dt'$$

Let: $\Psi(t') = \lambda$, a constant:

then:

(1D-3)

$$v(t) = (\lambda/4\pi\kappa) \int_0^t \left[e^{-(x^2+y^2)/4\kappa(t-t')/(t-t')}\right] \, dt'$$

(1D-4)

Let: $u = (x^2+y^2)/4\kappa(t-t')$

then:

(1D-5)

$$v(t) = (\lambda/4\pi\kappa) \int_{\frac{x^2+y^2}{4\kappa t}}^{\infty} \left[e^{-u}/(t-t')\right]\left[(x^2+y^2)/4\kappa\right]\left[du/u^2\right]$$

and:

(1D-6)

$$v(t) = (\lambda/4\pi\kappa) \int_{\frac{(x^2+y^2)}{4\kappa t}}^{\infty} (e^{-u}/u) \quad du$$

PART 2 - Conversion of the equations for pressure distribution in an infinite radial aquifer, constant rate case, to approximate polynominal expressions suitable for digital computer use.

Section A: Polynominal approximation for Bessel function of zero order, first kind. ($J_0(X)$)

From Handbook of Mathematical Functions(38), page 369, Section 9.4.

(2A-1)

$$-3 \leq X \leq 3$$

$$J_0(X) = 1 - 2.249997(X/3)^2 + 1.2656208(X/3)^4 - .3163866(X/3)^6 + .0444479(X/3)^8 - .0039444(X/3)^{10} + .0002100(X/3)^{12} + E$$

where: $|E| < 5 \times 10^{-8}$

or:

(2A-2)

$$3 \leq X < \infty$$

$$J_0(X) = X^{-\frac{1}{2}} f_0 \cos \theta_0$$

and: $$f_0 = .79788456 - .00000077(3/X) - .00552740(3/X)^2 - .00009512(3/X)^3 + .00137237(3/X)^4 - .00072805(3/X)^5 + .00014476(3/X)^6 + E$$

where: $|E| < 1.6 \times 10^{-8}$

and θ_0 is given later in Equation (2B-2).

Section B: Polynominal approximation for Bessel function of zero order, second kind . ($Y_0(X)$)

(2B-1)

$$0<X\leq 3$$

$$Y_0(X) = (2/\pi)\mathrm{Ln}(X/2)\, J_0(X) + .36746691 + .60559366(X/3)^2 - .74350384(X/3)^4 + .25300117(X/3)^6 - .04261214(X/3)^8 + .00427916(X/3)^{10} - .00024846(X/3)^{12} + E$$

where: $|E|<1.4 \times 10^{-8}$

or:

(2B-2)

$$3\leq X<\infty$$

$$Y_0(X) = X^{-\frac{1}{2}} f_0 \,\mathrm{SIN}\, \theta_0$$

where: f_0 is already defined in (2A-2) and θ_0 is given by

$$\theta_0 = X - .78539816 - .04166397(3/X) - .00003954(3/X)^2 + .00262573(3/X)^3 - .00054125(3/X)^4 - .00029333(3/X)^5 + .00013558(3/X)^6 + E$$

where: $|E|<7 \times 10^{-8}$

Section C: Polynominal approximations for Bessel function of first order, first kind. ($J_1(X)$)

(2C-1)

$$-3\leq X\leq 3$$

$$X^{-1} J_1(X) = \tfrac{1}{2} - .56249985(X/3)^2 + .21093573(X/3)^4$$
$$- .03954289(X/3)^6 + .00443319(X/3)^8$$
$$- .00031761(X/3)^{10} + .00001109(X/3)^{12} + E$$

where: $|E|<1.3 \times 10^{-8}$

(2C-2)

$3 \leq X < \infty$

$$J_1(X) = X^{-\frac{1}{2}} f_1 \cos \theta_1$$

where: $f_1 = .79788456 + .00000156(3/X) + .01659667(3/X)^2$
$$+ .00017105(3/X)^3 - .00249511(3/X)^4$$
$$+ .00113653(3/X)^5 - .00020033(3/X)^6 + E$$

and: $|E|<4 \times 10^{-8}$

also: $\theta_1 = X - 2.35619449 + .12499612(3/X) + .00005650(3/X)^2$
$$- .00637879(3/X)^3 + .00074348(3/X)^4 + .00079824(3/X)^5$$
$$- .000219166(3/X)^6 + E$$

with: $|E|<9 \times 10^{-8}$

Section D: Polynominal approximation for Bessel function of first order, second kind. ($Y_1(X)$)

(2D-1)

$0 < X \leq 3$

$$X Y_1(X) = (2/\pi) X \operatorname{Ln}(X/2) J_1(X) - .6366198$$
$$+ .2212091(X/3)^2 + 2.1682709(X/3)^4$$

$$- 1.3164827(X/3)^6 + .3123951(X/3)^8$$

$$- .0400986(X/3)^{10} + .0027873(X/3)^{12} + E$$

where: $|E|<1.1 \times 10^{-7}$

or:

(2D-2)

$$3 \leq X < \infty$$

then:

$$Y_1(X) = X^{-\frac{1}{2}} f_1 \text{SIN } \theta_1$$

where f_1 and θ_1 are already defined in Equation (2C-2) of Section C.

Section E: Approximations for functions used when TD≤.01. From the Handbook of Math Functions(38), page 299, Section 7.2.5.

(2E-1)

$$i^2\text{erfc}(Z) = -\frac{Z}{2}\,\text{ierfc}(Z) + \frac{1}{4}\,\text{erfc}(Z)$$

(2E-2)

$$\text{ierfc}(Z) = \frac{e^{-Z^2}}{\sqrt{\pi}} - Z(1-\text{erf}(Z))$$

(2E-3)

$$\text{ierfc}(Z) = \frac{e^{-Z^2}}{\sqrt{\pi}} - Z\,\text{erfc}(Z)$$

and since:

(2E-4)

$$\text{erfc}(Z) = \frac{2}{\sqrt{\pi}} \int_Z^\infty e^{-T^2}\,dt = 1-\text{erf}(Z)$$

For the purpose of this paper:

(2E-5)

$$Z = \frac{RD-1}{2\sqrt{TD}}$$

then:

(2E-6)

$$erf(Z) = \frac{2}{\pi} \int_0^Z e^{-T^2} \, dT$$

The function erf(Z) can be approximated by the polynominal:

(2E-7)

$$erf(Z) = 1 - \left(a_1T+a_2T^2+a_3T^3+a_4T^4+a_5T^5\right)e^{-Z^2} + E(Z)$$

where the error:

$$E(Z) \leq 1.5 \times 10^{-7}$$

and:

$T = 1/(1 + PZ)$ where: $P = .3275911$

$a_1 = .254829592$

$a_2 = - .284496736$

$a_3 = 1.421413741$

$a_4 = - 1.453152027$

$a_5 = 1.061405429$

thus Equation (2E-2) can be used to approximate ierfc(Z) with Equation (2E-7) being used for erf(Z).

For the second term of Equation (1B-13), the $i^2erfc(Z)$ term can be approximated as follows:

From (2E-1):

$$i^2\text{erfc}(Z) = -\frac{Z}{2}\,\text{ierfc}(Z) + \frac{1}{4}\,\text{erfc}(Z)$$

then, as has been shown, (2E-2) can be used to approximate ierfc(Z) and (2E-4) or the erfc(Z) can be taken as:

$$\text{erfc}(Z) = 1 - \text{erf}(Z)$$

In the actual computer programs the following subroutines are called:

(2E-8)

$$\text{err} = \text{ierfc}(Z)$$
$$\text{erfx} = \text{erf}(Z) \qquad Z = \frac{RD-1}{2\sqrt{TD}}$$
$$\text{ec} = 1-\text{erf}(Z)$$

thus Equation (1B-13) is written as:

(2E-9)

$$PD(RD,TD) = \frac{2\sqrt{TD}}{\sqrt{RD}}\,(\text{err}) - \frac{(3RD+1)\sqrt{TD}}{4RD}\left(-\frac{Z}{2}(\text{err}) + \frac{1}{4}(\text{ec})\right)$$

where the subroutines are called using the argument Z.

Section F: Approximations for the functions used when TD>500. These approximations are used to evaluate Equation (1C-8).

From Handbook of Mathematical Functions(38), page 231, Section 5.1.53.

The E_i function (exponential integral) can be approximated when:

(2F-1)

$$0 \leq X \leq 1$$

then:

$$E_i(X) + Ln(X) = a_0+a_1X+a_2X^2+a_3X^3+a_4X^4+a_5X^5+ E(X)$$

where: $|E(X)|<2 \times 10^{-7}$

and:

$a_0 = - .57721566$
$a_1 = .99999193$
$a_2 = - .24991055$
$a_3 = .05519968$
$a_4 = - .00976004$
$a_5 = .00108757$

But when:

(2F-2)

$1 \leq X < \infty$

then:

$$E_i(X) = \frac{X^4+a_1X^3+a_2X^2+a_3X+a_4}{X^4+b_1X^3+b_2X^2+b_3X+b_4} \left(\frac{e^{-X}}{X}\right) + E(X)$$

where:

$a_1 = 8.5733287401$ $\quad$ $b_1 = 9.5733223454$
$a_2 = 18.0590169730$ $\quad$ $b_2 = 25.6329561486$
$a_3 = 8.6347608925$ $\quad$ $b_3 = 21.0996530827$
$a_4 = .2677737343$ $\quad$ $b_4 = 3.9584969228$

where: $|E(X)|<2 \times 10^{-8}$

Equations (2F-1) and (2F-2) are both used in subroutine SUBTA to calculate EIMX when X is introduced as the argument, where:

$X = \frac{RD^2}{4TD}$ and thus $E_i(-X) = -(2F-2)$

as a result Equation (1C-8) becomes:

(2F-3)

$$PD(RD,TD) = \frac{1}{2} (-EIMX)$$

PART 3 - Expansion of the SIN and COS functions to accommodate very large arguments.

Section A: Expansion of the COS Function.

From the C.R.C. Standard Mathematical Tables(39), page 379 the following functions of multiple angles are given.

(3A-1)

$$\cos 3X = 4\cos^3 X - 3\cos X$$

$$\sin 3X = 3\sin X - 4\sin^3 X$$

and since: $\cos 6X = \cos(3X+3X)$

then:

(3A-2)

$$\cos 6X = \cos(3X+3X) = \cos 3X \cos 3X - \sin 3X \sin 3X$$

(3A-3)

$$\cos(3X+3X) = (4\cos^3 X - 3\cos X (4\cos^3 X - 3\cos X)) - (3\sin X - 4\sin^3 X (3\sin X - 4\sin^3 X))$$

therefore:

(3A-4)

$$\cos 6X = 16\cos^6 X - 24\cos^4 X + 9\cos^2 X - 9\sin^2 X + 24\sin^4 X - 16\sin^6 X$$

and since: $\sin^2 X = 1 - \cos^2 X$

then:

(3A-5)

$$\cos 6_X = 32\cos^6 X - 48\cos^4 X + 18\cos^2 X - 1$$

thus in the same manner as COS6X was developed in (3A-2):

$$\cos 12X = \cos(6X + 6X)$$

and:

$$\cos 12X = \cos 6X \cos 6X + \sin 6X \sin 6X$$

Then using the expansion for the SIN6X developed in Section B, page 242, Equation (3B-4):

(3A-6)

$$COS12X = ((32COS^6X - 48COS^4X+18COS^2X - 1)^2 - (32SINX\ COS^5X - 32SINX\ COS^3X+6SINX\ COSX)^2)$$

thus:

(3A-7)

$$COS12X = 2048COS^{12}X - 6144COS^{10}X+6912COS^8X - 3584COS^6X + 840COS^4X - 72COS^2X + 1$$

Equation (3A-7) is used in the Bessel functions subroutines BESJO and BESJ1 and the large argument of the COS is divided by 12 and evaluated by means of Equation (3A-7). The value of COS12X is then used as the value of COSX.

Section B: Expansion of the SIN Function.

From the C.R.C. Standard Mathematical Tables, page 379, the following functions of multiple angles are given:

(3B-1)

$$SIN6X = SIN2(3X)$$

$$SIN6X = 2(SIN3X)(COS3X)$$

then from Equation (3A-1):

(3B-2)

$$SIN6X = 2(3SINX - 4SIN^3X)(4COS^3X - 3COSX)$$

thus:

(3B-3)

$$SIN6X = 24SINX\ COS^3X - 32SIN^3X\ COS^3X - 18SINX\ COSX + 24SIN^3X\ COSX$$

Using: $SIN^2X = 1 - COS^2X$

then:

(3B-4)

$$SIN6X = 32SINX\ COS^5X - 32SINX\ COS^3X + 6SINX\ COSX$$

and thus by the same method that SIN6X was developed:

$$SIN12X = SIN2(6X)$$

$$SIN12X = 2(SIN6X)(COS6X)$$

and:

(3B-5)

$$SIN12X = 2(32SINX\ COSX - 32SINX\ COSX + 6SINX\ COSX)$$
$$(32COSX - 48COSX + 18COSX - 1)$$

Equation (3B-5) can be simplified to give:

(3B-6)

$$SIN12X = 2048SINX\ COS^{11}X - 5120SINX\ COS^9X + 4608SINX\ COS^7X -$$
$$1792SINX\ COS^5X + 280SINX\ COS^3X - 12SINX\ COSX$$

Equation (3B-6) is used in the Bessel function routines BESY0 and BESY1 and the large X argument is divided by 12 and evaluated by Equation (3B-6). The value of the SIN12X is then used as the value of SINX.

PART 4 - Development of the transformation of limits.

The transformation of the limits of integration from zero to infinity into zero to one was performed upon Equation (1A-9) in the following manner:

(1A-9)

$$PD(RD,TD) = \frac{2}{\pi}\int_0^{\infty} \frac{(1-e^{-X^2TD})\left[J_1(X)Y_0(X,RD)-Y_1(X)J_0(X,RD)\right]}{X^2\left[J_1^2(X)+Y_1^2(X)\right]}\,dX$$

then if:

(4A-1)

$$u = \frac{\bar{X}^*}{1-\bar{X}}$$

NOTE: This is not the same X as that used in (1A-9).

where: $0 \leq \bar{X} < 1.0$, and u is equivalent to the X of (1A-9)

(4A-2)

$$u^2 = \frac{\bar{X}^2}{(1-\bar{X})^2}$$

(4A-3)

$$du = \frac{(1-\bar{X})d\bar{X}-\bar{X}(-d\bar{X})}{(1-\bar{X})^2} = \frac{d\bar{X}}{(1-\bar{X})^2}$$

and then upon substituting (4A-1), (4A-2), and (4A-3) into Equation (1A-9):

(4A-4)

$$PD(RD,TD) = \frac{2}{\pi}\int_0^{1} \frac{\left(1-e^{-\left(\frac{\bar{X}^2}{(1-\bar{X})^2}\cdot TD\right)}\right)\left(J_1\left(\frac{\bar{X}}{1-\bar{X}}\right)Y_0\left(\frac{\bar{X}}{1-\bar{X}}, RD\right) - Y_1\left(\frac{\bar{X}}{1-\bar{X}}\right)J_0\left(\frac{\bar{X}}{1-\bar{X}}, RD\right)\right)\frac{d\bar{X}}{(1-\bar{X})^2}}{\bar{X}^2/(1-\bar{X})^2\left(J_1\left(\frac{\bar{X}}{1-\bar{X}}\right)+Y_1^2\left(\frac{\bar{X}}{1-\bar{X}}\right)\right)}$$

which can be reduced to:

(4A-5)

$$PD(RD,TD) = \frac{2}{\pi} \int_0^1 \frac{\left[1-e^{-u^2 TD}\right]\left[J_1(u)Y_0(u,RD)-Y_1(u)J_0(u,RD)\right]}{\bar{X}^2\left[J_1^2(u)+Y_1^2(u)\right]}\, d\bar{X}$$

Equation (4A-5) is the equation actually solved in this study by Romberg integration. This equation fills the TD range over which Mortada used a finite difference solution to calculate PD(RD,TD) for the constant rate case.

PART 5 - Reduction of Equation (4-6) to an equation similar to the Hurst, Haynie, and Walker equation.

The Hurst, Haynie, Walker equation was developed from the graphical solutions of Van Everdingen-Hurst and therefore the equation for the effective radius of drainage developed in this study should be approximately equal to the Hurst, Haynie, and Walker equation if the equation developed in this study is reduced to a point-source solution.

(4-6)

$$RD = 1 + 2.915\,(TD)^{.4821}$$

$$\frac{r}{r_b} = 1 + 2.915\,(TD)^{.4821}$$

$$r = r_b\,(1+2.915(TD)^{.4821})$$

(5A-1)

$$r = r_b\left(1+2.915\left(\frac{.006328Kt}{\phi\mu c r_b^{\,2}}\right)^{.4821}\right)$$

(5A-2)

$$r = r_b\left(1+2.915(.006328)^{.4821}\left(\frac{Kt}{\phi\mu c r_b^{\,2}}\right)^{.4821}\right)$$

(5A-3)

$$r = r_b\left[1+2.915(.087)\left(\frac{Kt}{\phi\mu c r_b^{\,2}}\right)^{.4821}\right]$$

(5A-4)

$$r = r_b\left[1+.2535\left(\frac{Kt}{\phi\mu c r_b^{\,2}}\right)^{.4821}\right]$$

$$\left(\frac{1}{X}\right)^{.4821} = .2535$$

$$X = 16.68$$

(5A-5)

$$r = r_b\left[1+\left(\frac{Kt}{\phi\mu c r_b^2 16.68}\right).4821\right]$$

(5A-6)

$$\frac{r}{r_b} - 1 = \left(\frac{Kt}{16.68\phi\mu c r_b^2}\right).4821$$

(5A-7)

Letting .4821 ≈ .500

$$\frac{r-r_b}{r_b} = \frac{1}{r_b}\sqrt{\frac{Kt}{16.68\phi\mu c}}$$

Then letting $r_b \to 0$ for the approximation to the point-source solution:

(5A-8)

$$r = \sqrt{\frac{Kt}{16.68\phi\mu c}} \qquad \text{in field units}$$

Converting (5A-8) to C.G.S. units results in:

(5A-9)

$$r = 2.76\sqrt{\frac{Kt}{\phi\mu c}}$$

The stabilization time can be expressed by

(5A-10)

$$t_s = \frac{16.68\phi\mu c r^2}{K} \qquad \text{in field units}$$

or in C.G.S. units as:

(5A-11)

$$t_s = \frac{\phi \mu c r^2}{7.62K}$$

Equations (5A-9) and (5A-11) can be compared with the Hurst, Haynie, and Walker equations by referring to Table 2-8.

APPENDIX C

COMPLETE COMPUTER RESULTS FOR PD(RD,TD)

INFINITE RADIAL RESERVOIR,RD=1.0,CHATAS

PD= 1.000

TD	PD
0.00050000	0.02493132
0.00100000	0.03513248
0.00150000	0.04346264
0.00200000	0.05030386
0.00250000	0.05623485
0.00300000	0.06155345
0.00350000	0.06644381
0.00400000	0.07099622
0.00450000	0.07526526
0.00500000	0.07930741
0.00550000	0.08315786
0.01500000	0.13114059
0.02000000	0.15027183
0.02500000	0.16688699
0.03000000	0.18172115
0.04000000	0.20763540
0.05000000	0.23002869
0.06000000	0.24993408
0.06999999	0.26796305
0.07999998	0.28451073
0.08999997	0.29985440
0.09999996	0.31419283
0.14999998	0.37510788
0.19999999	0.42421103
0.29999995	0.50238454
0.39999998	0.56457847
0.50000000	0.61682510
0.59999996	0.66216213
0.69999999	0.70238620
0.79999995	0.73863411
0.89999998	0.77168494
1.00000000	0.80211544
1.19999981	0.85667497
1.39999962	0.90468544
2.00000000	1.02221394
3.00000000	1.16631794
4.00000000	1.27488518
5.00000000	1.36245632
6.00000000	1.43603039
7.00000000	1.49957371
8.00000000	1.55554867
9.00000000	1.60560799
10.00000000	1.65090179
15.00000000	1.82934189
20.00000000	1.95345263
30.00000000	2.14699541
40.00000000	2.28227901
50.00000000	2.38841820
60.00000000	2.47577095
70.00000000	2.54999733
80.00000000	2.61441612
90.00000000	2.67143726
100.00000000	2.72260189
150.00000000	2.92055511
200.00000000	3.06132480
250.00000000	3.17179775
300.00000000	3.26183987
350.00000000	3.33800292
400.00000000	3.40421963
450.00000000	3.46261024
500.00000000	3.51487732
550.00000000	3.55972576
600.00000000	3.60321236
650.00000000	3.64321709
700.00000000	3.68025780
750.00000000	3.71474266
800.00000000	3.74700069
850.00000000	3.77730465
900.00000000	3.80587578
950.00000000	3.83290100
1000.00000000	3.85854149

INFINITE RADIAL RESERVOIR-CONSTANT RATE CASE

PD= 1.100

TD	PD
0.00050000	0.00001278
0.00100000	0.00037332
0.00200000	0.00289574
0.00300000	0.00674738
0.00400000	0.01107736
0.00500000	0.01553681
0.00600000	0.01997988
0.00700000	0.02434349
0.00800000	0.02860095
0.00900000	0.03274245
0.01000000	0.03676661
0.01500000	0.05548135
0.02000000	0.07186043
0.02500000	0.08657485
0.03000000	0.09999603
0.04000000	0.12391669
0.05000000	0.14494681
0.06000000	0.16383433
0.06999999	0.18107712
0.07999998	0.19699591
0.08999997	0.21181887
0.09999996	0.22572029
0.14999998	0.28515106
0.19999999	0.33338881
0.29999995	0.41055137
0.39999998	0.47216189
0.50000000	0.52401489
0.59999996	0.56907308
0.69999999	0.60907793
0.79999995	0.64514798
0.89999998	0.67806280
1.00000000	0.70837247
1.19999981	0.76275653
1.39999962	0.81062555
2.00000000	0.92788804
3.00000000	1.07175446
4.00000000	1.18020153
5.00000000	1.26768684
6.00000000	1.34120655
7.00000000	1.40470886
8.00000000	1.46065426
9.00000000	1.51068401
10.00000000	1.55595684
15.00000000	1.73433208
20.00000000	1.86440849
30.00000000	2.05191385
40.00000000	2.18713052
50.00000000	2.29331017
60.00000000	2.38064957
70.00000000	2.45488548
80.00000000	2.51945400
90.00000000	2.57630539
100.00000000	2.62742996
150.00000000	2.82534027
200.00000000	2.96659946
250.00000000	3.07653713
300.00000000	3.16657639
350.00000000	3.24282265
400.00000000	3.30894566
450.00000000	3.36733532
500.00000000	3.41958904
550.00000000	3.46446323
600.00000000	3.50794601
650.00000000	3.54794788
700.00000000	3.58498573
750.00000000	3.61946774
800.00000000	3.65172386
850.00000000	3.68202591
900.00000000	3.71059513
950.00000000	3.73761940
1000.00000000	3.76325893

INFINITE RADIAL RESERVOIR-CONSTANT RATE CASE

PD= 1.200

TD	PD
0.00050000	0.00000000
0.00100000	0.00000006
0.00200000	0.00002438
0.00300000	0.00021683
0.00400000	0.00070999
0.00500000	0.00152500
0.00600000	0.00262535
0.00700000	0.00396020
0.00800000	0.00548132
0.00900000	0.00714786
0.01000000	0.00892679
0.01500000	0.01673754
0.02000000	0.02712988
0.02500000	0.03743327
0.03000000	0.04744135
0.04000000	0.06636453
0.05000000	0.08386123
0.06000000	0.10009730
0.06999999	0.11524755
0.07999998	0.12946332
0.08999997	0.14286077
0.09999996	0.15555370
0.14999998	0.21087146
0.19999999	0.25666136
0.29999995	0.33096743
0.39999998	0.39090133
0.50000000	0.44163644
0.59999996	0.48588496
0.69999999	0.52527148
0.79999995	0.56085360
0.89999998	0.59336907
1.00000000	0.62334657
1.19999981	0.67720312
1.39999962	0.72467083
2.00000000	0.84116465
3.00000000	0.98435944
4.00000000	1.09243870
5.00000000	1.17968941
6.00000000	1.25304222
7.00000000	1.31642818
8.00000000	1.37228012
9.00000000	1.42223549
10.00000000	1.46744919
15.00000000	1.64563751
20.00000000	1.77561569
30.00000000	1.96292400
40.00000000	2.09323322
50.00000000	2.20432854
60.00000000	2.29165077
70.00000000	2.36587238
80.00000000	2.43042755
90.00000000	2.48755074
100.00000000	2.53860283
150.00000000	2.73633003
200.00000000	2.87758255
250.00000000	2.98751163
300.00000000	3.07755661
350.00000000	3.15379524
400.00000000	3.21992111
450.00000000	3.27830505
500.00000000	3.33057213
550.00000000	3.37750435
600.00000000	3.42098236
650.00000000	3.46098042
700.00000000	3.49801540
750.00000000	3.53240454
800.00000000	3.56474876
850.00000000	3.59504795
900.00000000	3.62361526
950.00000000	3.65063858
1000.00000000	3.67627525

INFINITE RADIAL RESERVOIR-CONSTANT RATE CASE

PD= 1.300

TD	PD
0.00050000	0.00000000
0.00100000	0.00000000
0.00200000	0.00000003
0.00300000	0.00000168
0.00400000	0.00001605
0.00500000	0.00006616
0.00600000	0.00017679
0.00700000	0.00036633
0.00800000	0.00064505
0.00900000	0.00101649
0.01000000	0.00147946
0.01500000	0.00551154
0.02000000	0.01044778
0.02500000	0.01620011
0.03000000	0.02239358
0.04000000	0.03530369
0.05000000	0.04826579
0.06000000	0.06094182
0.06999999	0.07320946
0.07999998	0.08503288
0.08999997	0.09641349
0.09999996	0.10736978
0.14999998	0.15662414
0.19999999	0.19870847
0.29999995	0.26859951
0.39999998	0.32592666
0.50000000	0.37490785
0.59999996	0.41787916
0.69999999	0.45628923
0.79999995	0.49109524
0.89999998	0.52297962
1.00000000	0.55242676
1.19999981	0.60544956
1.39999962	0.65228474
2.00000000	0.76754373
3.00000000	0.90966749
4.00000000	1.01715374
5.00000000	1.10403538
6.00000000	1.17712593
7.00000000	1.24031353
8.00000000	1.29601955
9.00000000	1.34585567
10.00000000	1.39097404
15.00000000	1.56886482
20.00000000	1.69868279
30.00000000	1.88582802
40.00000000	2.02105618
50.00000000	2.12709904
60.00000000	2.21438599
70.00000000	2.28958185
80.00000000	2.35311508
90.00000000	2.41022682
100.00000000	2.46144485
150.00000000	2.65897465
200.00000000	2.80018330
250.00000000	2.91009808
300.00000000	3.00012779
350.00000000	3.07637882
400.00000000	3.14250469
450.00000000	3.20087910
500.00000000	3.25313854
550.00000000	3.29751873
600.00000000	3.34099197
650.00000000	3.38098621
700.00000000	3.41801739
750.00000000	3.45249367
800.00000000	3.48474503
850.00000000	3.51504230
900.00000000	3.54360771
950.00000000	3.57062912
1000.00000000	3.59626389

INFINITE RADIAL RESERVOIR-CONSTANT RATE CASE

RD= 1.400

TD	PD
0.00050000	0.00000000
0.00100000	0.00000000
0.00200000	0.00000000
0.00300000	0.00000000
0.00400000	0.00000012
0.00500000	0.00000119
0.00600000	0.00000578
0.00700000	0.00001841
0.00800000	0.00004480
0.00900000	0.00009095
0.01000000	0.00016227
0.01500000	0.00123094
0.02000000	0.00305143
0.02500000	0.00562380
0.03000000	0.00881606
0.04000000	0.01644036
0.05000000	0.02501579
0.06000000	0.03403272
0.06999999	0.04320906
0.07999998	0.05238656
0.08999997	0.06147518
0.09999996	0.07042342
0.14999998	0.11245674
0.19999999	0.14996195
0.29999995	0.21424115
0.39999999	0.26818949
0.50000000	0.31487525
0.59999996	0.35617059
0.69999999	0.39328945
0.79999995	0.42706335
0.89999998	0.45810276
1.00000000	0.48685336
1.19999931	0.53876239
1.39999962	0.58475858
2.00000000	0.69835503
3.00000000	0.83903790
4.00000000	0.94573271
5.00000000	1.03210068
6.00000000	1.10484314
7.00000000	1.16777039
8.00000000	1.22327137
9.00000000	1.27295303
10.00000000	1.31793499
15.00000000	1.49542236
20.00000000	1.62502956
30.00000000	1.81105259
40.00000000	1.94706440
50.00000000	2.05303860
60.00000000	2.14027882
70.00000000	2.21444225
80.00000000	2.27895069
90.00000000	2.33604050
100.00000000	2.38724232
150.00000000	2.58476353
200.00000000	2.72593880
250.00000000	2.83584309
300.00000000	2.92534705
350.00000000	3.00209236
400.00000000	3.06820679
450.00000000	3.12659359
500.00000000	3.17884731
550.00000000	3.22347164
600.00000000	3.26694012
650.00000000	3.30693054
700.00000000	3.34305695
750.00000000	3.37843037
800.00000000	3.41067982
850.00000000	3.44097328
900.00000000	3.46953678
950.00000000	3.49655533
1000.00000000	3.52212000

INFINITE RADIAL RESERVOIR-CONSTANT RATE CASE

RD= 1.500

TD	PD
0.00050000	-0.00674446
0.00100000	-0.00953810
0.00200000	-0.01343892
0.00300000	-0.01652049
0.00400000	-0.01907615
0.00500000	-0.02132777
0.00600000	-0.02336320
0.00700000	-0.02523397
0.00800000	-0.02697282
0.00900000	-0.02860079
0.01000000	-0.03013194
0.01500000	-0.00032813
0.02000000	0.00015598
0.02500000	0.00108205
0.03000000	0.00245669
0.04000000	0.00636774
0.05000000	0.01144376
0.06000000	0.01729585
0.06999998	0.02364576
0.07999998	0.03030315
0.08999997	0.03713853
0.09999996	0.04406352
0.14999998	0.07846123
0.19999999	0.11091423
0.29999995	0.16876221
0.39999998	0.21874374
0.50000000	0.26269090
0.59999996	0.30196983
0.69999999	0.33752835
0.79999995	0.37005746
0.89999998	0.40007520
1.00000000	0.42796266
1.19999981	0.47851294
1.39999962	0.52346849
2.00000000	0.63503975
3.00000000	0.77392828
4.00000000	0.87964082
5.00000000	0.96538121
6.00000000	1.03768730
7.00000000	1.10028839
8.00000000	1.15554237
9.00000000	1.20501995
10.00000000	1.24984360
15.00000000	1.42682076
20.00000000	1.55516474
30.00000000	1.74281502
40.00000000	1.87778664
50.00000000	1.98367500
60.00000000	2.07085800
70.00000000	2.14497566
80.00000000	2.20945358
90.00000000	2.26651573
100.00000000	2.31770229
150.00000000	2.51553059
200.00000000	2.65636635
250.00000000	2.76624203
300.00000000	2.85624027
350.00000000	2.93245983
400.00000000	2.99856663
450.00000000	3.05603340
500.00000000	3.10917854
550.00000000	3.15454388
600.00000000	3.19800663
650.00000000	3.23799229
700.00000000	3.27501583
750.00000000	3.30948544
800.00000000	3.34173107
850.00000000	3.37202263
900.00000000	3.40058327
950.00000000	3.42760086
1000.00000000	3.45323277

INFINITE RADIAL RESERVOIR-CONSTANT RATE CASE

PD= 1.600

TD	PD
0.00050000	-0.00758649
0.00100000	-0.01072891
0.00200000	-0.01517297
0.00300000	-0.01858303
0.00400000	-0.02145780
0.00500000	-0.02399058
0.00600000	-0.02628029
0.00700000	-0.02838594
0.00800000	-0.03034577
0.00900000	-0.03218619
0.01000000	-0.03392604
0.01500000	-0.00018196
0.02000000	-0.00007840
0.02500000	0.00019198
0.03000000	0.00068847
0.04000000	0.00243641
0.05000000	0.00513010
0.06000000	0.00860025
0.06999999	0.01266869
0.07999998	0.01718520
0.08999997	0.02202997
0.09999996	0.02711226
0.14999998	0.05413918
0.19999999	0.08139163
0.29999995	0.13239890
0.39999998	0.17798865
0.50000000	0.21886885
0.59999996	0.25585234
0.69999999	0.28963292
0.79999995	0.32073361
0.89999998	0.34957093
1.00000000	0.37646842
1.19999981	0.42543364
1.39999962	0.46918559
2.00000000	0.57837236
3.00000000	0.71516377
4.00000000	0.81971729
5.00000000	0.90471518
6.00000000	0.97649407
7.00000000	1.03871727
8.00000000	1.09367180
9.00000000	1.14291668
10.00000000	1.18754673
15.00000000	1.36392593
20.00000000	1.49295139
30.00000000	1.67927456
40.00000000	1.81407642
50.00000000	1.91986084
60.00000000	2.00697136
70.00000000	2.08104134
80.00000000	2.14548111
90.00000000	2.20251560
100.00000000	2.25367641
150.00000000	2.45162773
200.00000000	2.59227467
250.00000000	2.70211411
300.00000000	2.79209328
350.00000000	2.86831760
400.00000000	2.93441963
450.00000000	2.99277878
500.00000000	3.04502678
550.00000000	3.09007645
600.00000000	3.13353348
650.00000000	3.17351437
700.00000000	3.21053314
750.00000000	3.24499893
800.00000000	3.27724171
850.00000000	3.30753040
900.00000000	3.33608818
950.00000000	3.36310387
1000.00000000	3.38873291

INFINITE RADIAL RESERVOIR-CONSTANT RATE CASE

PD= 1.700

TD	PD
0.00050000	-0.00947758
0.00100000	-0.01198910
0.00200000	-0.01695516
0.00300000	-0.02076574
0.00400000	-0.02397819
0.00500000	-0.02680846
0.00600000	-0.02936719
0.00700000	-0.03172017
0.00800000	-0.03391022
0.00900000	-0.03596730
0.01000000	-0.03791276
0.01500000	-0.00170098
0.02000000	-0.00168219
0.02500000	-0.00161646
0.03000000	-0.00146471
0.04000000	-0.00078037
0.05000000	0.00050348
0.06000000	0.00238551
0.06999999	0.00480181
0.07999998	0.00766926
0.08999997	0.01090749
0.09999996	0.01444580
0.14999998	0.03485176
0.19999999	0.05708284
0.29999995	0.10113841
0.39999998	0.14212638
0.50000000	0.17969030
0.59999996	0.21418411
0.69999999	0.24600226
0.79999995	0.27552044
0.89999998	0.30304444
1.00000000	0.32883960
1.19999981	0.37603861
1.39999962	0.41843438
2.00000000	0.52492607
3.00000000	0.65933537
4.00000000	0.76255679
5.00000000	0.84670228
6.00000000	0.91789228
7.00000000	0.97966754
8.00000000	1.03427792
9.00000000	1.08325577
10.00000000	1.12766171
15.00000000	1.30334949
20.00000000	1.43201351
30.00000000	1.61795998
40.00000000	1.75256920
50.00000000	1.85823441
60.00000000	1.94526577
70.00000000	2.01927376
80.00000000	2.08367062
90.00000000	2.14067268
100.00000000	2.19180679
150.00000000	2.38967037
200.00000000	2.53059959
250.00000000	2.64009953
300.00000000	2.73006725
350.00000000	2.80625629
400.00000000	2.87234402
450.00000000	2.93070602
500.00000000	2.98293114
550.00000000	3.02952671
600.00000000	3.07297802
650.00000000	3.11295319
700.00000000	3.14996624
750.00000000	3.18442917
800.00000000	3.21666813
850.00000000	3.24695396
900.00000000	3.27550993
950.00000000	3.30252171
1000.00000000	3.32814980

INFINITE RADIAL RESERVOIR-CONSTANT RATE CASE

RD= 1.800

TD	PD
0.00050000	-0.00941771
0.00100000	-0.01331865
0.00200000	-0.01883542
0.00300000	-0.02306857
0.00400000	-0.02663729
0.00500000	-0.02979142
0.00600000	-0.03262390
0.00700000	-0.03523785
0.00800000	-0.03767083
0.00900000	-0.03995594
0.01000000	-0.04211722
0.01500000	-0.00074802
0.02000000	-0.00074309
0.02500000	-0.00072819
0.03000000	-0.00068748
0.04000000	-0.00045049
0.05000000	0.00010097
0.06000000	0.00103613
0.06999999	0.00236712
0.07999998	0.00407218
0.08999997	0.00611475
0.09999996	0.00845313
0.14999998	0.02326788
0.19999999	0.04089199
0.29999995	0.07817036
0.39999998	0.11448389
0.50000000	0.14863396
0.59999996	0.18048352
0.69999999	0.21021712
0.79999995	0.23802805
0.89999998	0.26413769
1.00000000	0.28873014
1.19999981	0.33400470
1.39999962	0.37491024
2.00000000	0.47843599
3.00000000	0.61019385
4.00000000	0.71193445
5.00000000	0.79512680
6.00000000	0.86564708
7.00000000	0.92692935
8.00000000	0.98116231
9.00000000	1.02982903
10.00000000	1.07398701
15.00000000	1.24889565
20.00000000	1.37715530
30.00000000	1.56267643
40.00000000	1.69706535
50.00000000	1.80259323
60.00000000	1.88953781
70.00000000	1.96348476
80.00000000	2.02783298
90.00000000	2.08479118
100.00000000	2.13589001
150.00000000	2.33366680
200.00000000	2.47486591
250.00000000	2.58403969
300.00000000	2.67396545
350.00000000	2.75013828
400.00000000	2.81622314
450.00000000	2.87456131
500.00000000	2.92579882
550.00000000	2.97244740
600.00000000	3.01589203
650.00000000	3.05586147
700.00000000	3.09287071
750.00000000	3.12732887
800.00000000	3.15956497
850.00000000	3.18984699
900.00000000	3.21840000
950.00000000	3.24540997
1000.00000000	3.27103519

INFINITE RADIAL RESERVOIR-CONSTANT RATE CASE

PD= 1.900

TD	PD
0.00050000	-0.01040690
0.00100000	-0.01471758
0.00200000	-0.02081381
0.00300000	-0.02549160
0.00400000	-0.02943513
0.00500000	-0.03290952
0.00600000	-0.03605055
0.00700000	-0.03893905
0.00800000	-0.04162759
0.00900000	-0.04415275
0.01000000	-0.04654108
0.01500000	0.00279939
0.02000000	0.00279297
0.02500000	0.00279731
0.03000000	0.00280812
0.04000000	0.00288299
0.05000000	0.00309850
0.06000000	0.00352535
0.06999999	0.00420667
0.07999998	0.00515692
0.08999997	0.00637321
0.09999996	0.00784042
0.14999998	0.01819143
0.19999999	0.03177362
0.29999995	0.06269151
0.39999998	0.09440929
0.50000000	0.12508637
0.59999996	0.15424943
0.69999999	0.18179280
0.79999995	0.20782119
0.89999998	0.23242837
1.00000000	0.25574702
1.19999981	0.29995663
1.39999962	0.33827120
2.00000000	0.43858171
3.00000000	0.56744993
4.00000000	0.66756862
5.00000000	0.74971300
6.00000000	0.81949812
7.00000000	0.88023639
8.00000000	0.93404490
9.00000000	0.98237592
10.00000000	1.02625942
15.00000000	1.20030975
20.00000000	1.32811451
30.00000000	1.51316261
40.00000000	1.64731216
50.00000000	1.75269413
60.00000000	1.83953285
70.00000000	1.91340733
80.00000000	1.97769928
90.00000000	2.03461456
100.00000000	2.08568287
150.00000000	2.28335190
200.00000000	2.42449760
250.00000000	2.53402138
300.00000000	2.62355423
350.00000000	2.69970989
400.00000000	2.76577854
450.00000000	2.82411098
500.00000000	2.87633419
550.00000000	2.91846466
600.00000000	2.96190166
650.00000000	3.00186539
700.00000000	3.03886986
750.00000000	3.07332325
800.00000000	3.10555458
850.00000000	3.13583469
900.00000000	3.16438389
950.00000000	3.19139099
1000.00000000	3.21701431

INFINITE RADIAL RESERVOIR-CONSTANT RATE CASE

RD= 2.000

TD	PD
0.01500000	0.00110434
0.02000000	0.00110749
0.02500000	0.00111057
0.03000000	0.00111425
0.04000000	0.00113800
0.05000000	0.00121568
0.06000000	0.00139609
0.06999999	0.00172069
0.07999998	0.00221804
0.08999997	0.00290230
0.09999996	0.00377729
0.14999998	0.01074211
0.19999999	0.02092011
0.29999995	0.04606157
0.39999998	0.07336026
0.50000000	0.10062277
0.59999996	0.12706482
0.69999999	0.15241194
0.79999995	0.17657876
0.89999998	0.19963861
1.00000000	0.22162557
1.19999981	0.26267087
1.39999962	0.30029112
2.00000000	0.39718693
3.00000000	0.52294618
4.00000000	0.62131280
5.00000000	0.70231998
6.00000000	0.77130067
7.00000000	0.83144337
8.00000000	0.88479471
9.00000000	0.93275899
10.00000000	0.97634107
15.00000000	1.14945507
20.00000000	1.27676201
30.00000000	1.46129990
40.00000000	1.59517860
50.00000000	1.70039749
60.00000000	1.78712749
70.00000000	1.86092091
80.00000000	1.92515087
90.00000000	1.98202515
100.00000000	2.03305054
150.00000000	2.23060703
200.00000000	2.37169838
250.00000000	2.48143101
300.00000000	2.57070065
350.00000000	2.64681721
400.00000000	2.71285820
450.00000000	2.77118397
500.00000000	2.82339764
550.00000000	2.86725903
600.00000000	2.91068935
650.00000000	2.95064640
700.00000000	2.98764610
750.00000000	3.02209473
800.00000000	3.05432224
850.00000000	3.08459759
900.00000000	3.11314392
950.00000000	3.14014912
1000.00000000	3.16576958

INFINITE RADIAL RESERVOIR-CONSTANT RATE CASE

RD= 2.500

TD	PD
0.01500000	0.00091539
0.02000000	0.00091739
0.02500000	0.00091938
0.03000000	0.00092132
0.04000000	0.00092526
0.05000000	0.00092832
0.06000000	0.00093233
0.06999999	0.00093812
0.07999998	0.00094852
0.08999997	0.00096765
0.09999996	0.00100106
0.14999998	0.00156830
0.19999999	0.00316693
0.29999995	0.00987723
0.39999998	0.02031331
0.50000000	0.03310345
0.59999996	0.04724779
0.69999999	0.06210481
0.79999995	0.07726985
0.89999998	0.09248608
1.00000000	0.10760862
1.19999981	0.13720608
1.39999962	0.16563493
2.00000000	0.24338645
3.00000000	0.35117632
4.00000000	0.43915236
5.00000000	0.51334745
6.00000000	0.57750142
7.00000000	0.63403004
8.00000000	0.68456274
9.00000000	0.73028004
10.00000000	0.77201825
15.00000000	0.93933600
20.00000000	1.06357861
30.00000000	1.24490833
40.00000000	1.37712765
50.00000000	1.48132610
60.00000000	1.56736660
70.00000000	1.64066315
80.00000000	1.70451736
90.00000000	1.76109219
100.00000000	1.81188583
150.00000000	2.00372231
200.00000000	2.14945221
250.00000000	2.25907898
300.00000000	2.34891129
350.00000000	2.42501354
400.00000000	2.49077988
450.00000000	2.54863739
500.00000000	2.60056400
550.00000000	2.64462662
600.00000000	2.68801403
650.00000000	2.72793579
700.00000000	2.76490402
750.00000000	2.79932594
800.00000000	2.83152962
850.00000000	2.86178493
900.00000000	2.89031315
950.00000000	2.91730118
1000.00000000	2.94290638

INFINITE RADIAL RESERVOIR-CONSTANT RATE CASE

RD= 3.000

TD	PD
0.01500000	0.00211945
0.02000000	0.00212032
0.02500000	0.00212121
0.03000000	0.00212205
0.04000000	0.00212389
0.05000000	0.00212562
0.06000000	0.00212733
0.06999999	0.00212858
0.07999998	0.00213003
0.08999997	0.00213172
0.09999996	0.00213348
0.14999998	0.00216013
0.19999999	0.00229488
0.29999995	0.00343413
0.39999998	0.00626564
0.50000000	0.01083673
0.59999996	0.01688095
0.69999999	0.02407758
0.79999995	0.03213520
0.89999998	0.04081868
1.00000000	0.04994639
1.19999981	0.06900465
1.39999962	0.08852518
2.00000000	0.14641517
3.00000000	0.23406833
4.00000000	0.30287024
5.00000000	0.37587678
6.00000000	0.43411863
7.00000000	0.48616838
8.00000000	0.53320062
9.00000000	0.57609057
10.00000000	0.61550289
15.00000000	0.77543032
20.00000000	0.89571875
30.00000000	1.07288456
40.00000000	1.20293331
50.00000000	1.30579472
60.00000000	1.39093208
70.00000000	1.46357441
80.00000000	1.52693653
90.00000000	1.58312321
100.00000000	1.63360500
150.00000000	1.82949448
200.00000000	1.96974277
250.00000000	2.07908535
300.00000000	2.16972311
350.00000000	2.24468422
400.00000000	2.31060505
450.00000000	2.36882687
500.00000000	2.42096329
550.00000000	2.46292877
600.00000000	2.50526469
650.00000000	2.54614162
700.00000000	2.58307266
750.00000000	2.61746216
800.00000000	2.64963818
850.00000000	2.67986679
900.00000000	2.70837307
950.00000000	2.73534107
1000.00000000	2.76092815

INFINITE RADIAL RESERVOIR-CONSTANT RATE CASE

RD= 3.500

TD	PD
0.01500000	0.00091052
0.02000000	0.00091076
0.02500000	0.00091106
0.03000000	0.00091133
0.04000000	0.00091203
0.05000000	0.00091267
0.06000000	0.00091334
0.06999999	0.00091403
0.07999998	0.00091474
0.08999997	0.00091551
0.09999996	0.00091607
0.14999998	0.00091980
0.19999999	0.00092925
0.29999995	0.00106065
0.39999998	0.00161461
0.50000000	0.00286793
0.59999996	0.00494127
0.69999999	0.00783012
0.79999995	0.01146487
0.89999998	0.01575058
1.00000000	0.02058857
1.12999981	0.03155822
1.39999962	0.04375684
2.00000000	0.08382809
3.00000000	0.15166199
4.00000000	0.21460408
5.00000000	0.27167052
6.00000000	0.32333624
7.00000000	0.37033314
8.00000000	0.41335374
9.00000000	0.45298141
10.00000000	0.48969810
15.00000000	0.64092785
20.00000000	0.75650436
30.00000000	0.92866635
40.00000000	1.05607796
50.00000000	1.15732288
60.00000000	1.24135208
70.00000000	1.31310714
80.00000000	1.37595177
90.00000000	1.43166447
100.00000000	1.48176289
150.00000000	1.67649364
200.00000000	1.81615543
250.00000000	1.92513847
300.00000000	2.01453586
350.00000000	2.09032917
400.00000000	2.15611744
450.00000000	2.21424007
500.00000000	2.26630020
550.00000000	2.30951500
600.00000000	2.35278988
650.00000000	2.39261532
700.00000000	2.42950058
750.00000000	2.46385193
800.00000000	2.49599361
850.00000000	2.52619362
900.00000000	2.55467319
950.00000000	2.58161736
1000.00000000	2.60718346

INFINITE RADIAL RESERVOIR-CONSTANT RATE CASE

RD= 4.000

TD	PD
0.09999996	0.00254093
0.14999998	0.00254392
0.19999999	0.00254686
0.29999995	0.00256223
0.39999998	0.00264460
0.50000000	0.00291177
0.59999996	0.00348501
0.69999999	0.00444883
0.79999995	0.00584407
0.89999998	0.00767756
1.00000000	0.00993202
1.19999981	0.01558367
1.39999962	0.02251636
2.00000000	0.04835462
3.00000000	0.09831041
4.00000000	0.14880824
5.00000000	0.19673973
6.00000000	0.24152136
7.00000000	0.28313357
8.00000000	0.32183391
9.00000000	0.35790998
10.00000000	0.39164048
15.00000000	0.53318304
20.00000000	0.64340490
30.00000000	0.80981135
40.00000000	0.93417788
50.00000000	1.03352642
60.00000000	1.11627293
70.00000000	1.18717957
80.00000000	1.24922371
90.00000000	1.30438042
100.00000000	1.35402966
150.00000000	1.54739475
200.00000000	1.68635845
250.00000000	1.79492760
300.00000000	1.88404274
350.00000000	1.95963383
400.00000000	2.02526951
450.00000000	2.08327293
500.00000000	2.13523579
550.00000000	2.17683315
600.00000000	2.22003651
650.00000000	2.25980282
700.00000000	2.29663754
750.00000000	2.33094406
800.00000000	2.36304760
850.00000000	2.39321327
900.00000000	2.42166138
950.00000000	2.44857883
1000.00000000	2.47412014

INFINITE RADIAL RESERVOIR-CONSTANT RATE CASE

RD= 4.500

TD	PD
0.01500000	0.00171505
0.02000000	0.00171545
0.02500000	0.00171598
0.03000000	0.00171644
0.04000000	0.00171750
0.05000000	0.00171841
0.06000000	0.00171931
0.06999999	0.00172012
0.07999998	0.00172096
0.08999997	0.00172177
0.09999996	0.00172261
0.14999998	0.00172631
0.19999999	0.00172879
0.29999995	0.00173434
0.39999998	0.00174691
0.50000000	0.00179376
0.59999996	0.00192341
0.69999999	0.00219207
0.79999995	0.00264865
0.89999998	0.00332895
1.00000000	0.00425402
1.19999981	0.00686414
1.39999962	0.01045192
2.00000000	0.02597562
3.00000000	0.06103957
4.00000000	0.10012299
5.00000000	0.13936955
6.00000000	0.17727286
7.00000000	0.21340621
8.00000000	0.24762934
9.00000000	0.27999531
10.00000000	0.31057984
15.00000000	0.44170445
20.00000000	0.54605341
30.00000000	0.70605201
40.00000000	0.82699430
50.00000000	0.92420340
60.00000000	1.00548172
70.00000000	1.07532978
80.00000000	1.13656330
90.00000000	1.19108582
100.00000000	1.24022293
150.00000000	1.43202400
200.00000000	1.57019329
250.00000000	1.67827892
300.00000000	1.76707172
350.00000000	1.84243011
400.00000000	1.90789318
450.00000000	1.96576023
500.00000000	2.01761436
550.00000000	2.06001186
600.00000000	2.10313606
650.00000000	2.14283371
700.00000000	2.17961121
750.00000000	2.21386719
800.00000000	2.24592590
850.00000000	2.27605343
900.00000000	2.30446720
950.00000000	2.33135319
1000.00000000	2.35686684

INFINITE RADIAL RESERVOIR-CONSTANT RATE CASE

RD= 5.000

TD	PD
0.01500000	-0.00031733
0.02000000	-0.00031660
0.02500000	-0.00031621
0.03000000	-0.00031593
0.04000000	-0.00031528
0.05000000	-0.00031473
0.06000000	-0.00031419
0.06999999	-0.00031372
0.07999998	-0.00031319
0.08999997	-0.00031267
0.09999996	-0.00031214
0.14999998	-0.00030978
0.19999999	-0.00030751
0.29999995	-0.00030452
0.39999998	-0.00030048
0.50000000	-0.00029186
0.59999996	-0.00026621
0.69999999	-0.00020272
0.79999995	-0.00007425
0.89999998	0.00014568
1.00000000	0.00048035
1.19999981	0.00156120
1.39999962	0.00325385
2.00000000	0.01195843
3.00000000	0.03542574
4.00000000	0.06464261
5.00000000	0.09587598
6.00000000	0.12731642
7.00000000	0.15809554
8.00000000	0.18782884
9.00000000	0.21641999
10.00000000	0.24380445
15.00000000	0.36404580
20.00000000	0.46211797
30.00000000	0.61517715
40.00000000	0.73234493
50.00000000	0.82719040
60.00000000	0.90684221
70.00000000	0.97550929
80.00000000	1.03584480
90.00000000	1.08965302
100.00000000	1.13821793
150.00000000	1.32826710
200.00000000	1.46554089
250.00000000	1.57308388
300.00000000	1.66151142
350.00000000	1.73660851
400.00000000	1.80187511
450.00000000	1.85958862
500.00000000	1.91131973
550.00000000	1.95572567
600.00000000	1.99876022
650.00000000	2.03838348
700.00000000	2.07509518
750.00000000	2.10929489
800.00000000	2.14130497
850.00000000	2.17138863
900.00000000	2.19976425
950.00000000	2.22661591
1000.00000000	2.25209904

INFINITE RADIAL RESERVOIR-CONSTANT RATE CASE

PD= 5.500

TD	PD
0.01500000	0.00065997
0.02000000	0.00065939
0.02500000	0.00065931
0.03000000	0.00065926
0.04000000	0.00065935
0.05000000	0.00065938
0.06000000	0.00065942
0.06999999	0.00065945
0.07999998	0.00065953
0.08999997	0.00065964
0.09999996	0.00065980
0.14999998	0.00066051
0.19999999	0.00066145
0.29999995	0.00066313
0.39999998	0.00066521
0.50000000	0.00066794
0.59999996	0.00067354
0.69999999	0.00068713
0.79999995	0.00071890
0.89999998	0.00078150
1.00000000	0.00088845
1.19999981	0.00129154
1.39999962	0.00201957
2.00000000	0.00658221
3.00000000	0.02156575
4.00000000	0.04267164
5.00000000	0.06685913
6.00000000	0.09233260
7.00000000	0.11808079
8.00000000	0.14355147
9.00000000	0.16841602
10.00000000	0.19259942
15.00000000	0.30172938
20.00000000	0.39326423
30.00000000	0.53892589
40.00000000	0.65203404
50.00000000	0.74430650
60.00000000	0.82219070
70.00000000	0.88955760
80.00000000	0.94890255
90.00000000	1.00193024
100.00000000	1.04986477
150.00000000	1.23797894
200.00000000	1.37426281
250.00000000	1.48120403
300.00000000	1.56922722
350.00000000	1.64403343
400.00000000	1.70907974
450.00000000	1.76662159
500.00000000	1.81821823
550.00000000	1.86560088
600.00000000	1.90453720
650.00000000	1.94407749
700.00000000	1.98071766
750.00000000	2.01485634
800.00000000	2.04681206
850.00000000	2.07684708
900.00000000	2.10518074
950.00000000	2.13199425
1000.00000000	2.15744209

INFINITE RADIAL RESERVOIR-CONSTANT RATE CASE

RD= 6.000

TD	PD
0.01500000	0.00163098
0.02000000	0.00163189
0.02500000	0.00163217
0.03000000	0.00163222
0.04000000	0.00163233
0.05000000	0.00163234
0.06000000	0.00163236
0.06999999	0.00163235
0.07999998	0.00163239
0.08999997	0.00163245
0.09999996	0.00163257
0.14999998	0.00163299
0.19999999	0.00163361
0.29999995	0.00163501
0.39999998	0.00163614
0.50000000	0.00163774
0.59999996	0.00163973
0.69999999	0.00164332
0.79999995	0.00165074
0.89999998	0.00166694
1.00000000	0.00169781
1.19999981	0.00183339
1.39999962	0.00211989
2.00000000	0.00435757
3.00000000	0.01349511
4.00000000	0.02822176
5.00000000	0.04646448
6.00000000	0.06664366
7.00000000	0.08776569
8.00000000	0.10920751
9.00000000	0.13058811
10.00000000	0.15167338
15.00000000	0.24970335
20.00000000	0.33450192
30.00000000	0.47242659
40.00000000	0.58121854
50.00000000	0.67073601
60.00000000	0.74671441
70.00000000	0.81267643
80.00000000	0.87094855
90.00000000	0.92313302
100.00000000	0.97037363
150.00000000	1.15638351
200.00000000	1.29158592
250.00000000	1.39786530
300.00000000	1.48544407
350.00000000	1.55993176
400.00000000	1.62473583
450.00000000	1.68209171
500.00000000	1.73353481
550.00000000	1.77588654
600.00000000	1.81371605
650.00000000	1.85816479
700.00000000	1.89472675
750.00000000	1.92879772
800.00000000	1.96069431
850.00000000	1.99067783
900.00000000	2.01896381
950.00000000	2.04573631
1000.00000000	2.07114601

INFINITE RADIAL RESERVOIR-CONSTANT RATE CASE

RD= 6.500

TD	PD
0.01500000	0.00264880
0.02000000	0.00264972
0.02500000	0.00265003
0.03000000	0.00265019
0.04000000	0.00265060
0.05000000	0.00265092
0.06000000	0.00265118
0.06999999	0.00265141
0.07999998	0.00265167
0.08999997	0.00265191
0.09999996	0.00265221
0.14999998	0.00265326
0.19999999	0.00265422
0.29999995	0.00265600
0.39999998	0.00265696
0.50000000	0.00265805
0.59999996	0.00265940
0.69999999	0.00266071
0.79999995	0.00266314
0.89999998	0.00266742
1.00000000	0.00267587
1.19999981	0.00271775
1.39999962	0.00282125
2.00000000	0.00385038
3.00000000	0.00917827
4.00000000	0.01910755
5.00000000	0.03249488
6.00000000	0.04814136
7.00000000	0.06514162
8.00000000	0.08289522
9.00000000	0.10098690
10.00000000	0.11914259
15.00000000	0.20635802
20.00000000	0.28434801
30.00000000	0.41429633
40.00000000	0.51855922
50.00000000	0.60517150
60.00000000	0.67910767
70.00000000	0.74357313
80.00000000	0.80069411
90.00000000	0.85196489
100.00000000	0.89847028
150.00000000	1.08220005
200.00000000	1.21623039
250.00000000	1.32179260
300.00000000	1.40889072
350.00000000	1.48303032
400.00000000	1.54757500
450.00000000	1.60472679
500.00000000	1.65600491
550.00000000	1.69725227
600.00000000	1.73996449
650.00000000	1.77931499
700.00000000	1.81579304
750.00000000	1.84978962
800.00000000	1.88162231
850.00000000	1.91154861
900.00000000	1.93978500
950.00000000	1.96651173
1000.00000000	1.99188137

INFINITE RADIAL RESERVOIR-CONSTANT RATE CASE

PD= 7.000

TD	PD
0.01500000	-0.00101824
0.02000000	-0.00101942
0.02500000	-0.00101977
0.03000000	-0.00101981
0.04000000	-0.00101951
0.05000000	-0.00101924
0.06000000	-0.00101896
0.06999999	-0.00101871
0.07999998	-0.00101848
0.08999997	-0.00101822
0.09999996	-0.00101793
0.14999998	-0.00101690
0.19999999	-0.00101601
0.29999995	-0.00101452
0.39999998	-0.00101324
0.50000000	-0.00101260
0.59999996	-0.00101173
0.69999999	-0.00101068
0.79999995	-0.00100971
0.89999998	-0.00100816
1.00000000	-0.00100558
1.19999981	-0.00099305
1.39999962	-0.00095833
2.00000000	-0.00051348
3.00000000	0.00245891
4.00000000	0.00893221
5.00000000	0.01849406
6.00000000	0.03035472
7.00000000	0.04379418
8.00000000	0.05825020
9.00000000	0.07333654
10.00000000	0.08876175
15.00000000	0.16560990
20.00000000	0.23682702
30.00000000	0.35863906
40.00000000	0.45820063
50.00000000	0.54175401
60.00000000	0.61355549
70.00000000	0.67643148
80.00000000	0.73232788
90.00000000	0.78263086
100.00000000	0.82834822
150.00000000	1.00963497
200.00000000	1.14240837
250.00000000	1.24720097
300.00000000	1.33378029
350.00000000	1.40754509
400.00000000	1.47180557
450.00000000	1.52873516
500.00000000	1.57983875
550.00000000	1.62466240
600.00000000	1.66724968
650.00000000	1.70549338
700.00000000	1.74287987
750.00000000	1.77679825
800.00000000	1.80856133
850.00000000	1.83842659
900.00000000	1.86660862
950.00000000	1.89328575
1000.00000000	1.91861248

INFINITE RADIAL RESERVOIR-CONSTANT RATE CASE

RD= 7.500

TD	PD
0.01500000	0.00016393
0.02000000	0.00016173
0.02500000	0.00016114
0.03000000	0.00016089
0.04000000	0.00016083
0.05000000	0.00016080
0.06000000	0.00016080
0.06999999	0.00016078
0.07999998	0.00016081
0.08999997	0.00016086
0.09999996	0.00016094
0.14999998	0.00016121
0.19999999	0.00016158
0.29999995	0.00016238
0.39999998	0.00016347
0.50000000	0.00016383
0.59999996	0.00016451
0.69999999	0.00016511
0.79999995	0.00016597
0.89999998	0.00016667
1.00000000	0.00016784
1.19999981	0.00017197
1.39999962	0.00018318
2.00000000	0.00036504
3.00000000	0.00195304
4.00000000	0.00603473
5.00000000	0.01268376
6.00000000	0.02147743
7.00000000	0.03189801
8.00000000	0.04343077
9.00000000	0.05588615
10.00000000	0.06882215
15.00000000	0.13591534
20.00000000	0.20045251
30.00000000	0.31403863
40.00000000	0.40379393
50.00000000	0.48917806
60.00000000	0.55873835
70.00000000	0.61995101
80.00000000	0.67455906
90.00000000	0.72383660
100.00000000	0.76871914
150.00000000	0.94741935
200.00000000	1.07884502
250.00000000	1.18281651
300.00000000	1.26983507
350.00000000	1.34220028
400.00000000	1.40615940
450.00000000	1.46285439
500.00000000	1.51376343
550.00000000	1.55729771
600.00000000	1.59975052
650.00000000	1.63388073
700.00000000	1.67516994
750.00000000	1.70900345
800.00000000	1.74069214
850.00000000	1.77040160
900.00000000	1.79861546
950.00000000	1.82524109
1000.00000000	1.85052013

INFINITE RADIAL RESERVOIR-CONSTANT RATE CASE

RD= 8.000

TD	PD
1.00000000	-0.00125174
1.19999981	-0.00124991
1.39999962	-0.00124607
2.00000000	-0.00117542
3.00000000	-0.00036124
4.00000000	0.00212744
5.00000000	0.00663103
6.00000000	0.01300655
7.00000000	0.02093620
8.00000000	0.03007644
9.00000000	0.04012656
10.00000000	0.05083292
15.00000000	0.10880464
20.00000000	0.16692084
30.00000000	0.27231622
40.00000000	0.36215782
50.00000000	0.43927503
60.00000000	0.50650918
70.00000000	0.56598669
80.00000000	0.61925191
90.00000000	0.66744900
100.00000000	0.71145117
150.00000000	0.88742113
200.00000000	1.01741982
250.00000000	1.12051487
300.00000000	1.20594215
350.00000000	1.27887821
400.00000000	1.34251308
450.00000000	1.39895248
500.00000000	1.44966221
550.00000000	1.49449635
600.00000000	1.53680706
650.00000000	1.57581520
700.00000000	1.61200142
750.00000000	1.64574337
800.00000000	1.67735291
850.00000000	1.70708275
900.00000000	1.73514366
950.00000000	1.76171398
1000.00000000	1.78694248

INFINITE RADIAL RESERVOIR-CONSTANT RATE CASE

RD= 8.500

TD	PD
2.00000000	-0.00015051
3.00000000	0.00025024
4.00000000	0.00171886
5.00000000	0.00468904
6.00000000	0.00921282
7.00000000	0.01513263
8.00000000	0.02222282
9.00000000	0.03024902
10.00000000	0.03900458
15.00000000	0.08860958
20.00000000	0.14061713
30.00000000	0.23788476
40.00000000	0.32275367
50.00000000	0.39654005
60.00000000	0.46138138
70.00000000	0.51905817
80.00000000	0.57092315
90.00000000	0.61800307
100.00000000	0.66108388
150.00000000	0.83413512
200.00000000	0.96268010
250.00000000	1.06484699
300.00000000	1.14965057
350.00000000	1.22213173
400.00000000	1.28542423
450.00000000	1.34150565
500.00000000	1.39203889
550.00000000	1.43571854
600.00000000	1.47787666
650.00000000	1.51675701
700.00000000	1.55283165
750.00000000	1.58647823
800.00000000	1.61800385
850.00000000	1.64765930
900.00000000	1.67565441
950.00000000	1.70216465
1000.00000000	1.72734070

INFINITE RADIAL RESERVOIR-CONSTANT RATE CASE

RD= 9.000

TD	PD
0.01500000	-0.00012424
0.02000000	-0.00012261
0.02500000	-0.00012119
0.03000000	-0.00012043
0.04000000	-0.00011964
0.05000000	-0.00011937
0.06000000	-0.00011917
0.06999999	-0.00011906
0.07999998	-0.00011892
0.08999997	-0.00011877
0.09999996	-0.00011857
0.14999998	-0.00011802
0.19999999	-0.00011757
0.29999995	-0.00011689
0.39999998	-0.00011634
0.50000000	-0.00011586
0.59999996	-0.00011518
0.69999999	-0.00011504
0.79999995	-0.00011487
0.89999998	-0.00011456
1.00000000	-0.00011417
1.19999981	-0.00011341
1.39999962	-0.00011255
2.00000000	-0.00010224
3.00000000	0.00008777
4.00000000	0.00092703
5.00000000	0.00283481
6.00000000	0.00597473
7.00000000	0.01031330
8.00000000	0.01572297
9.00000000	0.02204169
10.00000000	0.02910583
15.00000000	0.07115024
20.00000000	0.11733222
30.00000000	0.20669389
40.00000000	0.28657162
50.00000000	0.35698384
60.00000000	0.41937542
70.00000000	0.47520179
80.00000000	0.52561849
90.00000000	0.57153696
100.00000000	0.61365844
150.00000000	0.78376436
200.00000000	0.91067958
250.00000000	1.01187134
300.00000000	1.09601021
350.00000000	1.16801548
400.00000000	1.23094463
450.00000000	1.28683472
500.00000000	1.33709812
550.00000000	1.38051414
600.00000000	1.42251205
650.00000000	1.46125698
700.00000000	1.49721432
750.00000000	1.53075981
800.00000000	1.56219673
850.00000000	1.59177303
900.00000000	1.61969852
950.00000000	1.64614677
1000.00000000	1.67126560

INFINITE RADIAL RESERVOIR-CONSTANT RATE CASE

RD= 9.500

TD	PD
2.00000000	0.00010355
3.00000000	0.00028066
4.00000000	0.00074536
5.00000000	0.00193887
6.00000000	0.00407097
7.00000000	0.00719278
8.00000000	0.01125310
9.00000000	0.01615513
10.00000000	0.02178193
15.00000000	0.05707958
20.00000000	0.09779721
30.00000000	0.17950088
40.00000000	0.25442135
50.00000000	0.32140690
60.00000000	0.38131231
70.00000000	0.43524033
80.00000000	0.48416698
90.00000000	0.52838685
100.00000000	0.57003129
150.00000000	0.73701370
200.00000000	0.86227572
250.00000000	0.96244937
300.00000000	1.04580081
350.00000000	1.11739540
400.00000000	1.17994308
450.00000000	1.23553562
500.00000000	1.28555489
550.00000000	1.33150933
600.00000000	1.37033844
650.00000000	1.40993936
700.00000000	1.44477463
750.00000000	1.47821236
800.00000000	1.50955486
850.00000000	1.53904915
900.00000000	1.56690121
950.00000000	1.59328270
1000.00000000	1.61834240

INFINITE RADIAL RESERVOIR-CONSTANT RATE CASE

RD= 10.000

TD	PD
1.00000000	0.00042031
1.19999981	0.00042071
1.39999962	0.00042117
2.00000000	0.00042353
3.00000000	0.00046245
4.00000000	0.00071191
5.00000000	0.00143963
6.00000000	0.00285603
7.00000000	0.00506011
8.00000000	0.00805062
9.00000000	0.01180828
10.00000000	0.01623156
15.00000000	0.04558896
20.00000000	0.08123976
30.00000000	0.15561664
40.00000000	0.22559357
50.00000000	0.28913647
60.00000000	0.34653038
70.00000000	0.39852929
80.00000000	0.44593292
90.00000000	0.48941672
100.00000000	0.52954453
150.00000000	0.69329929
200.00000000	0.81684554
250.00000000	0.91595554
300.00000000	0.99866819
350.00000000	1.06964302
400.00000000	1.13179111
450.00000000	1.18706894
500.00000000	1.23683929
550.00000000	1.27938461
600.00000000	1.32103634
650.00000000	1.35948753
700.00000000	1.39519310
750.00000000	1.42851925
800.00000000	1.45976257
850.00000000	1.48917007
900.00000000	1.51694393
950.00000000	1.54325676
1000.00000000	1.56825352

INFINITE RADIAL RESERVOIR-CONSTANT RATE CASE

RD= 15.000

TD	PD
2.00000000	0.00073178
3.00000000	0.00073202
4.00000000	0.00073254
5.00000000	0.00073439
6.00000000	0.00074192
7.00000000	0.00076680
8.00000000	0.00082627
9.00000000	0.00094312
10.00000000	0.00113975
15.00000000	0.00393982
20.00000000	0.01040158
30.00000000	0.03257025
40.00000000	0.06192833
50.00000000	0.09419918
60.00000000	0.12713468
70.00000000	0.15959430
80.00000000	0.19107598
90.00000000	0.22140455
100.00000000	0.25046694
150.00000000	0.37790853
200.00000000	0.48132730
250.00000000	0.56766593
300.00000000	0.64156109
350.00000000	0.70609300
400.00000000	0.76330941
450.00000000	0.81470060
500.00000000	0.86133164
550.00000000	0.90130615
600.00000000	0.94075251
650.00000000	0.97732592
700.00000000	1.01141453
750.00000000	1.04333305
800.00000000	1.07334137
850.00000000	1.10165596
900.00000000	1.12845421
950.00000000	1.15389156
1000.00000000	1.17810059

INFINITE RADIAL RESERVOIR-CONSTANT RATE CASE

RD= 16.000

TD	PD
10.00000000	0.00018542
15.00000000	0.00175900
20.00000000	0.00599094
30.00000000	0.02243113
40.00000000	0.04609326
50.00000000	0.07336104
60.00000000	0.10204864
70.00000000	0.13095224
80.00000000	0.15939456
90.00000000	0.18709546
100.00000000	0.21391165
150.00000000	0.33365744
200.00000000	0.43260705
250.00000000	0.51603293
300.00000000	0.58789396
350.00000000	0.65090054
400.00000000	0.70696211
450.00000000	0.75743443
500.00000000	0.80331331
550.00000000	0.84344149
600.00000000	0.88235903
650.00000000	0.91848135
700.00000000	0.95218086
750.00000000	0.98376036
800.00000000	1.01346970
850.00000000	1.04151821
900.00000000	1.06808090
950.00000000	1.09330654
1000.00000000	1.11732292

INFINITE RADIAL RESERVOIR-CONSTANT RATE CASE

RD= 20.000

TD	PD
1.00000000	-0.00043887
1.19999981	-0.00043887
1.39999962	-0.00043888
2.00000000	-0.00043879
3.00000000	-0.00043855
4.00000000	-0.00043868
5.00000000	-0.00043877
6.00000000	-0.00043874
7.00000000	-0.00043863
8.00000000	-0.00043831
9.00000000	-0.00043732
10.00000000	-0.00043483
15.00000000	-0.00032260
20.00000000	0.00027436
30.00000000	0.00441935
40.00000000	0.01311466
50.00000000	0.02558330
60.00000000	0.04067794
70.00000000	0.05744993
80.00000000	0.07521290
90.00000000	0.09348929
100.00000000	0.11195391
150.00000000	0.20153213
200.00000000	0.28210115
250.00000000	0.35325927
300.00000000	0.41634250
350.00000000	0.47277981
400.00000000	0.52373743
450.00000000	0.57013112
500.00000000	0.61268127
550.00000000	0.65070486
600.00000000	0.68725777
650.00000000	0.72135592
700.00000000	0.75330305
750.00000000	0.78335238
800.00000000	0.81171227
850.00000000	0.83856249
900.00000000	0.86405373
950.00000000	0.88831615
1000.00000000	0.91146183

INFINITE RADIAL RESERVOIR-CONSTANT RATE CASE

RD= 25.000

TD	PD
20.00000000	0.00030886
30.00000000	0.00080791
40.00000000	0.00264210
50.00000000	0.00631606
60.00000000	0.01184616
70.00000000	0.01900696
80.00000000	0.02749391
90.00000000	0.03701087
100.00000000	0.04730190
150.00000000	0.10443801
200.00000000	0.16281694
250.00000000	0.21824092
300.00000000	0.26969308
350.00000000	0.31720221
400.00000000	0.36111140
450.00000000	0.40177792
500.00000000	0.43959647
550.00000000	0.47318774
600.00000000	0.50632954
650.00000000	0.53748989
700.00000000	0.56588023
750.00000000	0.59468412
800.00000000	0.62105751
850.00000000	0.64613676
900.00000000	0.67004013
950.00000000	0.69286966
1000.00000000	0.71471739

INFINITE RADIAL RESERVOIR-CONSTANT RATE CASE

RD= 30.000

TD	PD
1.00000000	0.00014879
1.19999981	0.00014875
1.39999962	0.00014871
2.00000000	0.00014872
3.00000000	0.00014864
4.00000000	0.00014858
5.00000000	0.00014847
6.00000000	0.00014851
7.00000000	0.00014850
8.00000000	0.00014839
9.00000000	0.00014823
10.00000000	0.00014814
15.00000000	0.00014792
20.00000000	0.00014848
30.00000000	0.00018775
40.00000000	0.00046543
50.00000000	0.00129383
60.00000000	0.00291794
70.00000000	0.00544753
80.00000000	0.00888478
90.00000000	0.01316553
100.00000000	0.01820143
150.00000000	0.05124409
200.00000000	0.09074295
250.00000000	0.13162220
300.00000000	0.17164671
350.00000000	0.21011454
400.00000000	0.24667466
450.00000000	0.28128505
500.00000000	0.31402940
550.00000000	0.34370279
600.00000000	0.37310463
650.00000000	0.40101510
700.00000000	0.42755634
750.00000000	0.45284259
800.00000000	0.47697520
850.00000000	0.50004768
900.00000000	0.52214336
950.00000000	0.54333687
1000.00000000	0.56369638

INFINITE RADIAL RESERVOIR-CONSTANT RATE CASE

RD= 32.000

TD	PD
40.00000000	0.00244252
50.00000000	0.00286665
60.00000000	0.00380143
70.00000000	0.00538408
80.00000000	0.00767139
90.00000000	0.01065939
100.00000000	0.01430427
150.00000000	0.04014811
200.00000000	0.07325608
250.00000000	0.10889107
300.00000000	0.14472634
350.00000000	0.17963427
400.00000000	0.21329862
450.00000000	0.24548334
500.00000000	0.27616251
550.00000000	0.30199826
600.00000000	0.32985431
650.00000000	0.35641211
700.00000000	0.38176042
750.00000000	0.40598708
800.00000000	0.42917252
850.00000000	0.45139372
900.00000000	0.47271979
950.00000000	0.49321437
1000.00000000	0.51293612

INFINITE RADIAL RESERVOIR-CONSTANT RATE CASE

RD= 35.000

TD	PD
1.00000000	-0.00111746
1.19999981	-0.00111750
1.39999962	-0.00111753
2.00000000	-0.00111751
3.00000000	-0.00111758
4.00000000	-0.00111764
5.00000000	-0.00111768
6.00000000	-0.00111773
7.00000000	-0.00111784
8.00000000	-0.00111770
9.00000000	-0.00111778
10.00000000	-0.00111790
15.00000000	-0.00111834
20.00000000	-0.00111844
30.00000000	-0.00111679
40.00000000	-0.00108661
50.00000000	-0.00094317
60.00000000	-0.00056073
70.00000000	0.00017921
80.00000000	0.00136100
90.00000000	0.00302793
100.00000000	0.00519032
150.00000000	0.02256515
200.00000000	0.04744651
250.00000000	0.07597220
300.00000000	0.10584575
350.00000000	0.13582987
400.00000000	0.16521174
450.00000000	0.19381350
500.00000000	0.22141790
550.00000000	0.24816644
600.00000000	0.27368659
650.00000000	0.29818916
700.00000000	0.32171661
750.00000000	0.34431857
800.00000000	0.36604697
850.00000000	0.38695323
900.00000000	0.40708804
950.00000000	0.42649859
1000.00000000	0.44522893

INFINITE RADIAL RESERVOIR-CONSTANT RATE CASE

RD= 40.000

TD	PD
50.00000000	-0.00069316
60.00000000	-0.00062085
70.00000000	-0.00044162
80.00000000	-0.00009678
90.00000000	0.00046436
100.00000000	0.00127970
150.00000000	0.00960550
200.00000000	0.02422788
250.00000000	0.04306798
300.00000000	0.06433886
350.00000000	0.08683401
400.00000000	0.10979414
450.00000000	0.13275224
500.00000000	0.15541840
550.00000000	0.17758071
600.00000000	0.19924992
650.00000000	0.22033113
700.00000000	0.24080145
750.00000000	0.26065707
800.00000000	0.27990597
850.00000000	0.29856414
900.00000000	0.31665081
950.00000000	0.33418840
1000.00000000	0.35120010

INFINITE RADIAL RESERVOIR-CONSTANT RATE CASE

RD= 45.000

TD	PD
80.00000000	-0.00190446
90.00000000	-0.00174110
100.00000000	-0.00147126
150.00000000	0.00217613
200.00000000	0.01019204
250.00000000	0.02197690
300.00000000	0.03645553
350.00000000	0.05269676
400.00000000	0.07000768
450.00000000	0.08790261
500.00000000	0.10604507
550.00000000	0.12568873
600.00000000	0.14368343
650.00000000	0.16145557
700.00000000	0.17893451
750.00000000	0.19607598
800.00000000	0.21285295
850.00000000	0.22925186
900.00000000	0.24526668
950.00000000	0.26089835
1000.00000000	0.27615124

INFINITE RADIAL RESERVOIR-CONSTANT RATE CASE

RD= 50.000

TD	PD
100.00000000	0.00102450
150.00000000	0.00248826
200.00000000	0.00659807
250.00000000	0.01357445
300.00000000	0.02299920
350.00000000	0.03428767
400.00000000	0.04691334
450.00000000	0.06045764
500.00000000	0.07459694
550.00000000	0.08767909
600.00000000	0.10233635
650.00000000	0.11718315
700.00000000	0.13182616
750.00000000	0.14636552
800.00000000	0.16074991
850.00000000	0.17494303
900.00000000	0.18891978
950.00000000	0.20266336
1000.00000000	0.21616328

INFINITE RADIAL RESERVOIR-CONSTANT RATE CASE

RD= 55.000

TD	PD
100.00000000	-0.00012648
150.00000000	0.00041291
200.00000000	0.00238202
250.00000000	0.00629918
300.00000000	0.01215941
350.00000000	0.01971164
400.00000000	0.02862299
450.00000000	0.03857851
500.00000000	0.04931252
550.00000000	0.06035933
600.00000000	0.07202399
650.00000000	0.08394748
700.00000000	0.09602410
750.00000000	0.10817164
800.00000000	0.12045628
850.00000000	0.13255012
900.00000000	0.14457071
950.00000000	0.15648890
1000.00000000	0.16828269

INFINITE RADIAL RESERVOIR-CONSTANT RATE CASE

RD= 60.000

TD	PD
100.00000000	0.00203603
150.00000000	0.00221883
200.00000000	0.00310157
250.00000000	0.00518543
300.00000000	0.00867568
350.00000000	0.01353519
400.00000000	0.01961793
450.00000000	0.02672696
500.00000000	0.03466665
550.00000000	0.04092616
600.00000000	0.05000973
650.00000000	0.05948263
700.00000000	0.06924194
750.00000000	0.07920414
800.00000000	0.08930123
850.00000000	0.09947866
900.00000000	0.10969186
950.00000000	0.12003553
1000.00000000	0.13020319

INFINITE RADIAL RESERVOIR-CONSTANT RATE CASE

RD= 64.000

TD	PD
250.00000000	0.00143945
300.00000000	0.00367143
350.00000000	0.00699979
400.00000000	0.01137266
450.00000000	0.01668726
500.00000000	0.02280925
550.00000000	0.02964979
600.00000000	0.03697100
650.00000000	0.04473871
700.00000000	0.05285996
750.00000000	0.06125563
800.00000000	0.06985945
850.00000000	0.07861614
900.00000000	0.08747959
950.00000000	0.09641182
1000.00000000	0.10538125